



IMPLICATIONS OF ENVIRONMENTAL CONDITIONS ON ARID GYPSEOUS SOILS FOR GEOTECHNICAL ENGINEERING APPLICATIONS

by

Huda Najih Taher Alnomani

A thesis submitted to
the University of Birmingham
for the degree of
Doctor of Philosophy

School of Civil Engineering
College of Engineering and Physical Sciences
University of Birmingham
July 2019

UNIVERSITY OF
BIRMINGHAM

University of Birmingham Research Archive

e-theses repository

This unpublished thesis/dissertation is copyright of the author and/or third parties. The intellectual property rights of the author or third parties in respect of this work are as defined by The Copyright Designs and Patents Act 1988 or as modified by any successor legislation.

Any use made of information contained in this thesis/dissertation must be in accordance with that legislation and must be properly acknowledged. Further distribution or reproduction in any format is prohibited without the permission of the copyright holder.

ABSTRACT

Loosely packed sandy soil, created via aeolian deposition and stabilised by interparticle bonding via gypsum crystals (dispersed within the soil fabric), are a significant geohazard in hot, arid environments such as the Middle East (for example, these deposits cover a large area of Iraq). Gypsum, being a moderately soluble salt, can have a substantial influence on the engineering properties of soils, and changes in water content can result in rapid collapse of the soil fabric, damaging surrounding structures; i.e. these deposits are metastable.

A search of the literature illustrated that no research focused on the behaviour of an aeolian gypseous soil in environmental conditions. Also, employing electrical resistivity, which might be a helpful tool to monitor water movement in the soil deposit, has not been considered previously. This study, therefore, examined two interconnected experiments. The first aimed to study the impact of groundwater movement (the dimensions of the samples were 144 mm diameter and 300 mm height, with 10% and 20% gypsum content) due to evaporation through an unsaturated column of gypseous soil. These samples were exposed to various conditions, including changing gypsum content, groundwater, temperature gradients, and a breeze across the upper surface of the samples. The second study aimed to determine the stress-settlement characteristics of a pad footing resting on gypseous soil deposit (the dimensions of the samples were 349 mm diameter and 300 mm height, with 20% gypsum content) when exposed to groundwater flow, with and without exposure to the environmental conditions used in the previous study (temperature gradient, and breeze). Electrical resistivity was used to monitor the movement of salty water through the samples in ‘quasi-real-time’, without having to dissect the samples.

Obtaining undisturbed samples of this soil to study in the laboratory can be problematic for logistical reasons. Therefore, a method has been developed that produces repeatable samples with the desired properties to facilitate a systematic investigation of these soils without the need for sampling. This method offers flexibility so that large and small samples can be created for investigation. Samples with a range of gypsum content (from 5% to 30%) were investigated with an oedometer and with unconfined compressive strength apparatus, and it is clear that increasing the gypsum content results in stronger material that exhibits greater

collapse potential when inundated with water. Secondary compression and creep appear to be important mechanisms when considering settlements with inundation of water, suggesting that longer duration load steps should be used in compression tests (90 days were used herein) than the normal 24-hour period if the metastable nature of these materials is not to be underestimated.

It is apparent from the evaporation test that, over time, manufactured soil experiences partial dissolution and re-precipitation of its gypsum, with precipitation taking place in the upper layers of the soil as the water evaporates from the soil under increasing temperatures. While the dissolution of gypsum does not appear to be the dominant mechanism dictating the metastable response of the soil samples in the three footing tests, where partial dissipation of suction and possible softening of cementitious bonds via the gypsum crystals, appears to have a more pronounced impact due to both the time required for a collapse to occur and the volume of water required to trigger a collapse event.

The soil resistivity was very sensitive to moisture, temperature, and load-induced variations rather than crystal gypsum variation. Conditions of stress, temperature, and moisture substantially affected the current passing through the soil fabric. It was found that increasing the gypsum content provides more ions for electrical conduction, leading to an increase in the pore water conductivity and therefore diminishing soil resistivity. However, the soil resistivity for the three footing tests was completely different upon failure, and this due to the test conditions (amount of water, densification of the upper layer, temperature, and test time).

To My Mother; My Husband Hussain; My Kids Fatimah, Kawther and Ali

ACKNOWLEDGEMENT

Foremost, I would like to express my sincere gratitude to my supervisors- Dr. Alexander Royal and Prof. Ian Jefferson for the continuous support of my PhD study and research, for their patience, motivation, enthusiasm, and immense knowledge. Their guidance helped me in all the time of research and writing of this thesis.

My special thanks go to Mr Phil Atkins for his technical expertise in solving the electrical-resistivity-acquisition system problems. I would also like to express my deep gratitude to Professor Nigel Cassidy for his help in the design the ER for the evaporation pipe.

I would like to thank the reviewers: Prof. David Chapman and Prof. Gurmel Ghataora for their insightful comments and valued feedback during the annual progress reviews.

I would like to express my deepest thanks to the technical staff at Civil Engineering laboratory for their assistance in the lab.

Many thanks to Dr Anna Faroqy and Dr Giulio Curioni for their support, discussions and sharing literature.

I would like to express my greatest gratitude to my family, specially my mother for her invaluable love, support and guidance throughout my research, my husband for his love, patience and support, and for my kids Fatimah, Kawther and Ali for their innocence and spontaneity.

I would like to thank the Ministry of Higher Education and Scientific Research (MOHESR) of Iraq for financial support during my study.

Lastly, my loyalty and thankfulness to every person regarded, encouraged and taught me since my childhood till the end of this thesis. Undoubtedly, there is a share for everyone of them in my career.

TABLE OF CONTENTS

UNIVERSITY OF BIRMINGHAM RESEARCH ARCHIVE.....	i
ABSTRACT	ii
ACKNOWLEDGEMENT.....	v
TABLE OF CONTENTS	vi
TABLES	xii
FIGURES.....	xiii
ABBREVIATIONS AND SYMBOLS	xxi
CHAPTER ONE: INTRODUCTION	1
1.1 Introduction	1
1.2 Need and Motivations of the Research.....	2
1.3 Key Knowledge Gaps.....	6
1.4 Aim and objectives	7
1.5 Thesis Organization.....	8
CHAPTER TWO: LITERATURE REVIEW.....	11
2.1 Introduction	11
2.2 Gypseous Soil.....	11
2.2.1 Properties of Gypsum as a Mineral within Soil.....	12
2.2.2 The Gypsum-Anhydrite Cycle.....	14
2.2.2.1 Example of Civil Engineering Challenges Encountered with the Anhydrite to Gypsum Conversion	16
2.2.3 Formation of Gypseous Soil.....	18
2.2.4 Distribution of Gypseous Soils in the World.....	19
2.2.5 Summary of the Variation in Terminology Used when Attempting to Describe Soil Deposits Containing Gypsum.....	20
2.2.6 Dissolution of Gypsum.....	24

2.2.6.1 Example of Civil Engineering Challenges Encountered with Dissolution of Gypsum.....	25
2.3 Gypsum's Effect on Soil Properties	27
2.3.1 Consistency Limits	27
2.3.2 Compaction Parameters	28
2.3.3 Hydraulic Conductivity	29
2.3.4 Compressibility of Gypseous Soil	32
2.3.4.1 Collapsibility of Gypseous Soil.....	32
2.3.4.2 Compression and Swelling Index of Gypseous Soil	35
2.3.5 Swelling Behaviour	38
2.3.6 Shear Strength of Gypseous Soil	41
2.3.6.1 Effect of Gypsum Content on Shear Strength in Dry State.....	42
2.3.6.2 Effect of Soaking on Shear Strength of Gypseous Soils	44
2.4 Gypseous Soils in Iraq and Britain	47
2.4.1 Gypsum Forms Encountered in Iraq.....	47
2.4.2 Gypsum Forms Encountered in Britain.....	49
2.5 Uncertainties with Geotechnical Engineering Applications in Arid, Metastable, Gypseous Soils	51
2.6 Summary.....	53
CHAPTER THREE: MANUFACURING GYPSEOUS SOIL AND VALIDATION TEST..	56
3.1 Introduction	56
3.2 Creation of a Laboratory-Synthesized Gypseous Soil.....	57
3.2.1 Understanding the Natural Soil Deposits that the Manufactured Samples are Attempting to Simulate.....	57
3.2.2 Previous Methods Used to Manufacture Gypseous Soils within the Laboratory and the Associated Limitations	61
3.2.3 A Summary of the Method Developed for this Investigation	65
3.3 Materials Properties of the Manufactured Soils and Classification Tests	66
3.3.1 Materials Used in the Soil	66
3.3.2 Physical Tests	68

3.3.2.1 Particle Density.....	68
3.3.2.2 Water Content.....	69
3.3.3 Determination of Gypsum Content.....	69
3.4 Creating Gypseous Samples Using the Pluviation Technique	71
3.4.1 Air-Pluviation Method.....	71
3.4.2 Factors Affecting the Pluviation Method	72
3.4.3 Design of Pluviation Apparatus.....	74
3.4.4 Sample Preparation.....	77
3.4.4.1 Issues with the Sand-Gypsum Mixtures during Pluviation	77
3.4.4.2 Manufactured Gypseous Samples	78
3.5 Feasibility of the New Method	80
3.5.1 Discussion of Sample Preparation by the Pluviation Method	80
3.5.2 Gypsum Determination by the Thermogravimetric Method	84
3.6 Validation Testing	85
3.6.1 Compaction Test.....	86
3.6.1.1 Compaction Test Results	87
3.6.2 Oedometer Testing	90
3.6.2.1 Investigating the Collapse Potential of the Manufactured Gypseous Soils.....	91
3.6.2.1.1 Results and Discussions of the SOT.....	92
3.6.2.1.2 Results and Discussion of DOT.....	96
3.6.2.2 Results and Discussion of Standard Consolidation Test	98
3.6.2.3 Results and Discussion of Delayed Compression (Creep)	101
3.6.3 Unconfined Compressive Strength Tests and Associated Deformation Response	104
3.6.3.1 Sample Preparation for UCS Testing	105
3.6.3.2 Outcome of UCS Testing	108
3.6.3.2.1 Single-Layer Samples with Changing Gypsum Content and Curing Age	108
3.6.3.2.2 Deformation Response of Single- and Multi-Layered Samples with Changing Gypsum Content Levels on the UCS	109
3.6.3.2.3 Implications of Multiple Layers on Large-Scale Sample Manufacture ..	114
3.6.4 Suction Test	117

3.7.4.1 Testing Device	117
3.7.4.2 Sample Preparation and Testing Procedure	118
3.7.4.2.1 Chilled-Mirror Dew Point Technique	118
3.7.4.2.2 HYPROP Technique	120
3.7.4.3 Results and discussion	123
3.8 Summary	126
CHAPTER FOUR: BESPOKE EXPERIMENTS: SAMPLE CREATION AND CELL DEVELOPMENT	129
4.1 Introduction	129
4.2 Sample Sizes for the Bespoke Tests	130
4.3 Electrical Resistivity (ER)	132
4.3.1 ER Theory and Factors that Influence ER	132
4.3.2 Electrode Configuration for the Current Study	135
4.3.3 The Data Logging System	137
4.4 Experimental Setup of Evaporation Test	138
4.4.1 Lab Equipment and Apparatus	138
4.4.2 Soil Deposit Formation	144
4.4.2.1 Requirements for the Filter Layer	144
4.4.2.2 Formation of the Manufactured Pluviated Gypseous Soil Sample	144
4.4.3 Investigating the Response of a Trial Sample	147
4.4.4 Running the Evaporation Test	149
4.5 Setup of Footing Test	150
4.5.1 Lab Equipment and Apparatus	150
4.5.1.1 Model Footing	153
4.5.1.2 Loading and Measurement Apparatus	154
4.5.2 Formation of the Soil Column	156
4.5.2.1 Formation of the Filter Layer	157
4.5.2.2 Manufacture of the Gypseous Soil	157
4.5.3 Investigating the Homogeneity of a Trial Sample	158
4.5.4 Running the Footing Test	160

4.6 Electrical Resistivity Calibration.....	162
4.6.1 Calibration of the Configuration.....	162
4.6.2 Temperature Correction.....	164
4.6.2.1 Investigating the Temperature-Resistivity Relationship for the Gypseous Soils using McMiller Boxes	165
4.6.2.2 Limitations with ER Corrections	167
4.7 Summary.....	168
CHAPTER FIVE: EXPERIMENTAL RESULTS AND DISCUSSION.....	169
5.1 Introduction	169
5.2 Experimental Results and Analysis of Evaporation Test	169
5.2.1 Evaporation, Temperature Gradient, and ER Results with Respect to the Experimental Timeline	170
5.2.2 Investigating the Water Content, Gypsum Content, Temperature and ER at the End of Test.....	177
5.3 Results and Analysis of the Simulated Footing Experiment	182
5.3.1 Mechanism of Wetting the Soil.....	183
5.3.2 Stress-Settlement Characteristics of the Foundation before Wetting Stage	184
5.3.3 Time-Settlement, -ER and -Temperature and Failure Profiles of the Foundation- Manufactured Soil upon Wetting	185
5.3.3.1 Case 1: Quick Test without Heating Source and Breeze.....	185
5.3.3.2 Case 2: Slow Test without Heating Source and Breeze	192
5.3.3.3 Case 3: Slow Test with Heating Source and Breeze	196
5.4 Discussion.....	201
5.4.1 Producing a Metastable Response in Samples of Various Sizes	201
5.4.2 Observations on the Collapse of the Metastable Soils in the Footing Experiments and Comments on the Possible Mechanisms Controlling this Response	202
5.4.2.1 Gypsum Dissolution and Precipitation within Soil Columns.....	203
5.4.2.2 Failure Observations in the Footing Tests.....	205
5.4.3 Observations on the Use of Resistivity to Monitor Changes in Geotechnical Properties of the Gypseous Soil Samples with Movement of Water through the Soil Columns.....	209

5.5 Summary.....	211
CHAPTER SIX: CONCLUSION AND RECOMMENDATIONS	214
6.1 Introduction	214
6.2 Conclusions	216
6.2.1 Manufacturing Gypseous Soil and the Associated Validation Testing	216
6.2.2 Bespoke Testing (Evaporation Column and the Simulated Foundation)	219
6.2.3. Reflections on the Use of Electrical Resistivity	221
6.4 Recommendations for Further Work.....	222
LIST OF REFERENCES.....	224

TABLES

Table 1-1: Problems which occurred for structures constructed on gypseous soil.	4
Table 2-1: Chemical proportions of gypsum and anhydrite (Klein and Hurlbut, 1985).	13
Table 2-2: Classification of gypsiferous soil below 50% gypsum content (Barzanji, 1973). ..	23
Table 2-3: The proposed applied classification of gypsiferous soils (Al-Dabbas et al., 2012).	23
Table 2-4: Previous laboratory studies on the effect of gypsum on compaction parameters. ..	29
Table 2-5: Variation of the coefficient of permeability with gypsum content.	31
Table 2-6: Comparison of the compression index (C_c) and swelling index (C_s) values in standard consolidation and oedometer leaching tests of undisturbed samples.	37
Table 3-1: Physical properties of sand.	67
Table 3-2: Particle densities with different of gypsum contents.	69
Table 3-3: Variation in initial void ratios and dry densities through sample preparation.	83
Table 3-4: Gypsum content determined by Al-Mufti and Nashat's (2000) method.	85
Table 3-5: Properties of standard compaction test.	88
Table 3-6: CPs for various gypsum content levels from SOT and DOT.	95
Table 3-7: The severity of collapse according to the value of the CP, as defined by Jennings and Knight (1975).	95
Table 3-8: Data of the UCS test.	112
Table 3-9: Dry density and void ratio for the UCS samples.	114
Table 4-1: Popular electrode arrangements (Samouëlian et al., 2005).	133
Table 4-2: Defining a sequence of electrodes for automated data acquisition.	136
Table 5-1: Water content and gypsum content measurements with depth (with 0 cm taken at the upper surface) for all soil columns at the end of test.	180
Table 5-2: Volume of water for each wetting stage for all cases.	184

FIGURES

Figure 1-1: (a) and (b) Cracks in the walls of a house and historical building (rebuilt three years ago), respectively, due to differential settlement from Al-Najaf city, Iraq (by the author, 2017), (c) and (d) Differential settlement and collapse in a house in Iraq (Awn, 2010), (e) Sinkhole, 500 m downstream from Mosul Dam in Iraq (Salih, 2013), (f) Sinkhole at Ure Bank Terrace, Ripon, UK; the hole formed in April 1997, 10 m across and 5.5 m deep (Cooper, 2007).....	5
Figure 2-1: Gypsum-anhydrite equilibrium (Berner, 1971).	14
Figure 2-2: Equilibrium gypsum/anhydrite as a function of temperature and water vapour partial pressure (P_{H_2O}) for total pressure of 1 bar, according to various authors. (1) and (2) Van Hoff et al. (in Motensen, 1933). (3) Blount and Dickson (1973). The curve $\varepsilon = 100\%$ represents the saturating vapour pressure for a total pressure of 1 bar. The curves $\varepsilon = 75, 50, 30\%$ represent the water vapour partial pressure equivalent to the relative atmospheric moistures ε (Horta, 1980).	16
Figure 2-3: Geological profile along high-speed railway line, Spain (Alonso and Ramon, 2013).....	17
Figure 2-4: Heave profile in August and September 2007 compared with in September 2002, Spain (Alonso and Ramon, 2013).....	18
Figure 2-5: Distribution of gypseous soils in the world (FAO, 1990).	20
Figure 2-6: Hydraulic conductivity over time; (a) Arutyunyan and Manukyan (1982), (b) AlNouri and Saleam (1994) for 25% gypsum content, (c) Namiq and Nashat (2011) upon hydraulic gradient equal to 131.579, (d) Aldaood et al. (2015).	32
Figure 2-7: Typical effect of gypsum content on the CP (AlQaissy, 1989).....	34
Figure 2-8: Swelling index (C_s) versus gypsum content; (1) silty clay gypseous soil (AlNouri and AlQaissy, 1990), (2) silty sand gypseous soil (AlNouri and Saleam, 1994), (3) poorly graded silty sand gypseous soil (Fattah et al., 2012), (4) sandy silt gypseous soil (Ahmed, 2013), (5) sand gypseous soil (Fattah et al, 2015).....	35
Gypseous soils exhibit appreciable secondary consolidation, or creep, which increases with higher applied load, gypsum content, and water content (Seleam, 1988; Alaithawi, 1990; Sirwan et al., 1991; AlNouri and Saleam, 1994; Fattah et al., 2008; Estabrag et al., 2013; Afaj	

and Mohammed, 2018). This phenomenon is ascribed to the continuous dissolution process of gypsum with time and to particle reorientation (Figure 2-9).....	36
Figure 2-9: Total settlement for high plasticity clay soil (CH) with time for different gypsum content during leaching (Estabrag et al., 2013).	36
Figure 2-10: Swell pressure of expansive clay and calcium sulphate phases (Azam et al., 1998).	39
Figure 2-11: Variation of swell pressure with gypsum content (Yilmaz and Civelekoglu, 2009).	41
Figure 2-12: Effect of gypsum content on unconfined compressive strength; (a) sand-gypsum mixture with dry unit weight and gypsum content (GC) from 12 to 19 kN/m ³ and 0% to 20%, respectively (Huang and Airey, 1998), (b) gravely sand with 3%, 6% and 9% gypsum content (Haeri et al., 2005), (c) expansive bentonite soil (Yilmaz and Civelekoglu, 2009), (d) soil-1 (21% clay) and soil-2 (50% clay) with gypsum content from 0% to 40% (Estabragh et al., 2013).	43
Figure 2-13: Effect of soaking period on strength ratio of soaked CBRs relative to unsoaked CBRu for gypseous soils; (1) well graded gypseous silty sand (Razouki and El-Janabi, 1999), (2) well graded silty sand (Razouki and Al-Azawi, 2003), (3) and (4) high plasticity clay (Razouki and Kuttah, 2006), (5) and (6) sandy clay (Razouki et al., 2010). (NB. The force represented in the figure captions are those applied to the samples and GC refers to gypsum content).	45
Figure 2-14: Gypsum map of Iraq (Buringh, 1960).	48
Figure 2-15: Gypsum map of Iraq (Barzanji, 1973).	49
Figure 2-16: Distribution of Permian and Triassic strata and the location of anhydrite and gypsum sites (Bell, 1994).	50
Figure 2-17: Soil profile of the estimated sequence of layers with sinkhole at Ure Bank Terrace (Cooper and Waltham, 1999).	51
Figure 3-1: Map of study area (Al-Anbari et al., 2016)	58
Figure 3-2: Dust storm in the western desert of Iraq (Sissakian et al, 2013).	59
Figure 3-3: Photographs of sedimentary rocks in the Al-Najaf Sea (some of them have cavities) (Aziz, 2008).	60
Figure 3-4: Particle size distribution of sand.	68

Figure 3-5: Air pluviation apparatus; (a) photograph of pluviation apparatus, (b) systematic diagram, (c) shutter with a porosity of 15.84%, (d) diffuser (two-sieves) with 3.35 mm sieve aperture.	76
Figure 3-6: Variations of sand density with FH.	76
Figure 3-7: Gypsum segregation when the mixture is pluviated in dry conditions; (a) gypsum powder on the pipe surface, (b) gypsum powder accumulated around the mould on the tray.	77
Figure 3-8: Steps for sample preparation; (a) oedometer ring preparation, (b) pluviation stage, (c) levelling the sample surface and weighing it to calculate the dry density for the pluviation stage, (d) loading stage, (e) soaking stage, (f) drying stage.	80
Figure 3-9: The initial void ratio and corresponding dry unit weight versus gypsum content for the pluviation stage (stage 1) and the loading, soaking, and drying stages (stages 2, 3, and 4).	81
Figure 3-10: Variation in initial void ratio (e_0) versus initial gypsum content (d_0 , %); sand and clay are referred to by 1 and 2 on the graph, respectively (Petrukhin and Arakelyan, 1984).	82
Figure 3-11: Preparing the batches of sand-gypsum mixtures before starting the test.	87
Figure 3-12: Standard compaction test for various gypsum content.	88
Figure 3-13: Effect of gypsum addition on maximum dry density and optimum moisture content.	89
Figure 3-14: Results from the SOT with inundation upon 200 kPa for 24 hours; (a) 5% GC, (b) 10% GC, (c) 15% GC, (d) 20% GC, (e) 25% GC, (f) 30% GC.	93
Figure 3-15: CP versus gypsum content level in SOT.	95
Figure 3-16: DOT versus SOT for three gypsum content levels; (a) 10% GC, (b) 20% GC, (c) 30% GC.	96
Figure 3-17: CP versus vertical stress in logarithmic scale for three gypsum content levels.	98
Figure 3-18: Standard consolidation test for three gypsum content levels.	100
Figure 3-19: Effect of gypsum content on compression and swelling index.	101
Figure 3-21: Unconfined compression sample steps; (a) mould preparation, (b) loading system, (c) soil pluviated and loaded, (d) soaking by capillary action, (e) left after wetting at lab temperature to drain the water, (f) extraction process, (g) sample after extraction, (h) repeated samples.	107
Figure 3-22: (a) After drying process, (b) Scarifying the upper surface of the layer before pluviating the next layer.	108

Figure 3-23: Behaviour of UCS for single layer versus the curing time for various of gypsum content. It should be noted that curing times are included the draining time (2 days) and drying time in the oven (which are: 1, 3, 7, 14, and 28 days), i.e. the total curing time is: 3, 5, 9, 16, and 30 days.	109
.....	111
Figure 3-24: Deformation response for the three gypsum contents; (a) 10% GC, (b) 20% GC, (c) 30% GC. The labels are categorised as 9 samples, which are presented alongside mean single layer, two layer and four layers samples. The numerical designations of: 1, 2, and 3 refer to the three single layer samples; 4, 5, and 6 refer to the three double layers samples; 7, 8, and 9 refer to three quadruple layers samples. The terms one layer, two layers and four layers refer to mean response for all three of the samples for each gypsum content previously presented (in samples 1-9).	111
Figure 3-25: Distribution of gypsum content in single-layer and multi-layered samples (one layer = 1L, two layers = 2L, and four layers = 4L).	113
Figure 3-26: Behaviour of unconfined compressive strength with; (a) number of layers with different gypsum content, (b) multi-layer samples with gypsum content.	115
.....	116
Figure 3-27: Example of failed samples (NB. The labelling system refers to the gypsum content (%) and number of layers in the sample); (i) 10%, 20%, 30%-1L ‘cured’ for 9 days, (ii) 10%, 20%, 30%-2L with the second layer ‘cured’ for 9 days, (iii) 10%, 20%, 30%-4L with the fourth layers ‘cured’ for 9 days.	116
Figure 3-28: Sample preparation of chilled-mirror dew point technique.	119
Figure 3-29: Chilled mirror hygrometer test (WP4C Dew Point PotentialMeter).	119
Figure 3-30: Sample preparation for the HYPROP technique.	120
Figure 3-31: (a) Vacuum pump stage to remove the air bubbles inside the sensor and unit sensor, (b) Tools to prepare the holes’ sample ((1) auger positioning tool, (2) silicon gasket, (3) HYPROP auger), (c) Placing the auger positioning tool on the sampling ring to do the holes, (d) Two holes for attaching the sensor unit, (e) Set up the HYPROP system.	122
.....	122
Figure 3-32: Composition of the HYPROP test apparatus.	122
Figure 3-33: Drying path; Gravimetric water content with total suction for different gypsum contents (measured by using the chilled-mirror dew point technique).	124

Figure 3-34: Wetting path; Gravimetric water content with total suction for different gypsum contents (measured by using the HYPROP and chilled-mirror dew point techniques).	125
Figure 3-35: Combined drying and wetting paths for the four percentages of gypsum.	125
Figure 3-36: Parameters of total suction SWCCs for various percentages of gypsum (for drying path).....	126
Figure 4-1: Electrode configuration; (left) evaporation cell, (right) settlement tank.	136
Figure 4-2: ER-Acquisition System II (ER-Acq-II).	138
Figure 4-3: Sketch of the evaporation test (NB. This does not depict the ER probes installed in a line up one side of the pipe nor the internal temperature sensors buried at various depths).	139
Figure 4-4: Evaporation cell; (left) photographic picture, (right) schematic view illustrating the layout of the resistivity probes and location of the thermistors.	140
Figure 4-5: Waterproof (DS18B20) probe used to measure soil temperature.	142
Figure 4-6: Data logging of temperature sensors; (a) (top) Arduino board and (bottom) Arduino MEGA prototype shield, (b) the completed ensemble.	142
Figure 4-7: Photograph of pin electrode.	143
Figure 4-8: Steps of sample preparation; (a) installation of the gravel layer, (b) installation of the crushed stones layer, (c) completion of the filter layer with the addition of the punching needle fabric, (d) the layer of soil has been pluviated and the PVC plate has been installed ready for loading (note the notch to ensure the ER probe is not damaged), (e) loading stage, (f) scarifying the surface layer and installing the temperature sensors, (g) the completed gypseous sample after drying and ready for testing.	147
Figure 4-9: Water and gypsum contents of trial samples for 10% and 20% gypsum content before testing.	148
Figure 4-10: Running test. From left to right; soaking the soil by capillary action, starting the test, water tank and temperature controller.	150
Figure 4-11: Sketch of the footing test illustrating the settlement tank and the loading frame.	151
Figure 4-12: Settlement tank; (left) photograph shows the cylindrical tank used as a cell test including the circular and vertical arrangement of the electrodes, (right) schematic view illustrating only the vertical arrangement of the electrodes and location of the thermistors..	152

Figure 4-13: (a) Movable steel cylinder using to transmit the loading from the frame to the footing model, (b) Steel cylinder with both bases, (c) Closer view of the hinge between the small base and steel cylinder.	155
Figure 4-14: (a) Linear displacement sensor (LDS) to measure vertical displacement of footing, (b) The four channels connection side, (c) USB connection attached to the PC via a cable.....	156
Figure 4-15: Filter and soil formation steps; (a) gravel layer, (b) crushed stones layer, (c) punching needle fabric, (d) pluviated and loading stages, (e) wetting stage, (f) two temperature sensors installed over each new layer.....	158
Figure 4-16: Water and gypsum contents profiles of the trial sample for 20% gypsum content before testing.	159
Figure 4-17: Photograph of the test setup; (left) test in laboratory conditions (without heat and breeze), (right) test with heating and breeze sources.....	162
Figure 4-18: Calibration of the electrodes; (a) evaporation cell, (b) settlement cell.....	164
Figure 4-19: McMiller resistivity box.	165
Figure 4-20: Resistivity variation with temperature ranging 14-47°C.	167
Figure 5-1: Running test. From left to right; soaking the soil by capillary action, starting the test, water tank and temperature controller.	170
Figure 5-2: Time evolution of cumulative evaporation in manufactured gypseous soil columns with 10% and 20% gypsum contents.....	171
Figure 5-3: The drop daily in water height within the water tank during the whole experiment for 10% and 20% gypsum content.....	173
Figure 5-4: Variation in temperature and ER for; (a) 10% GC-Sample 2, (b) 10% GC-Sample 1. (NB. All these distances start from the surface of the soil; D/2: at centre of sample (7.2 cm); D/4: at distance 3.6 cm from cell wall).	174
Figure 5-5: Variation in temperature and ER for; (a) 20% GC-Sample 2, (b) 20% GC-Sample 1. (NB. All these distances start from the surface of the soil; D/2: at centre of sample (7.2 cm); D/4: at distance 3.6 cm from cell wall).	175
Figure 5-6: Profile of water content, gypsum content, temperature and ER along the soil column at the end of the test with 10% gypsum content, the first sample (10% GC-1) investigated without ER, while the second sample (10% GC-2) tested with ER.....	178

Figure 5-7: Profiles of water content, gypsum content, temperature and ER along the soil column at the end of the test with 20% gypsum content, the first sample (20% GC-1) investigated without ER, while the second sample (20% GC-2) tested with ER.	179
Figure 5-8: Stress-settlement relationships of the foundation settled on dry manufactured gypseous soils (with 20% gypsum content).	185
Figure 5-9: Vertical displacement of footing during wetting over time for Case 1. (NB. Ch1, Ch2, Ch3, and Ch4 refer to the channel numbers for the LDS sensors).	187
Figure 5-10: ER values along soil deposit during wetting over time for Case 1. (NB. A and B refer to the arrays, number refers to the depth of ER value from the soil surface).	187
.....	188
Figure 5-11: Temperature variation along soil deposit during wetting with time for Case 1. (NB. All these distances start at the surface of the soil; D/2: at centre of sample; D/4: at distance 8.73 cm from cell wall).	188
Figure 5-12: Photographs showing the footing failure in Case 1.	188
Figure 5-13: Salty spot on the soil surface after drying process.	189
Figure 5-14: Water and gypsum contents and temperature profiles over depth after failure for Case 1.	191
Figure 5-15: Vertical displacement of footing during wetting over time for Case 2. (NB. Ch1, Ch2, Ch3, and Ch4 refer to the channel numbers for the LDS sensors).	193
Figure 5-16: ER values along soil deposit during wetting over time for Case 2. (NB. A and B refer to the arrays, number refers to the depth of ER value from the soil surface).	193
Figure 5-17: Temperature variation along soil deposit during wetting with time for Case 2. (NB. All these distances start at the surface of the soil; D/2: at centre of sample; D/4: at distance 8.73 cm from cell wall).	194
Figure 5-18: Photographs of the soil surface before and after the failure for Case 2; (a) salt over the soil surface when water approached the upper layer, (b) and (c) punching shear and cracking around the footing model.	194
Figure 5-19: Water and gypsum contents and temperature profiles over depth after failure for Case 2.	195
Figure 5-20: Vertical displacement of footing during wetting over time for Case 3. (NB. Ch1, Ch2, Ch3, and Ch4 refer to the channel numbers for the LDS sensors).	197

Figure 5-21: ER values along soil deposit during wetting over time for Case 3. (NB. A and B refer to the arrays, number refers to the depth of ER value from the soil surface).	197
Figure 5-22: Temperature variation along soil deposit during wetting with time for Case 3. (NB. All these distances start at the surface of the soil; D/2: at centre of sample; D/4: at distance 8.73 cm from cell wall).	198
Figure 5-23: The profile of failure of Case 3; (a) first crack after 24 hours after adding 8 litres (W4), (b) and (c) close view for the final failure, (d) failure after switching off the heating system, (f) the area under the footing, (d) the duricrust around the footing area.	198
Figure 5-24: Water and gypsum contents and temperature profiles over depth, after failure for Case 3.	200
Figure 5-25: Single and double oedometer test for 20% gypsum content.....	202
Figure 5-26: Post-testing gypsum content profiles for initial gypsum contents of 10% (left) and 20% (right) (both repeated twice) (previously presented in Figures 5-6 and 5-7), after 40 days of testing.	204
Figure 5-27: Schematic presentation of settlement depth, groundwater level (GWT), and stress bulb for each case (Case 1= 45.13 kPa at settlement 40.7 mm and water content (WC)= 18.7%, Case 2= 47.4 kPa at settlement 38.7 mm and WC= 16.8%, and Case 3= 77.1 kPa at settlement 12.2 mm and WC=7.2%).	206
Figure 5-28: Gravimetric water content versus total suction for 20% gypsum content.	207

ABBREVIATIONS AND SYMBOLS

α	Temperature correction factor
Δe	The change in void ratio
ρ	Electrical resistivity
ρ_{dmax}	Maximum dry density
ρ_{dmin}	Minimum dry density
ϕ'	Effective internal of angle
AEV	Air-entry value
C_c	Compression index (compression testing)
C_c	Coefficient of curvature (classification testing)
CBR	California bearing ratio
CP	Collapse potential
C_s	Swelling index
C_u	Coefficient of uniformity (classification testing)
c'	Effective cohesion
DOT	Double oedometer collapse potential test
D10	Particle diameter corresponding to 10% passing
D30	Particle diameter corresponding to 30% passing
D50	Particle diameter corresponding to 50% passing
D60	Particle diameter corresponding to 60% passing
EC	Electrical conductivity
e_d	Void ratio of the dry sample at a given load step
e_{max}	Maximum void ratio
e_{min}	Minimum void ratio

e_s	Void ratio of the saturated sample at a given load step
e_0	Initial void ratio
FD	Falling distance: the depth between shutter and the diffuser
FH	Falling height; the depth between diffuser and sample
GC	Gypsum content (%)
G_s	Particle density
K	Geometric factor
LDS	Linear displacement sensor
OMC	Optimum moisture content
R	Electrical resistance
SOT	Single oedometer collapse potential test
SP	Poorly graded sand (under USCS)
SWCC	Soil water characteristic curve
UCS	Unconfined compressive strength
USCS	Unified soil classification system

CHAPTER ONE

INTRODUCTION

1.1 Introduction

Gypseous soils are distributed in many regions in the world, including arid and semiarid areas, accounting for more than 20% of the soil in Iraq (Al-Mufti, 1997). These soils constitute a significant geohazard in Iraq as they can be metastable having open structures stabilised by gypsum crystals, this causing many engineering problems related to construction in, or above these soils. The main cause of said problems is softening with changing water contents this causing dissolution of the gypsum.

Gypseous soil is typically stiff and strong when it is dry because of the cement-like bond between soil particles by gypsum crystals. However, it undergoes a substantial decrease in stiffness, strength and a sudden increase in compressibility when this soil experiences a change in water content resulting in an increase in saturation. The dissolution of cementing gypsum, results in a loss of solids, the softening of the soil structure resulting in a loss of strength. This can cause the collapse of gypseous soil under loading (Seleam, 1988; Al-Ani and Seleam, 1993; Al-Farouk et al., 2009; Ahmad et al., 2012; Aldaood et al., 2015).

Obtaining undisturbed samples of gypseous soil is, in many cases, very difficult. This has led to many researchers attempting (with various degrees of success) to manufacture gypseous soils in the laboratory. The behaviour of a gypseous soil in the laboratory is dependent upon a number of factors, including whether the soil was originally gypseous or prepared by adding

gypsum to soil that did not contain gypsum and whether the soil is undisturbed, disturbed or compacted. In addition, the initial water content, void ratio and gypsum content of manufactured samples play essential roles in directing the engineering behaviour of such soils. The laboratory behaviour may also be controlled by other factors such as the type of the soil constituents, test conditions and test type. As such, the development of a method that creates a gypseous soil with similar properties to that encountered in situ, and having the ability to apply environmental and loading conditions that also approximate conditions on site, are of key importance.

1.2 Need and Motivations of the Research

All civil engineering structures are founded directly, or indirectly, on the ground, therefore, the stability of both super-and subsurface structures depends on the stability of the ground, this a locality specific issue (Fang, 1997). In general, all structural design is based on loads. However, design criteria dependent on load factors alone does not give the whole picture, neglecting the other important factors that control the overall stability of civil engineering structure: environmental design criteria. For example, metastable gypseous soils in arid ground conditions are sensitive to factors in the local environment such as temperature, water content and water movement as well as the changing nature of pore fluids in soil voids. These will all impact significantly on soil behaviour because gypsum dissolution is strongly related to environmental conditions such as groundwater movement and the presence of other dissolved salts (such as sodium chloride) in pore fluid as well as the temperature of pores. Environmental changes may influence the geotechnical characteristics of gypsum crystals within the soil, for example is mechanical properties, crystal structures and stress-strain responses over time (James and Lupton, 1978; James and Kirkpatrick, 1980; Gumusoglu and

Ulker, 1982; Fooks et al., 1985; Klimchouk, 1996; Ahmed, 2013). The anhydrite-gypsum cycle is also dramatically influenced by environmental conditions including humidity, air temperature and water, these resulting in detrimental effects to foundations (i.e. swelling or shrinkage due to gypsification of anhydrite or dehydration of gypsum, respectively) (Blatt et al., 1980; Zambak and Arthur, 1986; Yilmaz, 2001; Sievert et al., 2005). Furthermore, the formation and redistribution of gypsum in the soil profile is significantly influenced by groundwater, rainfall, evaporation and capillary action (Akili and Torrance, 1981; Fookes et al., 1985; Furley and Zouzou, 1989; Chen, 1997; Royal, 2012). Consequently, environmental factors play an important role when considering gypseous soil responses in arid areas. This is all in addition to the load response of these gypseous soils, usually stiff and very low compressibility in their dry state due to the cementing action provided by the gypsum (Akili and Torrance, 1981; Fooks et al., 1985). Dissolution of gypsum in arid (often aeolian) deposits, has caused difficult civil engineering conditions throughout the world as illustrated in Table 1-1.

Alongside the economic losses caused by gypsum dissolution, fatalities are also recorded. These post-dissolution problems are related to soil collapse, increasing hydraulic conductivities which may result in increased seepage rates, softening of the soil, the creation of cavities or sinkholes and sulphate attacks on concrete (Figure 1-1). All these problems are correlated to the gypsum dissolution by seeping water through the gypsum-rich soil (James and Lupton, 1978; Arutyunyan and Manukyan, 1982; Klimchouk, 1996; Livneh et al., 1998; Azam, 2000; Cooper and Saunders, 2002; Razouki and Ibrahim, 2007; Razouki et al., 2007; Sajedi et al., 2008; Fattah et al., 2012; Estabragh et al., 2013; Aldaood et al., 2015). Water entering the soil and changing its water content, may originate from leaking infrastructure

(water pipes, sewers, heating, irrigation, etc.), groundwater level changes and surface water movements.

Table 1-1: Problems which occurred for structures constructed on gypseous soil.

Reference	Observations
Ransome (1928)	The dissolution of conglomerate cementing by gypsum in the Saint Francis dam at Los Angeles, destroyed the dam, killing more than 400 people.
Redfield (1963)	Due to the anhydrite-gypsum cycle, the concrete lining in the Vobarno Tunnel, Italy suffered heave, fractures and cracking.
Brune (1965)	The McMillan Dam, New Mexico suffered damaged due to seepage and collapse of gypsum karst on the left side of the dam.
Lee et al. (1984)	A foundation crack related to soil differential settlement, appeared in an apartment building in Syracuse University. Gypsum dissolution created cavities which then collapsed under its foundations.
Cooper (1989)	Ground collapse cause by gypsum dissolution, created hollow subsidence (10–80 m diameter and 30 m depth) in the Ripon area, England.
Saaed et al. (1989)	A modern, 400 dwelling village, Saudi Arabia, was severely damaged due to unequal and excessive settlement of the gypseous foundation soil. In Iraq, Karbala city's elevated water tank overturned and fell due to differential settlement caused by the water percolating into the gypseous base.
Nashat (1990)	Mosul dam, Iraq, was constructed on gypseous rocks. Continuous grouting using cement to replace the dissolving gypsum underneath the dam costs thousands of dollars annually. Cavities can be up to 50 m below the surface, some in critical locations with the dam facility.
Abduljawwad (1993)	Damage to structures and pavements in Eastern Saudi Arabia is due to heaving caused by the hydration of anhydrite.
Sissakian and Al-Mousawi (2007)	Some of the Baiji Electric Power Station north of Baghdad, Iraq, is constructed over highly gypseous soil. Its water treatment facilities have caused continuous subsidence due to the development of surface and subsurface karst features because of dissolving gypsum. The subsidence has decreased the efficiency of the station.
Pando et al. (2013)	In Oviedo, Spain, during excavation works for an underground parking lot, two buildings of 362 flats were threatened by structural collapse, resulting in losses of 18 million euros due to the appearance of sinkholes over the gypsum layer. Water pumped from a confined aquifer, related to excavation work during construction, modified the natural hydrological regime and thus water leaching gypsum from soil.
Kadhim (2014)	In Iraq, severe cracking and premature loss of serviceable pavements constructed on gypseous soil subgrade.



Figure 1-1: (a) and (b) Cracks in the walls of a house and historical building (rebuilt three years ago), respectively, due to differential settlement from Al-Najaf city, Iraq (by the author, 2017), (c) and (d) Differential settlement and collapse in a house in Iraq (Awn, 2010), (e) Sinkhole, 500 m downstream from Mosul Dam in Iraq (Salih, 2013), (f) Sinkhole at Ure Bank Terrace, Ripon, UK; the hole formed in April 1997, 10 m across and 5.5 m deep (Cooper, 2007).

In Iraq, roads, pipelines, sewers, canals and irrigation channels, all require routine repairs for failures caused by the continuous dissolution of gypsum which results in subsequent softening of the soil, or in the development of sinkholes (Sissakian and Al-Mousawi, 2007). Leaking pipes in, or close to, buildings may also cause total or differential settlements (AlNouri and Saleam, 1994; Ahmed, 2013). As such, the application of geotechnical interventions in these soils requires an understanding of the response of the soil under likely loading and environmental conditions. Undertaking such tests in situ, is problematic; laboratory testing is preferable. However, as noted above, manufacturing gypseous soils in the laboratory is yet to be perfected. Testing under conditions likely to be encountered in hot arid environments has also lacked due attention, these points forming the focus of this study.

1.3 Key Knowledge Gaps

Previous research has investigated the effects of physical and environmental factors of arid gypseous soil, including the soaking, wetting-drying cycle, thawing-freezing and leaching on the collapse, compressibility, creep and shear strength, using standard apparatus such as the oedometer, triaxial, California Bearing Ratio (CBR), Unconfined Compressive Strength (UCS) and direct shear (Arutyunyan and Manukyan, 1982; AlNouri and AlQaissy, 1990; Livneh et al., 1998; Razouki and El-Janabi, 1999; Azam, 2000; Razouki and Kuttah, 2006; Razouki and Ibrahim, 2007; Razouki et al., 2007; Sajedi et al., 2008; Estabragh et al., 2013; Aldaood et al., 2015; Fattah et al., 2015). However, small-scale experimentation, focusing on the relative changes in small samples via what is effectively parametric studies, do not comprehensively inform engineers how soil deposits will respond in more complex, realistic conditions. The behaviour of foundations in this material is poorly understood, with little research focused on this area. This is specifically the case where the soil is partially covered

by a floor above the foundation, resulting in exposure of the soil to differential surface temperatures between covered and uncovered ground surface, and thus potentially preferential groundwater movements towards the surface. It would appear that groundwater movement under thermal gradients through these soils, has not been investigated in the laboratory. This will form the main operationalised focus of this study: to develop a technique to manufacture reproducible gypseous soil samples of different sizes, in the laboratory. This study will also monitor the motion of groundwater and the migration and precipitation of gypsum in the capillary fringe as a response to heat, and how this motion could influence settlement of foundations. Trail electrical resistivity (ER) as a non-destructive monitoring method (see further details in Chapter Four), will be used to determine if changes in water content and gypsum content can be observed since water seeps vertically upwards through a soil column under a thermal gradient. The potential for using this approach to monitor gypseous soil under loading and environmental conditions, has not been considered to date.

1.4 Aim and objectives

To address key gaps in knowledge, the main aim of this research is to develop an understanding of the effect of environmental conditions (groundwater movement under thermal gradients and surface breezes) on manufactured gypseous samples, including those under simulated foundation loadings.

To meet this, aim the following objectives are proposed:

- 1) To develop a method to manufacture reproducible, gypseous soils in the laboratory that allows for the creation of samples of varying sizes, from oedometer sized samples to samples over 349 mm in diameter. This will involve producing samples with parameters

that approximate those of soils investigated in situ, and undertaking a parametric analysis to confirm samples can be re-created while retaining the same properties.

- 2) To develop a bespoke experimental apparatus that will allow:
 - i. Study of the movement of groundwater and the dissolution and precipitation of gypsum within gypseous soil columns experiencing various combinations of the modelled ‘evaporation mechanisms’: application of temperature gradient, simulated breeze across the upper surface and unsaturated fluid flow vertically upwards from a water table near the base of the sample.
 - ii. Study of the behaviour of the metastable soil under loading of a simulated shallow (pad) foundation, with and without environmental conditions (above).
- 3) To deploy an electrical resistivity array to determine if changes in fluid flow and dissolution/precipitation of the gypsum, in association with the ‘evaporation mechanism’, can be observed during a non-destructive test in order to confirm final water content and gypsum content profile, post-test, using sampling.

1.5 Thesis Organization

The overall structure of this thesis takes the form of six chapters, including this introductory chapter, the remainder are summarised below:

- **Chapter Two: Literature Review.** This chapter considers the existence, formation, distribution and dissolution of gypseous soils. A general review of the types of engineering problems related to construction on gypseous soils and the ways to classify

these soils, are also given. This chapter also reviews the physico-chemical behaviour of gypsum and aspects of the physical properties of gypsum bearing soils, outlining the areas of geotechnical performance that are still poorly understood/addressed using conventional techniques.

- ***Chapter Three: Manufacturing Gypseous Soil and Validation Test.*** This section details the sample manufacturing process (four stage pluviation), developed for this study. This includes the materials selected (sand and gypsum) to manufacture gypseous soil in the laboratory, and the classification properties of these materials. The preparation of sand-gypsum mixtures and their resulting index properties are presented. This chapter discusses the factors that effect the design of the pluviation apparatus which in turn, impacts the dry density achieved. Validation tests are reported, including the details of the devices used, sample preparation, test procedures and calculations. The analyses of results and discussion for these series of standard conventional tests are also included. These tests comprise standard compaction tests, oedometer tests, unconfined compressive tests and suction tests, including wetting and drying paths.

- ***Chapter Four: Bespoke Experiments: Sample Creation and Cell Development.*** This chapter describes the development of bespoke tests: the evaporation and footing tests, providing details of the design and description of a bespoke test arrangement and the justification for the decisions made. It also includes the description of the experimental apparatus, experimental set up, soil formation, tests programme and procedures for running the tests. Details on the design of the resistivity cells which were developed and

the full progress of the test procedure, including calibration tests and data processing, are also included.

- ***Chapter Five: Experimental Results and Discussion.*** This chapter presents the findings and discussions of the research, focusing on the three key themes concerning the response of the soil to changes in environmental conditions (application of temperature gradient, simulated breeze across the upper surface and unsaturated fluid flow vertically upward from a water table near the base of the sample), the change in response of the soil under a simulated foundation load with and without these environmental conditions, and the observed changes in geophysical properties using ER. It also considers the observed data, and discusses the potential correlation between geotechnical and geophysical changes in the soil properties.

- ***Chapter Six: Conclusions and Recommendations.*** Here, a summary of the conclusions derived from this research and the recommendations for further researches are presented.

CHAPTER TWO

LITERATURE REVIEW

2.1 Introduction

In this chapter, an extensive literature review has been conducted to give a comprehensive understanding of soils containing gypsum. The literature explored features topics and arguments that would benefit from further research and justification, and has helped to clarify the aims and objectives of the project.

2.2 Gypseous Soil

Gypseous soils predominantly form under geomorphological processes associated with hot, dry lands, reflecting the influence of both geological and climatic factors (Buringh, 1960; Fookes, 1976; Tomlinson, 1978; Porta and Herrero, 1990; Chen, 1997; Herrero and Porta, 2000; Royal, 2012). While they are common in many countries, deposits of gypseous soils in temperate and wetter climates are relatively small and confined to deeper geological formations that were formed during past geological epochs when climates were hot and dry (Horta, 1980; Boyadgiev and Verheye, 1996; Cooper and Waltham, 1999; Herrero and Porta, 2000; Czerewko et al., 2006). The characteristics of these soils are heavily influenced by the extent to which gypsum is distributed throughout the soil profile as the result of hydrogeological cycles, i.e. rainfall and infiltration; groundwater movements; and evaporation, which results in the dissolution and reprecipitation of gypsum crystals within the soils (AlNouri and AlQaissy, 1990; Royal, 2012). Therefore, it might be argued that the accumulation (and subsequent redistribution) of gypsum within the soil profile correlates

more strongly with the hydrogeological regime than to ground-air temperature regime. As a consequence, the soils with high gypsum percentages are concentrated in the aridic and xeric moisture regimes (Watson, 1983; FAO, 1990).

Gypseous soils present significant problems to engineers because of the chemically active and metastable nature of the ground conditions associated with such soils. For example, problems created by the chemical changes in the calcium sulphate crystals within gypseous soils (arising from interactions with water) are settlements (which can be very rapid, and difficult to predict beforehand) caused by the dissolution of the crystals, heave caused by hydration of anhydrite crystals to gypsum crystals, and the chemical weathering of concrete with the release in sulphate ions (Fookes et al., 1985; Akili, 2006).

2.2.1 Properties of Gypsum as a Mineral within Soil

The name gypsum is given to the hydrated calcium sulphate mineral ($\text{CaSO}_4 \cdot 2\text{H}_2\text{O}$) and to the rocks that are formed by this mineral. Gypsum exists in different forms within soil deposits; the form encountered depends on the morphology, origin, purity, shape, and crystallization mode of the gypsum crystals as well as the climatic and formation factors of the host soil (Chen, 1997; Poch et al., 2010). Accordingly, gypsum can be found in many forms, varying from soft, powdery, well-developed crystals to sand-like textures, rock fragments, or crusts (Verheye and Boyadgiev, 1997; Poch et al., 2010; Yamnova and Pankova, 2013). Based on the crystal morphologies of the gypsum, there are various terms that are commonly used to describe gypsum crystals in soils and sediments of arid and semiarid regions, namely: lenticular, acicular, prismatic, tabular, and hemi-bipyramidal. The lenticular habit or ‘spindle’ shaped crystals have been described by many authors and are considered the most common

morphology of gypsum in soils (Watson, 1979; Herrero and Porta, 1987; Eswaran and Gong, 1991; Jafarzadeh and Burnham, 1992; Chen, 1997). The morphology of lenticular gypsum occurs as single crystals or as crystal intergrowths, as in the case of desert rose, and can also form as massive crystallizations. The formation of acicular crystals in soil is relatively rare, although if adequately confined (along with other factors (Eswaran and Gong, 1991)) acicular or tabular forms of gypsum can occur. Moreover, gypsum can be found in pockets or isolated strata dispersed in the soil in lamellar, selenite, alabaster (fine-grained, usually massive), stain spar (fibrous gypsum), or clustered together to form a flower-like shape called a desert rose (Mashali, 1986).

The temperature of formation can influence the structure of the calcium sulphate crystals: between 0°C and 65°C, gypsum ($\text{CaSO}_4 \cdot 2\text{H}_2\text{O}$) is formed. As temperature increases, water is driven from the crystals, thus the gypsum can be transformed into hemihydrate (bassanite) ($\text{CaSO}_4 \cdot 0.5\text{H}_2\text{O}$) at 70°C. From approximately 95°C, the hemihydrate completely converted to anhydrite (CaSO_4). Hence, calcium sulphate crystals can be found in three chemical forms in natural soils, although gypsum is the dominant form (Horta, 1980; Klein and Hurlbut, 1985; Solis and Zhang, 2008). Table 2-1 presents the chemical proportions of the gypsum and anhydrite compounds.

Table 2-1: Chemical proportions of gypsum and anhydrite (Klein and Hurlbut, 1985).

Mineral type	CaO %	SO ₃ %	H ₂ O %
Gypsum	32.6	46.5	20.9
Anhydrite	41.2	58.8	0

The gypsum mineral has a particle density of approximately 2.32, a monoclinic crystallography and hardness value of 2 (i.e. a soft crystal) on the Mohs scale, and a perfect

cleavage parallel to the side faces of the crystal (Klein and Hurlbut, 1985). In massive compact forms, it is likely that no cleavage can be seen, while fibrous gypsum cleaves parallel to the fibers (Klein and Hurlbut, 1985). Pure gypsum may be colourless or white, although red, grey, and brown crystals have been encountered, and these are due to impurities within the crystal structures. In contrast, the anhydrite mineral (CaSO_4) has a particle density of approximately 2.96, an orthorhombic crystallography, a rectilinear cleavage, and a hardness value of 3 to 3.5 (Klein and Hurlbut, 1985). Anhydrite changes to gypsum if it is exposed to air and water.

2.2.2 The Gypsum-Anhydrite Cycle

The variation of calcium sulphate crystals comes about as a result of the activity of water (the relative humidity expressed in decimal fractions) and the temperature of the system, as shown in Figure 2-1 (Berner, 1971). Thus, decreasing the activity of water, decreases with temperature at which anhydrite becomes the stable species.

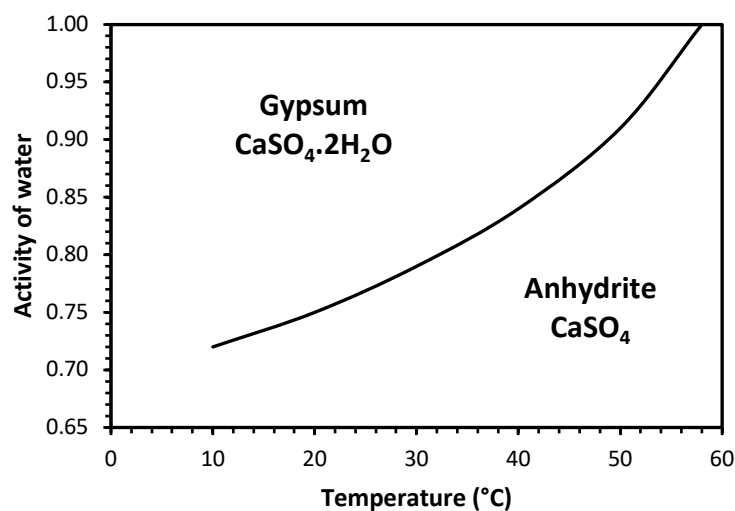


Figure 2-1: Gypsum-anhydrite equilibrium (Berner, 1971).

Gypsum is more abundant in Earth's crust than anhydrite (Krauskopf, 1979), although at depth anhydrite appears to form from the gypsum due to the increased heat and pressure (when compared to the conditions where gypsum is formed), resulting in the dehydration of the gypsum. Dehydration of gypsum involves a reduction in the volume of the crystal structure (estimated loss of at least 38%), which may result in further settlement of the overlying structures (Zanbak and Arthur, 1986). In contrast, upon hydration, the transition of anhydrite to gypsum is associated with an approximate volume increase of around 60% with respect to the original volume of the anhydrite crystals (Holiday, 1978; Blatt et al. 1980; Yilmaz, 2001), and this will exert swell pressures (Brune, 1965). Sievert et al. (2005) found that temperature significantly affects the hydration process of anhydrite crystals; the required time for the hydration of anhydrite to form gypsum at 40°C is double that which is required at 10°C. It has also been observed that the anhydrite-gypsum cycle usually results in a loss of the original primary textures, with new secondary variants being formed instead (Horta, 1980).

Horta (1980) indicated the equilibrium curves for gypsum as a function of temperature and water vapor partial pressure for a total pressure of 1 atmosphere (1 bar) (Figure 2-2). Gypsum is stable at low temperatures and at high water vapor pressures, whereas anhydrite is stable under the opposite conditions. Horta (1980) illustrated that gypsum encountered in the Sahara Desert in Algeria becomes unstable during summer periods due to this relationship; potentially resulting in the pavements cracking.

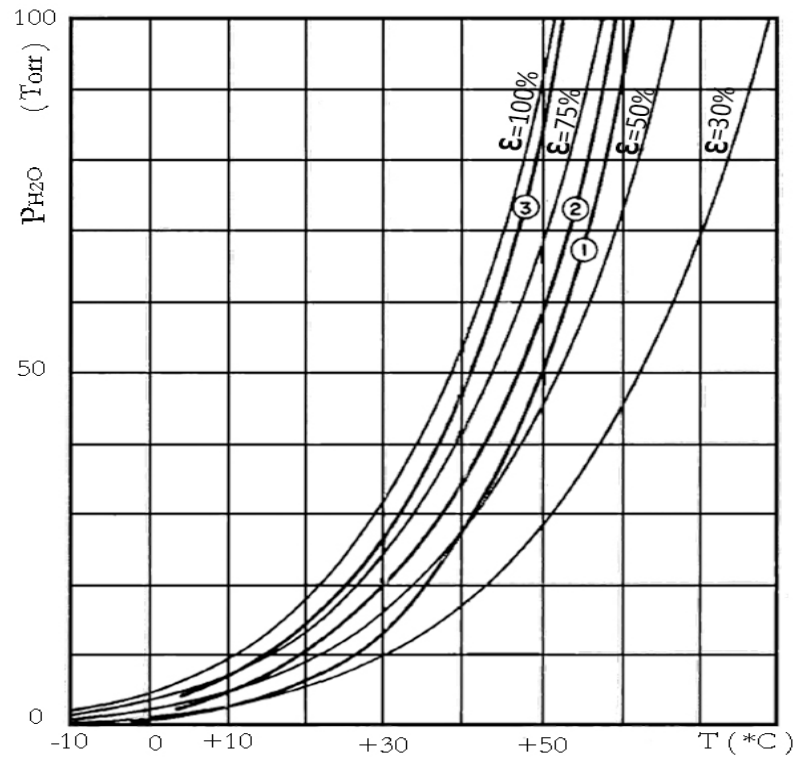


Figure 2-2: Equilibrium gypsum/anhydrite as a function of temperature and water vapour partial pressure (P_{H_2O}) for total pressure of 1 bar, according to various authors. (1) and (2) Van Hoff et al. (in Motensen, 1933). (3) Blount and Dickson (1973). The curve $\varepsilon = 100\%$ represents the saturating vapour pressure for a total pressure of 1 bar. The curves $\varepsilon = 75, 50, 30\%$ represent the water vapour partial pressure equivalent to the relative atmospheric moistures ε (Horta, 1980).

2.2.2.1 Example of Civil Engineering Challenges Encountered with the Anhydrite to Gypsum Conversion

(Alonso and Ramon, 2013) reported heave encountered on a bridge constructed for a high-speed railway on ground containing both gypsum and anhydrite in Spain (Figure 2-3). The total vertical heave of the central pillars exceeded 370 mm since the end of bridge construction (2001-2002) (Figure 2-4) and this was attributed to the swelling associated with anhydrite transforming into gypsum. A subsequent ground investigation suggested that the

installation of boreholes and the piles during construction created a hydraulic connection of upper aquifers (alluvium) with the lower anhydritic formation, resulting in a 12 to 15 m thick active zone below the pile bases (Figure 2-3) (no heave was detected in gypsum-rich claystones traced over the anhydritic layer). To reduce movements a 33 m embankment was constructed over the affected area of the valley floor. However, concern was raised that the ground movements might not have ceased in the longer term as it is believed that a secondary reaction involving the dissolution of the newly formed gypsum might result in long-term settlement (Alonso and Ramon, 2013).

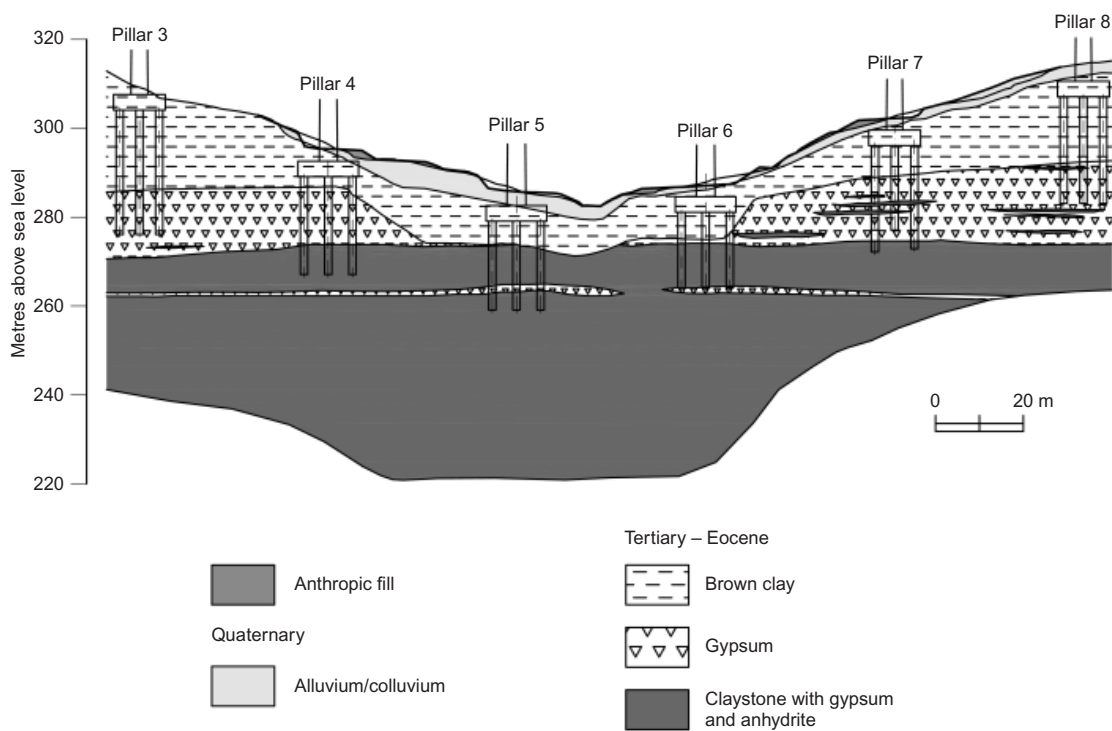


Figure 2-3: Geological profile along high-speed railway line, Spain (Alonso and Ramon, 2013).

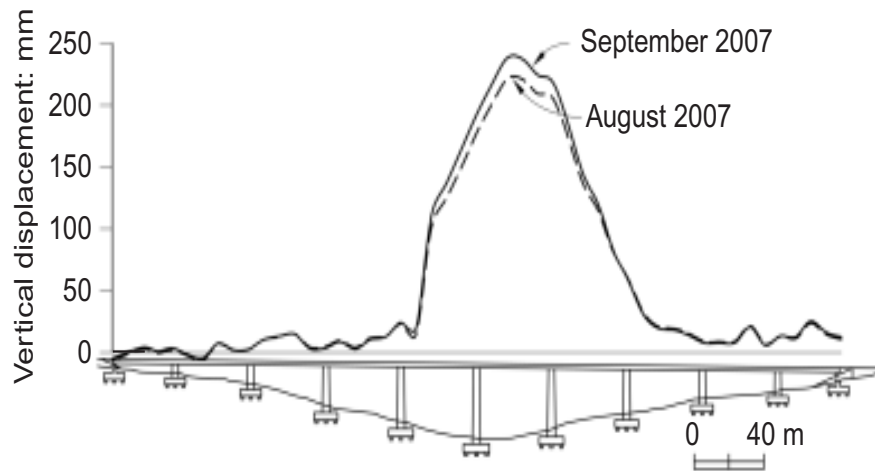


Figure 2-4: Heave profile in August and September 2007 compared with in September 2002, Spain (Alonso and Ramon, 2013).

2.2.3 Formation of Gypseous Soil

There are two ways in which gypsum forms in soils and rocks: the pedogenetic mechanism and the geogenetic mechanism (Van Alphen and Romero, 1971; Yamnova and Pankova, 2013). The pedogenetic phenomenon is the translocation and deposition of gypsum in a soil profile, resulting from infiltrating rainwater or evaporation and capillary rise (Van Alphen and Romero, 1971). The pedogenetic mechanism entails the formation of secondary gypsum in the soil due to the accumulation of gypsum crystals transported into the soil from other sources. An arid climate (a climate with a temperature higher than 20°C and a yearly rainfall lower than 400 mm) and an external source of gypsum are essential to the formation of gypsum in the soil deposit (Al-Mufti, 1997). This pedogenetic process of secondary gypsum forming in the soil is distinguished by several actions: dissolution from primary rocks (Buringh, 1960; Nafie, 1989), evaporation of groundwater containing dissolved calcium sulphates (Fookes et al., 1985; Furley and Zouzou, 1989), aeolian deposition of gypsum (Buringh, 1960; Akili and Torrance, 1981; Taimeh, 1992), and ion exchange between existing minerals and those in the pore water. It is worth mentioning that in all pedogenetic formations

of gypsum, seepage and evaporation of groundwater within the soil are required to achieve the redistribution of gypsum in the soil profile (Verheye and Boyadgiev, 1997).

Conversely, geogenetic processes include those of the diagenetic type (i.e. gypsum formed in place). These can be summarized as the weathering of gypsum-bearing rock (Nafie, 1989; Boyadgiev and Verheye, 1996), the evaporation of sea water, the chemical origins of gypsum (parent rocks that are rich in sulfur compounds, such as pyrite; upon oxidation, sulfuric acid is formed, which subsequently reacts with the calcite abundant in the rock to form gypsum) (Barzanji, 1973; Krauskopf, 1979; Taylor and Cripps, 1984), and the dolomisation of calcite (Krauskopf, 1979; Yamnova and Pankova, 2013).

2.2.4 Distribution of Gypseous Soils in the World

Gypseous soils, commonly encountered in semiarid and arid regions (where precipitation is insufficient to leach the calcium sulphate salts from the soil profile), are concentrated in Africa and central and southern Asia (Boyadgiev and Verheye, 1996). Whilst predominantly found in the aforementioned regions, these soils can also be encountered in Europe, central and south America, Australia, and countries of the former USSR (FAO, 1990). Figure 2-5 shows the distribution of gypseous soil in the world (FAO, 1990). In addition to those regions, many authors refer to the presence of gypsum in the UK, such as in the Cardiff area of Wales (Hawkins and Pinches, 1987) and in Ripon, North Yorkshire (Bell, 1981; Cooper, 1988).

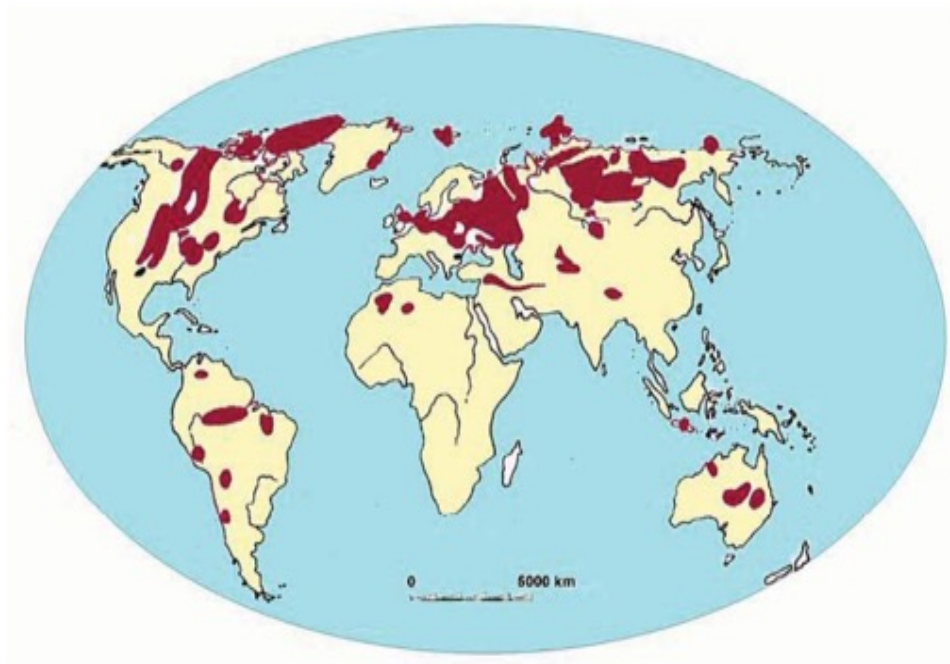


Figure 2-5: Distribution of gypseous soils in the world (FAO, 1990).

2.2.5 Summary of the Variation in Terminology Used when Attempting to Describe Soil Deposits Containing Gypsum

Geologists have developed classification systems to describe soils containing gypsum. Unfortunately, historically at least, more than one has been developed and used, leading to potential confusion. Furthermore, there are historical terms (such as gypseous) that predate these classification systems that are still used, erroneously or otherwise; or the classification terms are incorrectly applied, adding to the potential for confusion.

Terms used in classification of these soils can be found in the scientific literature (e.g. Spaargaren, 1994; FAO, 1998; Soil Survey Staff, 1998), and include ‘gypsic’, ‘petrogypsic’, ‘hypergypsic’, and ‘gypsiric’. A gypsic horizon refers to the subsurface diagnostic horizon that is enriched with secondary calcium sulphate. It is weakly cemented and occurs within 1 m of the surface, with a minimum thickness of approximately 15 cm, and contains at least 5%

more gypsum than the underlying layer (Spaargaren, 1994; FAO, 1998; Soil Survey Staff, 1998). A petrogypsic horizon is defined as a gypsic horizon with high gypsum content, typically greater than 60% (Boyadgiev and Verheye, 1996; Chen, 1997; Herrero, 2004), and is strongly cemented with gypsum and constitutes hard and massive accumulations (Barzanji, 1973; Nafie, 1989; FAO, 1998; Soil Survey Staff, 1998). ‘Hypergypsic’ describes a gypsum accumulation with high content, while ‘gypsiric’ can be applied to materials whose genesis is uncertain but has notable gypsum content (e.g. Spaargaren, 1994; FAO, 1998). Gypsum encrustation is a consolidated gypsum crust formed due to excessive evaporation and low rainfall in semiarid and arid regions that have high temperatures, relative humidity near 45%, and a highly gypsic sub-layer.

Additional terms include gypseous and gypsiferous, which are commonly used for soils containing gypsum, yet the actual meanings are less well defined. The suffixes ‘-eous’ and ‘-ferous’ mean ‘given to’, ‘abounding in’, and ‘full of’, and ‘conveying’, ‘bearing’, ‘producing’, ‘containing’, and ‘yielding’, respectively (Portland House, 1989; Merriam–Webster, 1994). Nevertheless, the term ‘gypseous’ (used after 1661) predates gypsiferous (used after 1799). The term ‘gypseous’ is more appropriate than gypsiferous for soils containing gypsum as a major soil component, especially in aridic and xeric climates (Herrero and Porta, 2000; Herrero et al., 2009; Lebron et al., 2009). On the other hand, the term ‘gypsiferous’ possibly arose from use for humid-temperate areas, where soils contain gypsum only as a minor component (Herrero and Porta, 2000). Moreover, gypsiferous soils vary distinctly in their morphology and behaviour from those formations in arid climates (i.e. gypseous soils), where aridity allows calcium sulphate enrichment. More specifically, Eswaran and Gong (1991), Boyadgiev and Verheye (1996), Lebron et al. (2009), Moret-

Fernández and Herrero (2015), and Pearson et al. (2015) state that the term ‘gypsiferous soil’ is used to describe soil that is between 1% and 40% gypsum, while the term ‘gypseous soil’ is used to describe soil that is more than 40% gypsum. Therefore, the appropriate terminology for referring to soil with gypsum in it is still a debatable issue.

Van Alphan and Romero (1971) suggest that soil that is 2% gypsum can be described as gypsiferous soil. At this percentage, it is able to cause a collapse of hydraulic structures, such as large irrigation canals. For the same purpose, other authors claim that soils with a gypsum content higher than 5% should be classified as gypsiferous soils (FAO, 1990; Verheye and Boyadgiev, 1997). Van Alphan and Romero (1971) consider a 14% gypsum-content level as the critical limit for distinguishing between gypsic and non-gypsic layers; in addition, they also assert that the characteristics that should be used in classifying gypseous soils are the depth of the gypsic layer, the percentage of gypsum, and the consistency of the soil layer (e.g. powdery, crusty, stony, etc.). Barzanji (1973) divides gypsiferous soils into classes according to their gypsum content, as shown in Table 2-2. Barzanji (1973) shows that gypsiferous soils can be recognized as such more easily when the gypsum content exceeds 3%. The gypsum does not interfere with ordinary soil characteristics, such as water holding capacity, consistency, and structure, until the gypsum content reaches 10%. In moderately gypsiferous soils, gypsum crystals tend more and more to break the continuity of the soil mass. A gypsum content higher than 25% causes the soil to lose plasticity, cohesion, and aggregation, and the soils becomes unstable when water is present. The soil becomes gypseous when the gypsum content exceeds 50% (Barzanji, 1973).

Table 2-2: Classification of gypsiferous soil below 50% gypsum content (Barzanji, 1973).

Gypsum content (%)	Classification
0.0-0.3	Non-gypsiferous
0.3-3.0	Very slightly gypsiferous
3.0-10	Slightly gypsiferous
10-25	Moderated gypsiferous
25-50	Highly gypsiferous

It can be noted that many authors neglect the soil texture, soil plasticity, and type of gypsiferous soil, with the gypsum content being the only criterion in classifying the soil as gypsiferous or not gypsiferous. However, Al-Dabbas et al. (2012) proposes that soil classification should take into account gypsum content, mineralogy, geochemistry, soil texture, and engineering properties (see Table 2-3).

Table 2-3: The proposed applied classification of gypsiferous soils (Al-Dabbas et al., 2012).

Gypsum (%)	Class	Initial void ratio	Coefficient of curvature	Uniformity coefficient	Collapse Potential (%)	Compressive strength (MN/m ²)	Cohesion (kN/m ²)	Plasticity index (%)	Fine-grained soil (%)	TDS of soil water extract (ppm)
0.5-25	Gypsiferous soil	<0.45	<2.5	<25	<1.5	<1	<15	<10	<50	<350
25-50	Highly gypsiferous soil	>0.45	>2.5	>25	>1.5	>1	>15	>10	>50	>350

In general, therefore, it seems that the minimum gypsum content for a soil to be classified as a gypsiferous one is controversial, as is the use of the terms ‘gypseous’ and ‘gypsiferous’. This study considers arid soils and therefore when reporting findings in the literature (where different terms may have been used to describe the same conditions), the term ‘gypseous’ will be used (this is not meant as a comment as to the appropriateness of either term) for the sake of consistency.

2.2.6 Dissolution of Gypsum

The dissolution of gypsum is a significant parameter that has a considerable effect on the geotechnical properties of gypseous soils, due to the creation of cavities or sinkholes; the collapse of metastable soils; and increasing hydraulic conductivities, which may result in increased seepage rates, which in turn may exacerbate the problem (James and Lupton, 1978). Gypsum dissolution is substantially correlated to environmental conditions such as groundwater, pressure, and temperature, which all have a strong influence upon the engineering characteristics of gypsum like crystal structure, mechanical behaviour, and stress-strain with time behaviour (Van Alphen and Romero, 1971; James and Lupton, 1978; Gumusoglu and Ulker, 1982; Fookes et al., 1985; Klimchouk, 1996; Cooper and Saunders, 2002; Salih, 2013).

Gypsum is considered a moderately soluble salt; in pure water, its solubility is 2.6 g/l at 25°C under one atmosphere of pressure (Barzanji, 1973; Boyadgiev and Verheye, 1996), compared to approximately 360 g/l for sodium chloride under similar conditions (Klimchouk, 1996). Gypsum is over one hundred times more soluble than limestone under the same conditions, and gypsum solubility is influenced by temperature and groundwater seepage velocity (Cooper, 1988; Feng-e et al., 2013). Zambak and Arthur (1986), Nafie (1989), and Klimchouk (1996) investigated the relationship between the solubility of gypsum and temperature and found that at temperatures below 40°C, gypsum solubility increases with the increase in temperature, reaching the highest solubility rate at 40°C. After this, the rate of gypsum solubility decreases with increasing temperature. The movement of water is problematic as the movement of water through the pore structure prevents the formation of a chemical equilibrium within the pore water (which can occur in hydrostatic conditions), thus although

the solubility of the compound is only moderate, the salt will continue to dissolve until equilibrium is reached.

In addition to the temperature and flow of groundwater, there are many other factors that directly influence the degree of solubility of gypsum, including the chemical composition of the groundwater, the presence of other evaporates, and the size of gypsum crystals formed. The groundwater chemistry can retard or accelerate the dissolution of gypsum. For example, the presence calcium bicarbonate ($\text{Ca}(\text{HCO}_3)_2$) and sodium sulphate (Na_2SO_4) in pore water reduces the dissolution rate due to the presence of common ions already within the solution (Cooper, 1988), whereas the existence of other salts in the solution, particularly sodium chloride (NaCl) and magnesium chloride (MgCl_2) (James and Lupton, 1978; James and Edworthy, 1985), potentially increases the dissolution rate. Al-Barrak and Rowell (2006) observe that calcite can impede gypsum dissolution when investigating this mechanism under in-situ conditions. Scanning Electron Microscopy (SEM) indicates that the precipitation of calcite on gypsum crystals can form a thin film that retards the dissolution of the gypsum crystal. It is also observed that the size of the gypsum crystal is inversely correlated with the solubility of the gypsum; hence the finer crystals of gypsum have greater dissolution rates (Khan, 1994; Al-Dabbas et al., 2012).

2.2.6.1 Example of Civil Engineering Challenges Encountered with Dissolution of Gypsum

The presence gypsum in earth dams can prove problematic as the potential for gypsum dissolution can result in excessive seepage through/under these structures; potentially making the dams vulnerable to failure (piping, suffusion, development of sinkholes, rupture or excessive settlements as was the case in the San Fernando, Olive Hills, and Rattlesnake dams

in California: Yilmaz, 2001; Johnson, 2008; Salih, 2013) and necessitate expensive remediation processes (as required in dams in Oklahoma and New Mexico, USA and a number of dams in Iraq, particularly, the Mosul dam: Johnson, 2008; Salah, 2013).

Mosul dam is a case in point, one that has entered general awareness (as evidenced by an article from the Independent Newspaper in 2017 entitled ‘Mosul Dam could collapse any minute killing 1.5 million people’). It was constructed in 1980 on the Tigris River near Mosul city, north Iraq in poor ground conditions (from the view point of a water retaining structure), which contains: limestone and gypsum in many places in the dam foundations and reservoir basin, along with beds of anhydrite and gypsum under the base of the dam (Al-Ansari et al., 1984; Hijab and Al-Jabbar, 2006; Sissakian et al., 2014; Adamo and Al-Ansari, 2016). Seepage of ground water through these strata has resulted in development of dissolution features and sinkholes (Kelley et al., 2007; SIGIR, 2007; Adamo and Al-Ansari, 2016), plaguing the dam since its construction. To date the dam has exhibited a many signs of distress, including: development of a number of cavities (particularly in the midline below the dam centre, close to the upstream shoulder beneath the reservoir; the downstream of the dam and the right bank about 900 m downstream the toe of the main embankment); large earth settlements have been observed around 100 m upstream from the dam centre line; considerable seepage happens along both sides of the concrete chute of the spillway; and lowlands downstream of the dam exhibit increased water content since the 1990s (Kelley et al., 2007; Johnson, 2008; Al-Taiee and Rasheed, 2009; Salah, 2013). In addition, dissolution rates appear both to be increasing with time and as a function of the reservoir level (quantity and rate dissolution in the east abutment increases when the water level is at or over 318 m) (Kelley et al., 2007; Johnson, 2008; Al-Taiee and Rasheed, 2009; Salah, 2013).

Saeedy (in MESF, 2007) reports that cement grouting has been used as a potential remediation option since 1985 but without noticeable abatement of the dissolution (indeed it has been argued that the application of grouting has contributed to deterioration of the dam as it is contributing to the growth of gypsum veins within the foundation soils; Kelley et al., 2007; Saeedy, in MESF, 2007).

2.3 Gypsum's Effect on Soil Properties

Many researchers have been investigated the effect of gypsum on the geotechnical characteristics of the soil in which it is found. In general, all geotechnical characteristics are influenced by the presence of gypsum. Al-Muftly (1997) stated that the influence of gypsum on the soil behaviours is based on the quantity of gypsum, the purity of the water, the concentration of salt, the velocity of water flow, and the area of gypsum that comes into contact with water.

2.3.1 Consistency Limits

The replacement of clay content with gypsum in fine-grained soils (manufactured or naturally occurring) results in the reduction of both the liquid limit and plastic limit, as gypsum crystals do not exhibit plasticity. These changes have been observed to increase in magnitude with an increase in gypsum content (Taha, 1979; Subhi, 1987; AlQaissy, 1989; Nashat, 1990; Sajedi et al., 2008; Yilmaze and Civelekoglu, 2009; Estabragh et al., 2013). Laboratory tests on a highly expansive clay (smectite content of 52%) demonstrate that both the liquid limit and the plastic limit diminish whilst the shrinkage limit increases with increases in the quantity of either gypsum or anhydrite (Azam et al., 1998; Azam and Abduljawwad, 2000).

2.3.2 Compaction Parameters

The results of previous studies on compaction characteristics are presented in Table 2-4. The contradictions in the results and the different behaviours that are stated in Table 2-4 may be explained by the role of gypsum in the compaction process. Firstly, at low gypsum content levels, the gypsum crystals appear to act as pore filling fines, especially if the added or the original gypsum crystals were of small sizes compared to the soil grains, thus increasing the maximum dry density. Secondly, gypsum crystals have a lower particle density (2.32) than the natural soil (without gypsum), thus increasing the gypsum content at the expense of soil particles will cause a reduction in the overall particle density of the soil (especially if at a high enough content level that the behaviour changes from pore infilling to disruption of the soil particles within the compacted fabric), causing a reduction in the maximum dry density. Thirdly, if the soil mixture is allowed to rest post mixing (for a sufficient time for the gypsum crystals to develop) prior to compaction, then the gypsum cements the soil particles, which improves resistance to the compaction effort, which in turn reduces the maximum dry density. Nonetheless, the interaction of the three effects yields the final behaviour. Moreover, the type of the soil and the shape and size of the gypsum crystals also affect the compaction parameters.

Table 2-4: Previous laboratory studies on the effect of gypsum on compaction parameters.

Reference	Soil Type	Observations
Kattab (1986)	Granular gypseous soil	Maximum dry density increases with a decrease in the optimum moisture content (OMC) up to 15%. Beyond that level, the effect of gypsum content is reversed.
Subhi (1987)	Sandy, silty clay soil with various sizes of gypsum crystals	Regardless of the crystal size of the gypsum, maximum dry density decreases with increases in gypsum. Addition of gypsum crystals sized <63 μm or, between 250-355 μm and 850-1000 μm , results in increases and decreases of the OMC with increases in gypsum, respectively.
Al-Dilaimy (1989)	Clayey gypseous soil	Maximum dry density increases while the OMC decreases with gypsum content up to 5%, after which the relationship is reversed.
Al- Khafaji (1997)	Sandy silt, 0-50% gypsum content	Maximum dry density decreases while the OMC increases with gypsum content.
Sajadi et al. (2008)	Silty low plasticity soil with gypsum content from 13.7% - 23.4%	Maximum dry density and OMC increase with increasing gypsum content from 1.61 to 1.69 Mg/m^3 and from 10.1% to 12.9%, respectively.
Fattah et al. (2012)	Poorly graded silty sand with 27%, 41.1%, and 60.5% gypsum	Maximum dry density increases (from 1.65 to 1.97 Mg/m^3), while the OMC decreases (from 13.8% to 10%) with increasing gypsum content from 27% to 60.5%.
Ahmed (2013)	Sandy silt with 0-80% gypsum content	From 0 to 30% gypsum content, the maximum dry density slightly increases related to a slight decrease in the OMC, after that the relationship is reversed. For soil with 80% gypsum, the dry density and OMC decreases and increases by 16% and 57%, respectively, in comparison with soil having 30% gypsum.
Estabrag et al. (2013)	Low plasticity clay (CL) and high plasticity clay (CH). Each with gypsum contents up to 40%	Maximum dry density decreases, and the OMC increases with gypsum. The results show that for 40% gypsum, the reduction of dry density is 8.4% and 40.4% for CL and CH soils, respectively, in comparison with natural soils. Hence the reduction in dry density for CH is 4.8 times that of CL soil. The OMC increases by 30.7% and 25% for CL and CH soils, respectively, in comparison with natural soil.

2.3.3 Hydraulic Conductivity

The hydraulic conductivity of gypseous soils is very difficult to evaluate because of the dissolution phenomena: as water seeps through the soil, a proportion of the gypsum will

dissolve, which will change the properties of the soil (i.e. void ratio, chemistry of the percolating waters, etc.) and hence change the hydraulic conductivity for the soil (Ismael, 1993; Al-Obaidi, 2014; Asghari et al., 2014; Aldaood et al., 2015). This process is affected by many factors, including the content, the crystal size and distribution of the gypsum, the hydraulic gradient, the stress conditions applied, and the chemistry of the water seeping through the soil (Keren et al., 1980; Arutyunyan and Manukyan, 1982; AlNouri and Saleam, 1994; Namiq and Nashat, 2011). These parameters will substantially influence the hydraulic conductivity derived for the soil, and hence the standard tests for measurement of hydraulic conductivity on gypseous soils are unreliable. However, in spite of this fact, ‘leaching hydraulic conductivity’ tests have been undertaken on various soil samples to assess the impact of gypsum dissolution upon the performance of the soil under various conditions, such as gypsum amount, size of gypsum crystal, stress levels, and hydraulic gradient. Tests were undertaken using the Rowe cell (AlNouri and Saleam, 1994; Namiq and Nashat, 2011), the oedometer (Arutyunyan and Manukyan, 1982), and the leaching column (Keren et al., 1980). Table 2-5 shows the methodology and the observation of permeability tests collected from several laboratory studies. The hydraulic conductivities were observed to fluctuate and decrease over time. These fluctuations are caused by the enlargement of void spaces due to the removal of gypsum between soil particles by dissolution process, resulting in an increase of permeability. However, leaching-induced collapses of the soil fabric (with dissolution of the gypsum crystals) will remove some flow paths through the soil fabric and hence reduce permeability. Consequently, whilst there have been intensive efforts to evaluate the coefficient of permeability in gypseous soil precisely, these results are still potentially unreliable due to the dissolution behaviour of gypsum.

Table 2-5: Variation of the coefficient of permeability with gypsum content.

Reference	Type of soil	Range of gypsum content (%)	Methodology	Variation of hydraulic conductivity(k) with gypsum content (%)
Keren et al. (1980)	Fine and coarse textured soils	(5% and 10%) for each soil. Crystal size: less than 44 μm and (0.25-1) mm	Leaching column soil (5 cm inner diameter and 20 cm height).	Gypsum crystals that are smaller than 44 μm cause significant decreases in k due to filling of pores with fine gypsum crystals. Conversely, the larger crystals (0.25-1) mm do not influence k because the resulting filling pores are still not sufficiently large to impede flow.
Arutyunyan and Manukyan (1982)	Gypseous soil	28.4%	Leaching-Permeability Oedometer Test.	At the first days (4 days), k increases sharply; after that, it fluctuates over time with a general decreasing trend (Figure 2-6a).
Ismael (1993)	Undisturbed low plasticity silt gypseous soil	60%	Constant Head Permeability Test. Hydraulic gradient: 10, using distilled water.	Over the leaching test, there is 100% increase in k value (from 1.75×10^{-3} cm/sec to 3.5×10^{-3} cm/sec) due to dissolution of the gypsum.
AlNouri and Saleam (1994)	Undisturbed silty sand gypseous soil	25%, 60%, and 80%	Leaching-Permeability Rowe Cell. (upon 50 and 200 kPa)	k decreases with increasing stress levels, in particular at 200 kPa. Since the solubility of gypsum increase with stress level and particle reorientation is greater under higher stresses (Figure 2-6b).
Namiq and Nashat (2011)	Undisturbed clayey gypseous soil	89%	Leaching-Permeability Rowe Cell. Hydraulic gradients: 131.579, 263.158, and 526.316 and stress levels: 100, 200, and 400 kPa.	k decreases with increasing magnitude of the hydraulic gradient and with the applied load; after that, k tends to a constant value (Figure 2-6c).
Al-Obaidi (2014)	Clayey, sandy silt	70%	Leaching-Permeability Test using UPC-Barcelona cell. Hydraulic gradient: 20. Net vertical stress (50, 100, 200, 400, and 800 kPa)	k significantly decreases with increasing in the leaching time and dissolved gypsum. This is due to the collapse of soil structure resulting in the reduction in micropore channels.
Asghari et al. (2014)	Silty sand, clayey sand, and clayey silt soils	From 2.9% to 57.3%	Leaching-Permeability Test using cell with 10.12 cm diameter and 12.17 cm height. Head: 90 cm.	Initially, k is high due to the dispersion and movement of particles, but it gradually decreases until approaches a constant value.
Aldaoood et al. (2015)	Low plasticity clay soil	0%, 5%, 15%, and 25%	Leaching test (cell with 97 mm diameter and 38.5 mm height) adopted constant head test. Hydraulic gradient: 20.	k increases with increasing in gypsum content and time until it reaches a constant value, which is mainly due to the gypsum dissolution making cavities and channels that ease water flow (Figure 2-6d).

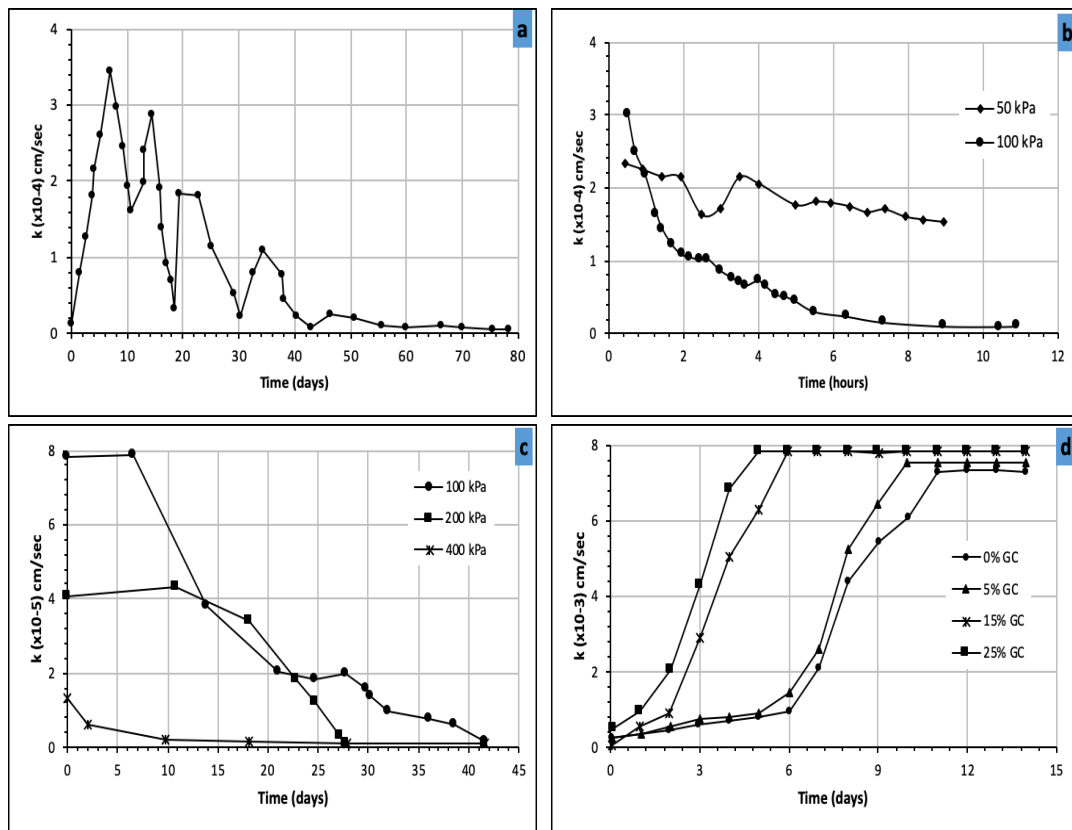


Figure 2-6: Hydraulic conductivity over time; (a) Arutyunyan and Manukyan (1982), (b) AlNouri and Saleam (1994) for 25% gypsum content, (c) Namiq and Nashat (2011) upon hydraulic gradient equal to 131.579, (d) Aldaood et al. (2015).

2.3.4 Compressibility of Gypseous Soil

2.3.4.1 Collapsibility of Gypseous Soil

The collapse of gypseous soil is a very common phenomenon. The value of collapse is dependent greatly on the void ratio and the permeability of the soil (Al-Mufti, 1997). The higher the void ratio or permeability, the greater the potential for collapse. This is confirmed by the work of Al-Mohmmadi et al. (1987). Collapse potential (CP) has been found by many studies to depend on the applied stress (Taha, 1979; Al-Khuzai, 1985; Al-Mohmmadi et al., 1987; Al-Ani and Seleam, 1993; Sheikha, 1994). An interesting work by Singh and Al-Layla

(1980) showed that the CP in natural gypseous soil was significantly higher than that for artificial soil with the same preconsolidation stress. This was attributed to the differences in the microstructure of the two soils. It was found that the artificial gypseous soil contained a larger aggregate of silt grains clothed in peels of flocculated clay, while the natural gypseous soil was composed of higher amounts of needle-like outgrowth of gypsum crystals. That means the simple method that is adopted by many authors (i.e. the simple practice of mixing the constituents and compacting them to form the samples) may not mimic the collapse behaviour of a natural soil unless an artificial soil is used to simulate the movement and precipitation of gypsum in natural soil (see Chapter Three).

Nonetheless, the CP value is also affected by the amount of gypsum in the soil. The greater the gypsum content, the higher the CP (Al-Heeti, 1990; Abood, 1994; Sheikha, 1994; Al-Dulaimi, 2004). This is true only for approximately equal void ratios at the stress level at which the CP is being calculated. In gypseous soils with low void ratios and high gypsum contents, the CP is lower than for soils with high void ratios but lower gypsum contents. Figure 2-7 shows a typical relationship between CP and gypsum content at a vertical stress of 200 kPa (AlQaissy, 1989).

Al-Mohmmadi et al. (1987) studied the effect of wetting-drying cycles on the gypseous soils under a constant stress of 100 kPa. The samples were air dried in the oedometer, keeping them stressed. It was found that rewetting caused a higher CP, but a CP that was still lower than that in the preceding cycle; that is, the additional CP gained decreases as the number of wetting-drying cycles increases. Consequently, Al-Mohmmadi et al., (1987) suggests that flooding gypseous foundation soils with sufficient amounts of water prior to construction may diminish the likelihood of collapse in the future.

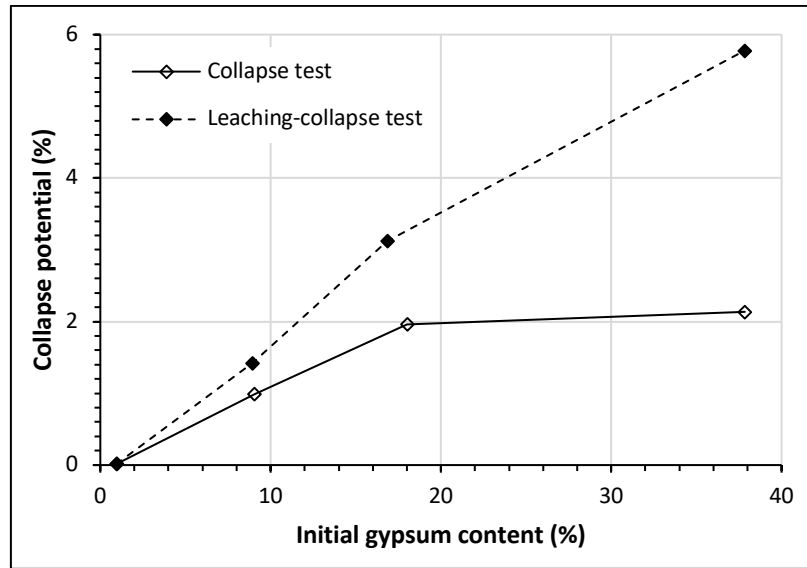


Figure 2-7: Typical effect of gypsum content on the CP (AlQaissy, 1989).

Regarding the purity of pore water, Azam (2000) investigated the influence of pore water chemistry on the compressibility and collapsibility of an anhydrite (CaSO_4)-clay mixture by using brine and distilled water when preparing the samples. The outcomes indicated that anhydrite was likely to be more compressible with the addition of clay soil. This effect was more noticeable when the brine water was permeated through the soil samples. This was attributed to the gypsification of the anhydrite in the first stage and of the gypsum dissolution in the second stage, forming cavities within the soil fabric. In addition to the dissolution, the fine clay particles in this mixture were highly compressible. It was also reported that the collapse of samples immersed in distilled water was half that observed in samples exposed to the brine, and it was suggested that this was due to the fact that the brine water contained a high ion concentration, especially Na^+ and Cl^- ions, which increased the solubility rate of the anhydrite. Moreover, these ions cause the breakdown of the crystalline bond of calcium sulphate, causing in further dissolution, making more and larger spaces, increasing the CP of the soil fabric (James and Lupton, 1978; James and Edworthy, 1985).

2.3.4.2 Compression and Swelling Index of Gypseous Soil

AlNouri and AlQaissy (1990), Sirwan et al. (1991), AlNouri and Saleam (1994), Livneh et al. (1998), Sajedi et al. (2008), Fattah et al. (2012), Ahmed (2013), Estabrag et al. (2013) and Fattah et al. (2015) have all investigated the effects of gypsum content on the compressive properties of gypseous soils using the oedometer. These authors observed that the compression index, (C_c), decreased as the gypsum content increased (in a dry state); this was probably due to cementing between soil particles, which increased the resistance to deformation. However, it was found that C_c increased upon wetting of a dry sample, because of the softening that occurs due to dissolution of the gypsum, especially at frictional grain contacts, etc., and hence the resultant loss/reduction of cementation and stiffness of the soil. The swelling index (C_s) does not follow the same trend as C_c , as its value depends highly upon the type of soil constituents (other than gypsum) and the way the gypsum and other particles are cemented (Figure 2-8).

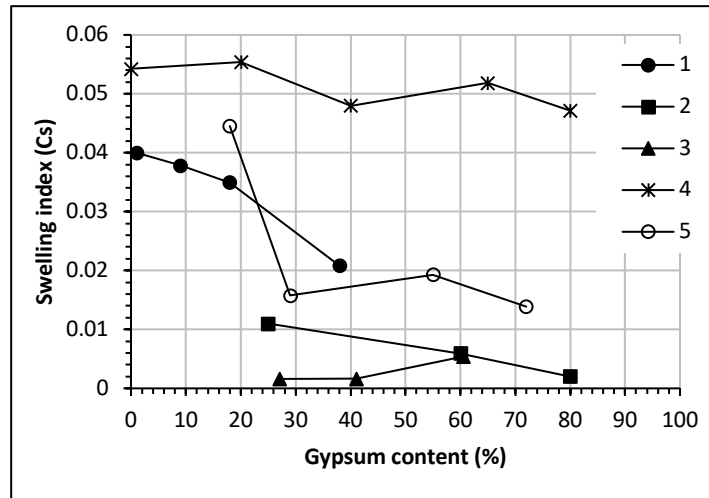


Figure 2-8: Swelling index (C_s) versus gypsum content; (1) silty clay gypseous soil (AlNouri and AlQaissy, 1990), (2) silty sand gypseous soil (AlNouri and Saleam, 1994), (3) poorly graded silty sand gypseous soil (Fattah et al., 2012), (4) sandy silt gypseous soil (Ahmed, 2013), (5) sand gypseous soil (Fattah et al, 2015).

Gypseous soils exhibit appreciable secondary consolidation, or creep, which increases with higher applied load, gypsum content, and water content (Seleam, 1988; Alaithawi, 1990; Sirwan et al., 1991; AlNouri and Saleam, 1994; Fattah et al., 2008; Estabrag et al., 2013; Afaj and Mohammed, 2018). This phenomenon is ascribed to the continuous dissolution process of gypsum with time and to particle reorientation (Figure 2-9).

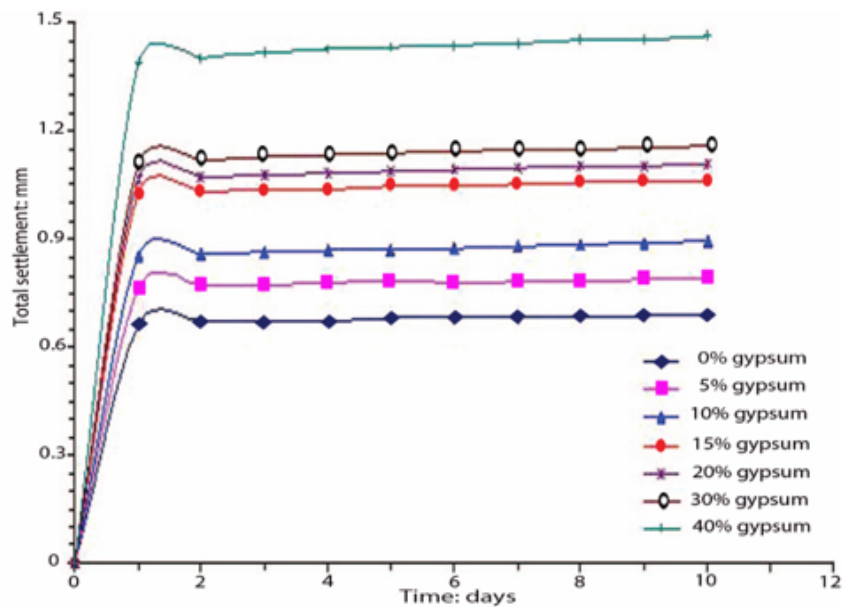


Figure 2-9: Total settlement for high plasticity clay soil (CH) with time for different gypsum content during leaching (Estabrag et al., 2013).

Seleam (1988) investigated a sandy soil and suggested that secondary compression was negligible when the soil is tested dry as no dissolution occurred, while in saturated specimens, it was very similar to the behaviour of clayey soils during secondary compression, although the soil tested was sandy in nature. This secondary compression was related to softening of the soil structure and partial dissolution of gypsum.

Samples experienced greater deformation under hydrodynamic conditions, where the flowing water retarded the development of an equilibrium within the pore spaces between the phases of the calcium sulphate (precipitate and dissolved) was coupled with the rearrangement of soil particles with loss of cementation (Seleam, 1988; Al-Ani and Seleam, 1993; Al-Mufti, 1997; Al-Farouk et al., 2009). Consequently, the C_c and settlement are greater during the leaching tests than the standard one-dimensional compression tests (Ismael, 1993; AlNouri and Saleam, 1994; Abduljawwad and Al-Amoudi, 1995; Ismael and Mollah, 1998; Namiq and Nashat, 2011; Estabrag et al., 2013). AlNouri and Saleam (1994) observed that this increase was more evident in samples with lower gypsum contents (see Table 2-6), it is presumed that the gypsum present in these soils is located mainly at the contact points, and is destroyed readily by the flowing water and hence the cementing effects of the gypsum would be removed from the soil fabric more quickly when compared to soils containing significantly greater proportions of gypsum (AlNouri and Saleam, 1994).

Table 2-6: Comparison of the compression index (C_c) and swelling index (C_s) values in standard consolidation and oedometer leaching tests of undisturbed samples.

Reference	Soil type	GC%	Before leaching		After leaching	
			C_c	C_s	C_c	C_s
Ismael (1993)	Low plasticity silt	60	0.15	0.010	0.21	0.015
AlNouri and Saleam (1994)	Silty sand	25	0.04	0.010	0.29	0.009
		80	0.03	0.007	0.04	0.007
Abduljawwad and Al-Amoudi (1995)	Poorly sand	6	0.13	0.018	0.17	0.018
Ismael and Mollah (1998)	Silty sand	28	0.10	0.020	0.12	0.028

2.3.5 Swelling Behaviour

Calcium sulphate hydrate, or gypsum ($\text{CaSO}_4 \cdot 2\text{H}_2\text{O}$), is a relatively stable crystal structure and thus does not swell to the same degree as calcium sulphate anhydrite (CaSO_4). This is due to the fact that the two bonding water molecules in gypsum permit the soil to imbibe minimal moisture without alteration of the gypsum chemical structure. In other words, soluble rocks in the form of hydrous calcium sulphate (gypsum) will not undergo larger expansion or heave compared with those without the bonding water within the crystal structure (calcium sulphate anhydrite) (Soils and Zhang, 2008). Accordingly, anhydrous calcium sulphate is one of the factors that leads to swelling during the hydration process, causing a variety of serious geotechnical hazards, such as massive rock uplift in dams, floor heave in tunnels, and damage to pavements and light structures (Brune, 1965; Holiday, 1978; Blatt et al., 1980; Abduljawwad, 1993; Yilmaz, 2001; Sajedi et al., 2008).

Azam et al. (1998) investigate the swell pressure of the three forms of calcium sulphate crystals and found that swell pressure in gypsum, bassanite (hemihydrate), and anhydrite are 330, 1400, and 1660 kPa, respectively. These swell pressures were far lower than those observed in expansive clay (3200 kPa) when tested under the same conditions, which dominantly contains smectite mineral (52%) (Figure 2-10).

Hydration and dissolution of calcium sulphate crystals are a function of changes in local environmental conditions and changes in climate conditions. Changes in seasonal rainfall, air temperature, soil temperature, soil water contents, cycles of wetting and drying, etc., will have an effect on the soil properties, impacting upon the behaviour of gypseous soil (potentially causing damages to geo-structures such as embankments and foundations).

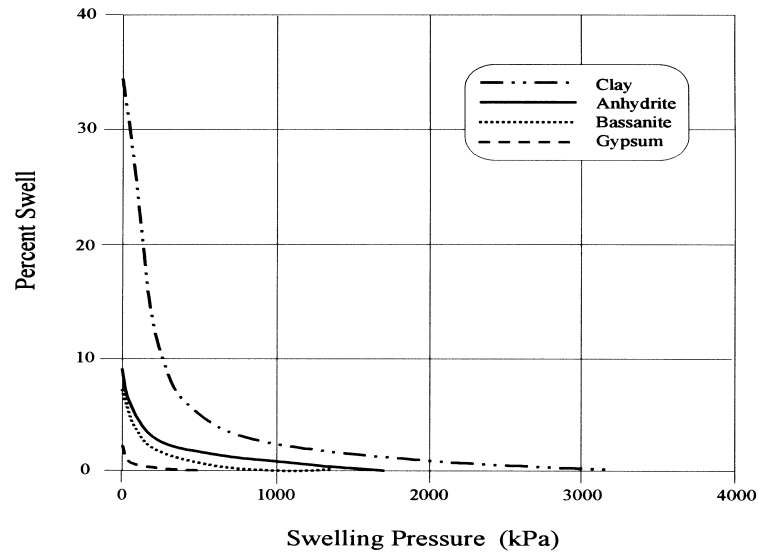


Figure 2-10: Swell pressure of expansive clay and calcium sulphate phases (Azam et al., 1998).

Sajedi et al. (2008) argue that the influence of the wetting-drying cycle using the free swelling test on the swell potential of gypseous soil results in an increase of the swelling potential from 10% to 15% upon rewetting, and this magnitude increases in a linear manner with increases in gypsum content. In contrast, Aldaood et al. (2014) conclude that the swell potential of clay-gypsum mixture decreases with multiple wetting-drying cycles. The greatest decrease in swell potential was observed after the completion of the first wetting-drying cycle: by the fourth wetting-drying cycle, the changes in swell pressure had approached an asymptote. The effects of the wetting-drying cycles on the swell potential were dependent on the gypsum content, and so the maximum reduction occurred for samples with the highest gypsum contents (15% and 25% by mass of dry soil). A possible explanation for this reduction in swell pressure is the disruption of the soil matrix (particularly the matrix of clay structure) during the wetting-drying cycles, as well as the partial breakdown of the soil macro-particles by reconstruction of the structure of aggregates that occurred during these cycles (Aldaood et al., 2014).

Shrink-swell is a well-known geohazard, and ground-improvement methods to limit this have been used in various soils. Ground improvement has been used in gypseous soils, and several authors (Czerewko et al., 2006; Aldaood, 2014; Jha and Sivapullaiah, 2016; Cheshomi et al., 2017) have noted that gypseous soil stabilized by lime is ineffective. This is due to the reaction between gypsum and lime leading to the formation of ettringite, which is an expansive mineral that contains a large amount of water in the crystal lattice. This tends to form in clumps of acicular crystals that push the soil fabric apart, creating internal stress inside the stabilized soil mass, resulting in the expansion and deterioration of the structure (Czerewko et al., 2006; Aldaood, 2014; Jha and Sivapullaiah, 2016; Cheshomi et al., 2017).

Gypsum (which does not heave to the same extent as expansive clays, as mentioned above) can be used effectively to stabilize expansive clay. Yilmaze and Civelekoglu (2009) investigated the effect of gypsum addition on expansive bentonite soil using fine natural gypsum as an improving material. Their study found, from carrying out the free swelling test, that the swelling potential of the clay decreased from 65% for clay samples without gypsum to 20% for clay samples mixed with 5% of gypsum; above these proportions, improvement was ineffective) (Figure 2-11). Similar behaviours are shown for high-plasticity clay with gypsum content (from 0% to 80%) (Azam et al., 1998; Abduljawwad et al., 1999). Azam et al. (1998) concluded that the reduction is due to the gypsum content; for samples containing up to 20% of fine gypsum, the porosity decreased with gypsum content, since gypsum acts mainly as an inert filler and tends to decrease the swell of the soil samples. For samples containing gypsum content higher than 20% and up to 80%, gypsum cementation is the controlling factor, resulting in the formation of clods, which partially restrict the swelling of

clay. These clods increase in the size as gypsum content increases in the mixture, leading to a further reduction in the swelling potential.

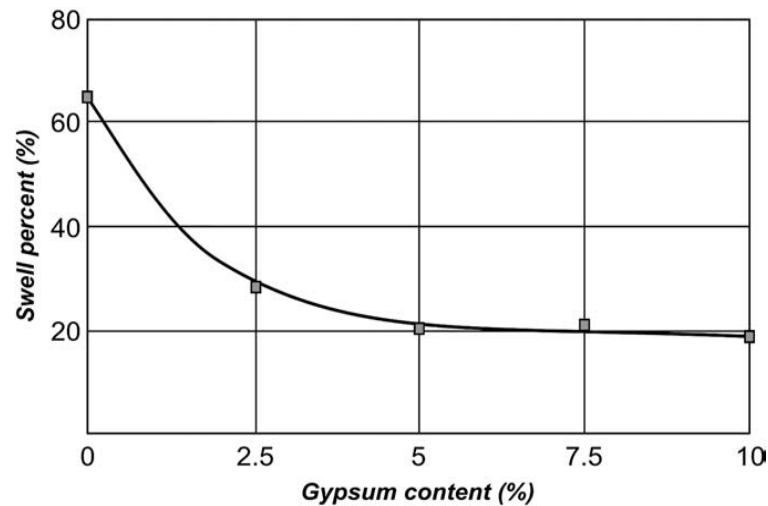


Figure 2-11: Variation of swell pressure with gypsum content (Yilmaz and Civelekoglu, 2009).

2.3.6 Shear Strength of Gypseous Soil

Gypseous soils in arid environments are likely to be relatively stiff and strong when dry, although both properties have been observed to decrease with wetting. Gypsum acts as a cementing agent between soil particles, and the decrease in strength and stiffness upon wetting is expected, as some of the cementing agent will be dissolved. The amount of loss in cementation depends on the void ratio, original gypsum content, the amount of water added to the soil and duration of exposure (if investigating in the laboratory the type and condition of the test undertaken are also important factors) (Fookes et al., 1985; Ahmad et al., 2012).

2.3.6.1 Effect of Gypsum Content on Shear Strength in Dry State

The effect of gypsum content on the parameters of shear strength (cohesion and internal angle of shearing resistance) of a sandy soil was examined by Seleam, (1988); increasing gypsum content (25% to 80%) caused an increase in both the internal angle of shearing and the cohesion. Similar behaviour was observed in gravel soil containing 0 to 6% gypsum (Haeri et al., 2005). Petrukhin and Arakelyan (1984) found that the internal angle of shearing in sandy soil increases with gypsum content up to 25%, due to the increase in mineral friction, and diminishes thereafter, due to the increase in porosity (due to the gypsum disrupting the fabric of the soil, akin to the findings when compacting these soils).

For fine-grained soils, the cohesion decreases whilst the internal angle of shearing increases, with increasing gypsum content (Salas et al., 1973; AlQaissy, 1989; AlNouri and AlQaissy, 1990). The decrease in the cohesion is attributed to the reduction in the fine materials (due to the increasing gypsum content). Nonetheless, the increase in the angle of shearing is because of the increased friction between the gypsum and soil particles, or between gypsum crystals, which is greater than that between the fine-grained soil particles. Petrukhin and Arakelyan (1984) found that cohesion of clayey soils increases with gypsum content up to 15% due to decrease in porosity caused by the formation of gypsum crystals in soil pores and decreases thereafter due to the failure of crystal bonds, while the internal angle of shearing increases up to 20% and decreases thereafter.

Huang and Airey (1998), Haeri et al. (2005), and Yilmaz and Civelekoglu (2009) undertook unconfined compressive strength testing (UCS) on gypseous soils containing varying gypsum contents. Huang and Airey (1998) investigated fine to medium sand soil mixed with gypsum

contents varying from 0% to 20%, and observed that compressive strength increased with increasing in gypsum content and dry unit weight. A similar trend was observed in the gravelly sand soil containing 3% to 9% gypsum content tested by Haeri et al. (2005); and expansive bentonite soil with 0% to 10% gypsum content (Yilmaz and Civelekoglu, 2009) (see Figure 2-12).

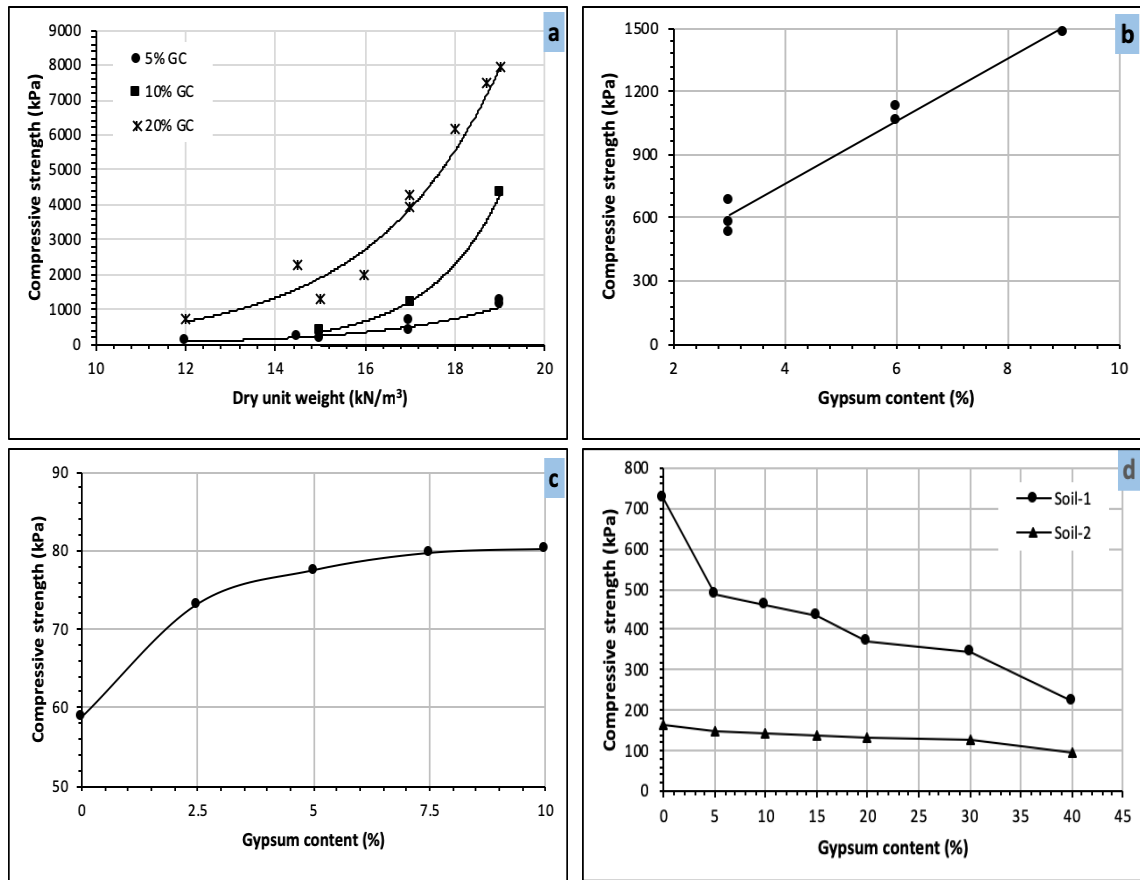


Figure 2-12: Effect of gypsum content on unconfined compressive strength; (a) sand-gypsum mixture with dry unit weight and gypsum content (GC) from 12 to 19 kN/m³ and 0% to 20%, respectively (Huang and Airey, 1998), (b) gravelly sand with 3%, 6% and 9% gypsum content (Haeri et al., 2005), (c) expansive bentonite soil (Yilmaz and Civelekoglu, 2009), (d) soil-1 (21% clay) and soil-2 (50% clay) with gypsum content from 0% to 40% (Estabragh et al., 2013).

However, Estabragh et al. (2013) undertook UCS on two clayey soils, containing respectively 21% and 50% clay, Figure 2-12d. The gypsum contents also varied and both the clay and gypsum contents were found to be important when investigating changes in UCS. Inclusion of gypsum in any of the samples appears to have reduced the UCS values, and this reduction in soil-1 greater than soil-2. This is a function of disruption of the soil fabric and clay content; thus, the gypsum crystals are held together by clay causing a higher reduction in compressive strength in soil-2 than soil-1 which has lower clay content.

2.3.6.2 Effect of Soaking on Shear Strength of Gypseous Soils

Due to the time required in the dissolution process of gypseous soil, short-term soaking (in laboratory tests) does not necessarily provide an insight as to the realistic in situ response of highly gypseous soils and can lead to significant overestimations of soil strength and stiffness. Therefore, it has been recommended that samples should be exposed to a soaking period of at least one month in order to allow the dissolution of gypsum and provide an indication as to the loss of strength with increased water content (Razouki and El-Janabi, 1999; Estabragh et al., 2013; Razouki and Salem, 2014).

A number of investigations have been undertaken that consider the effect of long-term soaking on the California Bearing Ratio (CBR) and/or the parameters of shear strength for some Iraqi gypseous soils that have different gypsum contents and textures (Razouki and El-Janabi, 1999; Razouki and Kuttah, 2006; Razouki et al., 2007; Razouki and Ibrahim, 2007). Razouki and El-Janabi (1999) soaked a well-graded gypseous silty sand with 64% gypsum content for various periods (Figure 2-13) and found that the CBR was reduced with increasing soaking periods, although the reduction was a non-linear decrease (Figure 2-13). The decrease

in CBR is due to the soil softening and loss in gypsum from the sample with increasing soaking period. Similar behaviour was observed in well graded silty sand containing 34% gypsum content (Razouki and Al-Azawi, 2003); high plasticity clay with 34% gypsum content (Razouki and Kuttah, 2006); silty sand with 28% gypsum content (Razouki and Ibrahim, 2007); sandy clay with 25.6% and 33% gypsum content (Razouki et al., 2010); and low and high plasticity clay soils with various gypsum contents from 5% to 40% for each soil (Estabrag et al., 2013).

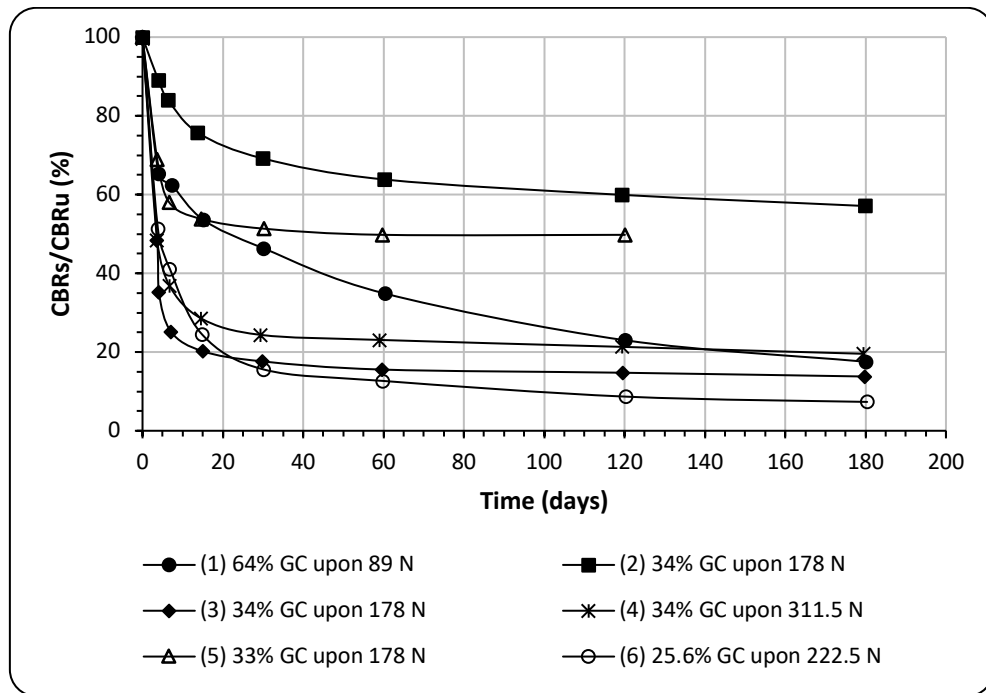


Figure 2-13: Effect of soaking period on strength ratio of soaked CBRs relative to unsoaked CBRu for gypseous soils; (1) well graded gypseous silty sand (Razouki and El-Janabi, 1999), (2) well graded silty sand (Razouki and Al-Azawi, 2003), (3) and (4) high plasticity clay (Razouki and Kuttah, 2006), (5) and (6) sandy clay (Razouki et al., 2010). (NB. The force represented in the figure captions are those applied to the samples and GC refers to gypsum content).

The results of strength ratio CBRs/CBRu (the suffixes s and u are for soaked and unsoaked tests respectively; the ratio expressed as a percentage) against soaking period for some soils and surcharge loads used in this analysis are shown in Figure 2-13. This shows that the strength ratio CBRs/CBRu is strongly affected by many factors, including the type of soil, the initial gypsum content, the applied surcharge load, and the soaking period

The effect of soaking period on shear strength parameters has also been considered and include unconsolidated, undrained triaxial tests on a low-plasticity clay soil containing 33% gypsum content (Razouki et al., 2007), as well as direct shear tests on both a silty clay (Gumusoglu and Ulker, 1982) and a sandy clay containing 33% gypsum (Razouki et al., 2008). These investigations exhibited a significant drop in effective cohesion, (c') and effective internal angle of shearing, (ϕ') with increased soaking period; the drop after 15 days is 58% and 6.7% for (c') and (ϕ'), respectively (Gumusoglu and Ulker, 1982); the drop in the (ϕ') and (c') at the end 120 days soaking is 61.8% and 40%, respectively, as compared to 4 days soaking (Razouki et al., 2007), while the (c') and (ϕ') for 4 days soaking is 1.35 times and 1.08 times, respectively, that for 30 days soaking (Razouki et al., 2008). The reduction in shear strength parameters with soaking was similar to that observed with the CBR upon soaking, and was once again attributed to dissolution of gypsum crystals from the contact areas between the soil particles and softening of the soil structure.

2.4 Gypseous Soils in Iraq and Britain

2.4.1 Gypsum Forms Encountered in Iraq

In Iraq, gypsum is found in the alabaster form (the fine-grained, compact, and non-crystalline form of gypsum), which is known locally as Mosul marble, or it is found as primary rocks of either gypsum or anhydrite. Also, secondary forms of gypsum, such as detrital and reprecipitated gypsum, are usually encountered in younger formations, such as Bakhitiari gravels; river terraces; and, to a lesser extent, in the Holocene fluvial deposits. It is crystalline or amorphous. Most secondary gypsum was formed during the pluvial phases of the Pleistocene, at the time when the climate was more humid and the valleys in the gypsum regions were formed (Al-Mufti, 1997). In the older clayey and silty deposits of the Pliocene, which are often somewhat reddish coloured, gypsum often occurs in monoclinic crystals, which are colourless and transparent, and is called selenite.

Some secondary gypsum has been blown from the gypseous desert areas and deposited in other areas. In the gypsum areas of Iraq, wind erosion is very active; therefore, aeolian sediments are extensive in the gypsum and sand deserts, forming thin sheets of sand, and low and high dune land. Some gypsum has been precipitated from irrigation water, whereas some is also formed by chemical reactions in the soil itself, especially when sulphur is present, which in moist soil reacts with lime (CaCO_3) with the help of micro-organisms. In the soils of the flood plain, secondary gypsum is present in both amorphous and crystalline forms. Finer textured soils usually have higher gypsum content than the similar coarse textured soils. As a result of the evaporation of groundwater in arid areas, most of the gypsum accumulates in the layer above the capillary water zone of a profile, reaching a depth of about 2.5 to 3 metres below the land's surface (Buringh, 1960).

Buringh (1960) investigated gypsum in Iraq and produced a map depicting the distribution of gypseous soils and their geological formation (Figure 2-14 presents this map). Buringh's map was divided to five zones: primary gypsum, primary gypsum mixed with limestone, secondary gypsum, gypsiferous alluvium, and non-gypsiferous and mainly limestone.

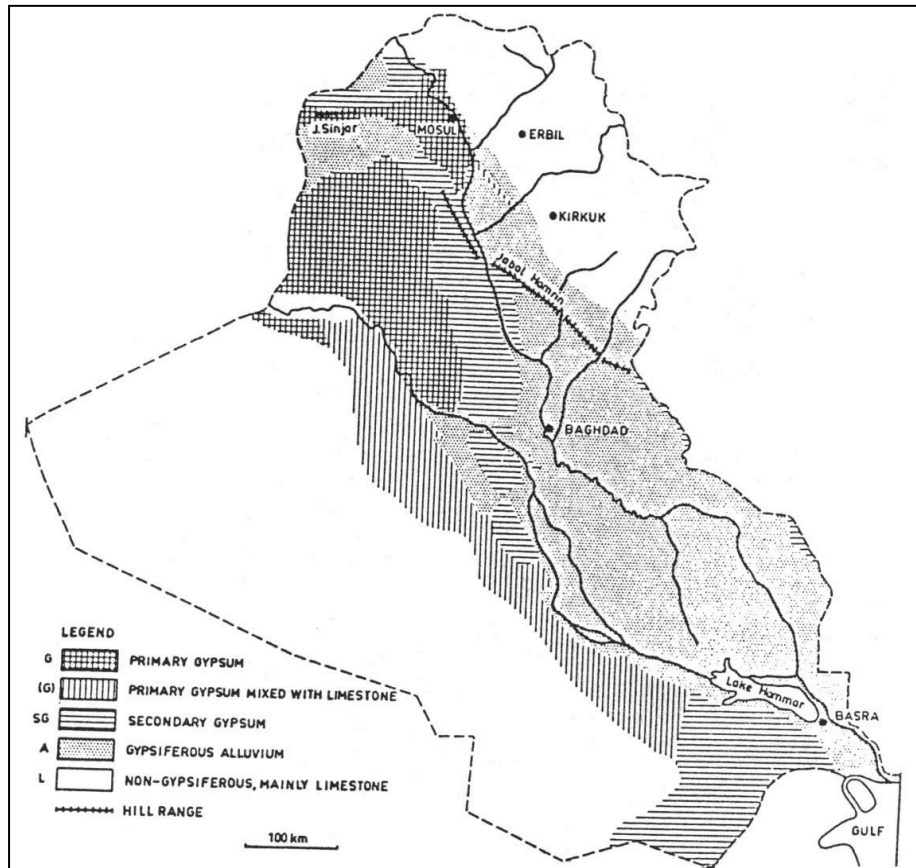


Figure 2-14: Gypsum map of Iraq (Buringh, 1960).

Barzanji, (1973) investigated the distribution of gypsum in different parts of Iraq. Six zones were identified according to their origin and gypsum content (Figure 2-15). Zone one denotes slightly gypseous soils laid on a gypsum bedrock in the far north of Iraq. Zone two is of moderately to highly gypseous soils above gypsum and anhydrite rock, located in the northern part between the Tigris and Euphrates rivers. Zone three is a gypsum desert located between

zone one and zone two in the north of Iraq. Zone four is highly gypseous soils upon Pleistocene terraces covering two narrow strips on the right and left of the Tigris. Zone five is non-gypseous to slightly gypseous soils, extending from the upper third of Iraq down to the south with the Kuwaiti borders. Zone six is moderately to highly gypsiferous soil correlated with lime, covering the west Jazeera.

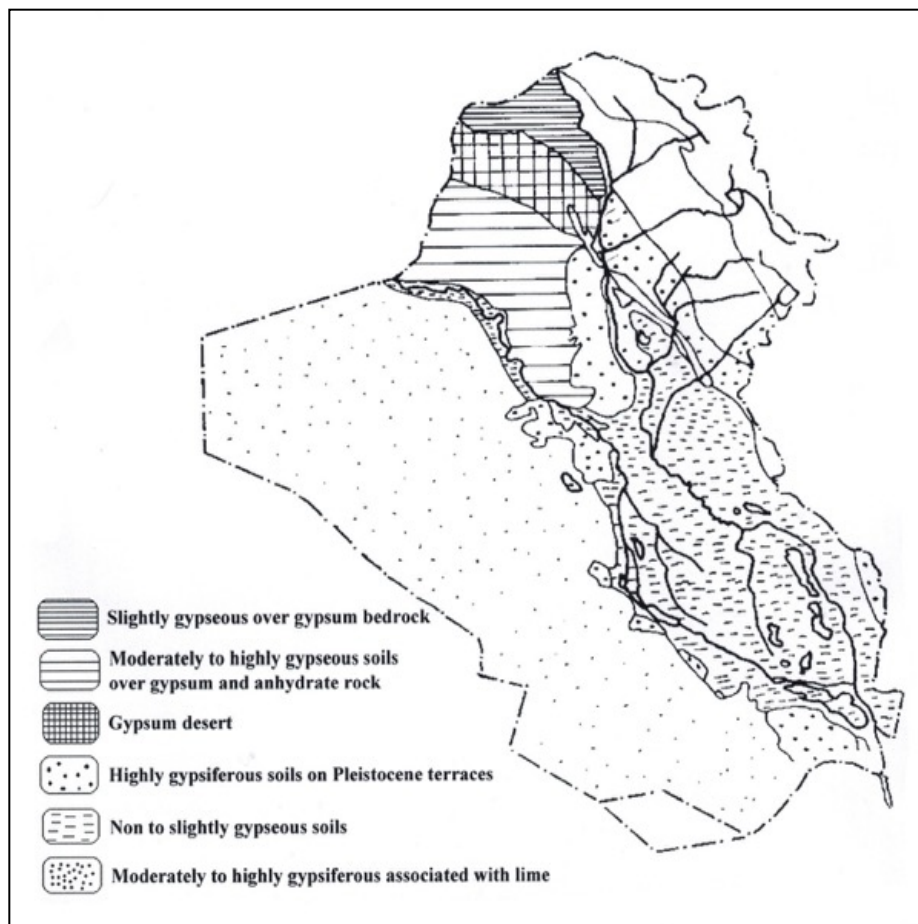


Figure 2-15: Gypsum map of Iraq (Barzanji, 1973).

2.4.2 Gypsum Forms Encountered in Britain

In the UK, calcium sulphate is found within rocks and soils in the forms of anhydrite and gypsum. These often occur in thick layers/beds formed in the Permian and Triassic ages, and

are widely distributed in the north and midlands of England (Bell, 1994; Cooper and Saunders, 2002; Czerewko et al., 2006) (Figure 2-16). Gypsum is present in the bedrock either as massive beds or as veins. Massive beds tend to be soft and fine-grained (alabaster) with a colour that is white or pale, or in a fibrous form known as satin spar (Czerewko et al., 2006).

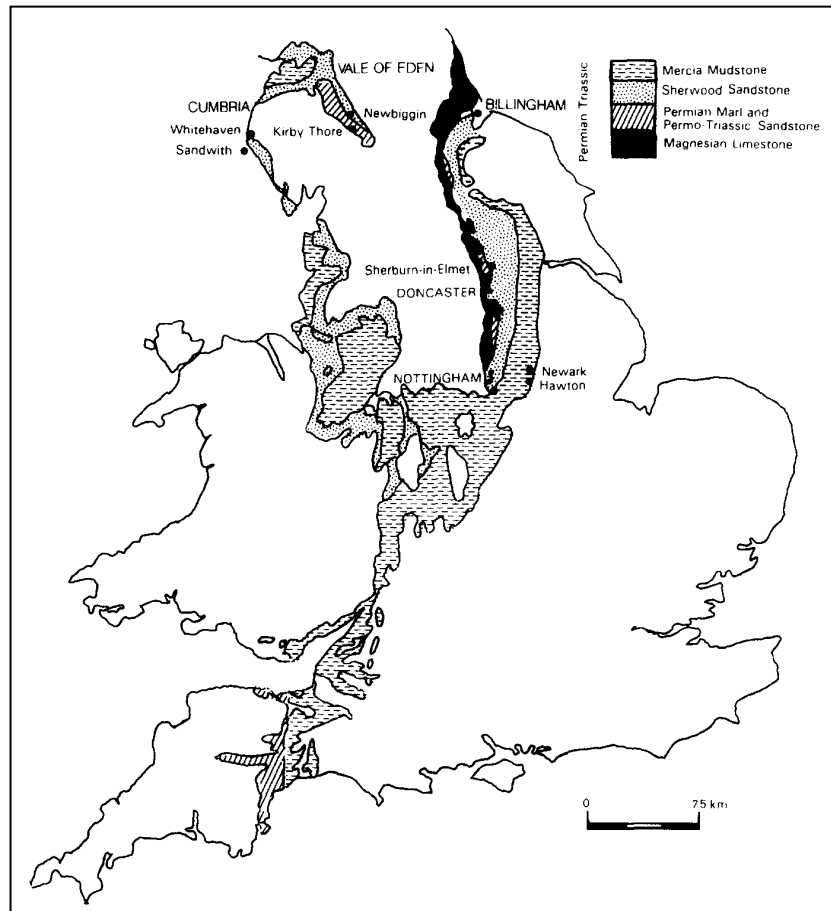


Figure 2-16: Distribution of Permian and Triassic strata and the location of anhydrite and gypsum sites (Bell, 1994).

Gypsum karsts found in the Permian rocks are considered to be significant geohazardous and are mostly found in the Ripon area of north Yorkshire (Cooper and Saunders, 2002). This region has two principal gypsum beds separated by dolomite and limestone aquifers, and these underlay the Triassic Sherwood Sandstone (Figure 2-17). Due to the thickness of

gypseous beds, which range between 80 m and 120 m, large caves (up to 30 m across and 20 m deep) that are susceptible to surface collapses have been identified (Cooper and Waltham, 1999; Cooper and Saunders, 2002). Based on the test of UCS, it was found that the strength of anhydrite rock is strong to very strong, while gypsum rock is medium; this is due to the relatively low porosities (Bell, 1994).

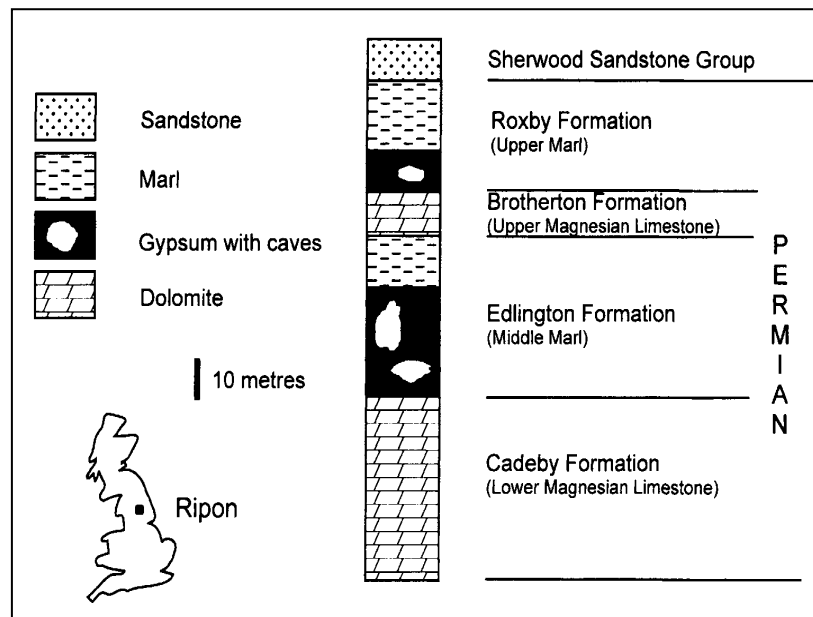


Figure 2-17: Soil profile of the estimated sequence of layers with sinkhole at Ure Bank Terrace (Cooper and Waltham, 1999).

2.5 Uncertainties with Geotechnical Engineering Applications in Arid, Metastable, Gypseous Soils

It is clear from the research effort undertaken to date that inclusion of gypsum within a soil changes the engineering response and if not properly handled may become metastable. Hence, constructing geotechnical structures (such as earth dams, embankments, foundations, highway and airfield pavements) over/in shallow gypseous deposits in hot, arid, environments

could potentially change the localised conditions experienced by the foundation soil (as illustrated with the distress exhibited by the high-speed railway bridge and Mosul dam), which in turn may change its engineering response. However, much is still poorly understood regarding the engineering response of gypseous materials and their interaction with structures. For example, calcium sulphate is known to change crystal structure with dehydration and hydration, which are processes that are affected by the pressure, ambient temperature and relative humidity. If a soil repeatably experience such changes on a regular basis, what impact does this have on the geotechnical properties of the soil and are standard geotechnical tests sufficient to determine these changes? If this is an issue, what type of geotechnical testing is appropriate to assess any such changes? In addition, soil exposed to hot ambient conditions may develop different thermal gradients with depth when compared to the same soil that is below a building, where the structure provides surface cover; this potentially could change groundwater movement in the vadose conditions. This in turn might result in differential dissolution of the gypsum, due to differential groundwater movement, leading to differential settlements of the structure. Furthermore, in arid aeolian sand deposits, loose deposits stabilised by cementation from gypsum crystals and negative pore water pressures, if there is a change in groundwater response, potentially leading to increased unsaturated flow upwards to the ground surface, is the changing in suction regime, or gradual (partial) dissolution of the gypsum crystals, of more critical importance to the change in geotechnical response?

The term gypseous soils clearly covers a range of soil types and properties, if these deposits are loose and metastable then sampling them is problematic and a number of researchers have attempted to manufacture gypseous soils within the laboratory (Akili and Torrance, 1981; AlNouri and AlQaissy, 1990; Huang and Airey, 1998; Haeri et al., 2005; Lee et al., 2010).

This is not without difficulty, manufacturing samples containing gypsum that provide both repeatable and representative samples is a challenge. For example, if attempting to compact samples the gypsum is likely to initially infill the voids (unless the gypsum content is too great) which produces a dense and relatively strong structure; this would be inappropriate when attempting to simulate a loose, metastable structure. In this case, pluviation seems an obvious alternative (Akili and Torrance, 1981; Lee et al., 2010) although difficulties arise in how to deal with the gypsum and how to ensure the repeatable samples. This raises a wider concern, are standard geotechnical methods for both laboratory sample creation (i.e. compaction, consolidation from slurry, pluviation of the solid particles) and testing suitable when considering the nature of arid, aeolian, gypseous soils? Are soil structures that are vulnerable to changes in properties with exposure to changing conditions, i.e. loading, water movements (including evaporation), temperature gradients, well characterised by standard triaxial, UCS, or the small-scale of a standard oedometer? it would appear that new standards are required to facilitate better characterisation of these materials to better explore their behaviour in transitory conditions. Therefore, it is believed that these arid, metastable, gypseous soils present not only a significant geohazard but also challenging materials to investigate properly within the laboratory setting, and it is argued that far more research effort in this area is required.

2.6 Summary

This chapter has reviewed the research into the implications of the inclusion of gypsum in soils in arid environments, where the gypsum/anhydrite is dispersed within the soil structure and not in massive formations, from a geotechnical engineering viewpoint. Based on the review, the following conclusions can be drawn:

- 1) Arid, metastable, gypseous soils (defined herein as soils which contain sufficient gypsum to adversely affect geotechnical engineering applications) are known to be problematic and a potential source of danger if they are not created for during design and construction. These soils can often be characterised as being stiff, with very low compressibility when in a dry (or low saturation) condition, hence they can appear to be ideal foundation soils. However, changes in groundwater conditions may result in partial or complete removal of gypsum, which may be combined with the gypsum being loaded beyond its strength, resulting in increased compressibility and reduced strength reduce, resulting in associated settlements and structural failure. In certain situations, these soils can experience rapid repacking akin to hydrocollapse in loess soils. Furthermore, the release of sulphates into the soils with dissolution of the gypsum can result in accelerated chemical degradation of concretes. These factors make these soils potentially less than ideal for geotechnical applications.

- 2) Physico-chemical changes in the calcium sulphate crystals (i.e. the anhydrite-gypsum cycle) is influenced by environmental conditions such as humidity, temperature, and the presence of water, which leads to detrimental effects to the foundation (i.e. swelling or shrinkage due to gypsification of anhydrite or dehydration of gypsum, respectively). The dissolution, transportation and redistribution of gypsum in the soil profile is extensively influenced by the hydrogeological cycle, i.e. rainfall and infiltration, groundwater movements, and evaporation as well as anthropogenic causes (leaking water pipes, excessive irrigation, etc.), which in turn may influence the engineering characteristics in response to loading.

- 3) The characteristics of arid gypseous soils are controlled by several factors including: types and forms of gypsum crystals (including their size and shape) and the gypsum content; presence of other salts (such as calcite and halite); environmental conditions (such as temperature, pressure and hydrological cycle) acting on the soil; particle size distribution and clay minerals (and content) present in the soil; mineralogical composition of soils; soil structure (i.e. dense or loose packing, hence stable or metastable); and loading applied. Therefore, prediction of the behaviour of these soils is difficult and complex and certainly merits addition research.
- 4) When considering the review, there appear to be potentially contradictory findings, including compaction test, hydraulic conductivity, swelling index, parameters of shear strength and unconfined compressive strength. This is due to the properties of gypseous soils that are influenced by many factors as mentioned in point 3, test conditions, test type, etc. Therefore, the common guideline for investigating gypseous soils needs to be developed to better realise safe design and construction of structures on these, potentially metastable soils.

In conclusion, all of the above points from the review have been indicated the need to conduct this study, as there is a clear lack of studies on the behaviour of gypseous soils under environmental conditions, such as temperature, breeze, water, and loading conditions.

CHAPTER THREE

MANUFACURING GYPSEOUS SOIL AND VALIDATION TEST

3.1 Introduction

To assess the effect of gypsum content on the geotechnical characteristics of a sand soil, an extensive laboratory methodology and programme was developed. This chapter considers the method developed to produce repeatable, laboratory-manufactured, gypseous soils required for the experimental phase of this research. The particle density of the sand, hydrated gypsum, and sand-gypsum mixtures, as well as the particle size distribution of sand, are presented. This chapter also covers the validation tests used to determine the collapse potential (CP) of the manufactured gypseous soil, and it also investigates the repeatability and applicability of the method used to create the gypseous soil used throughout this research (see Chapter Four). Single and double oedometer experiments have been conducted to investigate the collapse behaviour. Moreover, different subjects are presented, including the results of the standard consolidation tests, creep tests (post collapse), unconfined compressive strength tests, and the suction tests. The details of the devices used, the experimental setup, test procedures, calculations, testing programme, and the discussion of the experimental results of the laboratory test programme are considered in this chapter.

3.2 Creation of a Laboratory-Synthesized Gypseous Soil

3.2.1 Understanding the Natural Soil Deposits that the Manufactured Samples are Attempting to Simulate

The simulated gypseous soil samples are intended for use as a proxy for those naturally occurring in a region of Iraq. Laboratory-manufactured samples are being investigated due to the significant logistical challenges and legislation that effectively prevented the sourcing of undisturbed soil samples from Iraq.

The area of Iraq in question is the Al-Najaf province, which is located in the south-west of Iraq (see Figure 3-1). The reasons for selecting this area, and for focusing upon the engineering behaviour of gypseous soils in arid environments, is due to the frequent observation of cracks that develop within the walls and roofs of buildings that have been constructed on highly gypseous soils in this region. Furthermore, some buildings have experienced sudden failures in these soils, due to what is believed to be the formation of cavities (or loss of strength) under their foundations as a result of the dissolution and leaching processes of gypsum by groundwater, permeation of surface water (from irrigation or rainfall), or broken sewage/water pipes (NCCLR, 2005). Overall, the reports of damage to structures constructed in these soils due to loss of localised strength indicates that the soils of this region are metastable.

Al-Najaf has a desert climate and the mean rainfall is approximately 88 mm, falling mainly in the winter season; on average, evaporation exceeds precipitation (Sissakian et al., 2013; Al-Bahrani et al., 2014).

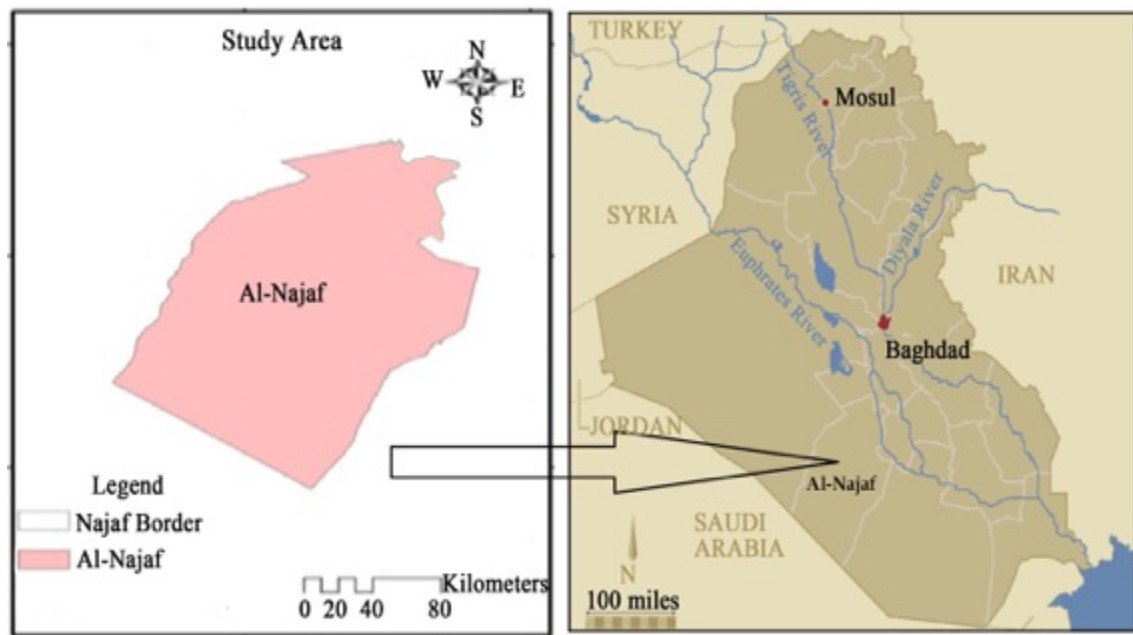


Figure 3-1: Map of study area (Al-Anbari et al., 2016)

The summer season is very hot, dry, and dusty; the mean ambient temperature is about 45°C, and on some days, particularly in August, the maximum temperature may increase to 50°C (Al-Bahrani et al., 2014). The ground conditions in Al-Najaf, like other areas in Iraq, is affected by the occurrence of sand and dust storms (Jassim and Goff, 2006; Abdul-Ameer, 2012; Sissakian et al., 2013). Accordingly, most of the secondary gypsum is formed through aeolian action due to the activity of wind erosion/deposition. In this case, secondary gypsum has been blown from the gypseous desert areas and has accumulated either a short or long distance away (depending upon the particle size of the material and the wind conditions), and the gypsum content for these soils, formed by this action, ranges from 6% to 30%, but the upper percentage is unusual (Buringh, 1960; Al-Zubaydi, 2017). It is suggested that two types of wind-transported material are commonly encountered during dust storms, these being as follows (Buringh, 1960; Sissakian et al, 2013):

- ‘Fine dust’, which consists of fine particles (maximum 0.06-0.2 mm) suspended in the air, often up to a height of 1 km. In stronger storms, the dust height reaches 3.5 km and can be transported over great distances.
- ‘Coarse dust’, which consists of coarser particles (0.15-0.25 mm and larger), which are transported along the Earth's surface in an air layer up to 15 m in height, or transported via saltation. It should be noted that this is the size (0.15-0.25 mm) that is used in this study to simulate the gypseous soil. Lees and Falcon (1952) estimated that the thickness of soil deposited each year in the Lower Mesopotamian Plain of Iraq by dust storms is approximately 2.5 mm. Figure 3-2 shows a heavy dust storm in the western desert of Iraq.



Figure 3-2: Dust storm in the western desert of Iraq (Sissakian et al, 2013).

Ideally, samples from the Al-Najaf region would have been used to investigate this behaviour, but this was not feasible; nor do the naturally occurring gypseous soils in the UK reflect those encountered in Iraq, and so they could not be used as a proxy. Therefore, in order to investigate the influence of gypsum minerals on soil properties under various environmental conditions, manufactured gypseous soil was prepared within a laboratory.

Al-Najaf soil comes in seven types; fluvial sediments, sabkha, sand dunes, aeolian sediments, sand sheet, gypsum sediments, and sedimentary rocks (limestone, sandy, silty, clayey with gravels), Figure 3-3 shows a photograph of some sedimentary rocks that are located in the Al-Najaf Sea (Aziz, 2008).

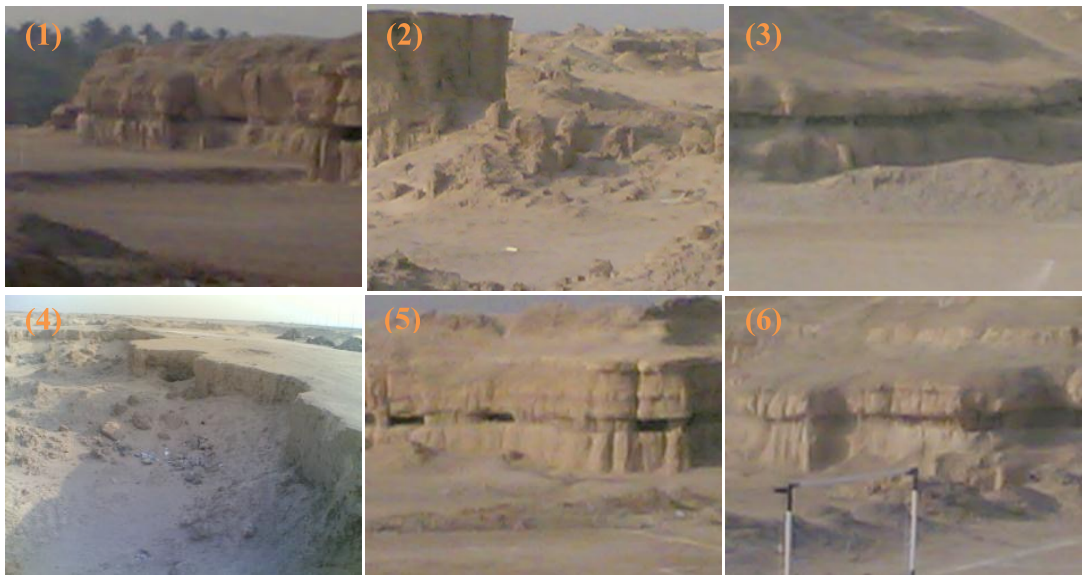


Figure 3-3: Photographs of sedimentary rocks in the Al-Najaf Sea (some of them have cavities) (Aziz, 2008).

In early prehistoric times, most of what is now Al-Najaf soil was under water (the Al-Najaf Sea); a remnant of the Al-Najaf Sea is located west of Al-Najaf city – the extent of its basin is 750 km². Accumulated sediments in this shallow sea eventually became limestone, shale, and sandstone. As a consequence of layered soil deposition, many sedimentary rocks are easily recognized today because of their stratified appearance. The limestone in the Al-Najaf Sea is predominantly crystalline calcium carbonate (calcite) formed under water. This rock forms from chemicals precipitated from solution, the remains of marine organisms, and the action of plant life. Gypsum formations can be found as crystals in the surface layer, as crusts, or can be recrystallized as a result of groundwater evaporation. The groundwater in the Al-Najaf Sea (Al-Najaf depression) is close to the surface. Previous periods of flooding have generated

changes in pore pressure, resulting in a continuous flow of ground water in the surrounding area (Aziz, 2008).

The soil profile in the Al-Najaf region is described as consisting predominantly of sand, which forms 76-100% of the (soil) particle size distribution, with gypsum mineral constituting 2-66% of the soil, a proportion that decreases as depth increases. It should be noted that the highest percentage of gypsum content (66%) is found in rock formations located in the Al-Najaf depression, whereas lower proportions (i.e. 6%-30%) are formed by the aeolian phase (secondary gypsum). Furthermore, the soil in general is classified as poorly graded, fine, medium, and fine-to-medium sand, with a cohesion varying from 0 to 21 kPa and an internal angle of shearing varying from 26.3 to 41.2 degrees (Aziz, 2008; Salih, 2013; Al-Dabbas et al., 2014; Fattah et al., 2015, Ali and Fakhraldin, 2016; Al-Zubaydi, 2017). Liquid and plastic limits vary from 21 to 29% and from 11 to 15%, respectively, but in most cases non plastic. The field dry density varies from 15.0 to 17.2 kN/m³, while the values of maximum dry density and optimum moisture content vary from 17.5 to 19.5 kN/m³ and 8.6 to 13.2%, respectively (Aziz, 2008; Al-Dabbas et al., 2014; Ali and Fakhraldin, 2016; Al-Zubaydi, 2017).

3.2.2 Previous Methods Used to Manufacture Gypseous Soils within the Laboratory and the Associated Limitations

Obtaining undisturbed samples of gypseous soils in many cases is very difficult, which has led previous researchers to prepare the gypseous soils in the laboratory (Frydman, 1979; Ismail et al., 2000; Haeri et al., 2005). However, many experiments that fabricate gypseous soils for laboratory-scale experiments to simulate field conditions adopted the simple practice

of mixing the constituents and compacting them to form the samples (Keren et al., 1980; Subhi, 1987; Al-Khafaji, 1997; Azam et al., 1998; Yilmaze and Civelekoglu, 2009; Ahmed, 2013; Estabragh et al., 2013; Salih, 2013; Aldaood et al., 2014; Al-Obiadi, 2014; Jha and Sivapullaiah, 2016). The mixing and compacting of gypsum (calcium sulphate hydrate) and sand would not simulate the mechanism in which they are deposited in nature and so would not produce samples with the required geotechnical parameters. Therefore, these methods were not embraced in this study; instead, a method was developed that better approximates the formation mechanisms to try to improve the quality (and suitability) of the samples created.

Akili and Torrance (1981) suggested a technique for the simulation of the development of cementation in sabkha material: chemically precipitating calcium carbonate or calcium sulphate within pluviated (i.e. sand-raining) sand samples. Laboratory experiments were carried out to model the sabkha materials of the Persian Gulf coasts in the laboratory. Sabkha soils consist predominantly of reworked aeolian sands with varying amounts of cementing agents, such as calcium carbonate and calcium sulphate (gypsum and anhydrite) (Fookes, 1976; Akili and Torrance, 1981; Fookes et al., 1985; Al-Amoudi, 1994). Sabkha soils appear to have high strengths under dry conditions but are significantly weakened, with an increase in compressibility, when fully or partially saturated. To reproduce sabkha at laboratory-scale, the 'evaporative pumping mechanism' was achieved. A solution that was saturated with calcium carbonate or calcium sulphate was passed through the sand layer. As a consequence of applying a heat source above the sand surface, the oversaturated calcium sulphate soluble salt moves towards the soil's surface via capillary action. The calcium sulphate solution evaporates, leaving the gypsum crystals throughout the unsaturated sand above the water table

and mainly accumulated on the sample surface, forming a crust layer. Its thickness is a function of the sample's age, whereas underneath the crust layer there is no visible evidence of gypsum accumulation. However, the principle of precipitating the gypsum crystals once the soil fabric is produced was deemed to be an interesting approach when considering the methodology for creating gypseous soils.

French et al. (1982) and AlNouri and AlQaissy (1990) reproduced Akili and Torrance's (1981) method when producing gypseous soil samples, but once again compacted the soil instead of pluviating the soil. French et al. (1982) highlighted the significance of soil fabric on the 'deposition quality' of the gypsum crystals by noting that the fine sand content was critical when inducing capillary-driven advection of the calcium sulphate solution into the soil.

Akili and Torrance (1981) suggested an alternative approach. Instead of permeating the sample with the solution of calcium carbonate or calcium sulphate, a calcium chloride solution (CaCl_2) was permeated into a pulviated sample comprising a mixture of sand-powdered sodium carbonate (Na_2CO_3), or sand-granular sodium sulphate (Na_2SO_4). The solution permeated from the bottom (through a sand filter) and moved upwards through the soil column; the chemical compounds reacted to produce the calcium carbonate or gypsum. The solution was passed through the sample for one week to assure complete reaction, and after this point, the samples were dried by passing a warm dry air through the sample.

Whilst these approaches were an improvement on mixing the gypsum and soil together and compacting the mixture, there are certain drawbacks with the use of these alternative

methods. One of these is the time required to inundate the samples with the fluid, allow for the chemical reactions to take place, and then dry the sample to the desired water content level, particularly for manufacturing a large volume sample. Furthermore, there is difficulty in controlling the precipitation of the crystals within the soil profile. Whilst open fabrics were produced, this approach would appear to make it difficult to produce the ‘homogeneous’ samples (with constant gypsum contents with depth) desired for a parametric study.

Haeri et al. (2005) adopted an ‘undercompaction’ method, which was first proposed by Ladd (1978), to prepare samples cemented with gypsum for triaxial testing. In this approach, each subsequent layer is typically compacted to a lower density than the previous value by a predetermined value, to produce a sample with the desired properties. Hence, the basic principle of the ‘undercompaction’ method differs from the methods reported in the ASTM or BS specifications, which involve applying a constant comparative effort to each layer. The procedure incorporates a tamping method of compacting moist, sandy gravel soil with the desired amount of gypsum (1.5%-9%, already incorporated into the soil) in layers. Following this, the samples were extracted from the mould and allowed to cure in the oven at 50°C until no change in their weight was recorded. However, this method is not feasible for fabricating samples on a large scale due to the effort required and the difficulty in controlling the homogeneity of soil, and hence it was recommended that the maximum height of the layers should not exceed 25 mm for samples with diameters less than 102 mm (Ladd, 1978).

Lee et al. (2010) presented an alternative approach that purported to fabricate a homogenous sample within a ‘standard’ time, enabling the creation of large samples as well as small ones. It adopted the concept of air pluviation and the pre-wetting method, which were proposed by

Rad and Tumay (1986) and Puppala et al. (1995), in order to reduce the segregation between the sand particles and the gypsum. To reconstitute a homogeneous sand-gypsum mixture, a pre-wetted sand mixture (containing gypsum at content levels varying from 5% to 10%) was pluviated in a large chamber (with dimensions of 120 cm in diameter and 100 cm in length) as one layer. Seating pressure (vertical pressure) was applied to the sample (at 50, 100, and 200 kPa), and then distilled water was inundated to form the chemical bonds before a 24-hour curing period.

Although this method is considered to be a more suitable approach for obtaining a large, homogenous sample in a standard time than the chemical precipitation or evaporation approaches, it does suffer from a number of flaws. Firstly, there is the inconvenience of the compression; inserting the water from the base of the sample under a high seating pressure (at 50, 100, and 200 kPa) can lead to an exaggeration of the recorded settlement for the height of the sample. Secondly, the curing time is insufficient for developing the bonds between the gypsum and sand particles, as the sample is cured only for 24 hours under the loading and saturation conditions before testing.

3.2.3 A Summary of the Method Developed for this Investigation

There were clearly positive aspects in the sample-creation approaches of each of the previous methodologies for manufacturing gypseous soils, although each also had negative aspects (in some cases, significant ones). Therefore, a bespoke method was developed for this project (described in detail in Section 3.4).

Taking into consideration the origin of secondary gypsum deposits formed in the area of study

in Iraq (Al-Najaf), it seems that the air pluviation technique presented by Lee et al. (2010) for large and small samples is the most suitable method for simulating gypseous soil in the laboratory. However, modifications to this method were required. The problems of Lee et al.'s (2010) method were greatly minimized by a reduction of the seating load to 5 kPa and by circulating the water from the sample base after removing the seating load. A small sample (an oedometer-sized ring; 75 mm in diameter and 20 mm in height) was chosen to develop the new method and assessed for its suitability for use in the large test (details of the sample preparation are given in Section 3.4.4).

In this study, larger samples were manufactured in layers simulating the deposition in the field (more detail is presented in Chapter Four), with a small seating stress of 5 kPa (mirroring a certain pre-consolidation pressure) being applied to the sample after the creation of each layer. After two hours, the seating pressure was removed and then distilled water was circulated from the sample's base via capillary action. To form the bonds between the sand particles and the gypsum, each layer was given time to dry before the next layer was created on top in an attempt to imitate the arid climate (Note that small samples can be created using one layer). Finally, the whole sample was left to dry, at which point it was ready for testing. The following sections describe the materials used, the procedure involved in sample creation, and validity testing in more detail.

3.3 Materials Properties of the Manufactured Soils and Classification Tests

3.3.1 Materials Used in the Soil

Silica sand is a commercially available washed and sieved sand, which was supplied by Bathgate Silica Sand Ltd. It is a high-purity, fine sand, and is pale buff in colour, all of which

makes it similar to Al-Najaf soil. The British Standard tests (BSI, 1990) were carried out to determine the physical properties of the sand, such as particle size distribution, maximum and minimum index density, and particle density. The soil is classified as poorly graded sand (SP) according to the Unified Soil Classification System (USCS). The properties of the sand are tabulated in Table 3-1 and the particle size distribution performed for this sand is shown in Figure 3-4.

The gypsum used in this study for preparing the manufactured gypseous soil, supplied by the British Gypsum Company, is a very fine powder that can pass through an 80- μm sized sieve and has a purity of more than 99.0%. Gypsum was added to simulate the gypseous soil in the field, which contains varying gypsum content. Throughout this study, the expressed gypsum contents were calculated on a weight by weight basis of dry gypsum with oven-dried sand.

Table 3-1: Physical properties of sand.

Test Type	Parameter	Value	Specification
Grain size distribution	D10	0.09	BS 1377-2:1990, Clause 9.2
	D30	0.15	
	D50	0.18	
	D60	0.19	
	C_c	1.32	
	C_u	2.11	
	USCS	SP	
Particle density	Gs	2.64	BS 1377-2:1990, Clause 8.3
Maximum dry density	$\rho_{d\max} (\text{Mg/m}^3)$	1.79	BS 1377-4:1990, Clause 4.2
	e_{\min}	0.47	
Minimum dry density	$\rho_{d\min} (\text{Mg/m}^3)$	1.47	BS 1377-4:1990, Clause 4.4
	e_{\max}	0.80	

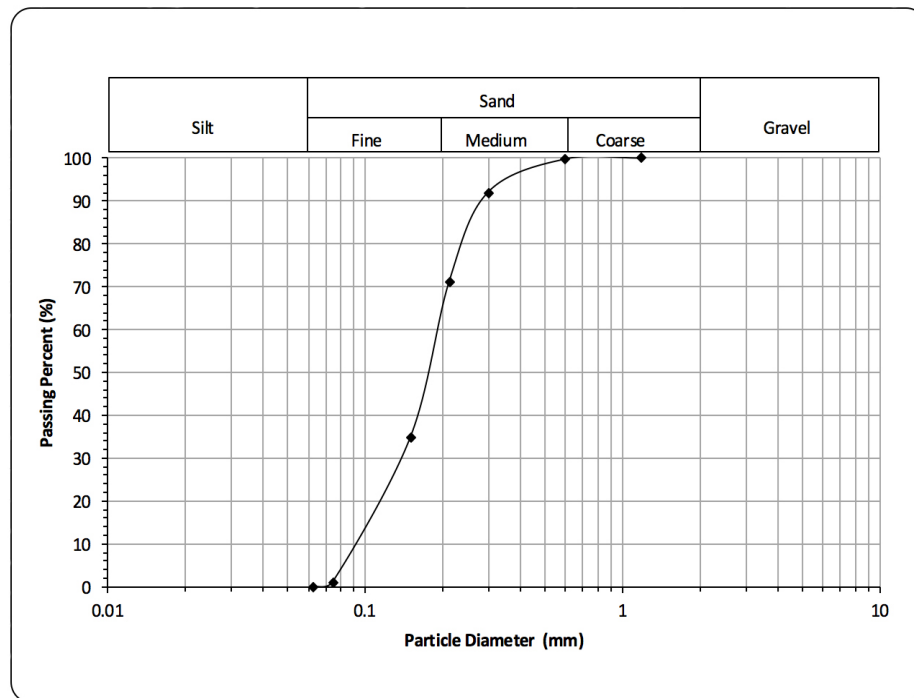


Figure 3-4: Particle size distribution of sand.

3.3.2 Physical Tests

The physical properties of the gypsum powder and the manufactured gypseous soil (i.e. the sand-gypsum mixture) were ascertained according to the British Standard (BS 1377-2:1990) procedures. These tests comprise the calculation of water content and particle density.

3.3.2.1 Particle Density

The particle density test was determined according to the procedure described in (BS 1377-2:1990, Clause 8.3). Distilled water is usually used for particle density determination, but for samples contain gypsum mineral, it may yield erroneous results, as the gypsum may dissolve and the solids may decrease in volume and mass. Therefore, white spirit was used in the determination of particle density instead of distilled water (BS 1377-2:1990, Clause 8.3).

The particle densities of the pure gypsum and the sand were calculated to be 2.32 and 2.64, respectively. Accordingly, the particle density for the sand-gypsum mixture reduced with increasing gypsum contents (see Table 3-2).

Table 3-2: Particle densities with different of gypsum contents.

Gypsum content (%)	Particle density
5	2.62
10	2.60
15	2.58
20	2.57
25	2.55
30	2.54
40	2.50

3.3.2.2 Water Content

The determination of water content was conducted by following the British Standard (BS 1377-2:1990, Clause 3). A standard drying temperature of 105°C was used for the sand sample (BS 1377-1:1990), while a drying temperature not exceeding 45°C was used for the gypseous samples in order to prevent the loss of crystallization water within the gypsum and prevent phase transform. Nelson et al. (1978), Sirwan et al. (1991), Porta (1998), and Al-Mufti and Nashat (2000) recommended that the drying temperature of gypseous soil should not exceed 40-50°C, in order to avoid gypsum transformation.

3.3.3 Determination of Gypsum Content

A number of methods have been developed to quantify gypsum content in soils. The available methods can be grouped, according to their basic principles of gypsum determination, into three categories: wet chemical methods, X-ray techniques, and thermogravimetric methods

(Hesse, 1976; Skarie et al., 1987; Porta, 1998; Lebron et al., 2009). The wet chemical methods are based on the dissolution of gypsum in water; when all the gypsum of the sample has been dissolved, it is possible to analyse SO_4^{2-} or Ca^{+2} concentrations to back-calculate the original amount of gypsum in the sample.

X-ray diffraction can be used for qualitative identification of the presence or absence of gypsum on oriented samples (Khan and Webster, 1968). Nevertheless, it needs complicated and expensive instruments and is time consuming, which was a logistical issue in this study. Furthermore, determination of gypsum content by using this method is not recommended because of its inaccurate results due to the preferred orientation of gypsum crystals (Skarie et al., 1987; Porta, 1998).

The thermogravimetric method is based on the loss of weight as a result of heating gypseous soil. The loss of weight is due to the dehydration of the gypsum (Porta, 1998). Nelson et al. (1978) proposed a method for gypsum content determination based on this principle. In this method, the gypsum content is determined from the loss of crystal water upon heating to 105°C for 24 hours. Al-Muftly and Nashat (2000) had developed this method. The gypsum content can be determined by oven drying the soil sample at 45°C until its weight becomes constant, thereafter the same sample is dried at 105°C until the weight becomes constant. The gypsum content is calculated from Equation 3.1:

$$X (\%) = \frac{W_{45^\circ\text{C}} - W_{105^\circ\text{C}}}{W_{45^\circ\text{C}}} \times 4.778 \times 100 \quad \text{Eq. 3.1}$$

Where X is the gypsum content as a percentage; $W_{45^{\circ}\text{C}}$ and $W_{105^{\circ}\text{C}}$ are the weights of the sample at 45°C and at 105°C , respectively; and 4.778 is a constant.

It is worth mentioning that the thermogravimetric method (by Al-Mufti and Nashat, 2000) was the method used in this study to calculate gypsum content (see Section 3.5.2).

3.4 Creating Gypseous Samples Using the Pluviation Technique

3.4.1 Air-Pluviation Method

The air pluviation method is carried out by allowing dry sand particles to fall freely through the air into a container from a perforated plate (shutter) located in the end of a hopper (sand storage). The apparatus should contain a diffuser (a set of sieves) below the shutter; this is because the sand flowing through the shutter can form ‘columns’ in the air. By passing the sand through the sieves, the fall of the sand columns is disrupted, resulting in a more uniform ‘sand rain’ into the collection chamber (considered in more detail in Sections 3.4.2 and 3.4.3). The air pluviation method mimics aeolian deposition (Khari et al., 2014; Huang et al., 2015) and has been widely validated for the preparation of repeatable and highly reliable homogenous sand beds with verifiable and controllable relative densities for laboratory studies (Oda et al., 1978; Rad and Tumay, 1987; Presti et al., 1992; Fretti et al., 1995; Dave and Dasaka, 2012). Moreover, the pluviation approach has a number of attractive features when compared to vibration and tamping methods, such as a higher level of maximum dry density, better control of the density (and hence air void content), negligible particles crushing, less segregation regardless of particle size, the ability to replicate natural soil deposition, and better repeatability (Rad and Tumay, 1987; Presti et al., 1992, 1993; Choi et al., 2009; Dave and Dasaka, 2012). In addition to these positive characteristics, this technique

yields good results when reproducing a large sample for laboratory testing (Fretti et al., 1995; Dave and Dasaka, 2012), which was a key consideration for this study. Therefore, pluviation of the sand particles through air was selected for manufacturing gypseous soil samples.

3.4.2 Factors Affecting the Pluviation Method

Factors found to be influencing the design of a sand pluviation apparatus, which in turn affect the relative density achieved, have been explored in several studies (Mori et al., 1977; Tumay et al., 1979; Miura and Toki, 1982; Vaid and Negussey, 1984; Rad and Tumay, 1986, 1987; Sweeney and Clough, 1990; Brandon et al., 1991; Presti et al., 1992, 1993; Fretti et al., 1995; Yamamuro and Wood, 2004; Ueng et al., 2005; Khari et al., 2014). The key findings from these studies concern the following:

- **Falling Height (FH):** the distance between the lower diffuser sieve (installed below the shutter) and the sand sample surface, or the distance from the perforated hopper base to the soil bed surface if there is no diffuser. In general, the kinetic energy of a single soil particle is directly correlated to the falling height and to the mass of the particles, i.e. the grain size. It is found that increasing the falling height increases the relative density. However, it is noted that the relative density increases with increasing FH up to a limiting value; or, in other words, beyond a certain value of FH, any further increase in height becomes negligible. Theoretically, critical height is expected to be greater for coarser soils than those for finer-grained soils.
- **Falling Distance (FD):** the distance between the shutter and the upper diffuser sieve. Since the velocity of the sand particle ‘columns’ (formed as the soil falls through the aperture(s))

in the shutter) upon reaching the sieve depends on the value of the FD, then this velocity determines the initial velocity of the sand rain emanating from the bottom sieve, which impacts upon the value of the FH. The higher the initial velocity, the lower the FH required. In other words, the FH and FD are related since both control the terminal velocity of the sand rain. For this reason, to diminish the effect of the FD on FH, many researchers confirmed that the FD should exceed 40 cm.

- Deposition Intensity (DI): the mass of soil falling in the mould per unit area per unit time. It has been indicated that for the same FH and shutter-hole pattern, the larger the shutter porosity (which is the ratio of the cross-sectional area of the holes against the cross-sectional area of the whole shutter), the lower the relative density. The relative density is inversely proportional to the shutter porosity and is affected significantly by the soil type.
- The diffuser sieve is used to disperse the sand columns in order to achieve a uniform sand distribution. It was observed that two diffuser sieves are adequate for homogeneous pluviation, and additional sieves have no effect on the homogeneity of the sample and only a minor effect on the relative density. Therefore, it was recommended that two completely parallel and horizontal sieves should be used in the construction of the diffuser and that they should be rotated 45° horizontally with respect to each other and be placed 5 to 10 cm apart. However, during the test, special attention has to be paid to verify that the sand particles do not collect on the sieves before being deposited in the collector, otherwise the FH is incorrect. The standard sieve size of 6.3 mm is recommended for most cases.

- It was suggested that samples be obtained at different relative densities by changing the shutter porosity (deposition intensity) and keeping the FH constant. This becomes important when attempting to produce large samples. Nevertheless, if the FH cannot be kept reasonably constant during a test, an FH in excess of the terminal FH (an FH above which an increase in the FH has little or no influence on the relative density) should be used.
- For a given set of factors, different results are obtained based on the mean grain size (D50) and the grain size distribution of the sand. It was noticed that the relative density increased with increasing D50. This is due to the fact that as the soil particles increase in size, its impact on the soil particles below will be higher.

Together, these studies indicate that shutter porosity, or deposition intensity, plays a vital role in the maintenance of relative density. The FH, the hole size of the diffuser sieve, and the shutter-hole pattern have less pronounced effects, and the effects of the sand height in the container, the FD, the distance between the diffuser sieves, and the number of sieves used in a diffuser on relative density are relatively negligible. These findings were used in the design of the experimental apparatus used in this study.

3.4.3 Design of Pluviation Apparatus

Based on the background (previously described in Section 3.4.2) and following the design steps presented by Rad and Tumay (1987), the air pluviation apparatus was developed to control the density and void ratio of manufactured gypseous sand soils. It is worth mentioning that all the parameters (shutter porosity, diffuser, and FH) basically depend on the sand

properties; as one sand was used in this study, these parameters were fixed, whilst the gypsum content was varied to investigate the influence of gypsum levels on the density and void ratio of sand soils. The apparatus used to prepare the samples is depicted in Figure 3-5, and consists of the following:

- The soil container (hopper).
- The shutter, which is a perforated plate positioned in the base of the hopper that allows the soil particles to fall. The shutter porosity was 15.84% (Figure 3-5c).
- Two horizontal sieves are used as the diffuser; the meshes of the two sieves are rotated 45° out of phase in order to increase the diffusion of the particles and to ensure the uniform deposition of particles (Figure 3-5d). The distance between them is 5 cm with 3.35 mm sieve aperture (based on the maximum sand particle size), as this did not result in the accumulation of the sand on the sieves.
- The FD is held constant and equal to 45 cm for all the tests (note the depiction of the sand falling in columns between the shutter and the sieves in Figure 3-5b).
- The FH is 20 cm, which was found to correspond to the average dry density of 1.61 Mg/m³ and the average relative density of 49% (Figure 3-6) (note the depiction of the sand falling as rain between the sieves and sample container in Figure 3-5b). This dry density was chosen as it represents the average for the study area (with the field dry density varying from 1.50 to 1.72 Mg/cm³, as mentioned in Section 3.2.1.).
- The sample container (otherwise known as the collector or mould).
- The top cap, which is placed over the sand and connected to the diffuser via four strings (to keep the FH constant).

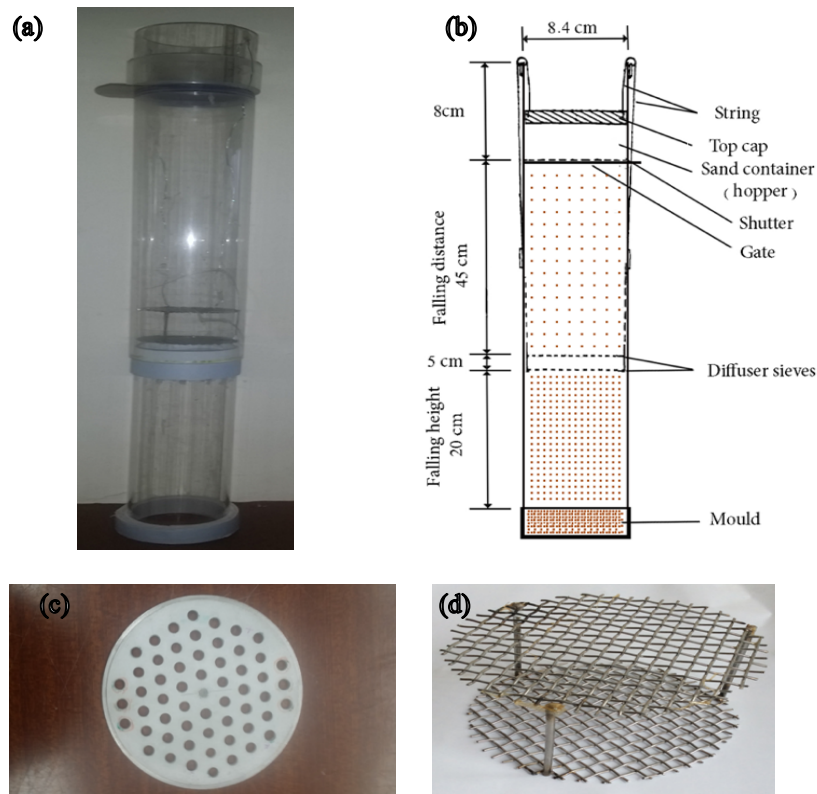


Figure 3-5: Air pluviation apparatus; (a) photograph of pluviation apparatus, (b) systematic diagram, (c) shutter with a porosity of 15.84%, (d) diffuser (two-sieves) with 3.35 mm sieve aperture.

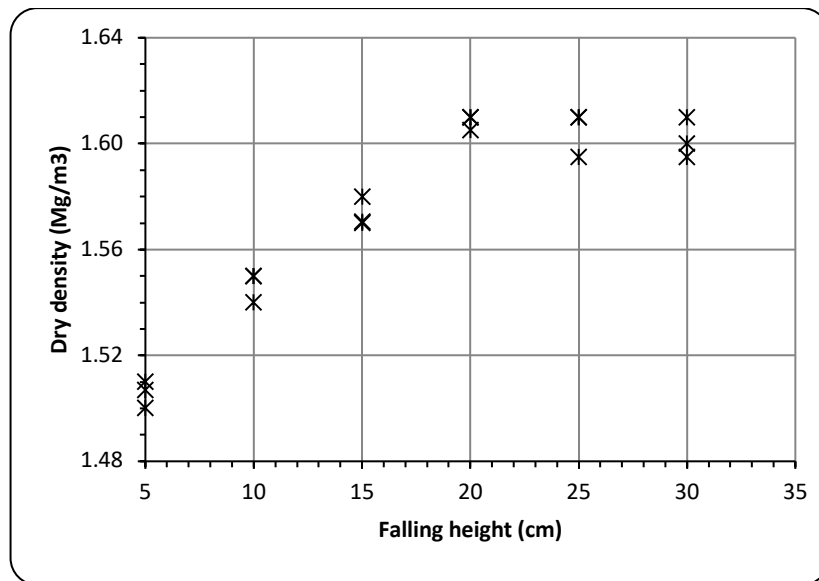


Figure 3-6: Variations of sand density with FH.

3.4.4 Sample Preparation

3.4.4.1 Issues with the Sand-Gypsum Mixtures during Pluviation

It was found that pluviating a dry sand-gypsum mixture resulted in segregation, as the sand particles and gypsum crystals have different falling velocities; in addition, the gypsum crystals are prone to adhering to the pipe surface (see Figure 3-7). Resulting in pluviated samples that may not be uniform. Therefore, a pre-wetting method, suggested by Rad and Tumay (1986) and Puppala et al. (1995) to reduce segregation between Portland cement and sand, was subsequently trialled. It was found that the pre-wetting of the sand potentially reduced the segregation between gypsum and sand during pluviation by moistening the surface of the sand grains, thus causing a uniform and homogenous coating of the grains with the gypsum crystals. A health and safety requirement necessitated the sand to be washed with distilled water through a 63 μm sieve and then oven dried at 105°C to reduce the dust generated during the raining method.

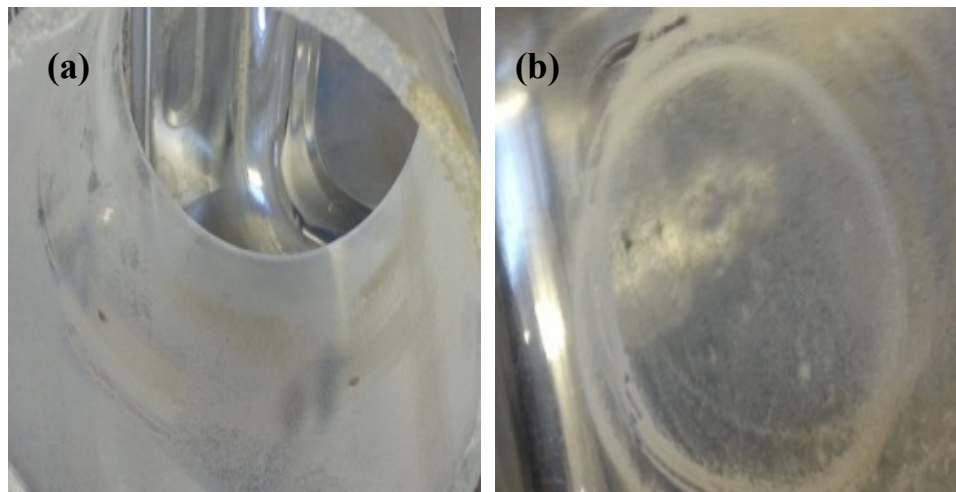


Figure 3-7: Gypsum segregation when the mixture is pluviated in dry conditions; (a) gypsum powder on the pipe surface, (b) gypsum powder accumulated around the mould on the tray.

3.4.4.2 Manufactured Gypseous Samples

This section described the development of a sample within small size (an oedometer-sized ring; 75 mm in diameter and 20 mm in height) to investigate the validity of pluviation method in terms of void ratio and gypsum content. A ring was fixed on a porous stone by adhesive to prevent movement during sample preparation, and then filter paper was inserted. It should be mentioned that only distilled water was used throughout this study. Sample preparation comprises four stages:

- 1) Pluviation stage: the required oven-dried sand is weighted and placed on a glass plate and an amount of water equivalent to 0.75% water content by dry sand is sprayed over the sand, which is then mixed manually using a palette knife. Then, the desired gypsum content is added to the moistened sand. This mixture is mixed gently to obtain a homogenous colour. Any gypsum on the knife blade is wiped off into the sample and the mixing is continued for an additional 2 minutes. The sand-gypsum mixture is then carefully transferred into the top chamber in the pluviation setup (hopper). The hopper is tapped by hand until the sand-gypsum mixture level reached a designated level and the top cap, connected to the diffusers with four strings, is then positioned over the sand. When ready, the shutter gate is removed, the mixture pours through the holes in the shutter, and the level of the mixture in the container is reduced (leading to a downward movement of the top cap). This movement raises the diffusers and keeps the FH for the sand particles constant in order to ensure a relatively homogeneous sample. Rad and Tumay (1987) experimentally proved that changes in the FD during a test caused by the diffuser ascending towards the hopper would not appreciably affect the relative density. When pluviation is complete, the pluviation apparatus is carefully

lifted from the mould, the upper surface is smoothed, and the sample is weighed to calculate the actual dry density for this stage.

- 2) Loading stage: having manufactured the samples in the pluviation apparatus, they are then secured in the oedometer cell. This is placed in the oedometer apparatus, and the loading arm and disc are lowered onto the samples. A vertical stress equivalent to 5 kPa is applied to the oedometer for 2 hours, which was found to be sufficient to allow the samples to come to equilibrium with no further deformation. This was achieved by monitoring the dial gauge reading. At the end of the 2-hour period, the loading and disc cap are released.
- 3) Soaking stage: to initiate gypsum crystal growth, distilled water is allowed to enter the samples from the bottom (porous stone) by capillary action for 4 hours to replace the air.
- 4) Drying stage: finally, in order to form the cementing bond between the sand particles, the samples were removed from the oedometer cell, drained and dried at 25°C in the oven for three days to obtain completely dry samples.

It is important to mention that application of the seating load and water clearly resulted in compression of the sample (the greater the gypsum content the more pronounced the change, Section 3.5.1). This seating load was undertaken to produce a relatively constant void ratio, regardless of gypsum content, to allow for investigation into the effects of gypsum content on the properties of the samples. To ensure the 'initial' sample height, dry density and void ratio

were known when testing commenced, the depth of settlement was recorded using a digital caliper. Figure 3-8 shows the steps of sample preparation.

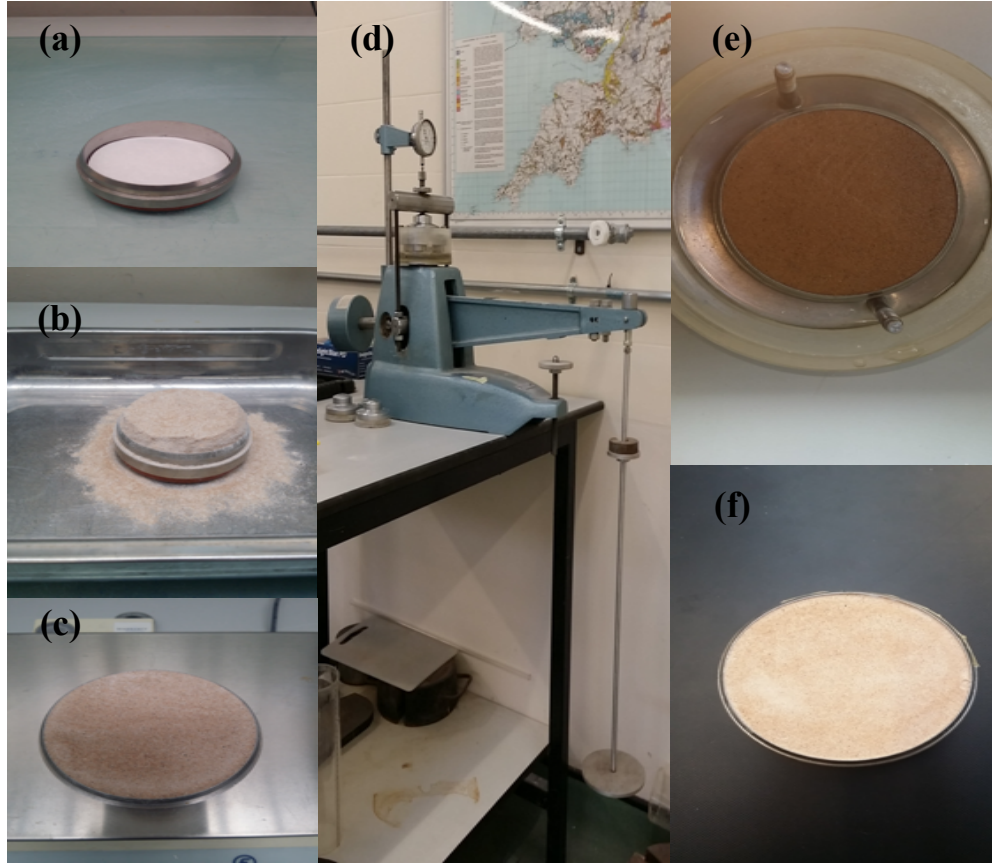


Figure 3-8: Steps for sample preparation; (a) oedometer ring preparation, (b) pluviation stage, (c) levelling the sample surface and weighing it to calculate the dry density for the pluviation stage, (d) loading stage, (e) soaking stage, (f) drying stage.

3.5 Feasibility of the New Method

3.5.1 Discussion of Sample Preparation by the Pluviation Method

The method selected in this study to manufacture the gypseous samples involved four preparatory stages: stage 1, pluviation; stage 2, loading; stage 3, soaking; and finally, stage 4, drying (which is essentially the cementing of the bonds between the sand particles and the gypsum). The initial void ratio and corresponding dry unit weight versus gypsum content are

shown in Figure 3-9 for the pluviation stage (stage 1) and the loading, soaking, and drying stages (stages 2, 3, and 4). It can be seen that at the pluviation stage, the void ratio significantly increases with increases in gypsum content, whereas the corresponding dry unit weight decreases with decreases in gypsum.

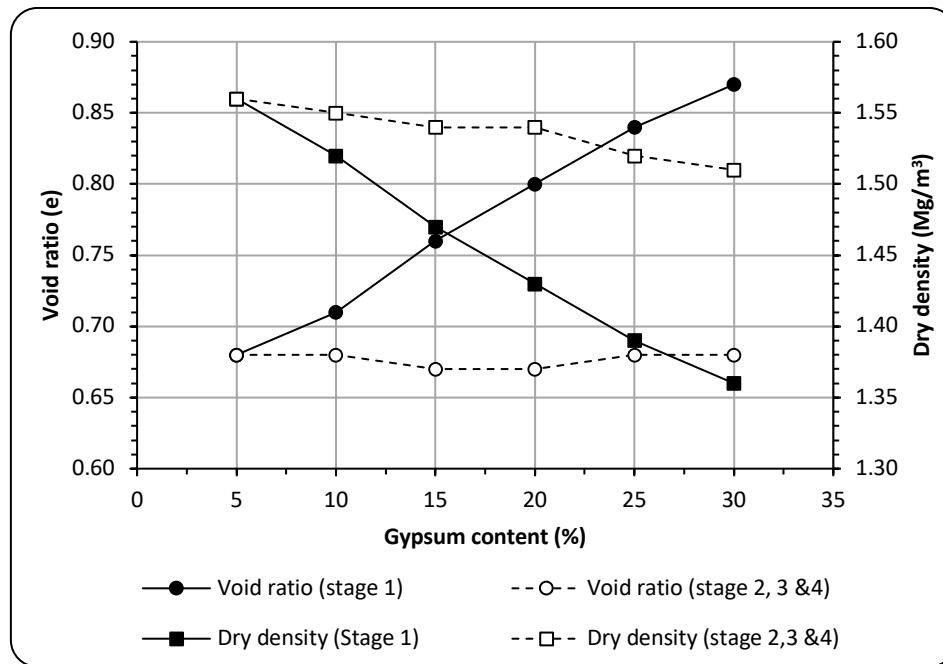


Figure 3-9: The initial void ratio and corresponding dry unit weight versus gypsum content for the pluviation stage (stage 1) and the loading, soaking, and drying stages (stages 2, 3, and 4).

The sample properties at the pluviation stage (stage 1) seem to be consistent with the findings of Petrukhin and Arakelyan (1984) and Livneh et al. (1998), who found that the variation in gypsum content in the soil impacts upon the initial void ratio (see Figure 3-10). It was found that increases in gypsum content within sand soils causes an increase in their void ratio, as there are little or no cohesive forces to prevent the enlargement of pores with crystal growth. In fact, this explanation is applicable for the pluviation stage, which simulates juvenile, gypseous, aeolian deposits (in arid environments) before they are buried under subsequent

layers of deposited material, or exposed to environmental changes (which stages 2-4 of the sample creation process attempt to simulate).

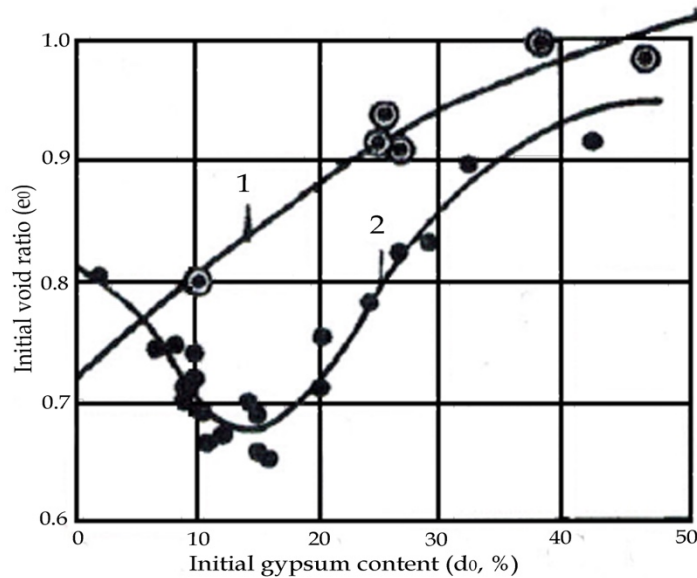


Figure 3-10: Variation in initial void ratio (e_0) versus initial gypsum content (d_0 , %); sand and clay are referred to by 1 and 2 on the graph, respectively (Petrukhin and Arakelyan, 1984).

This explanation (changing void ratios with changing gypsum content), therefore, is not complete, because the effect of the overburden pressure on the crystallization process was not taken into consideration. The variation of the initial dry unit weight with gypsum precipitation is expected to be the opposite of the variation of void ratio, insomuch that increasing the gypsum content yields lower dry densities if the porosity remains unchanged, as the particle density of the gypsum is lower than that of other soil constituents (once again, as observed in stage 1 of sample preparation).

During the loading stage, a decrease in the sample's height was observed with the application of 5 kPa of load, leading to a reduction in the initial void ratio. After the application of the load, water was introduced into the sample via capillary force, which also resulted in a

noticeable reduction in the height of the sample (Figure 3-9 presents the dry density and void ratio after stages 2, 3, and 4 as a combined stage). This reduction in the sample's height increases with increasing gypsum content, as exhibited in Table 3-3.

Table 3-3: Variation in initial void ratios and dry densities through sample preparation.

Gypsum content (%)	After pluviation stage		After loading, soaking, and drying stages		Height of surface collapse (mm)
	Initial void ratio (e_o)	Dry density (Mg/m^3)	Initial void ratio (e_o)	Dry density (Mg/m^3)	
0	0.64	1.61	0.64	1.61	0.0
5	0.68	1.56	0.68	1.56	0.0
10	0.71	1.52	0.68	1.55	0.4
15	0.76	1.47	0.67	1.54	0.9
20	0.80	1.43	0.67	1.54	1.4
25	0.84	1.39	0.68	1.52	1.7
30	0.87	1.36	0.68	1.51	2.0

The application of stages 2 and 3 to the pluviated samples resulted in a relatively consistent void ratio and dry density for the samples regardless of gypsum content. Hence, any increase observed in the collapse potential of the samples correlated with increasing gypsum content can be explained by considering the properties of the gypsum crystals that formed within the fabric of the soil and no other factors (such as higher initial void ratio). This was the fundamental reason for implementing stages 2 and 3 during sample manufacture (to provide a constant void ratio, or dry density, with changing gypsum content). To examine the efficiency of the designed and implemented sample preparation techniques by aeolian, gypseous sand soils, the reproducibility of samples is examined in terms of initial void ratio and gypsum content. Each sample was repeated five times, each with a specific gypsum percentage. Each result shown in Table 3-3 represents the average of five replicates.

It is believed, from the data presented above, that the method developed for this study offered several advantages when considering the manufacture of gypseous sand samples; namely, the successful production of repeatable samples, the relative simplicity of the equipment, flexibility, the relatively short time required to prepare a sample, and no particle crushing during the sample preparation in comparison with the compaction method (especially where gypsum particles that are soft crystals with a hardness rating on the Mohs scale of 2 are concerned) (Klein and Hurlbut, 1985).

Difficulties arose, however, when an attempt was made to prepare a sample with a gypsum content higher than 30%. This was due to the increase in the percentage of finer particles (i.e. gypsum crystals), and so to minimize segregation, more water was required during mixing prior to pluviation than was used for samples with lower gypsum-content levels. This led to flocculation of the gypsum and sand particles, which in turn blocked the shutter and hampered the raining of the particles. Nevertheless, as earlier mentioned in Section 3.2.1, soils with gypsum content much greater than 30% are considered to be relatively rare in the arid, aeolian, gypseous soils encountered in Iraq, and so 30% gypsum content was taken as the upper limit for this study.

3.5.2 Gypsum Determination by the Thermogravimetric Method

Whilst gypsum was introduced to the sample during the sand-gypsum mixing process and every effort was undertaken to ensure that gypsum was not lost during pluviation, some losses were to be expected. Therefore, a method was required to measure the gypsum content of the manufactured samples (i.e. post pluviation, loading, wetting and drying). Al-Muftly and Nashat's (2000) method, previously outlined in Section 3.3.3, was adopted to determine the

gypsum content of the prepared samples. Subsamples were taken from the samples produced and the gypsum content was measured five times, with the mean taken. The measured gypsum content after the completion of the sample preparation process (i.e. pluviation, loading, wetting and drying stages: Table 3-4) were found to be relatively close to that of the target contents. Hence, it was concluded that whilst a small proportion of gypsum was being lost during preparation, the magnitude of these losses was deemed an acceptable, if undesirable, error associated with the creation of the samples. Please note that when the gypsum content for the samples produced in this study are described (5%, 10%, etc.), those descriptions will refer to the gypsum content at the time of initial preparation of the soil prior to pluviation; as such, the actual gypsum content of the samples will vary slightly.

Table 3-4: Gypsum content determined by Al-Mufti and Nashat's (2000) method.

Target gypsum content during mixing (%)	Measured gypsum content after complete samples preparation process (%)
5	4.7
10	9.7
15	14.5
20	19.5
25	24.1
30	29.4

3.6 Validation Testing

In this section, a comprehensive validation of the experimental programme was carried out on the manufactured gypseous soils in an effort to determine their compaction, compressibility, compressive strength characteristics, and suction test including wetting and drying path. It also describes the sample-preparation procedure, the apparatus used, the testing procedure, the testing programme, and a discussion of the results.

3.6.1 Compaction Test

Compaction is the densification of soils with the application of mechanical energy to reduce the amount of air voids (Holtz and Kovacs, 1981). To investigate the influence of gypsum content on the optimum moisture content and the maximum dry density of the manufactured gypseous soil, the compaction characteristics were determined for the following gypsum levels: 0, 5, 10, 20, 30, and 40% (by weight of dry sand). The compaction characteristics of the manufactured gypseous soils are described according to the procedures in (BS 1377-4:1990, Clause 3). Standard Proctor compaction was used, applying 27 blows from 2.5 kg rammer, dropped from a height 300 mm, to compact the soil in three equal layers into a one-litre compaction mould. Gypsum is considered vulnerable to crushing during compaction due to the softness of gypsum crystals (which have a hardness rating of 2; Klein and Hurlbut, 1985). This could cause gypsum crystals to reduce in size due to the action of the 2.5 kg rammer. For example, Horta (1980) found out that gravel-sized particles of gypsum could be broken down to sand-sized particles under the compaction process. This is an unavoidable consequence of the process, although for the purposes of this investigation, an attempt was made to limit this effect by only using a mixture once (and not recycling it), thus using separate batches of sand-gypsum mixtures at each water content, (following BS 1377-4:1990, Clause 3).

To produce a mixture for compaction, a predetermined weight of dry sand was mixed with a predetermined amount of water, which was equivalent to the optimum moisture content for the sand, in an electrical mixer for 4 minutes. Then the desired gypsum content was added and mixed thoroughly for another 10 minutes in order to obtain a homogenous mixture. The

mixed soil was poured onto a tray and air-dried for one week to facilitate the growth of the gypsum crystals prior to the commencing of the compaction test (Figure 3-11).



Figure 3-11: Preparing the batches of sand-gypsum mixtures before starting the test.

3.6.1.1 Compaction Test Results

The results obtained from the compaction test are shown in Figure 3-12. Table 3-5 presents a summary of the statistics for the maximum dry densities and related optimum moisture contents, along with the void ratios, porosities, and saturation degrees that were calculated based on the volume-mass relationships. It can be seen from Figure 3-12 and the data in Table 3-5 that the compaction parameters are significantly affected by changes in gypsum content (which ranged from 0% to 40%).

The influence of gypsum content on compaction parameters is illustrated in Figure 3-13. The graph reveals that there was a marked increase in the maximum dry density with each

increase in gypsum content up to 30%; beyond that, the trend appeared to reverse. Similar trends have been stated by Kattab (1986) on granular gypseous soil and Ahmed (2013) on sandy gypseous soil, but the limited percentages of gypsum content that led to the enhancement in compaction parameters were 15% and 30% for Kattab (1986) and Ahmed (2013), respectively. Analysis of the soils suggests that these differences can be explained by the variance in pore size distribution of the sandy soils.

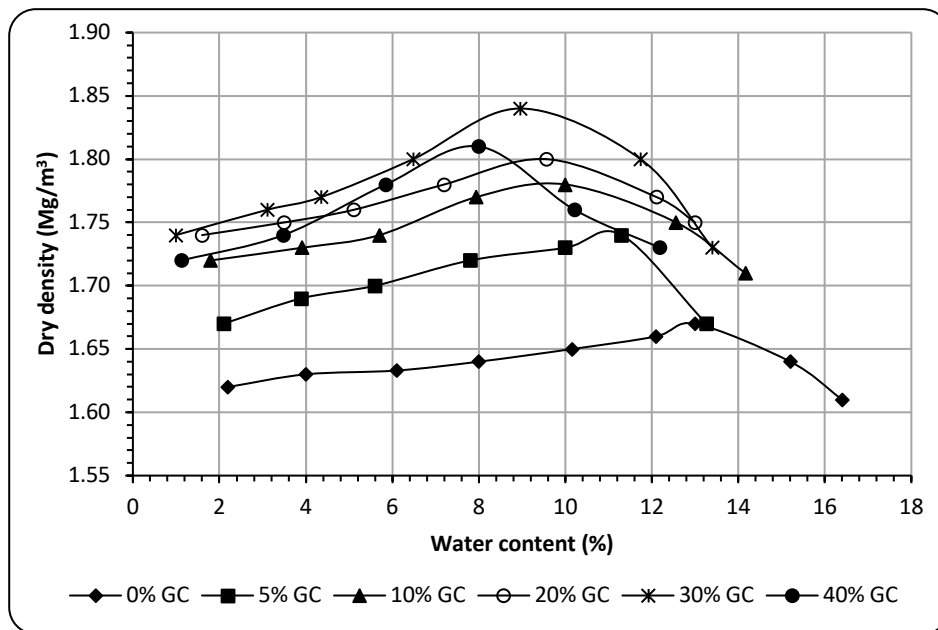


Figure 3-12: Standard compaction test for various gypsum content.

Table 3-5: Properties of standard compaction test.

Gypsum content, %	0	5	10	20	30	40
Optimum moisture content, %	13.0	11.3	10.0	9.6	9.0	8.0
Maximum dry density, Mg/m ³	1.67	1.74	1.78	1.80	1.84	1.81
Specific gravity	2.64	2.62	2.60	2.57	2.54	2.50
Minimum void ratio	0.58	0.51	0.46	0.43	0.38	0.38
Minimum porosity, %	37	34	32	30	28	28
Saturation degree, %	59	58	57	57	60	53

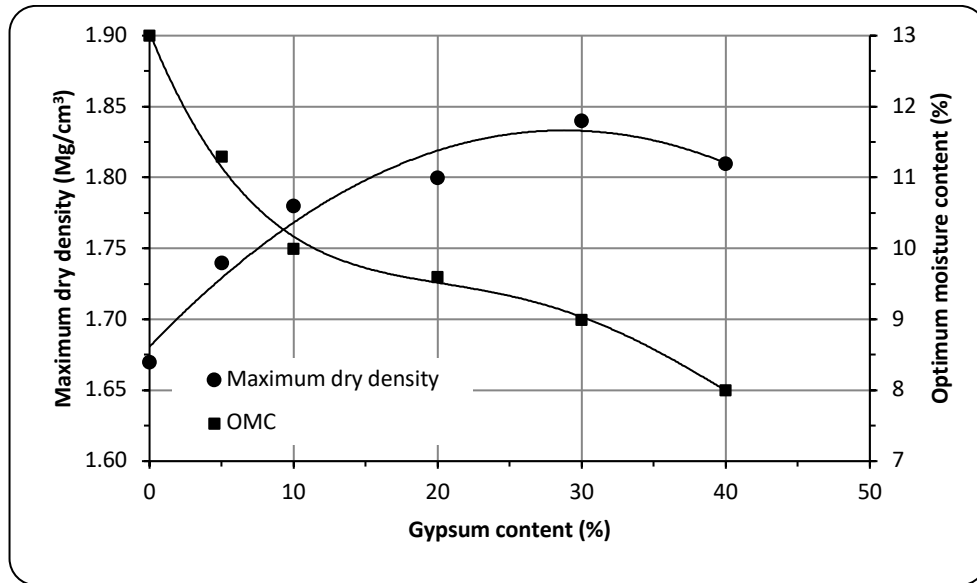


Figure 3-13: Effect of gypsum addition on maximum dry density and optimum moisture content.

Similarly, there is a clear trend of decreasing optimum moisture content with increasing gypsum content (from 0% to 40%). This is consistent with Al-Layla and Al-Obaydi (1993), Al-Bayati (2000), and Al-Gabri (2003), who all revealed that the optimum moisture content reduces with the increasing of gypsum content. It seems possible that these results are due to the role of gypsum in the compaction results. Two pertinent roles related to the presence of gypsum have to be considered here. First, the gypsum crystals act as a pore filling fines, especially when the added gypsum crystals are small in size (less than 80 μm) compared to the sand grains. In addition to this, gypsum is considered vulnerable to crushing during compaction, as gypsum particles are soft crystals, and consequently, it is possible for gypsum to fill various void shapes. Second, the reduction in the overall particle density of the soil mixture due to the increase in gypsum content, since the particle density of the gypsum used is 2.32, while it is 2.64 for the sand used.

It is believed that for gypsum content levels between 0% to 30%, gypsum predominantly serves as a filling material between sand grains, and so the maximum dry density increases with increases in gypsum content. Nevertheless, once the gypsum content level reaches 40%, it is suggested that there is sufficient gypsum within the soil not only to fill the pores but also to disrupt the distribution of sand, and as the particle density of the gypsum is lower than that of the sand, this results in reduced dry density.

When comparing these results with those that were obtained by the pluviation method, it is obvious that the same soil constituents (sand, gypsum, and water) produce very different fabrics when handled differently. For the gypsum content levels considered (0% to 30%), if the soil was formed via compaction, then the gypsum crystals would fill in the voids between the sand particles, producing a relatively dense material with low void ratios, due to the soft gypsum crystals having been compacted. Conversely, pluviating the samples created open structures, with void ratios and collapse potentials increasing with increasing gypsum content (if only stage 1 of preparation is completed). Therefore, it was obvious from the outcomes of this testing that compacting the soil was not a suitable alternative to pluviation and should not be used when attempting to manufacture gypseous samples that need to exhibit a certain CP (akin to those encountered in Iraq, Aziz, 2008; Salih, 2013; Fattah et al., 2015, Ali and Fakhraldin, 2016; Al-Zubaydi, 2017) or produce gypsum crystals within the fabric after loading and soaking.

3.6.2 Oedometer Testing

Front-lever loading, fixed-ring oedometers manufactured by Wykeham Farrance Engineering Limited were used for the oedometer tests. The sample used for the oedometer was 75 mm in

diameter and 20 mm in height. Vertical stress was applied using dead weights. Vertical displacements were measured using a strain gauge with 0.002 mm per division. No grease was applied to lubricate the internal surface of the oedometer's ring (this was to correspond to the bespoke cells, where the lubricant was not possible) (see Chapter Four). Sample preparation was explained in Section 3.4.4.2. Three sets of tests were undertaken on the oedometer, those being a collapse test, including a single oedometer test (SOT) and a double oedometer test (DOT); a standard consolidation test; and a creep test (post collapse). To ensure the measurement of reliable and accurate values, in the first two sets, each test was repeated three times, while creep testing took far longer and thus was repeated only twice.

3.6.2.1 Investigating the Collapse Potential of the Manufactured Gypseous Soils

Two classic approaches to investigating metastable soils in the oedometer are the single oedometer test, SOT (as proposed by Knight, 1963) for samples with gypsum contents of 5, 10, 15, 20, 25 and 30% and the double oedometer test, DOT (as proposed by Jennings and Knight, 1975) for samples with gypsum contents 10, 20, and 30%. Both were used in this study. The SOTs and DOTs were undertaken to observe whether hydrocollapse could be triggered in the samples and, if so, to determine the relative CP. The SOT involved a dry sample being progressively loaded up to 200 kPa, and at this loading level, the sample was flooded with water. The CP during this period was measured (Equation 3.2) and loading was continued up to 800 kPa.

To determine the CP at each stress level, the test should be repeated on many samples at different stress stages. Therefore, the DOT involved two identical samples being compressed independently, one being kept dry and the other being saturated from the outset. At each load

step, the difference in void ratios between the two samples was considered and the CP derived (Equation 3.3). In both approaches, loading was applied for 24 hours to ensure that the samples had reached equilibrium with the applied load.

$$CP \% = \left(\frac{\Delta e}{1+e_0} \right) * 100 \quad \text{Eq. 3.2}$$

$$CP \% = \left(\frac{e_s - e_d}{1+e_0} \right) * 100 \quad \text{Eq. 3.3}$$

Here, Δe is the change in void ratio and e_0 is the initial void ratio of the sample. e_d and e_s are the values of the void ratio of the samples at dry and at saturated conditions, respectively, under the same applied load.

3.6.2.1.1 Results and Discussions of the SOT

Typical void ratio-log stress relationships for the manufactured gypseous soils (at the various gypsum content levels), are shown in Figure 3-14. This figure reveals that the sample creation method not only produces the desired metastable behaviour but is also repeatable. In general, the sudden compression observed upon saturation is stark and indicates that all of the soils investigated exhibit CP. Upon further loading, the slope becomes steeper than that of the dry stage, indicating a loss of stiffness with the failure of the gypsum bonds. The observed relationships can be described as having three ‘phases’. In the first phase, the samples are unsaturated and the gypsum crystals have bonded the soil skeleton together, which makes the fabric relatively strong and the associated settlements relatively small. Thus, the rate of compressibility is low and the settlement ends within 2 to 4 hours of the load application.

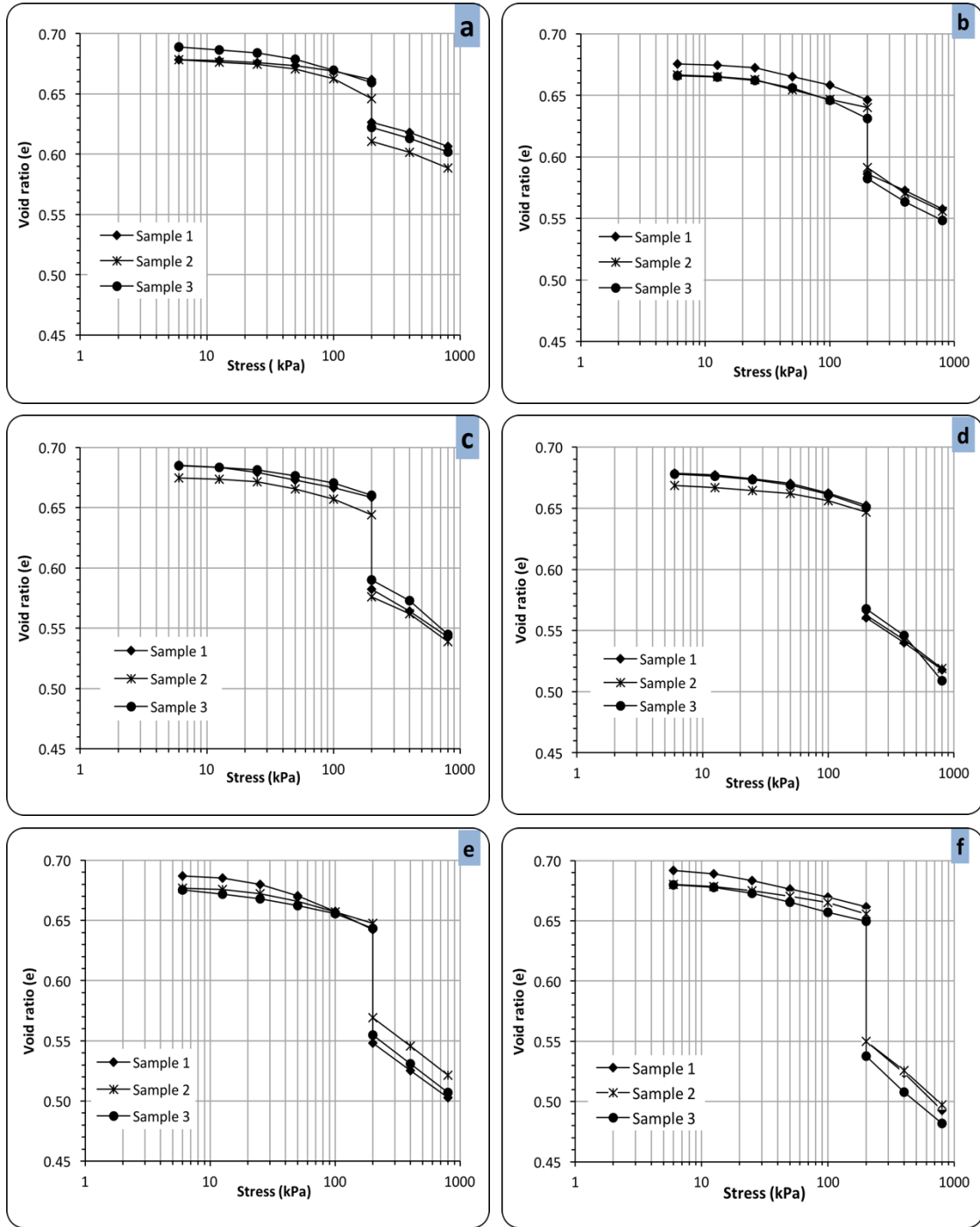


Figure 3-14: Results from the SOT with inundation upon 200 kPa for 24 hours; (a) 5% GC, (b) 10% GC, (c) 15% GC, (d) 20% GC, (e) 25% GC, (f) 30% GC.

The second phase corresponds with the flooding of the oedometer cell with distilled water; the compression (flooded at 200 kPa) is rapid and occurs immediately upon and then throughout saturation. Saturating the samples is believed to significantly weaken, or destroy, interparticle

bonding through gypsum dissolution, resulting in rapid particle reorientation synonymous with metastable soil (as exhibited by other arid gypseous soils: Seleam, 1988; AlQaissy, 1989; Nashat, 1990; Fattah et al., 2008; Fattah et al., 2012; Al-Obaidi, 2014; and loess, the classic metastable soil: Rogers et al., 1994; Al-Obaidi, 2014; Al-Obaidy, 2017). The third phase is almost a straight line extending over increasing load steps due to further dissolution of gypsum.

The relationship between gypsum content levels and the CP at a vertical stress of 200 kPa for those six sand-gypsum mixtures is demonstrated in Figure 3-15 (remembering that these samples all started the testing with approximately the same initial void ratio after the completion of stage 4 of sample preparation). The magnitude of the CP of this series is presented in Table 3-6. The results show that the CP is significantly influenced by gypsum content, as the value of CP increases dramatically with the increasing of gypsum content. Using the definitions suggested by Jennings and Knight (1975) (Table 3-7), the CPs observed in this testing are considered as ‘moderate trouble’ to ‘trouble’, suggesting that this material would be problematic if foundations were constructed in this type of soil and the soil subsequently experienced a significant increase in water content.

These outcomes – the metastable behaviour, the stiff and strong behaviour when dry, the rapid repacking with wetting, the loss of strength post wetting, etc. – suggest that the manufactured gypseous soil accurately simulates the behaviour of the gypseous soils found in Al-Najaf, Iraq (Fattah et al., 2008; Salih, 2013; Al-Dabbas et al., 2014; Fattah et al., 2015). As such, these manufactured soils can be used as a proxy to investigate the physical response of these metastable gypseous soils within controlled laboratory settings.

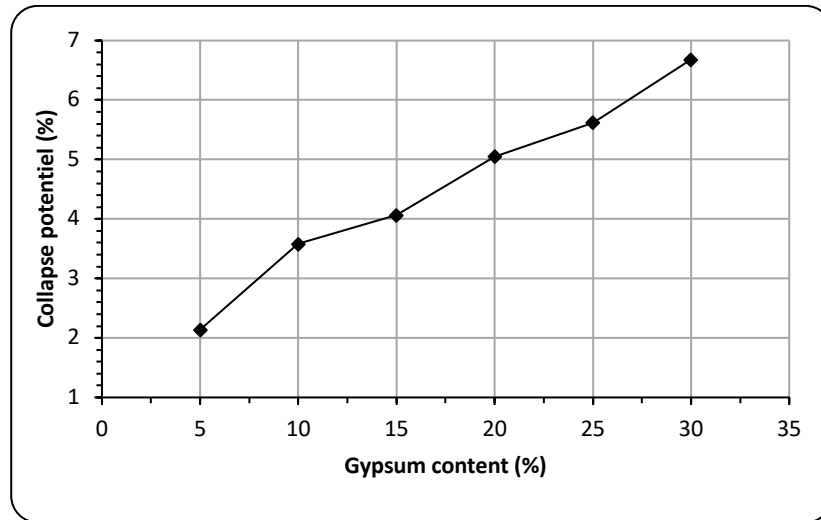


Figure 3-15: CP versus gypsum content level in SOT.

Table 3-6: CPs for various gypsum content levels from SOT and DOT.

Gypsum content (%)	Mean Collapse Potentials from SOT and DOT (%)		
	SOT		DOT
	24 hours	90 days	
5	2.11		
10	3.58	4.83	2.78
15	4.10		
20	5.10	8.55	4.10
25	5.62		
30	6.68	10.00	5.48

Table 3-7: The severity of collapse according to the value of the CP, as defined by Jennings and Knight (1975).

CP (%)	0-1	1-5	5-10	10-20	>20
Severity of collapse problem	No problem	Moderate trouble	Trouble	Severe trouble	Very severe trouble

3.6.2.1.2 Results and Discussion of DOT

In this section, two identical samples for each gypsum content level (those levels being 10%, 20% and 30% gypsum) were tested in parallel following the procedure described in Section 3.6.2.1. A typical result of the DOT versus the SOT is shown in Figure 3-16. The CP is determined for each load increment after adjustment. The curves for the saturated samples are lower than those for the samples tested at their dry state. Compression of the dry samples is a function of frictional forces between the particles and the cementing action of the gypsum. Increasing the applied load upon saturated state results in progressive failure of these interparticle bonds, with associated particle movements in the relatively open structure; hence large corresponding volumetric strains.

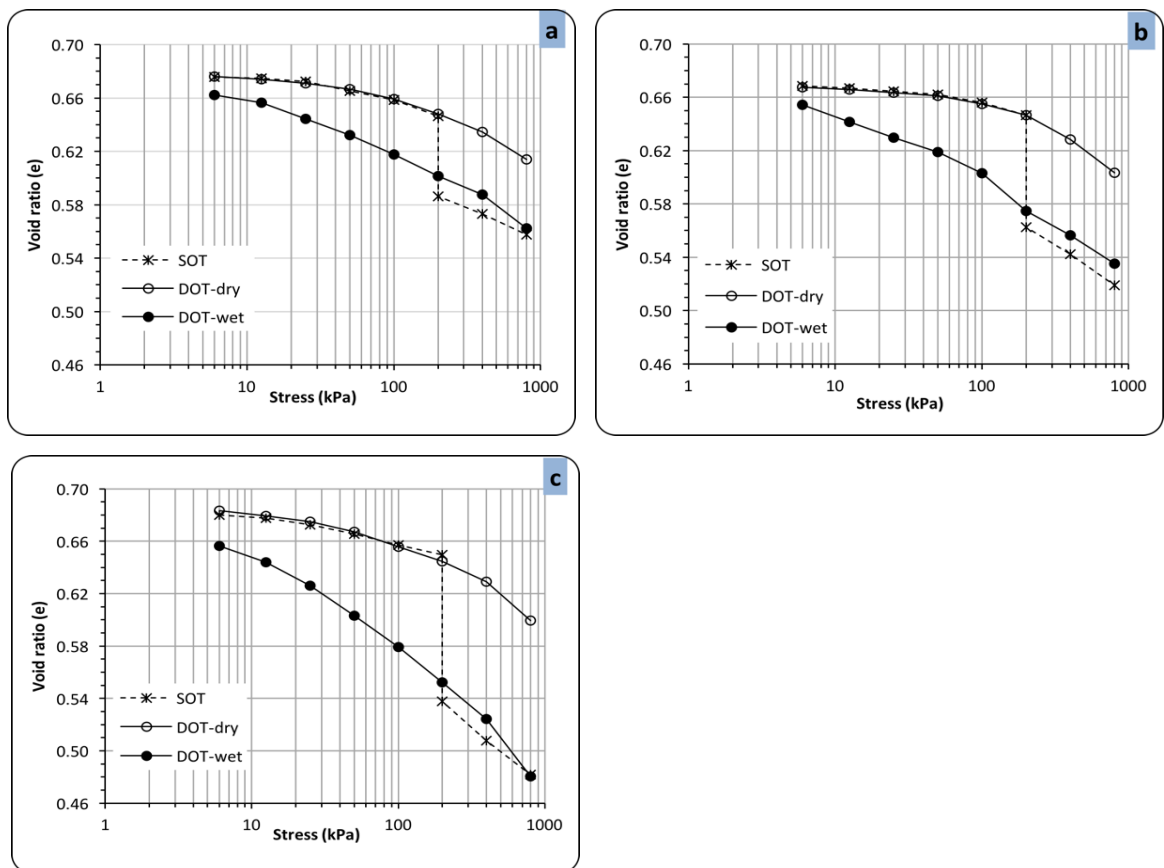


Figure 3-16: DOT versus SOT for three gypsum content levels; (a) 10% GC, (b) 20% GC, (c) 30% GC.

Accordingly, this test gives an indication of the collapse tendency of the soil at any pressure. This observation could be ascribed to the softening, and breaking of intergranular bonds as loading increases, with an associated repacking of the soil particles, resulting in greater volumetric strains. Similar findings have been found by Seleam (1988), Nashat (1990), and Al-Obaidi (2014). It is clear that the mean SOT response estimates a slightly greater CP than the corresponding DOT value, for the same vertical stress level, which is 200 kPa, as shown in Figures 3-16 and Table 3-6 (reported in the previous section, Section 3.6.2.1.1). These (slight) differences may be explained by the fact that soil structure until is rapidly disrupted with sudden inundation of water in the SOT. At that point, great and rapid deformations occurred as a result of volumetric strain development with weakening of the soil structure. Conversely, in the DOT method, the sample had been progressively weakening with time as the increment of load was increased in flooded conditions. This is consistent with results obtained by Al-Obaidi (2014), who worked on natural and manufactured gypseous soils.

Figure 3-17 shows the CP for each load increment with the stress applied in the logarithmic scale. From these results, it can be seen that for the 30% gypsum content samples, the CP increased progressively with the increase in inundation stress level in a linear manner, whereas for soil with 10% and 20% gypsum levels, it is observed that the CP increased until vertical stress approached 400 kPa, at which point the CP decreased. However, the reduction in the 10% gypsum sample is greater than that in the 20% gypsum sample, as the latter has a higher gypsum content level and so the cementing bonds at the contact points were stronger than those of the 10% gypsum sample. This behaviour can be attributed to the fact that when a higher load is applied to a structurally weak sample (that is, one with lower gypsum content),

the soil skeleton loses its integrity, the voids diminish (a denser soil sample is obtained), and thus the CP becomes negligible, especially under saturated conditions.

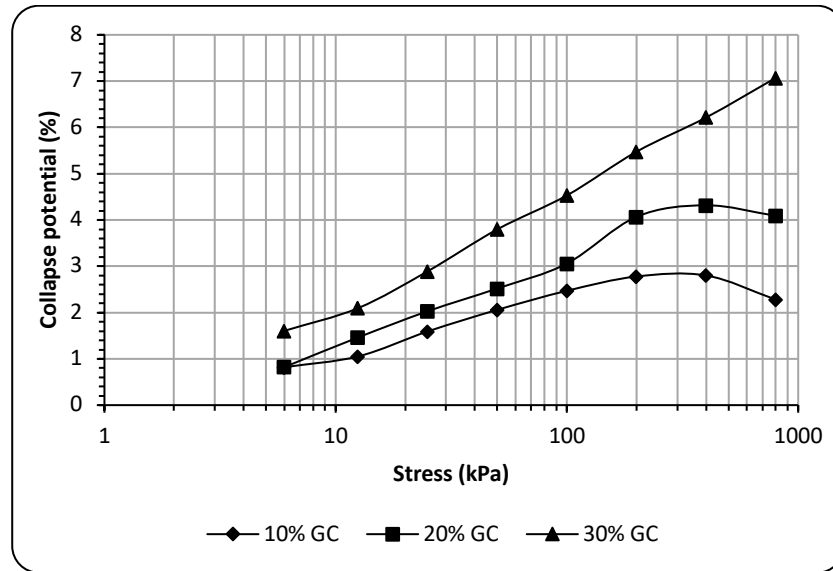


Figure 3-17: CP versus vertical stress in logarithmic scale for three gypsum content levels.

These findings further support the results of Kezdi (1974), who concluded that the CP value obtained from a similar test (DOT) reaches a constant maximum value at pressure of 200 to 300 kPa for most collapsible soils. With increasing inundation vertical pressure, the CP value tends to decrease due to the continuous breakdown of the intergranular bonds of the soil skeleton under higher loads.

3.6.2.2 Results and Discussion of Standard Consolidation Test

The consolidation tests were conducted on samples with gypsum content levels of 10%, 20%, and 30%, following BS 1377-5:1990, Clause 3, in an effort to examine the influence of gypsum content on the parameters of compressibility, such as the compression index (C_c) and the swelling index (C_s).

The tests began by compressing the prepared soil sample vertically in stepped increments of applied load, following BS 1377-5:1990. Each incremental load was maintained until the rate of primary settlement reached equilibrium with no further deformation. During this time, the reduction in the height of the sample was recorded at regular time intervals. After the desired applied stress was reached, the sample was unloaded in decrements (to 25 kPa) corresponding to the loading increment, and the expansion in the sample height was recorded regularly. Stress was applied in a sequence of 6, 12.5, 25, 50, 100, 200, 400, and 800 kPa over a 24-hour period. The C_c and C_s of the tested samples were determined.

The loading and reloading curves versus the log-effective stress for the gypseous soils are presented in Figure 3-18. The graph shows that there was a marked increase in the difference between the loading and reloading curves with increasing gypsum content. The following conclusion can be drawn regarding the mechanical behaviour of samples, where the reloading represents the elastic part of compression, and the inelastic part is the variance between the loading and reloading curves resulting from breakage and particle slippage. Gypsum crystals are soft, with a hardness rating of 2 on the Mohs scale (Klein and Hurlbut, 1985); as such, with an increase of gypsum content, it is anticipated that the slippage of sand particles would be easier and the breakage of crystals increased. Consequently, the increasing difference between the loading and the reloading curves (the plastic deformation) correlates with an increase in gypsum content, which can be justified by considering the properties of gypsum.

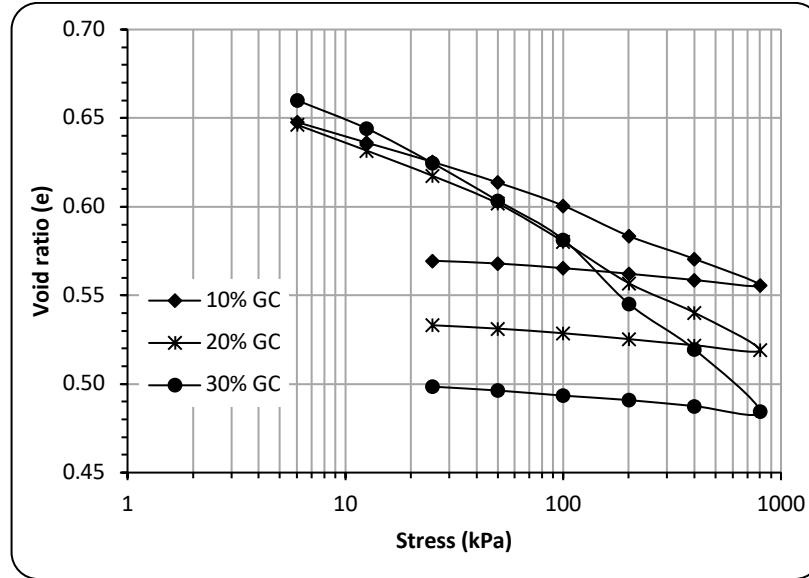


Figure 3-18: Standard consolidation test for three gypsum content levels.

Figure 3-19 indicates that as the gypsum content increases, the compression index increases, while the swelling index increased from 10% to 20% but decreased thereafter. It was reassuring that the observed behaviour of the manufactured samples in this regard mirrors so closely that exhibited by naturally occurring variants of these soils. For example, these results are consistent with Sirwan et al. (1991), AlNouri and Saleam (1994), Livneh et al. (1998), Ahmed (2013), Al-Obaidi (2014) and Fattah et al. (2015), who found that the C_c increased upon the wetting of a dry sample because of the softening that occurs due to the dissolution of the gypsum and the resultant loss/reduction of cementation, while the C_s does not follow the same trend as C_c as its value depends highly upon the types of soil constituents (other than gypsum) and the way the gypsum and other particles are cemented. This is encouraging and supports the thesis that these materials can be manufactured in the laboratory.

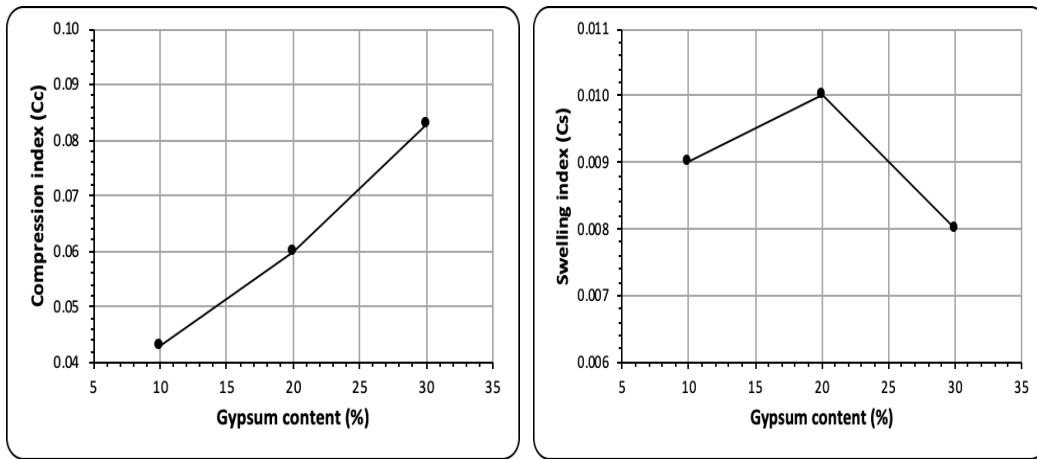


Figure 3-19: Effect of gypsum content on compression and swelling index.

3.6.2.3 Results and Discussion of Delayed Compression (Creep)

In gypseous soils, creep or delayed compression continues for a long time after collapse and after primary compression, which makes the CP for a standard test (24 hours) uncertain. Therefore, the creep testing initially adopted SOT procedures for samples with gypsum contents 10, 20, and 30%, although once the sample was inundated, the 200 kPa load remained in place for three months (90 days). After this time, the load was incrementally increased (once again, over 24-hour periods) until the desired pressure was achieved (800 kPa).

Void ratio-load plots as shown in Figure 3-20 illustrates that samples saturated for 90 days showed much greater volumetric changes than those of the samples with the 24-hour saturation period (though samples from both sets exhibited similar characteristics in unsaturated states), with increased magnitudes of 34.9%, 67.6% and 49.7% for 10%, 20% and 30% gypsum content, respectively. This indicates that the percentage of increase in the CP value is greater in soil that is 20% gypsum in comparison with soil that is 30% gypsum.

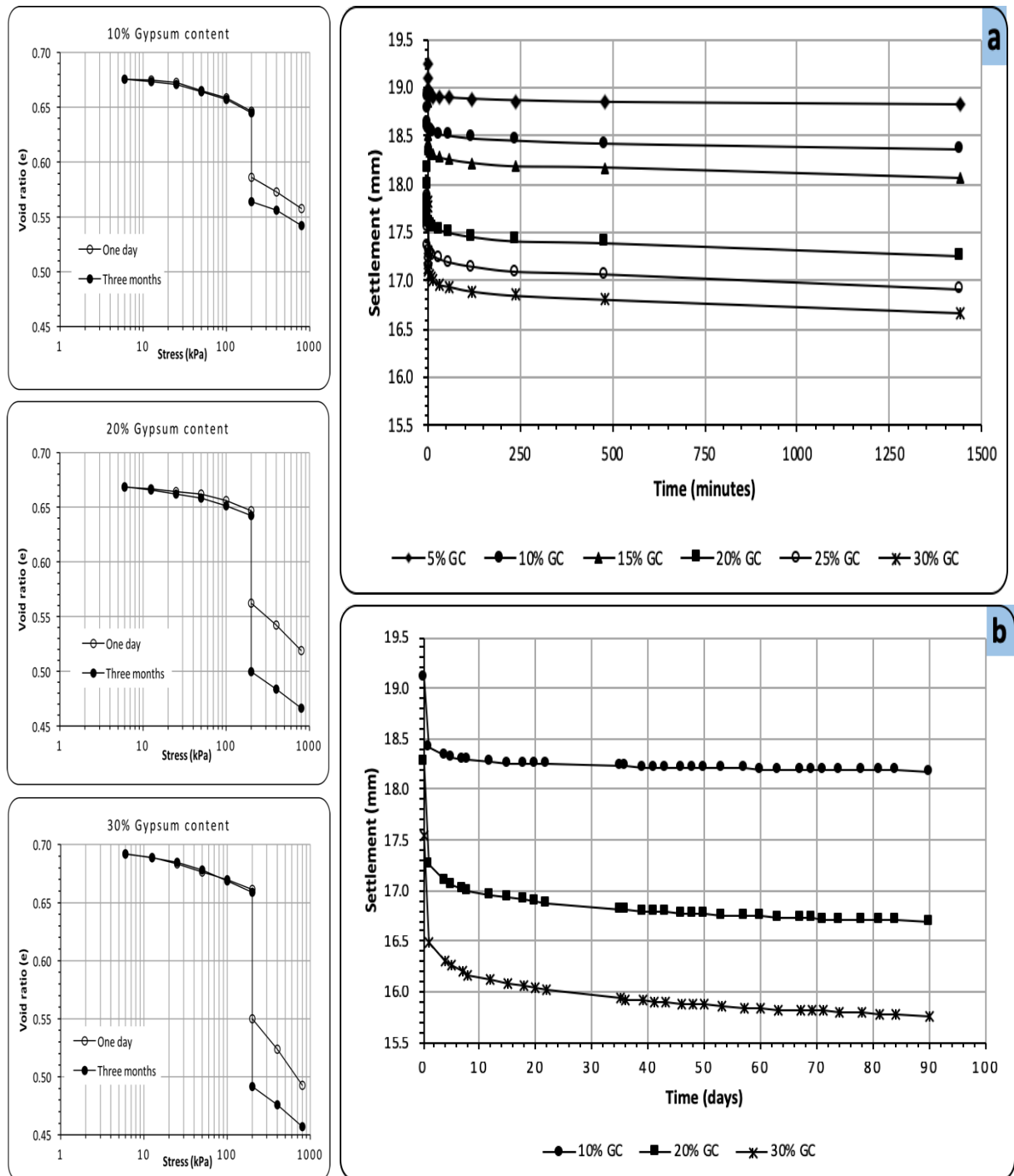


Figure 3-20: (Left) Change in voids with loading and inundation (200 kPa) for the three gypsum contents. (right) Mean settlements associated with the manufactured gypseous soils with time (a) over a 24-hour period, (b) over a 90 day period, each whilst experiencing 200 kPa load with inundation (inundation taking place at time zero) in SOT.

This may be due to the dissolution process being faster and more profound when the gypsum content is lower and gypsum is located mainly at the contact points, but that it is not so effective in dissolving large gypsum lumps present in soil that is 30% gypsum (AlNouri and Saleam, 1994). When considering the total movement over the 90 days, the soils change in classification (for 30% gypsum content) from 'trouble' to 'severe trouble' for foundation safety (Jennings and Knight, 1975). Therefore, secondary compression and creep are important mechanisms that must be considered when assessing the metastable behaviour of these soils.

To demonstrate that the significant settlements induced with wetting were indeed rapid collapses, mean settlement-time plots (SOT) are presented in Figure 3-20, along with settlements associated with longer term loading (creep tests). The mean settlements for the six gypsum contents indicate that the greater the gypsum content the smaller proportion of settlements take place in the first 15 minutes: approximately 80% of the total collapse for 5% gypsum content, 70% for 10 and 15% gypsum contents and 60% of the settlement for 20 to 30% gypsum contents, after which continued settlement is observed but at a much slower rate. This is in keeping with the findings of Al-Mohmmadi et al. (1987), Saleam (1988), Nashat (1990), and Al-Obaidi (2014), who observed that approximately 60% to 80% of the collapse occurred within a few minutes after wetting of natural gypseous soil, once again indicating that the manufacturing process produced samples with desired physical response. While for deformation upon 200 kPa for 90 days (Figure 3-20b), the majority of settlement is observed within the first day of inundation, and this is true for samples of all gypsum content levels. The significant amount of creep deformation is the result of the gradual breakdown of interparticle bonding within the soil skeleton, as well as the crushing of particles and the

dissolution process; with time, this deformation decreases, and grains tend to glide over each other to be rearranged into a more stable and denser configuration.

3.6.3 Unconfined Compressive Strength Tests and Associated Deformation Response

The unconfined compressive strength (UCS) test was conducted using a standard unconfined compression apparatus, following the procedure in British Standard (BS 1377-7:1990, Clause 7), with an LVDT and pressure cell (3 kN) to record deformation and force, respectively. The samples were prepared into a cylindrical acrylic mould with a 50 mm inner diameter and a 100 mm height using the pluviation method (discussed in detail in Section 3.4.4). Whilst the ratio of the sample diameter to its length should be approximately two, the sample length can differ, with an acceptable range being stated from 8% under-size to 12% over-size, without considerably affecting the results (BS 1377-7:1990, Clause 7). The British Standard (BS1377-7:1990, Clause 7) also states that brittle soils need a slower rate of strain than plastic soils, as the former fail at smaller deformation. Thus, the applied rate of vertical displacement was 0.2 mm/min (Huang and Airey, 1998).

The soil samples were prepared with gypsum content levels of 10%, 20%, and 30%, although these were grouped into three series. These series were named according to the number of layers formed during the manufacture of the sample: one layer, two layers, and four layers. The main objective of these tests was to investigate the potential significance of creating samples using multiple layers of gypseous soils on the deformation response. In order to assess possible impacts when using this approach to manufacture far larger samples, where it was feared that creating them in a single layer might not produce a metastable response

throughout the depth of the sample if created in one large layer, three samples were produced for each test to provide an indication of repeatability.

Curing time was considered for one-layer samples as it is a fundamental factor for understanding the behaviour of the bonding between sand and gypsum; therefore, an experimental schedule was arranged to accomplish the tests at curing periods of 3, 5, 9, 16, and 30 days (see Section 3.6.3.2.1) for the manufactured gypseous soils. Curing proved an issue with multi-layered samples: once the final layer was created, the sample experienced damage during the extraction process, and the sample preparation process proved time-consuming. It is estimated that during validation testing, only approximately two out of five samples were extracted in acceptable conditions for testing.

3.6.3.1 Sample Preparation for UCS Testing

Three series of unconfined compressive samples were prepared following the same overall procedures as those for the oedometer samples (see Section 3.4.4.2). However, before the pluviation phase, one of the open ends of the acrylic moulds was sealed, via an adhesive, with a filter paper and then placed over a dry porous stone (Figure 3-21a). The first series contained one layer, with a height of 100 mm. The second series comprised samples with two layers, each 50 mm in height. The third series comprised samples with four layers, each 25 mm in height.

For the one-layer sample, the soil was pluviated into the mould, then the seating load was applied (5 kPa, transmitted by a 49.6-mm diameter plastic rod; this is 0.4 mm smaller than the internal diameter of the acrylic tube: see Figure 3-21b and c) for 2 hours. Following this

period, the sample was exposed to water (seeping upwards through the porous stone) for four hours before being drained and left within the mould for two days (at laboratory temperature) to produce a material that could be extracted without being damaged, and this representing the initial curing. The sample was extracted (which is difficult, as it is granular soil) using a rubber cylinder (Figure 3-21e). Finally, the sample was oven dried at 25°C until a constant weight was obtained (which took approximately four days, and this representing the final curing, bringing the total curing time to 6 days). It should be noted that curing times are stated include the draining time (initial curing) and drying time (final curing). Figure 3-21 shows the main steps of sample preparation.

This procedure was repeated twice for the two-layer sample and four times for four-layer sample. Each pluviated layer was loaded, submerged, and then dried before the next layer was started, meaning for the four-layer sample, the first layer was exposed to four cycles of loading-soaking-drying, while the fourth layer was exposed for one cycle. It is worth noting that through the extraction process for multi-layered samples, particularly for the four-layer samples, it was challenging to obtain a sample that functioned as a single sample. This was due to weaknesses at the horizontal interfaces between layers, resulting in failure. Therefore, the sample production process was modified slightly: once each layer (except the final layer) had been prepared, the upper surface was gently scarified using a palette knife to improve bonding across the layers. This step alleviated these difficulties (Figure 3-22), although if this process were undertaken too vigorously, the sample would experience localised failure around the edges and have to be rejected. It should be noted that extracting the sample from the mould each time a layer is created, to facilitate oven drying, before reinstalling it back into the mould to allow for pluviation of the next layer was a tricky operation, and samples could have

been damaged if it was rushed; if this occurred, the samples were rejected. Therefore, this process was abandoned and each layer that was created was left to dry in the mould.

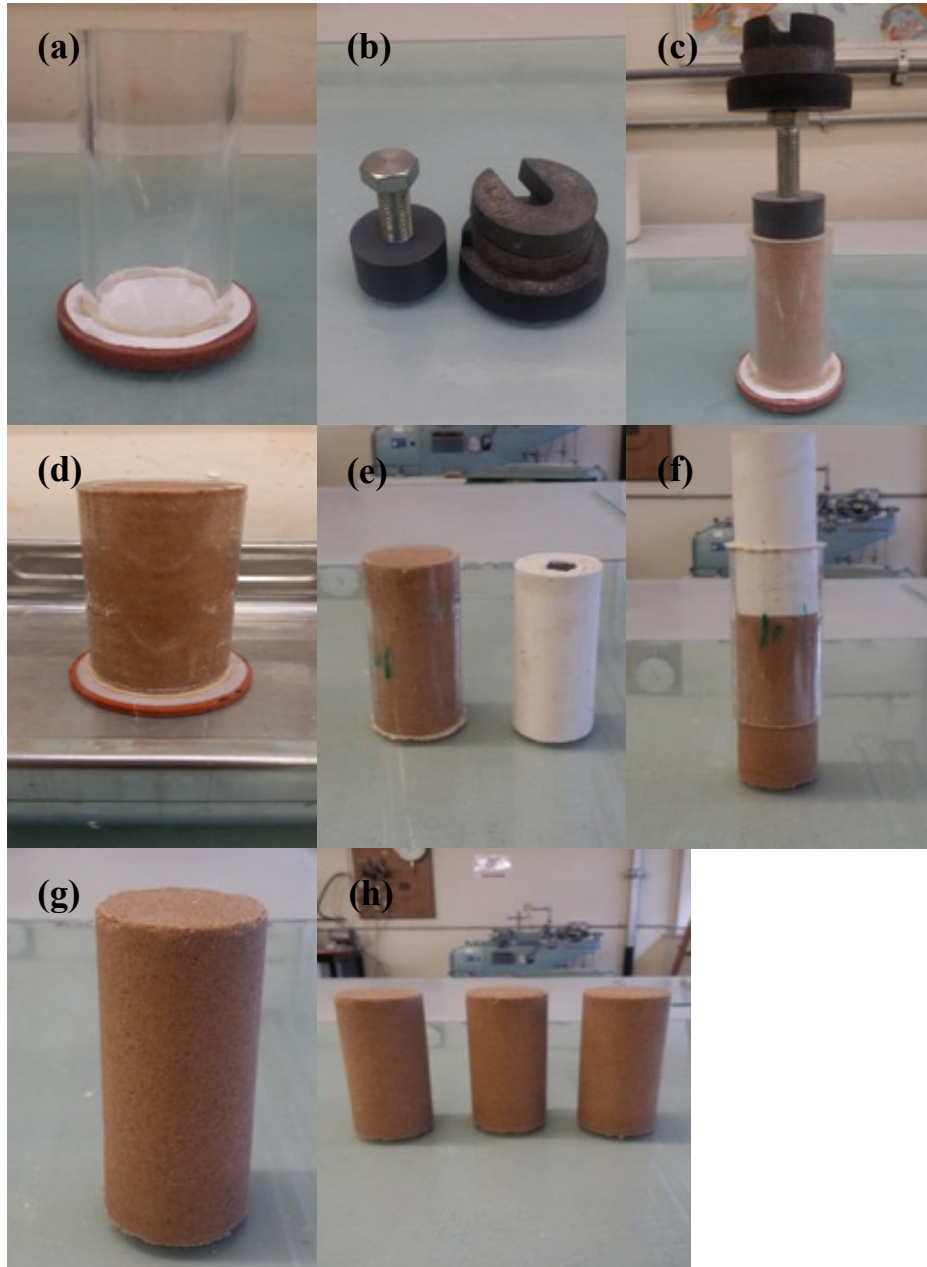


Figure 3-21: Unconfined compression sample steps; (a) mould preparation, (b) loading system, (c) soil pluviated and loaded, (d) soaking by capillary action, (e) left after wetting at lab temperature to drain the water, (f) extraction process, (g) sample after extraction, (h) repeated samples.

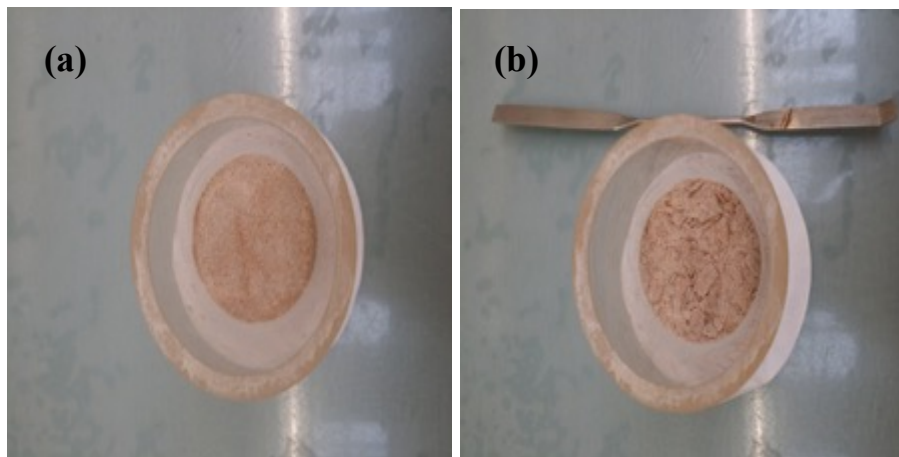


Figure 3-22: (a) After drying process, (b) Scarifying the upper surface of the layer before pluviating the next layer.

Samples created for the UCS also experienced changes in dimensions (due to the loading, wetting and drying processes). Therefore, sample dimensions were measured (taking a three-point mean) using a digital caliper prior to testing to determine dry density and void ratio.

3.6.3.2 Outcome of UCS Testing

3.6.3.2.1 Single-Layer Samples with Changing Gypsum Content and Curing Age

Oedometer testing indicates that samples containing 30% gypsum content were likely to experience the greatest volumetric changes with inundation whilst under load; however, of the gypsum content levels investigated in UCS testing, these samples were also the strongest, whilst the 10% gypsum content level sample was the weakest (Figure 3-23). This agrees with the findings of Huang and Airey (1998), and Haeri et al., (2005). When considering the age of the samples at the time of testing, it is evident that in the short term (up to 9 days after curing was initiated (the draining and drying stages)), the strength increases with age. However, after this point, the strength does not increase significantly with continued aging (up to the upper

limit considered herein: 30 days) (Figure 3-23). This has implications when developing laboratory investigations with these soils; gypsum bonding should be allowed to develop for at least 9 days, after which the strength should be representative for this type of gypsum-bonded soil as it is found in nature.

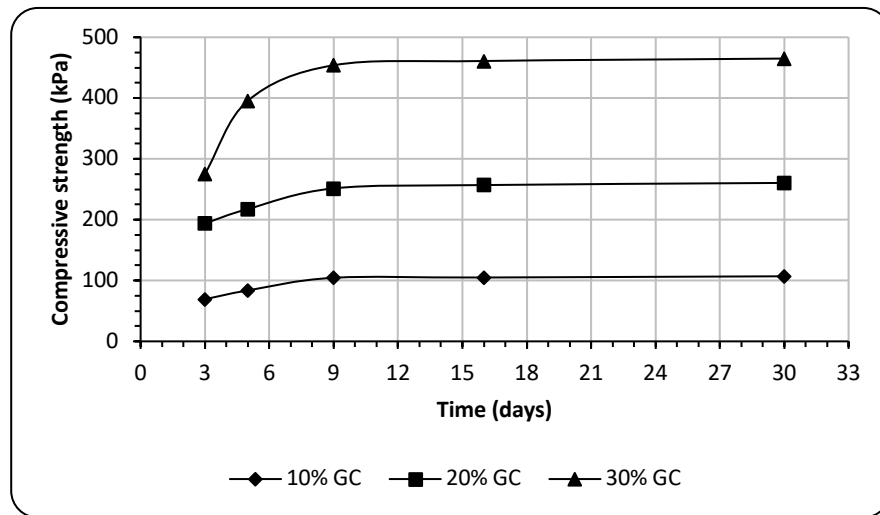
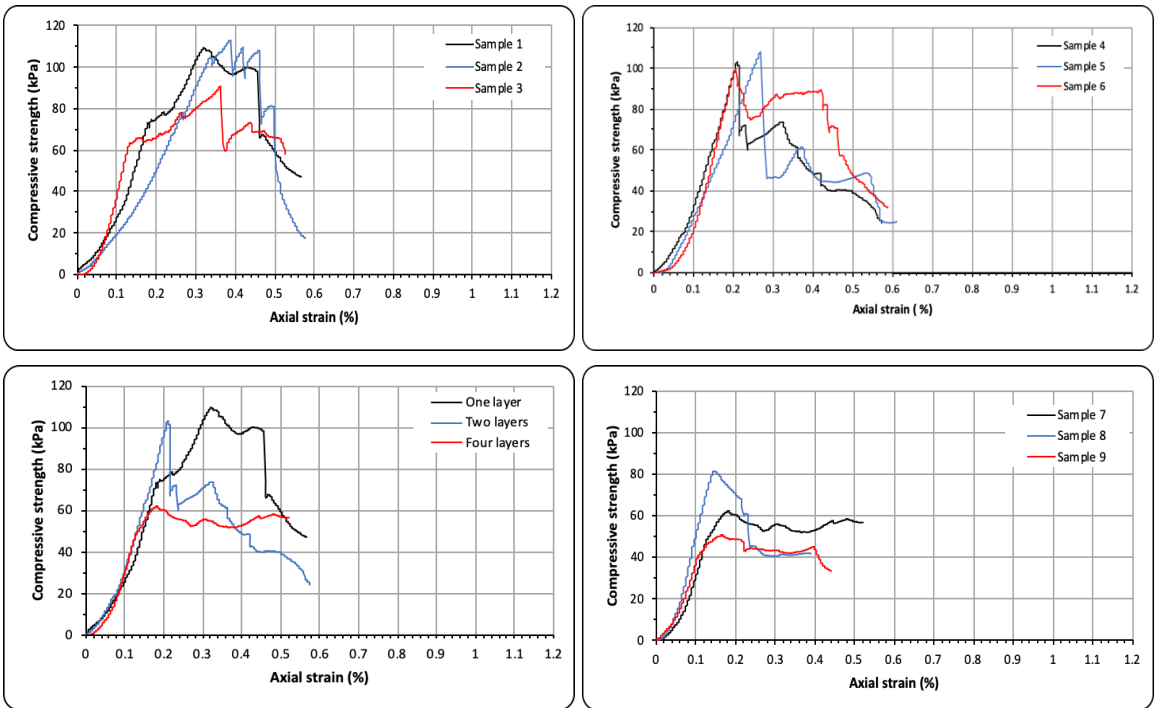


Figure 3-23: Behaviour of UCS for single layer versus the curing time for various of gypsum content. It should be noted that curing times are included the draining time (2 days) and drying time in the oven (which are: 1, 3, 7, 14, and 28 days), i.e. the total curing time is: 3, 5, 9, 16, and 30 days.

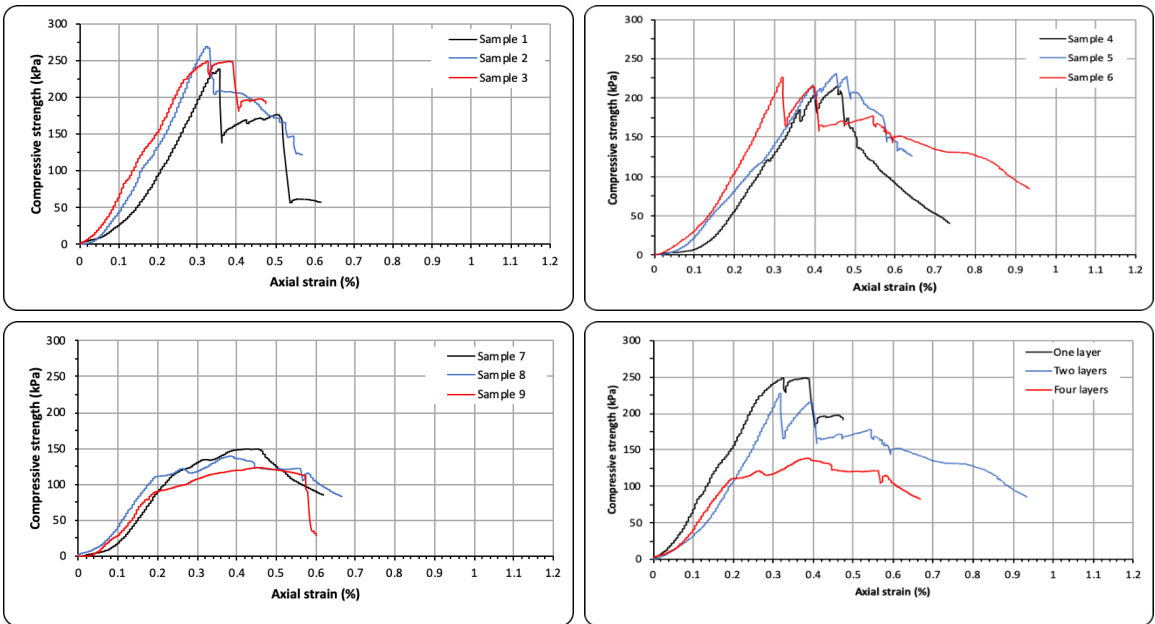
3.6.3.2.2 Deformation Response of Single- and Multi-Layered Samples with Changing Gypsum Content Levels on the UCS

The typical UCS-axial strain relationships of UCS tests for samples with three gypsum content levels are shown in Figure 3-24. Note that the single-layer samples are cured for the same time as the youngest layer for all samples, which is 9 days (i.e. the single-layer samples are cured for 9 days, the second layer in the two-layer samples are 9-days old, and the fourth

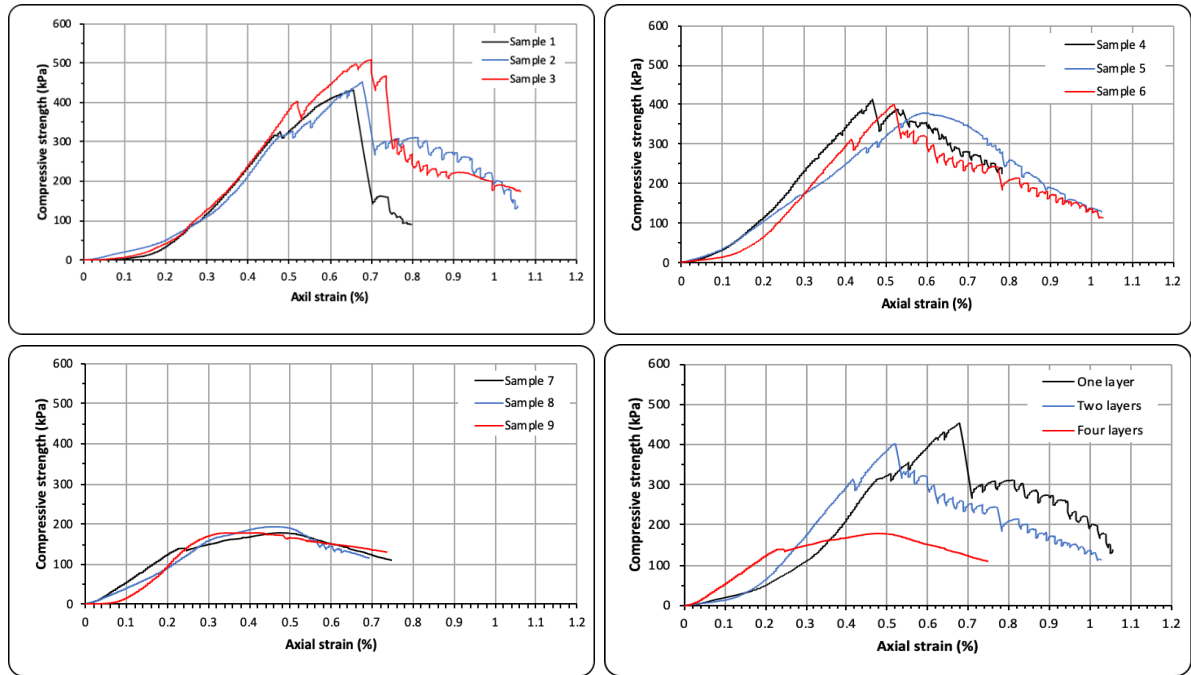
layer in the four-layer samples are also cured for 9 days). Layers below the upper layer in multi-layered samples are clearly older than 9 days.



(a)



(b)



(c)

Figure 3-24: Deformation response for the three gypsum contents; (a) 10% GC, (b) 20% GC, (c) 30% GC. The labels are categorised as 9 samples, which are presented alongside mean single layer, two layer and four layers samples. The numerical designations of: 1, 2, and 3 refer to the three single layer samples; 4, 5, and 6 refer to the three double layers samples; 7, 8, and 9 refer to three quadruple layers samples. The terms one layer, two layers and four layers refer to mean response for all three of the samples for each gypsum content previously presented (in samples 1-9).

The nature of the gypsum crystal bonds resulted in peak strengths being mobilised at very low strains (the range of strains being between 0.14 to 0.70%) (see Figure 3-24 and Table 3-8); hence the deformation response was brittle with strain-softening post peak strength. It was interesting to note that, in many cases, the deformation responses observed were not smooth curves, appearing instead to be ‘stepped’ in nature prior to peak strength. The ‘steps’ were small increments of increased strength followed by small increments of deformation under approximately the same stress, accumulation of these steps resulted in reducing stiffness. It is

suggested that deformation of the samples results in the failure of a proportion of the cementing bonds, potentially resulting in localised particle rearrangement, with associated volumetric loss but increased frictional contact. Once sufficient bonds have sheared, the peak strength of the bonded material is exceeded and the sample fails via the development of a cone below the load cap and vertical cracking down the length of the sample (akin to the failure mechanisms of other cemented soils as reported by Royal et al. (2013), (2018) and Alzayani et al. (2017).

Table 3-8: Data of the UCS test.

No. of layers	Gypsum content (%)	Compressive strength (kPa)	Mean (kPa)	Axial strain (%)
One layer	10	109.9	104.5	0.32
		112.9		0.39
		90.8		0.36
	20	237.8	251.5	0.36
		268.8		0.33
		248.0		0.38
	30	431.6	463.6	0.66
		452.1		0.68
		507.1		0.70
Two layers	10	103.6	103.9	0.21
		107.9		0.27
		100.3		0.21
	20	214.7	224.0	0.46
		231.0		0.45
		226.4		0.32
	30	412.2	398.1	0.47
		380.1		0.59
		402.0		0.52
Four layers	10	62.3	65.0	0.18
		81.6		0.14
		51.1		0.17
	20	148.8	137.3	0.43
		139.4		0.39
		123.7		0.46
	30	179.8	184.0	0.48
		192.3		0.47
		179.5		0.42

The formation of vertical cracks in the samples eventually forms wedges of material, and it is believed that the post peak strength strain-softening behaviour observed is a result of the widening of these cracks with reduced frictional interaction between them. There was variation within the brittle strain softening deformation behaviour, i.e. stiffness, peak strength and corresponding strain, magnitude of strain-softening. This variation was greater than that observed in the hydrocollapse and compression response, and it is presumed that this is linked to the pluviation of the samples and influence between layers (with the interface proving a zone of potential weakness, this is considered further in the following subsection). Analysis of the samples indicates that the gypsum content was relatively evenly distributed throughout the samples regardless of the number of layers used (which provides additional confidence in the sample production methodology) (Figure 3-25).

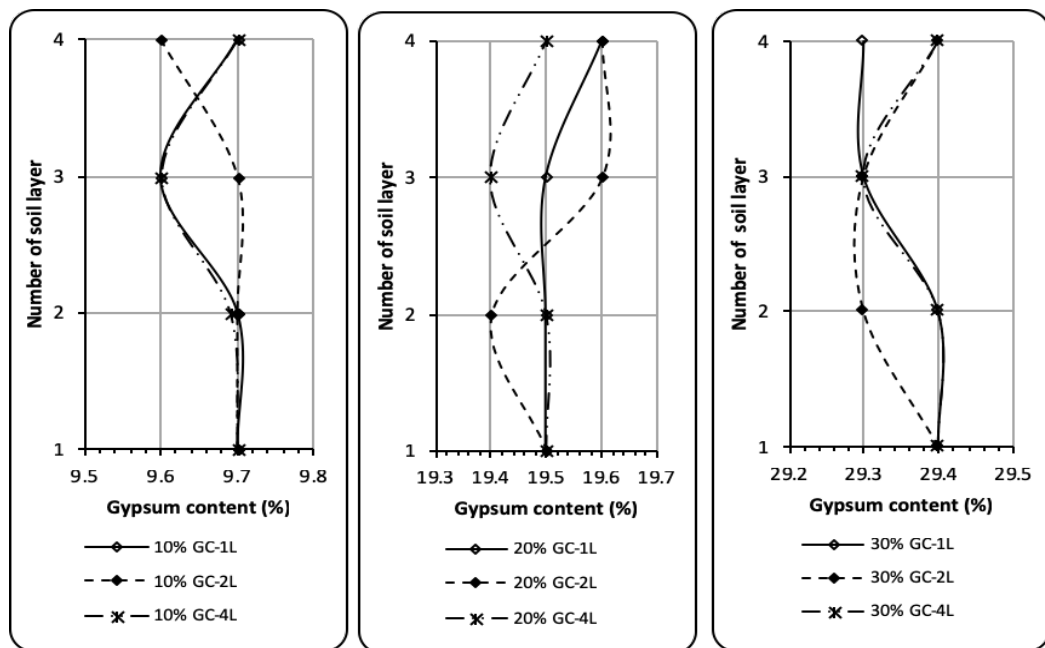


Figure 3-25: Distribution of gypsum content in single-layer and multi-layered samples (one layer = 1L, two layers = 2L, and four layers = 4L).

3.6.3.2.3 Implications of Multiple Layers on Large-Scale Sample Manufacture

Table 3-9 presents the mean dry density and void ratios for the three sample types. It is clear that these are directly comparable to those produced for the oedometer, which indicates that the method is flexible enough to cope with samples of different size.

Table 3-9: Dry density and void ratio for the UCS samples.

Gypsum content (%)	No. of layers	After sample preparation	
		Initial void ratio (e_0)	Dry density (Mg/m^3)
10	One layer	0.68	1.55
	Two layers	0.69	1.54
	Four layers	0.67	1.56
20	One layer	0.67	1.54
	Two layers	0.68	1.53
	Four layers	0.67	1.54
30	One layer	0.68	1.51
	Two layers	0.69	1.50
	Four layers	0.69	1.50

The multi-layer samples were trialled as the wider investigation used large samples (349 mm in diameter and 300 mm in height: see Chapter Four) and there was concern that pluviation of such samples in one layer might result in self-weight compression of the sample, affecting metastability. As such, three layer thicknesses were considered during UCS testing (100 mm, 50 mm, and 25 mm), and it is clear that the upper layer in the double-layer samples exhibited similar deformation response to the single-layer samples (after the same period of curing) (Figure 3-26). This was not the case for the four-layered samples, which were much weaker than the single-layer samples and exhibited lower stiffness levels.

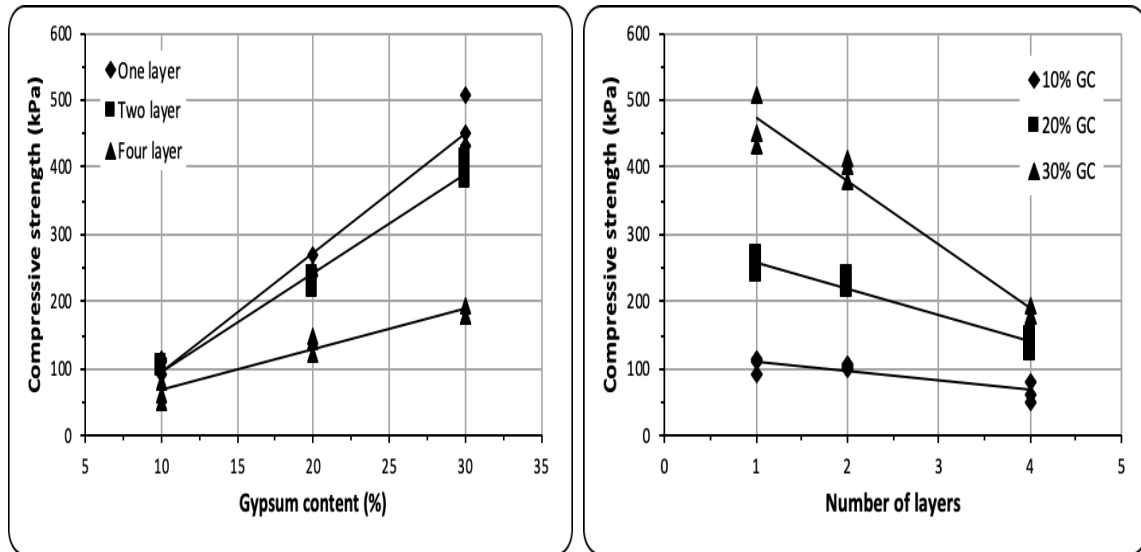


Figure 3-26: Behaviour of unconfined compressive strength with; (a) number of layers with different gypsum content, (b) multi-layer samples with gypsum content.

In addition, the failure tends to take place in the uppermost layer(s), with the interface between these and the lower layers acting as a crack-stop in many of the samples (Figure 3-27), supporting the notion that the interface between the layers (even if scarified prior to creation of the next layer) provides a plane of weakness. The exception to this would appear to be the 10% gypsum content samples, where cracks can propagate down the entirety of the multi-layered sample; it is suggested that these samples, which were the weakest in terms of UCS, had insufficient interparticle bonding within the soil skeleton for the resistance of the failure mechanism observed in the single-layered samples. It is clear that the thickness of the layer is critical: too thin and the strength and stiffness of the material is significantly reduced; the interface between layers, especially for samples with higher gypsum content levels, can dominate the development of the failure plane. However, it is apparent that if the layers are of sufficient thickness then the strength of the overall sample is not overly negatively affected and hence embracing a multi-layered approach to creation of much larger samples should prove feasible. In addition, if care is taken to ensure that the boundary between formed layers

is below potentially mobilised zones of soil during loading in the larger experiments (such as in simulated foundation testing), then using multiple layers could help maximise efficiencies during sample creation by reducing dry times required to promote gypsum bonding, whilst maintaining a metastable soil structure.

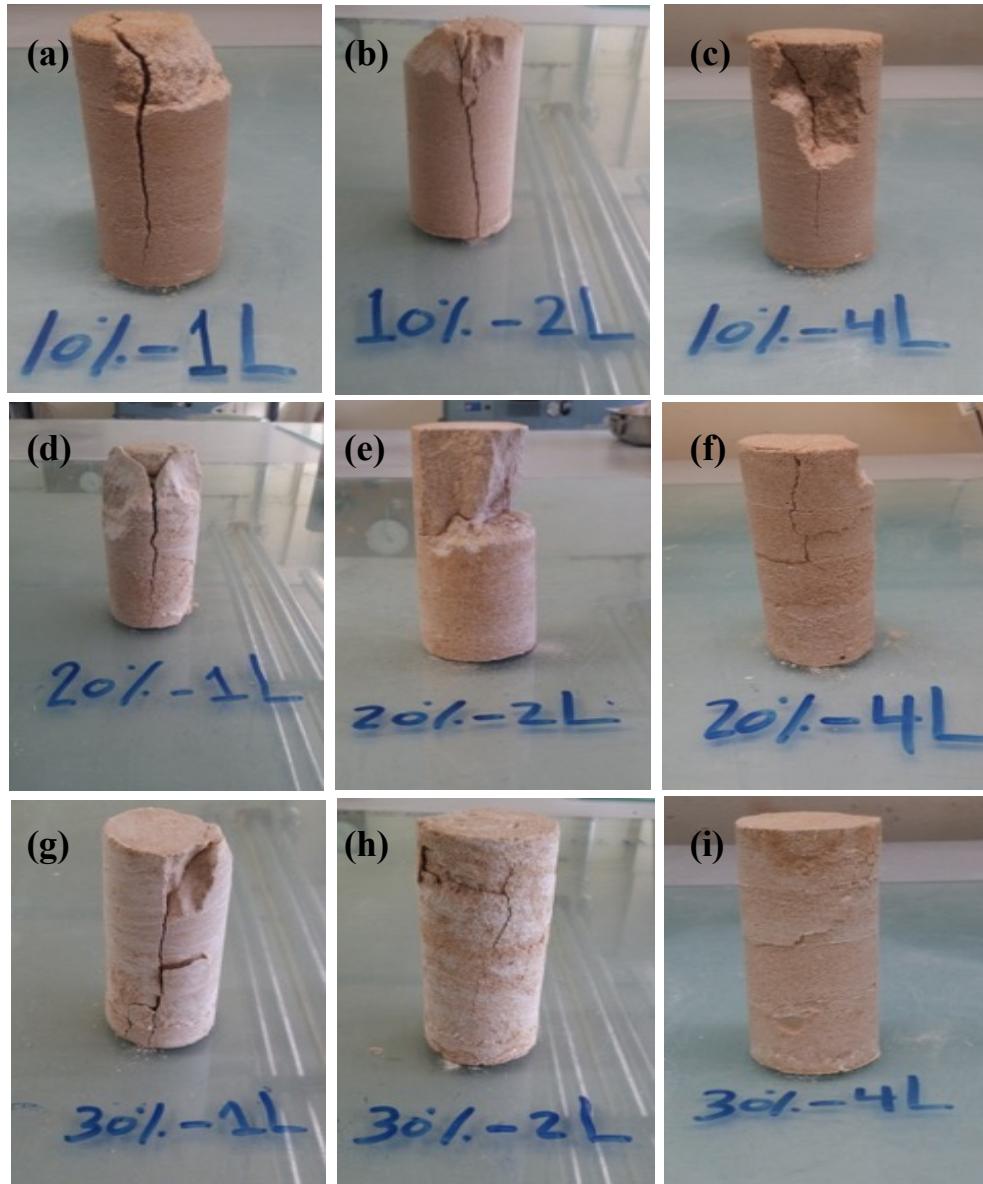


Figure 3-27: Example of failed samples (NB. The labelling system refers to the gypsum content (%) and number of layers in the sample); (i) 10%, 20%, 30%-1L ‘cured’ for 9 days, (ii) 10%, 20%, 30%-2L with the second layer ‘cured’ for 9 days, (iii) 10%, 20%, 30%-4L with the fourth layers ‘cured’ for 9 days.

3.7.4 Suction Test

This section determines the influence of various percentages of gypsum on soil-water characteristic curves (SWCC), within the manufactured gypseous soil. Four sand-gypsum mixtures containing 0%, 10%, 20%, and 30% gypsum were used. To establish the drying and wetting suction paths, the chilled-mirror dew point and the HYPROP system techniques were used.

3.7.4.1 Testing Device

The chilled-mirror dew point technique was used to determine drying paths in terms of total suction. In order to achieve this, a Decagon's WP4C Dew Point PotentialMeter was used according to the procedure in ASTM D 6836-07. This device is able to measure suction from 0 to 300 MPa with an accuracy of ± 0.05 MPa within a suction range of 0-5 MPa, and an accuracy of 1% from 5 to 300 MPa. For most samples, the time of precise mode of measurement was between 8 to 15 minutes. Before measuring suction, the device was calibrated by using a 0.5 molar potassium chloride (KCl) solution.

The chilled-mirror dew point technique can be used in combination with a HYPROP system to establish the entire SWCC in wetting paths. The HYPROP system is a laboratory evaporation method for the determination of the unsaturated hydraulic conductivity and water retention characteristics of soil samples. This device is able to measure suction 0-300 kPa. For most samples, measurements were taken between 10 to 15 days.

3.7.4.2 Sample Preparation and Testing Procedure

3.7.4.2.1 Chilled-Mirror Dew Point Technique

A sample of 37.4 mm diameter and 6 mm thickness was prepared inside a stainless-steel mould. This mould is very small when compared with the others moulds used in this study, hence pluviation was conducted by allowing the soil to fall freely into the mould via a glass funnel, its nozzle inserted in a clear tube to prevent the soil scattering and the generation of dust. To produce a similar dry density to those achieved for the oedometer and UCS samples, a 5 mm nozzle diameter and 300 mm falling height were used. Post pluviation, the sample was loaded by 5 kPa, then saturated from the soil surface as the mould base is not perforated. Consequently, the sample was moistened by placing a filter paper on the soil surface to maintain it without disturbance during the injection of distilled water by syringe. It was then dried at 25°C, the dry density and void ratio calculated. Figure 3-28 shows the main steps for the manufactured sample. This test was repeated three times for each percentage of gypsum content.

Once the samples were ready, they were inundated with a predefined weight of water (calculating the whole weight of the sample with the mould). Once again, filter paper was placed on the sample surface during inundation. The sample was then covered and stored overnight at 25°C in an incubator for water equalization. The mould was then inserted into the device to measure the total suction (Figure 3-29). Once the total suction was measured to the nearest 0.0001 g, the weight of the sample in the mould, was recorded to determine the water content gravimetrically, this constituting one point on the SWCC. To determine a second point on the SWCC, the sample was air dried until the next desired water content was achieved. This step was controlled by periodically monitoring the overall weight of the

sample within the mould. When the desired water content was achieved, the sample was left to equilibrate for 24 hours in the incubator. After this, as in the previous step(s), the total suction and the weight of the sample were recorded. This procedure was repeated till the values of total suction were equivalent to the entire range of water content calculated.

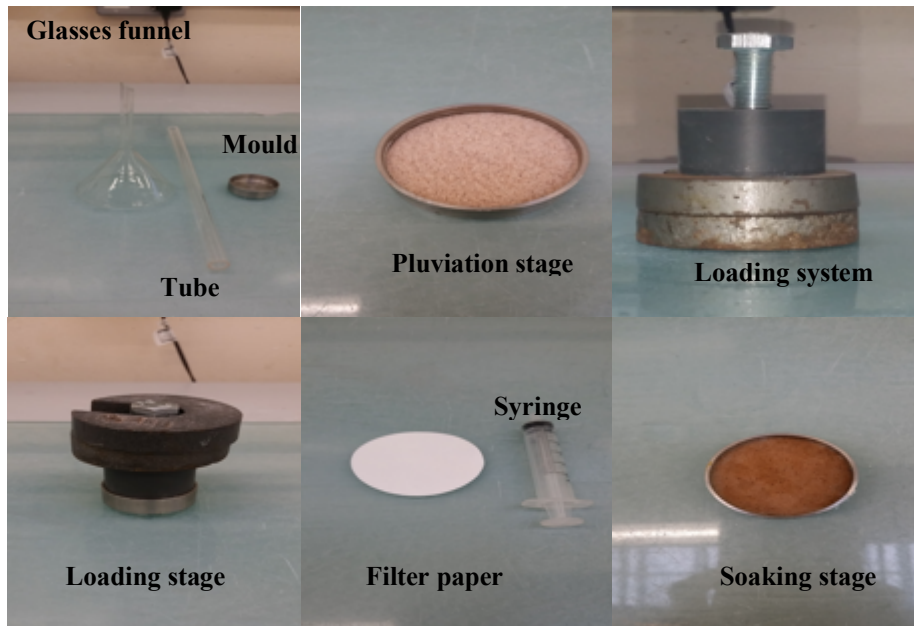


Figure 3-28: Sample preparation of chilled-mirror dew point technique.



Figure 3-29: Chilled mirror hygrometer test (WP4C Dew Point PotentialMeter).

After all measurements were taken, the samples were oven dried for 24 hours and the dry weight recorded to confirm the mass of dry solids within the samples and the gravimetric water contents used.

3.7.4.2.2 HYPROP Technique

A stainless-steel ring, 80 mm internal diameter and 50 mm height, was positioned on a mesh fabric (150 mm x 150 mm) which, in turn, was attached to a perforated saturation bowl. The sand-gypsum mixture was pluviated (using the same pluviation apparatus for the oedometer samples), levelled and weighed to calculate its dry density before loading (5 kPa), saturating and drying in the oven at 25°C. After the drying stage, the height of the sample was calculated to determine the real dry density. Figure 3-30 illustrates the basic steps to prepare the samples. Each gypsum content was repeated twice.



Figure 3-30: Sample preparation for the HYPROP technique.

To conduct the test, a dish was filled with distilled water, the water level 20 mm inside the dish, the sample placed on the perforated attachment, the sample therefore saturated by capillary action. After 4-6 hours, the water level was increased until it was 10 mm below the upper rim of the sampling ring, the sample left for 24 hours in the water. The saturated soil sample was then taken out of the dish, the auger positioning tool was placed directly over the sampling ring (Figure 3-31c). The auger tool was carefully inserted into the soil sample via the holes in the positioning tool to avoid compressing the soil, and rotated while pulling it out slowly. This made two holes in the sample, each at the desired depth. Finally, the sample was attached to the sensor unit and placed on the mass balance which was connected to a data logger (Figure 3-31e). Figure 3-31 shows the test preparation steps while Figure 3-32 illustrates the components of the HYPROP unit.

The weight and suction of each sample was measured periodically during drying process until the both the tensiometers dropped to 0 kPa (air entry). At the end of test, the soil sample was removed carefully and placed on a tray to avoid any soil loss, oven dried and weighed. The gravimetric water content of each measurement at all suction levels were then obtained via back-calculation.

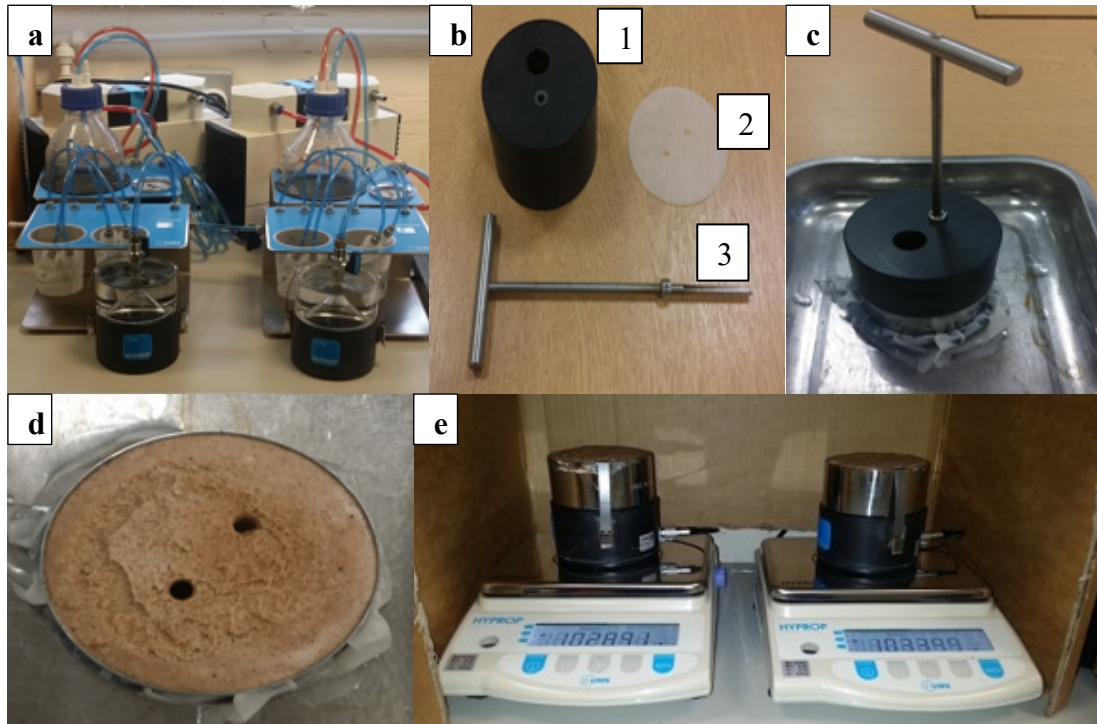


Figure 3-31: (a) Vacuum pump stage to remove the air bubbles inside the sensor and unit sensor, (b) Tools to prepare the holes' sample ((1) auger positioning tool, (2) silicon gasket, (3) HYPROP auger), (c) Placing the auger positioning tool on the sampling ring to do the holes, (d) Two holes for attaching the sensor unit, (e) Set up the HYPROP system.

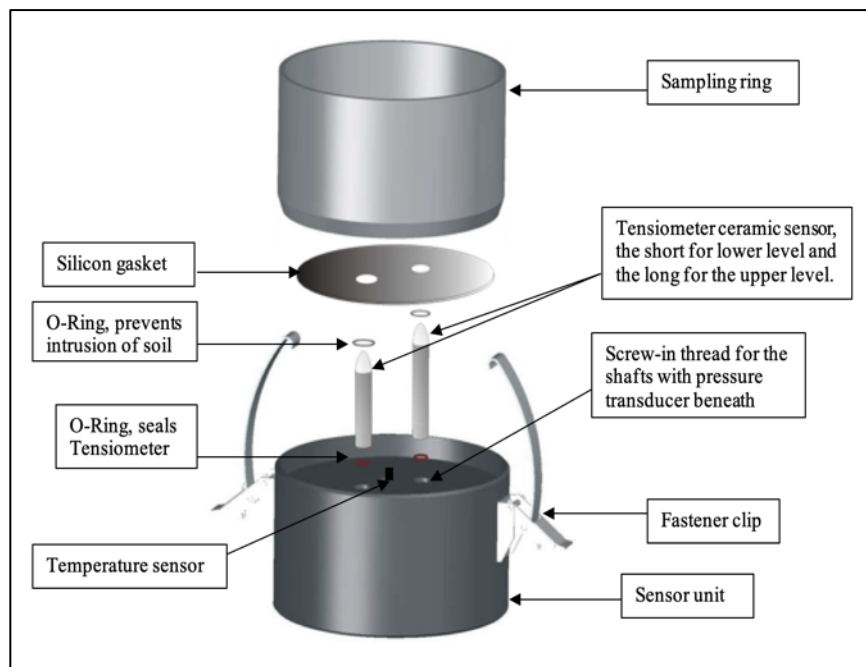


Figure 3-32: Composition of the HYPROP test apparatus.

3.7.4.3 Results and discussion

The drying and wetting paths results, over a wide suction range, are detailed in Figures 3-33 to 3-35. Figure 3-33 and 3-34 present the results of the gravimetric water content versus suctions for the drying and wetting paths, respectively, while Figure 3-35 illustrates the combined paths for each gypsum percentage.

Figure 3-33 and 3-34 reveal that as the gypsum content increases, the total suction significantly increases, as long as the residual value is lower than the water content. Nonetheless, all the total suction characteristic curves intersect at a total suction value of approximately 7 kPa and 5 kPa, corresponding to the drying and wetting paths, respectively. Below this, their response appears to reverse. This behaviour is due to the influence of gypsum content on osmotic suction which is generated at high values of water content progressively decreasing with reductions in water content. Osmotic suction is ascribed to the dissolved salt solutions in the soil pores. This finding is consistent with that of Fredlund and Xing (1994) who demonstrated that when the measured soil suction is higher than 1.5 MPa, the matric and total suctions indicate practically to the same meaning, i.e., there is no osmotic suction.

Figure 3-36 shows the results obtained from the preliminary analysis of Figure 3-33. This figure reveals that there has been a marked increase in residual total suction with an increase in gypsum content. Residual total suction increases from 120 kPa for a sample with 0% gypsum content to 590 kPa for a sample with 30% gypsum content. The equivalent residual water content decreases with increasing gypsum content. It drops from 3.5% in a sample without gypsum, to 1.2% for sample with 30% gypsum content. From the SWCCs of different

gypsum content soils, it can be noticed that the air-entry value (AEV), (this representing the value of the required suction to start the air to occupy the largest pores and cause water to be drawn from these voids within the soil system: Vanapalli et al., 1999; Lins, 2009; Fredlund et al., 2011) happened in a comparatively low range of suction values and slightly increases with increasing gypsum content. The AEV for gypseous soils obtained from the SWCC drying curve were 5, 7, 10, and 10.5 kPa corresponding to 0, 10, 20, and 30%, respectively. This finding is in agreement with Al-Obaidi's (2014) findings which showed that at the boundary effect zone, the soil fabric cannot hold water in the pore space due to its relatively coarse particle size even upon a low value of suction. This behaviour could be ascribed to the high permeability of the manufactured soil that produced by the presence of sand particles in parallel with the weak intergranular tension forces of the manufactured soil structure.

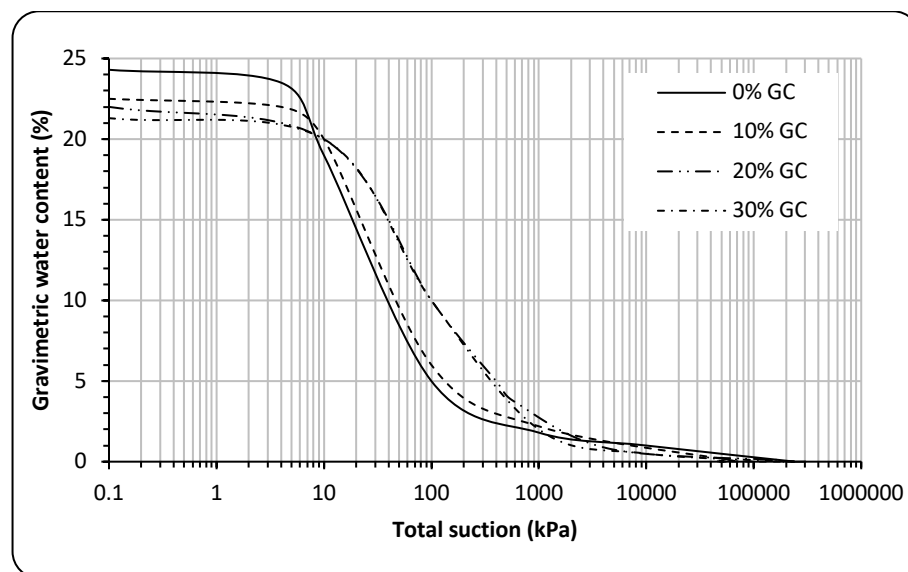


Figure 3-33: Drying path; Gravimetric water content with total suction for different gypsum contents (measured by using the chilled-mirror dew point technique).

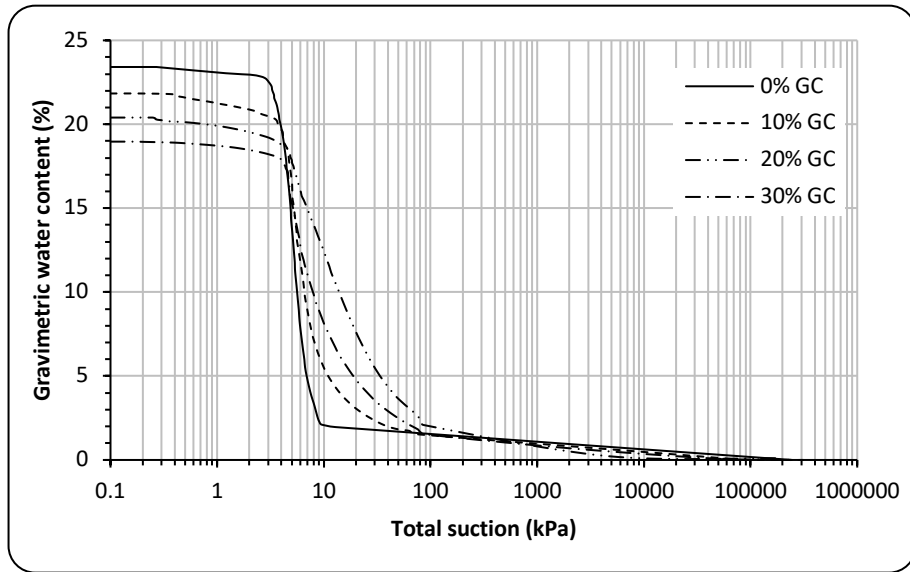


Figure 3-34: Wetting path; Gravimetric water content with total suction for different gypsum contents (measured by using the HYPROP and chilled-mirror dew point techniques).

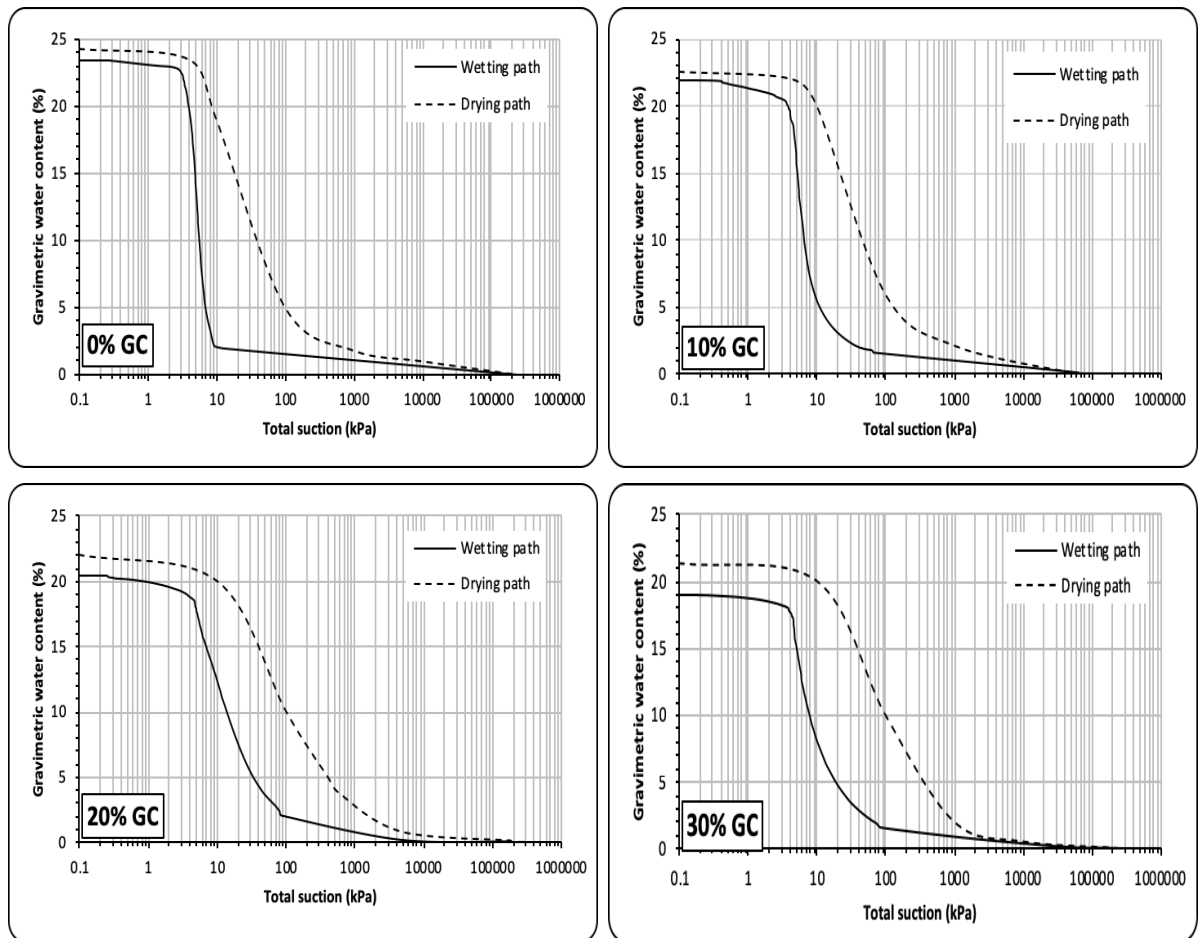


Figure 3-35: Combined drying and wetting paths for the four percentages of gypsum.

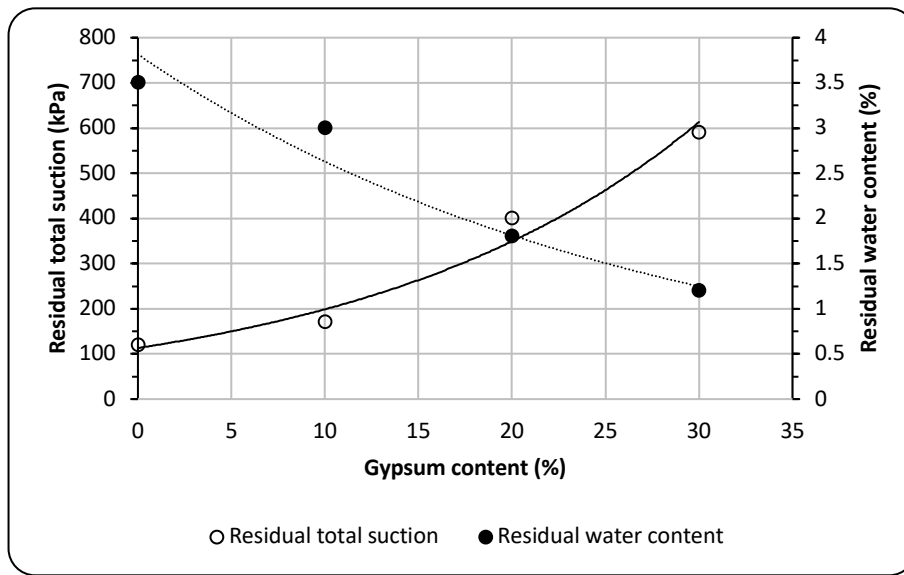


Figure 3-36: Parameters of total suction SWCCs for various percentages of gypsum (for drying path).

3.8 Summary

This chapter presents the development of a methodology to manufacture gypseous soils that reproduced metastable behaviour associated with aeolian deposits encountered in the Middle East (and potentially other hot, dry environments where aeolian deposition and secondary cementation processes may create metastable superficial soil deposits). These deposits are characterised as being strong and stiff when dry (or at low degrees of saturation), although can experience softening of the soil structure and rapid repacking with increasing water contents. Such deterioration in soil properties can lead to damage to surrounding structures. Therefore, the new method developed for this study, which used a modification of the pluviation technique in an effort to produce more consistent gypseous sand samples. A poorly graded sand, chosen to create an open structure, was pluviated with gypsum crystals and subsequent wetting and drying of the sample (in a low temperature oven, set at 25°C)

promoted the development of cemented bonds between the particles. This has produced ‘relatively homogeneous’ soil structures, which exhibit collapse potential, and thus are ideal for parametric study.

The compaction parameters were significantly affected by changes in gypsum content (which ranged from 0% to 40%). It was found that there is a marked increase in the maximum dry density with increase in gypsum content up to 30%; beyond that, the trend appeared to reverse. While, there is a clear trend of decreasing optimum moisture content with increasing gypsum content (from 0% to 40%).

Outcomes from compression and deformation response testing indicate that the samples produced following this method replicate behaviour prescribed to naturally occurring deposits: brittle deformation response, being stiff and strong when dry, becoming less stiff upon wetting, with associated repacking, which underlines the suitability of this approach (pluviation). It is clear that constructing a sample using multiple layers does not produce one with exactly the same properties as one created in a single layer, using multiple layer approach allows for the development of much larger soil samples whilst ensuring that the metastable response remains. It is clear that samples should be allowed to dry for at least 9 days, if not longer if drying larger samples in the atmosphere, to ensure that gypsum crystal growth develops the required interparticle bonding. In multiple-layered samples, each layer must be allowed to develop the gypsum bonding before the creation of the subsequent layer.

The manufactured samples experienced rapid repacking akin to hydrocollapse when inundated whilst transmitting load, although it is clear that secondary compression and creep

are critical to the compression behaviour of these soils. Discounting the impact of these fundamentally underestimates likely settlements that would be encountered if conditions in situ change, hence fundamentally underestimating the severity of these metastable soils. Therefore, in SOT, it is recommended that longer load steps (90 days used herein) are used than the commonly adopted 24-hour periods.

The suction test revealed that as the gypsum content increases, the total suction significantly increases, as long as the water content is greater than the residual value. The AEV, occurred in a comparatively low range of suction values and slightly increases with increasing gypsum content. The AEV values that obtained from the SWCC drying curve were 5, 7, 10, and 10.5 kPa corresponding to 0, 10, 20, and 30% gypsum content, respectively.

CHAPTER FOUR

BESPOKE EXPERIMENTS: SAMPLE CREATION AND CELL DEVELOPMENT

4.1 Introduction

The experimental phase of this investigation, undertaken after it was established that gypseous soil samples could be manufactured in the laboratory (Chapter Three), was undertaken in two, interconnected studies. The first study aimed to determine the impact of groundwater movement due to evaporation through an unsaturated column of gypseous soil. This was carried out using larger samples than those used for validation testing: 144 mm diameter and 300 mm height. These samples were exposed to various conditions including changing gypsum contents, groundwater, temperature gradients and a breeze fanning across the upper surface of the samples. The second study aimed to determine the change in response of the manufactured gypseous soil under a simulated foundation load. The samples used for this were the largest in this investigation: 349 mm diameter and 300 mm height. Measurements were taken when the samples were exposed to groundwater flow with and without exposure to the environmental conditions used in the previous study; temperature gradients and breeze.

This chapter reports the development of the experiments undertaken to meet the aims of the study. The first experiment was designed to simulate a ‘very simple proxy’ for conditions that superficial aeolian gypseous soils in hot arid environments, such as those in the Middle East, might be expected to experience, i.e. unsaturated conditions (drying), overlaying saturated deposits, temperature gradients (hot surface temperatures) and a surface breeze. The second

experiment was designed to simulate foundation loading when exposed to groundwater flow, with and without exposure to environmental conditions. Electrical resistivity (ER) was used to monitor the movement of salty water through the samples in ‘quasi real-time’, without having to dissect the samples. Dissection was undertaken at the end of the tests. Electrodes were installed into the sample housing in a single line, two lines corresponding to the evaporation cell and settlement tank, respectively. To calibrate the resistivity within the temperature gradient, the soil temperature was measured using thermistors installed within the sample at various depths.

In summary, this chapter includes the development of bespoke tests, the evaporation and footing tests, the method used to test electrical resistivity, details of the experimental design, construction, procedure of the experiment and calibration.

4.2 Sample Sizes for the Bespoke Tests

The samples created for validation testing were of the standard size used for classic geotechnical tests. These however, would not be of a suitable size for these bespoke experiments. Establishing a temperature gradient and unsaturated fluid flow through such small samples would be problematic at best, therefore a larger sample was required.

French et al. (1982), Gran et al. (2011), Smits et al. (2011), Song et al. (2013), and Yoon et al. (2015) each investigated sand(y) soils exposed to various conditions including salt behaviour in the capillary fringe and movement of water in soils experiencing a thermal gradient. The sample size used for the current work was chosen based on the practical findings of the above researches.

French et al. (1982) carried out experimental work simulating sabkha soil, similar to that found in the Arabian Gulf, to study the motions of saline groundwater and the dissolution and precipitation of inorganic salts (such as gypsum, halite and calcite) in the capillary fringe. In their study, the distance between the water table and the soil surface was allowed to vary, while the daily cycle of temperature and humidity was fixed. It was found that the rate of evaporation at the surface and capillary velocity are related to the groundwater depth from the surface, this impacting on the quantity of salts accumulated at the surface. French et al. (1982) found that a dry soil bed, 500 mm thick, requires three months to achieve equilibrium of moisture profile: upwards of one year is required for a sample 1 m thick under the same conditions. Therefore, French et al. (1982) recommended that in order to achieve results in a reasonable amount of time, the thickness of the soil bed in a model test has to be less than 500 mm.

Song et al. (2013) undertook a similar study to that of French et al. (1982) and developed a large-scale environmental chamber (800 mm width x 1000 mm length x 895 mm height) to investigate the process of soil water evaporation on sand beds. It was found that only the zone closest to the soil surface is subject to the effects of evaporation (within 60 mm). This was near the heating source, the volumetric water content showing significant changes. As such, it was recommended that the soil column be 300 mm high, this sufficient to achieve the evaporation targets in the laboratory. In addition to the height of the soil column, the internal diameter (144 mm) was chosen to obtain data in a reasonable time, based on the practical findings of Gran et al. (2011), Smits et al. (2011), and Yoon et al. (2015). Therefore, based on the aforementioned findings, the samples measured 144 mm in diameter by 300 mm in height for the evaporation test and 349 mm in diameter (see Section 4.5) by 300 mm in height for the

footing test. Due to the time required to create and test the samples, only two sand-gypsum mixtures (10% and 20% gypsum content) were considered in the evaporation test. Only 20% gypsum content was used in the footing test as it is very common in urban areas in Al-Najaf city (Aziz, 2008; Ali and Fakhraldin, 2016; Al-Zubaydi, 2017).

4.3 Electrical Resistivity (ER)

Electrical resistivity is a geophysical technique that has been used to determine subsurface resistivity distribution by taking measurements on the ground surface (Loke, 1999; Stummer et al., 2004; Jinguiji, 2011). These are then used to infer information regarding the properties of the ground profile. ER surveys have been used for many decades in mining, hydrogeological and geotechnical investigations (Kalinski and Kelly, 1993; Fukue et al., 1999; Guinea et al., 2012; Yan et al., 2012; Pandey et al., 2015). More recently, it has been used in environmental surveys (Slater and Lesmes, 2002; Kemna et al., 2004; Loke et al., 2011, 2013).

4.3.1 ER Theory and Factors that Influence ER

ER can be considered a basic property of a porous medium containing water and solutes (Kalinski and Kelly, 1993; Samouëlian et al., 2005). It measures the resistance of a material towards the flow of electric current. Four electrodes are normally needed to measure ER: the current is generated through two electrodes ('current electrodes'), the other two measuring the potential difference ('potential electrodes'). Ohm's law governs the resistance as shown in the following Equation 4.1:

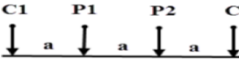
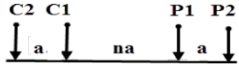
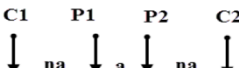
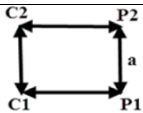
$$R = \frac{\Delta V}{I} \quad \text{Eq. 4.1}$$

The electrical resistance of the ground is denoted by R , the difference in voltage between the two potential electrodes shown by ΔV and the electrical current that is generated between the two current electrodes given by I . The measurement of the value of the apparent resistivity (ρ) from the resistance, R can be done by applying Equation 4.2:

$$\rho = R * K \quad \text{Eq. 4.2}$$

Where the geometric factor that relies on the four electrodes arrangement is given by K . Table 4-1 presents the values of geometric factors together with their common electrode configurations previously used in the laboratory and field.

Table 4-1: Popular electrode arrangements (Samouëlian et al., 2005).

Configuration type	Electrode arrangement	Geometric factor (K)
Wenner		$2\pi a$
Dipole-Dipole		$\pi n(n+1)(n+2)a$
Wenner-Schlumberger		$\pi n(n+1)a$
Square		$\frac{2\pi a}{2\sqrt{2}}$
Notes	a: electrode spacing; n: an integer; C: current electrode; P: potential electrode	

The calculated ER value is not the true ER of the subsurface, but an apparent value representing the ER of a homogenous ground that will give a similar resistance value for a similar electrode arrangement. There is complex relationship between the true and the apparent resistivity. Calculated apparent resistivity values have to be inverted through a computer program to reflect true subsurface resistivity (Loke, 1999; Samouëlian et al., 2005). Nevertheless, ER is a function of a number of soil properties (Kalinski and Kelly, 1993; Fukue et al., 1999; Samouëlian et al., 2003, 2005; Kim et al., 2010; Yan et al., 2012; Pandey et al., 2015) including the voids arrangement (porosity, pore size distribution and connectivity), degree of saturation (water content), the nature of the solid constituents (particle size distribution and mineralogy), temperature and ER of the fluid (solute concentration). The air is an insulator medium ('infinitely resistive'). The resistivity of water solution is a function of ionic concentration, the density of electrical charges at the surface of the constituents determining the resistivity of the solid grains. ER is influenced in various ways and degrees by these parameters.

An unsaturated, gypseous soil, experiencing upward seepage of water transporting dissolved gypsum under a thermal gradient and prior to precipitating the gypsum crystals into the soil fabric with evaporation, is likely to experience a complex chemico-physico-electromagnetic environment in transitory conditions. Accurately identifying the changes in resistivity in such a complex and changing, environment is beyond the scope of this research. However, it is hoped that relative changes in resistivity over time, might be used to identify the migration of solute-bearing water through the soil column, providing another source of data to augment traditional post-testing sampling synonymous with geotechnical testing.

4.3.2 Electrode Configuration for the Current Study

The principle of the conventional four electrodes method is used to develop automated multi electrode resistivity systems through multiplexing various electrodes. A regular fixed distance is maintained between the current and the potential electrodes and gradually moved along a line on the surface of the soil. One measurement is recorded at every step. In this investigation, the electrodes were installed into the sample housing in a single array and in two vertical arrays, corresponding to the evaporation cell and settlement tank, respectively. Each array consisted of sixteen, equidistant electrodes to measure the ER based on four electrodes. For laboratory scale measurements, it is preferable to use a 16 electrodes system which compromises between the noise introduced through many electrodes and computational time (Polydorides, 2002; Damasceno et al., 2009; Bera and Nagaraju, 2011; Devadasi et al., 2014).

To measure resistivity, the Wenner arrangement was used. In comparison to the more common arrangement, this facilitates a higher vertical resolution because it has relative sensitivity towards vertical variations in the subsurface resistivity underneath the central array (Reynolds, 1997; Dahlin and Loke, 1998; Loke, 1999; Olayinka and Yaramanci, 2000; Okpoli, 2013). By using each set of four adjacent electrodes, thirteen individual resistances are calculated using the sixteen-electrode configuration: the current electrodes are outer ones, the potential electrodes are the inner electrodes, as shown in Table 4-2. A typical sequence of resistance measurements on evaporation cell and settlement tank is shown in Figure 4-1. To give a good resolution, each measurement was repeated four times. After this, to achieve the apparent ER, the measured electrical resistance R was multiplied by the geometric factor (K) for this specific configuration.

Table 4-2: Defining a sequence of electrodes for automated data acquisition.

Readings No.	C1	P1	P2	C2
1	1	2	3	4
2	2	3	4	5
3	3	4	5	6
4	4	5	6	7
5	5	6	7	8
6	6	7	8	9
7	7	8	9	10
8	8	9	10	11
9	9	10	11	12
10	10	11	12	13
11	11	12	13	14
12	12	13	14	15
13	13	14	15	16

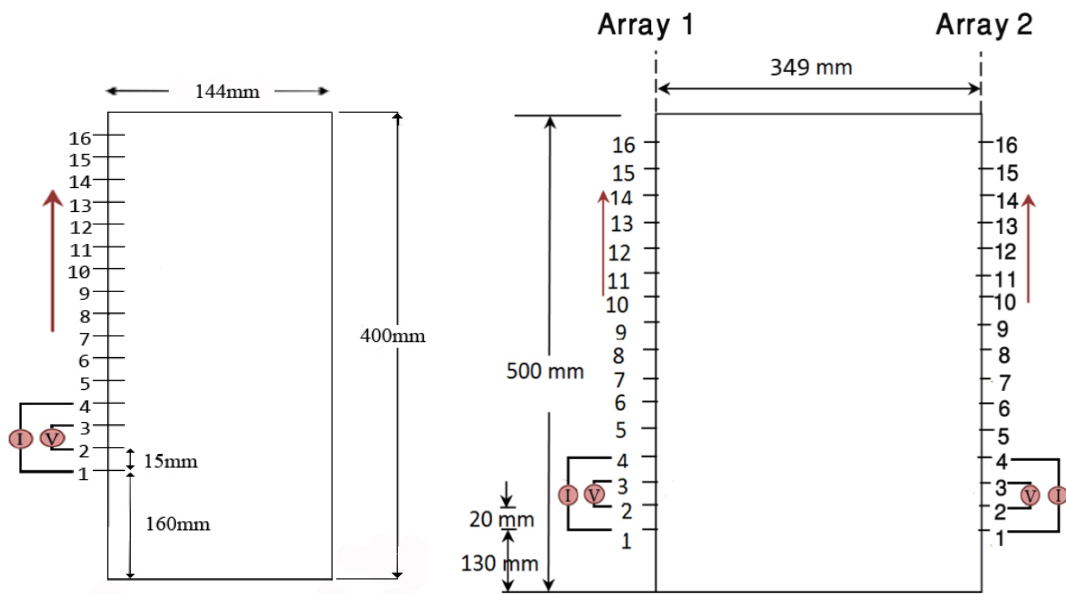


Figure 4-1: Electrode configuration; (left) evaporation cell, (right) settlement tank.

4.3.3 The Data Logging System

The ER Acquisition System II, was developed in the Department of Electrical Engineering at Birmingham University, to allow multifrequency measurements (courtesy of Mr P.A. Atkins) for a previous doctoral study undertaken within the Civil Engineering laboratory (Faroqy, 2018). Having determined that the contact resistance effects between the soil sample and the electrode are greatly reduced or totally eliminated by using an alternating current (AC) over a direct current (DC), (AC) was chosen. To facilitate automatic switching between the 32 electrodes, National Instruments modules NI9239 and NI9263 (ER-Acq-I) were integrated along with an automatic switching board into the data acquisition system. It was not possible to integrate more than 16 channels owing to the cost of the automatic switching board (Figure 4-2).

To obtain voltage and current readings from a switched array of electrodes, a MATLAB script was created by Mr P.A. Atkins. Two pairs of electrodes were used to take each measurement. Two current electrodes (C1 and C2) at a constant 1 mA, were used to inject the electrical current and to measure voltage across the 1 k Ω resistor, two potential electrodes (P1 and P2) also used, the time set at five seconds. Based on the results of previous research (Faroqy, 2018), it was concluded that high accuracy and high precision readings can be obtained by the ER-Acq-II. A sufficiently low frequency of 60 Hz was chosen in this study to avoid polarization as this alters the electrical properties of the soil (Arulanandan and Smith, 1973; Abu-Hassanein et al., 1996; ASTM G57, 2006).

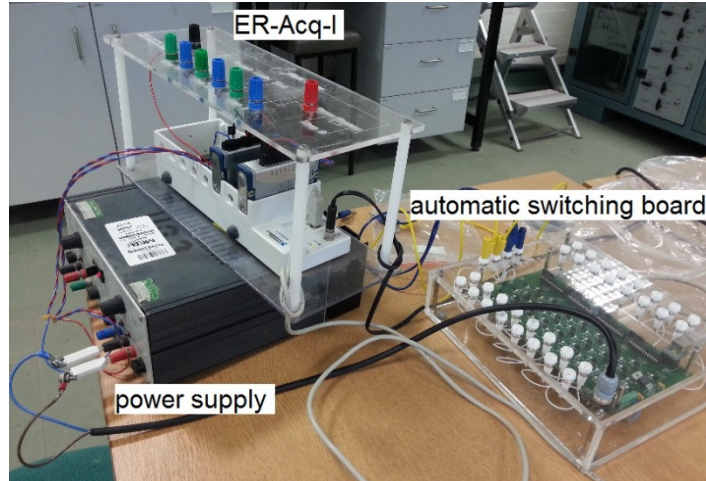


Figure 4-2: ER-Acquisition System II (ER-Acq-II).

4.4 Experimental Setup of Evaporation Test

4.4.1 Lab Equipment and Apparatus

This experimental apparatus (Figures 4-3 and 4-4) comprised a cylindrical pipe (the experimental cell), a water tank, an infrared lamp, a fan, thermistors (temperature sensors), resistivity probes and data loggers. Samples were pluviated into the experimental cell in 6 layers of 50 mm thickness each (described in more detail in Section 4.4.2.2). This thickness of layer was chosen based on the outcomes of the UCS testing whereby 50 mm layers appeared to not significantly impact upon the deformation response of the samples (unlike 25 mm thick layers). They also proved compatible with the installation of the resistivity probes (Figure 4-4). Thermistors were installed between each pluviated layer of soil. Unlike the samples created for UCS testing, the samples created for this study were not extracted from the cell, but instead allowed to dry in situ under ambient conditions (Section 4.4.2.2). The experimental cell comprised an acrylic, transparent pipe that was 400 mm in height with an internal diameter of 144 mm and a wall thickness of 3 mm. The bottom of the pipe base was glued to a base plate to seal it in order to prevent any leakage of water. A tap was installed 25

mm from the base of the cell to facilitate connection to the water tank. A 100 mm thick filter layer comprising well graded gravel and crushed stone with a layer of fabric between the filter and pluviated gypseous soil (described in more detail in Section 4.4.2.1), was installed prior to pluviation to ensure that water could easily flow into the base of the sample. The internal opening of the tap was covered by a fine plastic mesh to prevent the filter material entering it and blocking it, principally during the drying stage (see Section 4.4.2.2).

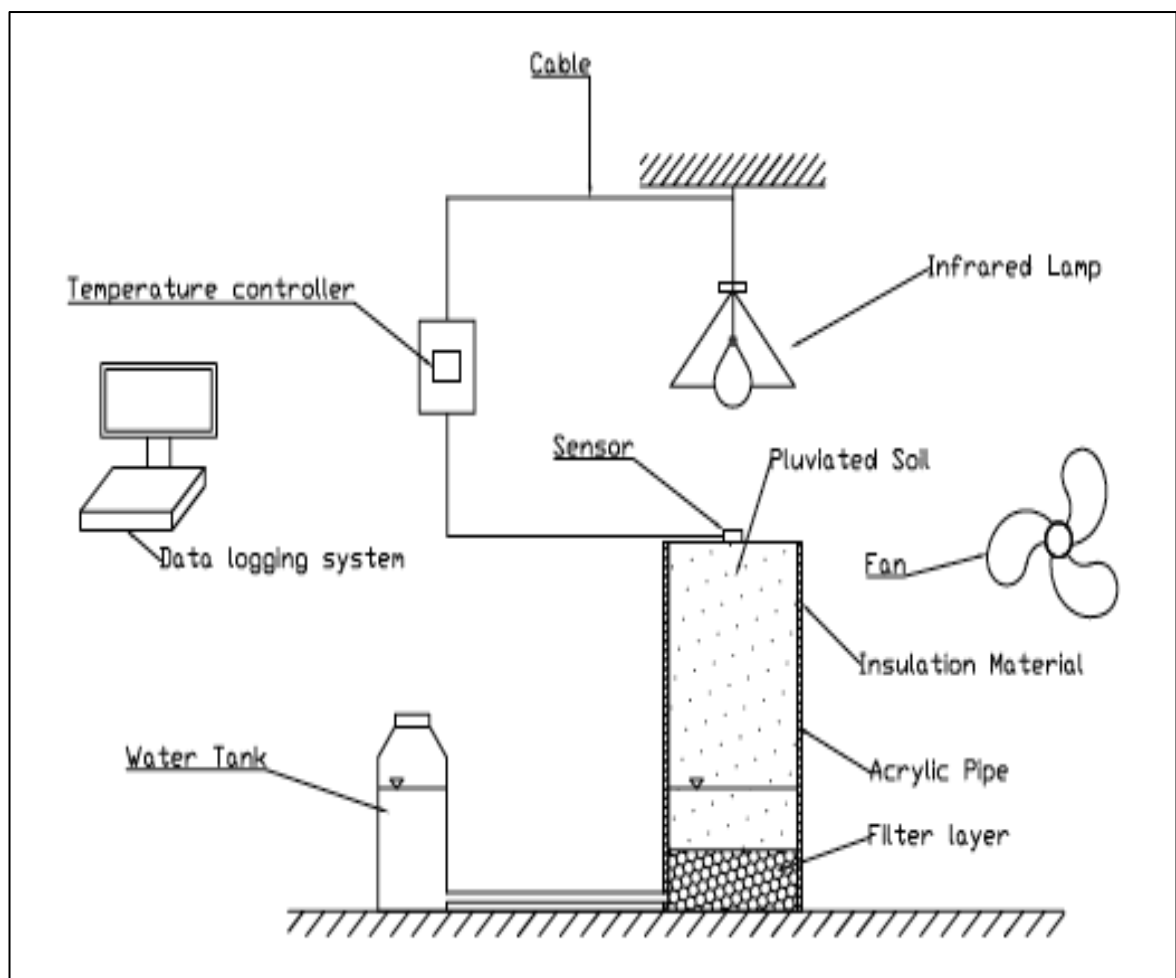


Figure 4-3: Sketch of the evaporation test (NB. This does not depict the ER probes installed in a line up one side of the pipe nor the internal temperature sensors buried at various depths).

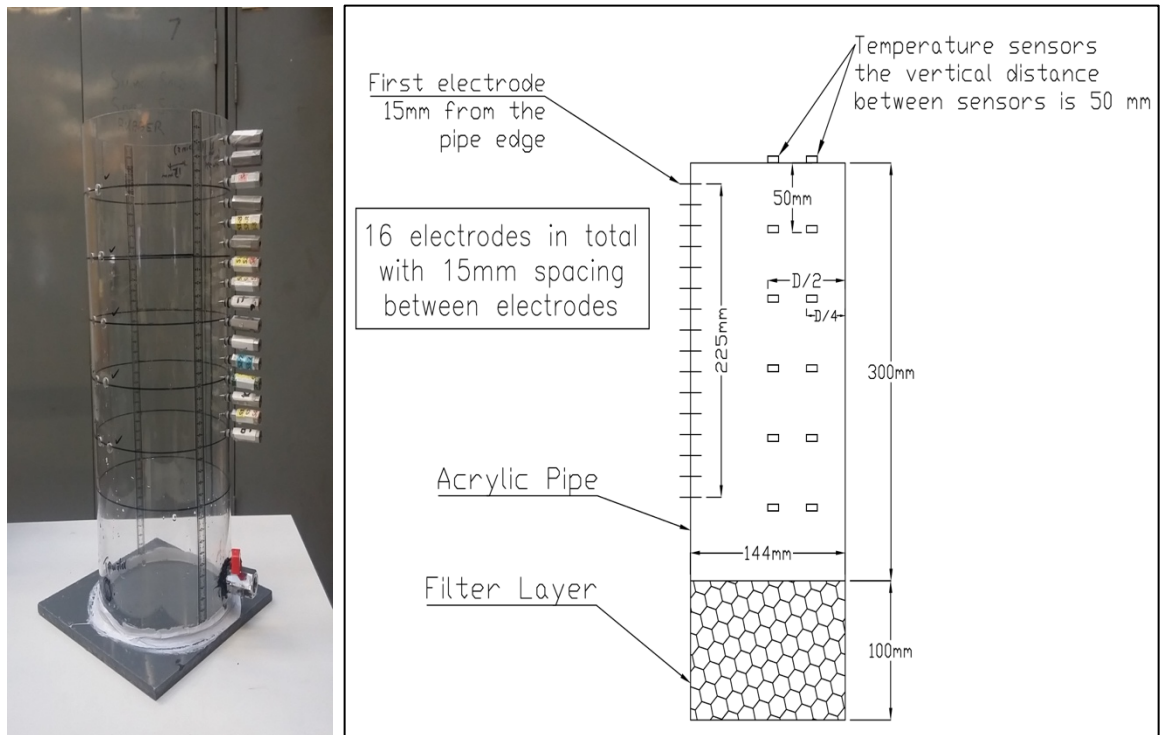


Figure 4-4: Evaporation cell; (left) photographic picture, (right) schematic view illustrating the layout of the resistivity probes and location of the thermistors.

The water tank took the form of a 5-litre capacity container that housed a tap near the base. The water tank supplied water to the experimental cell via a 5 mm internal diameter clear plastic tube. Hydrostatic conditions were maintained between the water tank and the experimental cell, with a water table formed 100 mm above the upper surface of the filter layer. The water tank was labelled with a measuring tape, allowing any change in the water table to be detected. As water was drawn up into the unsaturated soil sample, the water level slowly decreases. As such, the water tank requires to be topped up regularly throughout the duration of the experiment (see Section 4.4.4).

An infrared lamp (175-Watt, Philips 175R), partially covered by a lampshade was placed 200 mm directly above the manufactured soil surface to create an even distribution of temperature

within the soil. This lamp can heat the upper surface to 50-52°C, similar to the summer temperature encountered in Iraq (Sissakian et al., 2013; Al-Bahrani et al., 2014). To maintain the desired temperature, a temperature controller (INKBIRD, model ITC-106 with a stated accuracy $\pm 0.1^\circ\text{C}$ at more than 1000°C), was used to regulate the output from the lamp based on the output from a thermistor located on the soil surface. In order to minimise the influence of ambient conditions on the temperature gradient established within the soil column, the experimental cell was wrapped in a 4 mm thick layer of insulation comprising a double aluminium bubble wrap foil insulation. This insulation material was selected after undertaking several tests regarding different types and thickness of insulation material to determine the best configuration to minimise loss of heat into the laboratory. Testing also took into consideration the level of fire resistance of these materials as the lamp above the soil column operated continuously throughout the duration of the experiment when a temperature gradient was required.

In order to determine the temperature profile for the samples, waterproof probes (Figure 4-5: DS18B20, supplied by Cool Components Ltd Company) were installed at the surface and buried within the samples. 12 probes were installed, the number limited by the data logging facilities available, at the interface between the layers of soil, with the exception of the filter layer (i.e., 0, 50, 100, 150, 200, and 250 mm below the soil surface), which had two per layer. The first was installed in the centre of the sample and the second nearer the wall, 36 mm from the cell wall. The diameter and length of the probes are 7 mm and 26 mm, respectively, the twelve temperature sensors installed horizontally through the pipe wall. The cell wall was sealed using waterproof silicon sealant to prevent leaks. All of the sensors were installed horizontally through the wall of the experimental cell in order to reduce the potential for

preferential flow paths forming along the sensor wires vertically upwards through the soil column. The temperature range of the sensors was -55°C to $+125^{\circ}\text{C}$ with a stated accuracy $\pm 0.5^{\circ}\text{C}$ when recording temperatures between -10°C to $+85^{\circ}\text{C}$. This sensor was chosen as it was able to operate in wet conditions and did not need specialist dataloggers and software, making them a cost-effective solution. An Arduino board integrated with Arduino MEGA prototype shield was use as a data logger and could support up to 12 sensors (see Figure 4-6). The data from the thermistors were obtained with Termite software that operated from a PC.



Figure 4-5: Waterproof (DS18B20) probe used to measure soil temperature.

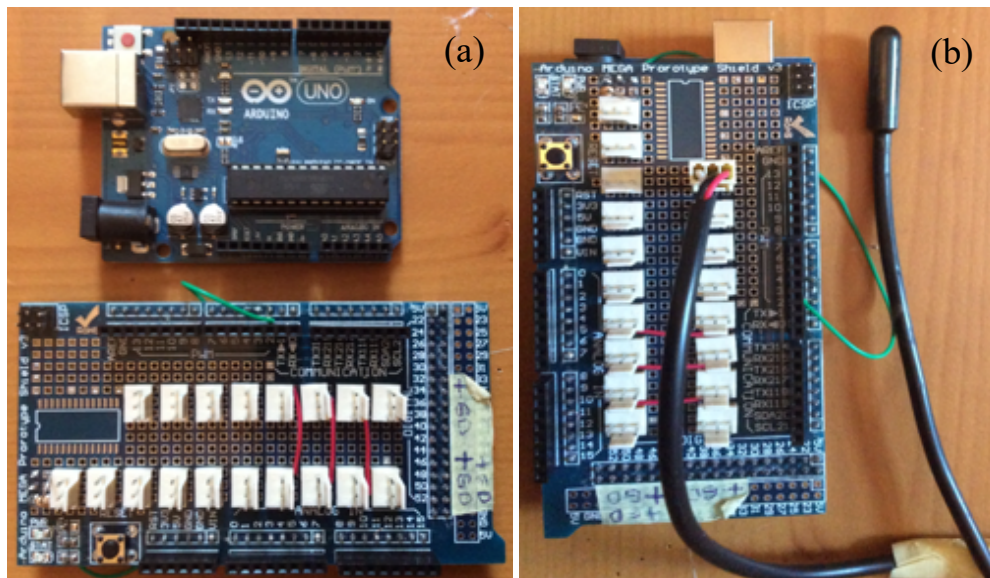


Figure 4-6: Data logging of temperature sensors; (a) (top) Arduino board and (bottom) Arduino MEGA prototype shield, (b) the completed ensemble.

A breeze acting across the upper surface of the soil columns was generated using a fan (Axial fan model RAH1245S1, brand X-Fan). This fan was positioned at a distance of 330 mm from experimental pipe and slightly above the pipe edge so as not to interfere with the positioning of the lamp. It is capable of generating wind speeds of up to 2400-2500 rpm.

The ER arrangement used 16 pin electrodes (Figure 4-7), aligned and equally spaced on one side of the experimental cell (Figure 4-4). The first electrode was positioned 15 mm from the upper surface of the cell, the 15 subsequent electrodes installed with a 15 mm gap between electrodes. The electrodes were fastened to the cell wall via a threaded outlet insulated with a plastic threaded washers and O-rings to ensure they did not leak. The pin electrode was made of threaded marine steel rod with a 3 mm diameter which sharpened to a point. The rod was embedded in a hexagonal shaped marine steel bar with an opening permitting the accommodation of a banana plug connection. The electrodes extended into the acrylic pipe by approximately 5 mm. The calibration of the array arrangement and the influence of temperature was determined following the procedure in Section 4.6.



Figure 4-7: Photograph of pin electrode.

4.4.2 Soil Deposit Formation

4.4.2.1 Requirements for the Filter Layer

A well-graded gravel up to 7 mm, which had previously been washed and oven-dried, was placed into the base of the acrylic pipe, lightly compacted by a wooden rod and levelled to give a height of 85 mm. The gravel layer was topped by 12 mm of crushed stones (ranging from 1 to 3 mm) that was tamped at the surface by a wooden rod and levelled to create an even filter layer. This was finally covered with 3 mm thick punching needle fabric, working as a filter paper. The total height of the filter layer was 100 mm. The purpose of the filter layer was to disperse the water and to allow an even distribution of water throughout the manufactured soil during inundation, without disturbing the contact soil particles.

4.4.2.2 Formation of the Manufactured Pluviated Gypseous Soil Sample

Following the procedure developed in Chapter Three, sand-gypsum mixtures of two gypsum contents, 10% and 20%, were pluviated separately in six layers, each 50 mm thick. Each layer was flooded and then left to dry within the experimental cell, before the upper surface was scarified and the subsequent layer pluviated. It should be noted that the apparatus used to create the oedometer and UCS samples was too small to create these samples. Therefore, a new pluviation apparatus was built with a wider internal diameter, although the shutter porosity, falling height, falling distance and diffuser were maintained in order to obtain the same dry unit weight as those formed during the validation testing.

The following procedure was used to prepare the samples for the evaporation test:

- To minimize the segregation between the sand and gypsum, 1300 g of dry sand was mixed with 10 g of distilled water (0.75% by dry sand) in an electrical mixer for 5 minutes until the moisture was evenly distributed. This percentage of water had been used for the preparation of samples for the validation testing.
- 130 g or 260 g of gypsum material, corresponding to 10% or 20% gypsum content by dry weight of sand, was added to the damp sand. This mixture was mixed for 10 minutes, any soil coated on the mixer blades wiped off into the sample and remixed again for another 3 minutes.
- The sand-gypsum mixture was weighed and then carefully transferred into the soil container in the pluviation setup (hopper). Once ready, the diffuser was properly positioned inside the pipe and the gate was opened to pluviate the sand-gypsum mixture.
- Once pluviation was completed, the top of the layer was levelled off to a predefined mark on the experimental cell, the remaining material removed and weighed and the dry density (at pluviation stage) calculated.
- An 8 kg (equivalent to 5 kPa) load was applied onto a 5 mm thick PVC plate which remained in place for 2 hours. The PVC loading plate contained a groove cut within the perimeter to ensure that the electrodes which were previously inserted into the pipe wall, were not damaged.
- Thereafter, the loading was removed and distilled water was introduced, via the filter layer, up to the upper surface of the filter to inundate the mixture by capillary action for 4 hours. It should be noted that the 4 hours started after the new layer was completely inundated by capillary action.

- The sample was drained by disconnecting the water tank and applying a gentle vacuum to the base tap of the experimental cell, hence the need for the plastic mesh to prevent particles being drawn into the vacuum pump, to remove as much liquid as possible. It was then air dried as there was no oven big enough. Oven drying the electrodes was deemed inadvisable for fear of unquantifiable changes in their properties. The extent of drying of the soil deposit was checked by weighing the cell regularly until measurements were constant.
- Prior to pluviation of the next layer, the upper surface of the existing sample was gently scarified and the two thermistors inserted horizontally via the holes in the experimental cell wall. This procedure was repeated for each layer.
- As for the preparation of samples for validation tests in Chapter Three, it was noted that the surface of each new layer experienced a collapse (approximately 1 and 3 mm, corresponding to 10% and 20% gypsum content, respectively) during loading and saturation stages. This collapse increases the dry density by 2.0% and 7.1% corresponding to 10% and 20%, respectively.
- These layers were formed over a six-week period. Once complete, the manufactured gypseous soil column was approximately 300 mm in depth. Figure 4-8 shows the steps of sample preparation.

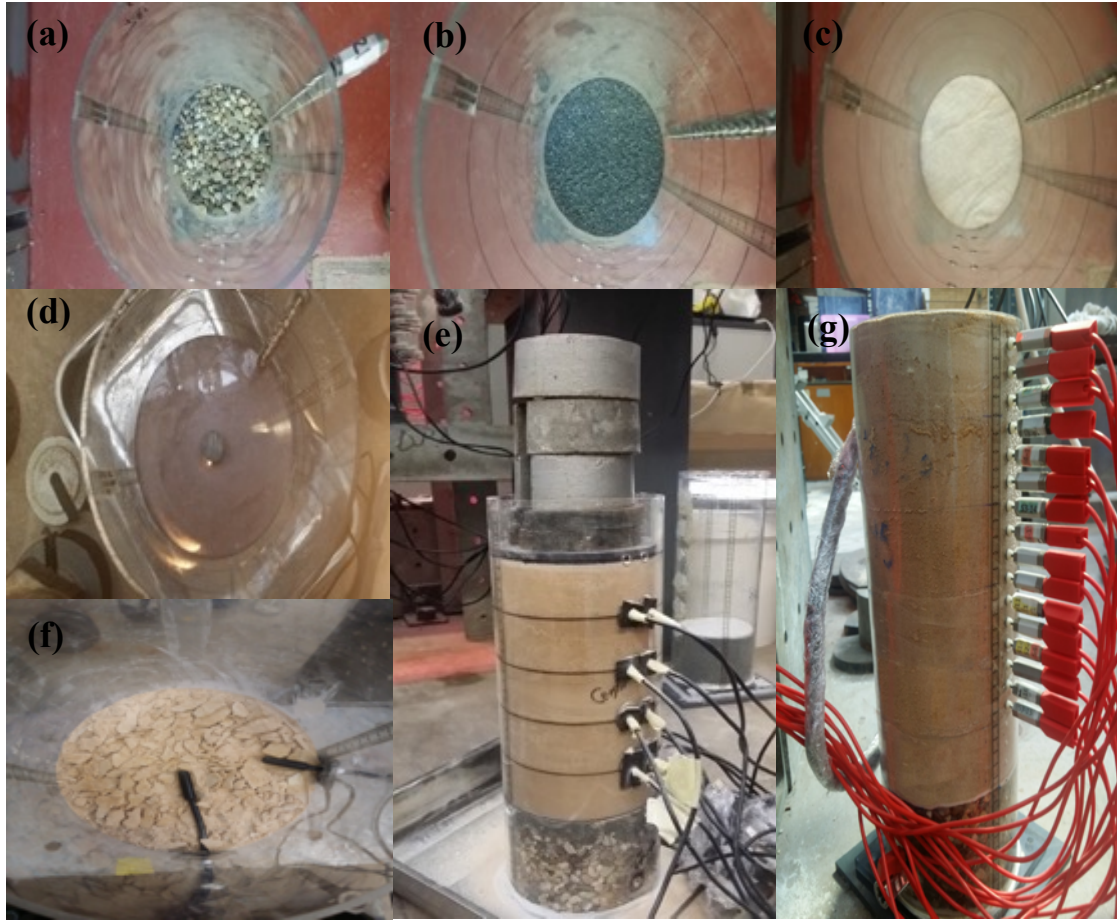


Figure 4-8: Steps of sample preparation; (a) installation of the gravel layer, (b) installation of the crushed stones layer, (c) completion of the filter layer with the addition of the punching needle fabric, (d) the layer of soil has been pluviated and the PVC plate has been installed ready for loading (note the notch to ensure the ER probe is not damaged), (e) loading stage, (f) scarifying the surface layer and installing the temperature sensors, (g) the completed gypseous sample after drying and ready for testing.

4.4.3 Investigating the Response of a Trial Sample

Before the main tests were undertaken, two pilot samples, one each of 10% and 20% gypsum contents, were created in order to determine the actual gypsum content and water content before implementing the real tests. This allowed identification of the consistency of the soil deposits inside the cell, identification of the practical limitations of the sample production technique and indication if it was suitable for a larger sample size. The experimental cell was

filled with soil layers in the same way as the procedure described in Section 4.4.2. Having created the samples via pluviation, loading, wetting and drying, they were divided into subsamples by digging, each approximately 25 mm in length. The gypsum and water contents were calculated (the gypsum content using Al-Muftly and Nashat's (2000) method, previously described in Chapter Three, Section 3.3.3) for each subsample, and the profile plotted (Figure 4-9).

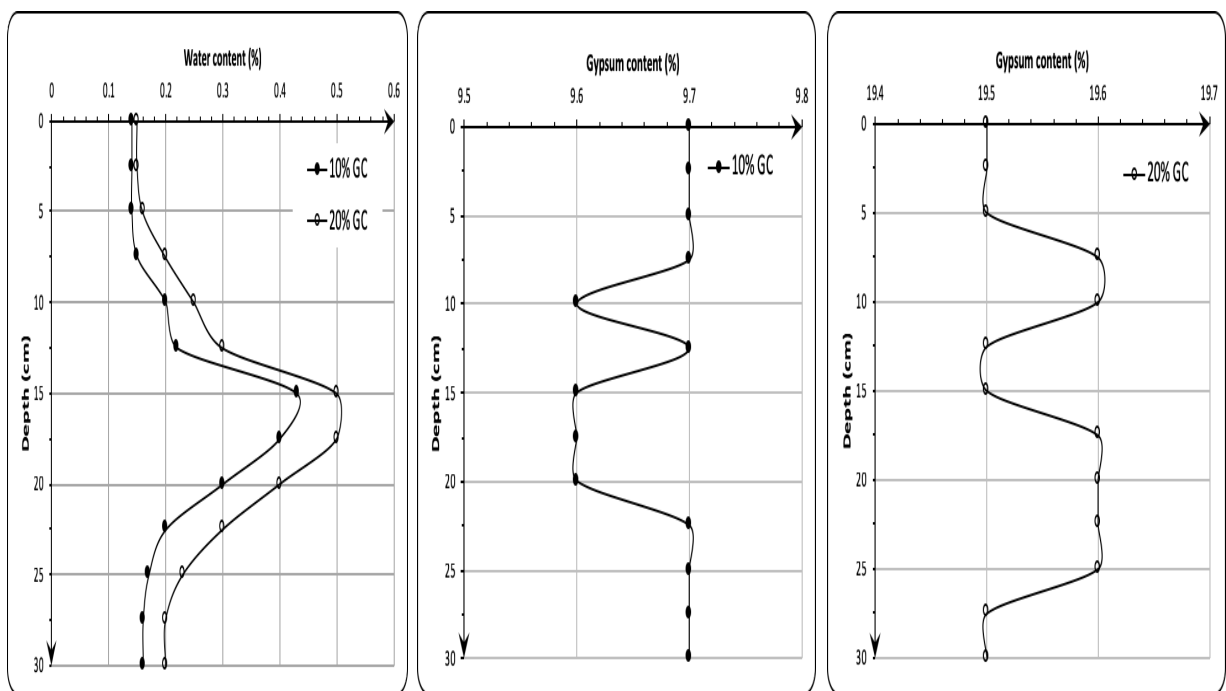


Figure 4-9: Water and gypsum contents of trial samples for 10% and 20% gypsum content before testing.

Figure 4-9 reveals that the water content in the middle layers was higher than the upper and lower layers. This is because evaporation of the water will be high at the top open to the air and the bottom because of contact with the filter layer. It was found that there was variation in the gypsum content as is expected using pluviation, both within the layer and down through the column. This variation is of similar magnitude to that encountered in the validation study, with a maximum variation from target gypsum content of 0.4% and 0.5% for the 10% and

20% gypsum content samples, respectively. This variation was deemed acceptable and formed an effective baseline when considering the changes in gypsum content with changing environmental conditions.

Subsampling for dry density calculation was trialled but found wanting due to the friability of the material; this issue was also encountered during validation testing. Therefore, the dry density calculated for each layer was based on the known layer volume and the mixture weight after the drying stage. Dry density was calculated to be $1.55 \text{ Mg/m}^3 \pm 2\%$ and $1.54 \text{ Mg/m}^3 \pm 2\%$ corresponding to 10% and 20% gypsum contents, respectively.

4.4.4 Running the Evaporation Test

Initially, the experimental cell was connected to the water tank and water allowed to seep into the previously dried sample to form the 100 mm deep groundwater table above the upper surface of the filter layer. It was left for one day afterwards to allow the level of the water table (within the sample and the water tank, which was topped up throughout this period) to achieve equilibrium. This was considered Day 1 of the experiment. After Day 1, the pipe wrapped with insulation material, the lamp and the fan were activated and remained on for the duration of the experiment which was completed on Day 41. This is because it takes time for the temperature gradient to enter a quasi-steady-state, this varying with gypsum content. The water level within the water tank fell as water was drawn up into the soil column, this fall recorded every one to two days, the water level topped up regularly to keep it constant and equivalent to 100 mm within the manufactured gypseous sand sample. Temperature measurements were collected every 1 minute. ER data was collected throughout the duration

of the experiment, the samples dissected post testing to determine changes in the soil sample. Figure 4-10 shows the test operation.

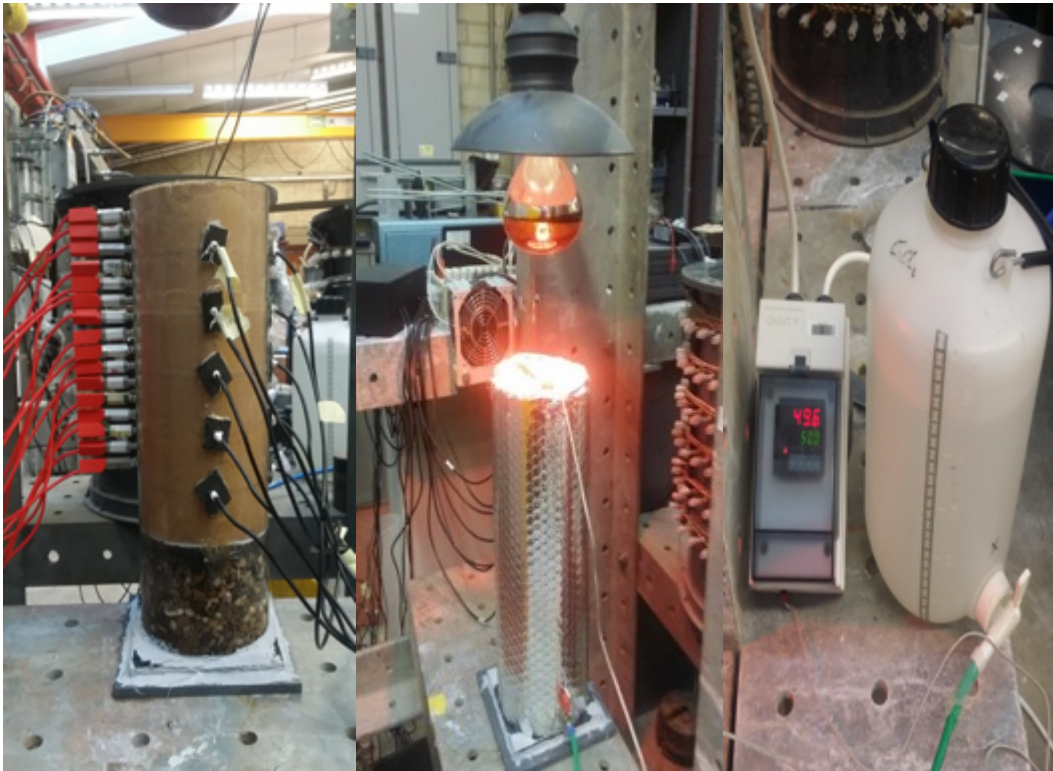


Figure 4-10: Running test. From left to right; soaking the soil by capillary action, starting the test, water tank and temperature controller.

4.5 Setup of Footing Test

4.5.1 Lab Equipment and Apparatus

This experimental apparatus (Figures 4-11 and 4-12) comprised three cylindrical tanks which were used for a previous doctoral study undertaken in the laboratory of Civil Engineering at the University of Birmingham (for more details see Al-Obaidy, 2017), a water tank, an infrared lamp, a fan, thermistors, resistivity probes and data loggers. Samples were pluviated into the experimental cell: 5 layers of 60 mm thickness (described in detail in Section 4.5.2.2).

The tanks were made of 3 mm thickness PVC with internal dimensions of 349 mm diameter and 500 mm height. Each tank contained 212 electrodes arranged in six horizontal circles and two vertical arrays. The test cells had flanges to make them sufficiently rigid. To simulate the rise of the groundwater table through the soil deposit, each tank was fitted with a tap 40 mm above the tank base and a 160 mm thick filter layer. The water tank supplied water to the experimental cell via a 5 mm internal diameter, clear plastic tube. Similar to the evaporation cell, the internal opening of the tap of the settlement cell was covered by a fine plastic mesh (see Section 4.5.2.2).

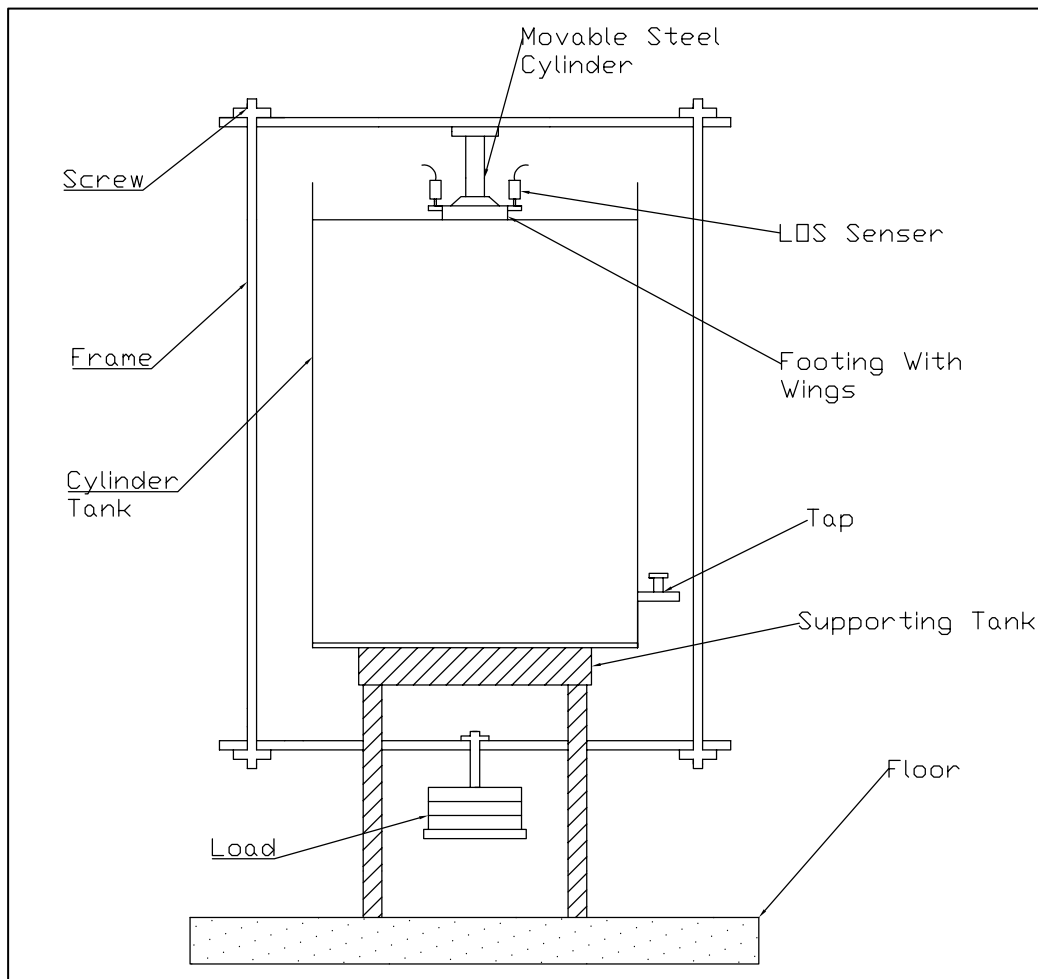


Figure 4-11: Sketch of the footing test illustrating the settlement tank and the loading frame.

sample and the second nearer the wall, 87.3 mm from the cell wall, as shown in Figure 4-12. In order to minimise the influence of ambient conditions on the temperature gradient established within the soil column, the experimental cell was wrapped in a 4 mm thick layer of insulation (double foil insulation), as described in Section 4.4.1.

As mentioned earlier, each tank has 212 electrodes as the previous researcher used an acquisition system that enabled simultaneous measurements at a set standard time, this borrowed from another university (Al-Obaidy, 2017). However, the acquisition system (ER-Acq-II) that was used in this study only read up to 16 electrodes (as previously mentioned in Section 4.3.3) and each electrode cable had to be connected manually. Consequently, it was decided to measure soil resistivity by the two vertical arrays aligned on both sides of the tank, each line containing 16 pins. The first electrode was positioned 130 mm from the base of the tank, the 16 electrodes were separated equally at 20 mm. The electrodes were made of M4 threaded stainless steel rods. They extended into the tank by approximately 6 mm and were strengthened by using a washer and nut. A banana plug connection was used to connect each electrode to the acquisition system. The calibration of the array arrangement was determined in Section 4.6.1.

4.5.1.1 Model Footing

The circular model footing was made of steel plate. The footing width was carefully chosen under two main considerations: to minimize the particle size effect and to contain most of the stress bulb within the tank. Tatsuoka et al. (1994) concluded that the footing size effect is a function of two factors: stress level dependency of the mechanical properties of granular soils and the variation of footing width to mean grain size (B/D_{50}) ratio. The second factor is also

termed as ‘particle size effect’. Based on modelling experiments, some researchers (e.g. Ovesen, 1975; Bolton and Lau, 1989; Kusakabe, 1995) reported that there is a threshold value of B/D_{50} ratio for small model tests above which the influence of particle size is insignificant. Kusakabe (1995) recommended that B/D_{50} ratio should be greater than 50-100 in order to avoid scale effects. On other hand, based on the bearing capacity effect, it was found that to avoid boundary effects, the horizontal distance from the edge of the footing to the internal face of the tank should be larger than $2B$, while the vertical distance from the bottom of the footing model to the strong layer in the tank, should be larger than $2.5B$ (Mandal and Manjunath, 1995; Al-Aghbari and Mohamedzein, 2004; El Sawwaf and Nazir, 2012). Consequently, and based on this information, the footing diameter was selected as 70 mm with a thickness 20 mm.

To facilitate the measurement of the settlement under the footing by the LDS sensors without touching the frame, four steel wings were connected to the footing extending approximately 20 mm out of the footing area. In order to avoid the influence of the embedded temperature sensor that was positioned directly underneath the footing (see Section 4.5.4), by footing temperature, double aluminium bubble wrap foil insulation was used to insulate the circular footing.

4.5.1.2 Loading and Measurement Apparatus

A loading frame was designed and manufactured to apply a static vertical load on the circular footing model in the settlement tank. A sketch of the main features of the loading assembly is given in Figure 4-11. The loading frame was constructed using two rigid steel plates. The end face of these plates was connected with two steel rods via a screw, to form the frame skeleton.

In addition, a hanger including a steel rod and square base, was screwed centrally to the bottom steel plate, this hanger used to hold the loading. This hanger applied the desired load centrally on the model footing through a movable solid steel cylinder which was placed concentrically on the footing model. This movable steel cylinder has two bases: the lower base (49.57 mm in diameter) which was positioned on the footing, and an upper base (69.84 mm diameter) which raises the frame. The hinge between the lower base and steel cylinder allows the frame to move freely with the footing, while the diameter of upper base prevents the frame sliding (Figure 4-13). This movable cylinder was used to transmit dead weights from the frame to the foundation. A stress of 80 kPa (this stress including the weight of the frame and moveable cylinder) was used to represent a building of two storey height.

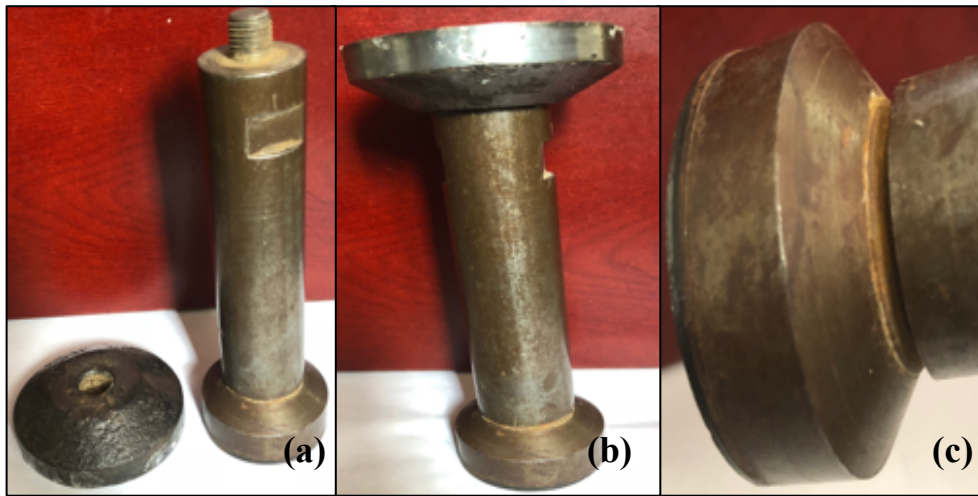


Figure 4-13: (a) Movable steel cylinder used to transmit the loading from the frame to the footing model, (b) Steel cylinder with both bases, (c) Closer view of the hinge between the small base and steel cylinder.

Footing settlement was measured by four linear displacement sensors (LDS) model HS50 (50 mm travel distance) with infinite resolution, supplied by Micro-Measurements Company. LDS sensors work within a temperature range of -10 to 60°C. A model D4 data acquisition

conditioner, supplied by the same company, was used to read the LDS sensors. The model D4 has four input channels. It is powered via the USB interface; its measurement accuracy is $\pm 0.1\%$. The operational temperature is 0 to 50°C, humidity up to 90%. Figure 4-14 shows the LDS sensor and data logger.



Figure 4-14: (a) Linear displacement sensor (LDS) to measure vertical displacement of footing, (b) The four channels connection side, (c) USB connection attached to the PC via a cable.

4.5.2 Formation of the Soil Column

As was explained in Section 4.2 and 4.5.1, the soil column was 300 mm high, the tank 500 mm high, respectively. In order to raise the soil deposit to the flange's tank to allow frame loading, it was decided to increase the filter layer's thickness to 160 mm. To manufacture substantial quantities of gypseous soil by pluvial deposition, a large pluviation apparatus was built, taking into account the factors and process used in Chapter Three. There was no variation in the soil properties (void ratio and gypsum content) above those investigated in this chapter.

4.5.2.1 Formation of the Filter Layer

19 kg of washed and dried gravel was placed into the base of the cylindrical tank, lightly compacted by a wooden rod and levelled to a height of 140 mm. 3.4 kg of crushed stones were laid over the gravel layer, compacted by the wooden rod, levelled to form an even filter layer and covered with punching needle fabric of thickness 3 mm. The total height of the filter layer was 160 mm. Distilled water was added to the filter layer via the base until the filter layer was covered. 5 litres of water were required to cover the 160 mm layer, this process taking 14 minutes. This amount of water will be referred to as W1 (see Chapter Five). This was an essential step as it allowed calculation of the quantity of water that was added to the soil. Figure 4-15 shows the steps followed to establish the filter layer.

4.5.2.2 Manufacture of the Gypseous Soil

A sand-gypsum mixture with 20% gypsum, was pluviated in five layers, each 60 mm thick, instead of six layers (see Section 4.4.2.2) to reduce the time required to obtain a whole dry sample. The cylindrical tank was marked inside in 60 mm sections for each layer. 7.2 kg of the dry sand was moistened with 54 g of distilled water and mixed thoroughly in an electrical mixer for 5 minutes until the moisture was evenly distributed throughout the dry sand. 1.4 kg of gypsum material, corresponding to 20% gypsum content by dry weight of sand, was added to the pre-wetting sand. This mixture was mixed for 10 minutes, any soil coating the mixer blades wiped off into the sample and remixed again for another 3 minutes. Exactly the same procedure as described in Section 4.4.2.2 was followed: pluviation; a seating pressure 5 kPa was applied on the PVC circle for two hours, its diameter smaller than that of the tank to avoid the electrode needles inside the tank; wetting and drying by applying a gentle vacuum to the base across the tap hole to remove as much liquid as possible and then air dried. Before

pluviating the next layer, each layer was scarified and two temperature sensors inserted horizontally via the holes that were previously made in the walls of the tank, this repeated for each layer. Application of the seating load and water clearly resulted in compression of each new layer by approximately 3-4 mm, leading to an increase in dry density. These layers were formed over a three month period until the manufactured gypseous soil column was approximately 300 mm. Figure 4-15 shows the sample preparation steps.

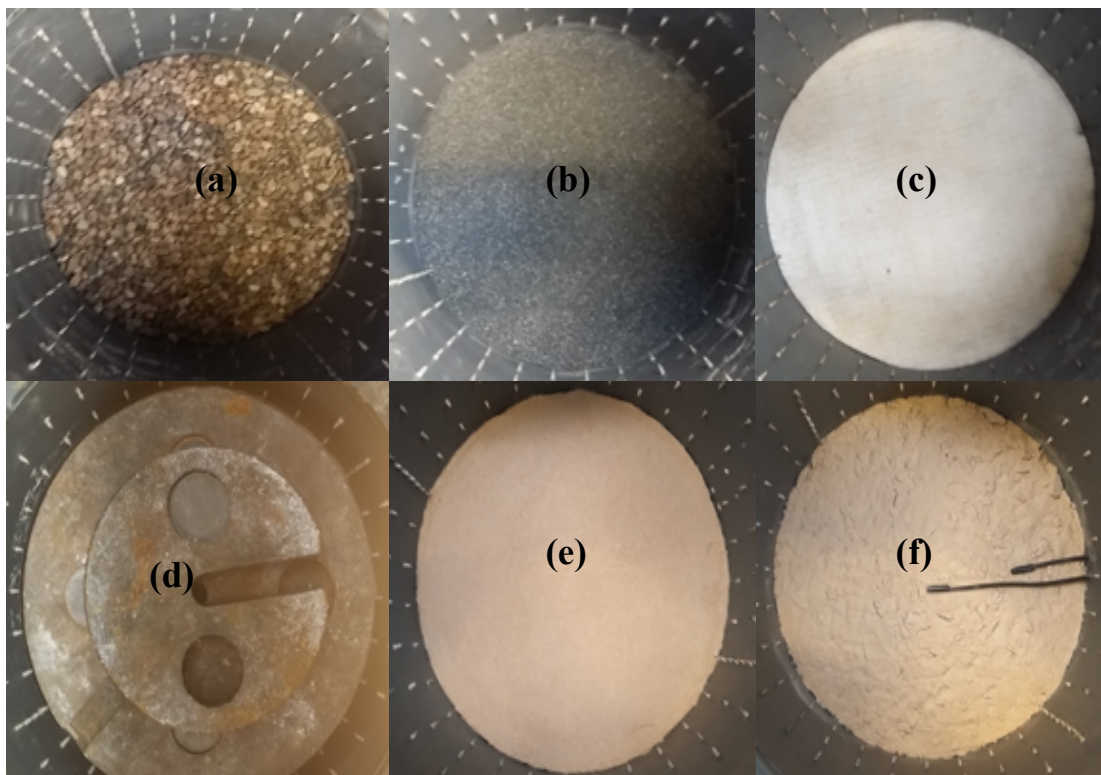


Figure 4-15: Filter and soil formation steps; (a) gravel layer, (b) crushed stones layer, (c) punching needle fabric, (d) pluviated and loading stages, (e) wetting stage, (f) two temperature sensors installed over each new layer.

4.5.3 Investigating the Homogeneity of a Trial Sample

As described in Section 4.4.3, to investigate the consistency of the sample before the main tests were conducted, a pilot sample, one at 20% gypsum content, was created in order to

determine the initial water content and actual gypsum content along the soil column. Once the gypseous soil sample was manufactured following the procedure described in Section 4.5.2, subsamples were taken from five depths along the sample produced and the water and gypsum contents was measured (see Figure 4-16). As noted in the trial evaporation samples (Section 4.4.3), the soil was dry at the upper and lower layers, the highest water content, an average 2.2%, was at a depth of 180 mm from the soil surface. The maximum variation of the gypsum content within the layer and down through the column from target gypsum content was found to be 0.5%. It was difficult to sample the dry soil in undisturbed condition; thus, the dry density was calculated for each layer based on the known of layer volume and the mixture weight. Dry density was calculated to be $1.55 \pm 2\%$ Mg/cm³ corresponding to 20% gypsum content.

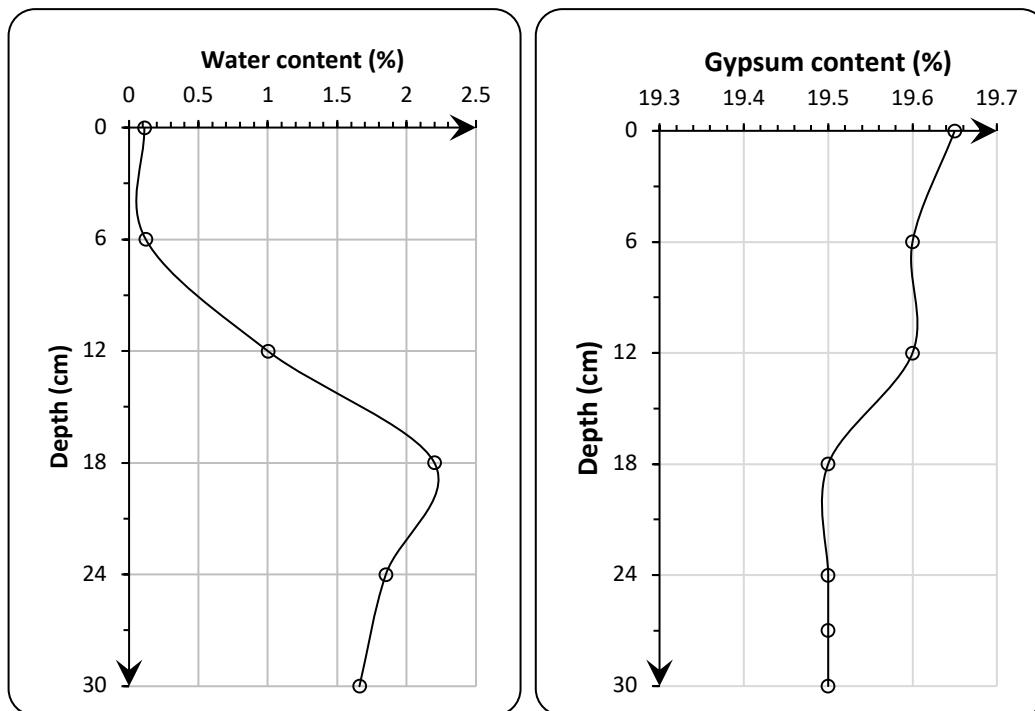


Figure 4-16: Water and gypsum contents profiles of the trial sample for 20% gypsum content before testing.

4.5.4 Running the Footing Test

Once the tank approached the desired curing time, it was transported to the loading frame. The surface was carefully levelled again using a straight edge and spirit level. Then, a temperature sensor was buried in the centre of the soil tank, located directly below the footing. To bury the temperature sensor, a hole with the same dimensions as the sensor was formed manually and then it was placed horizontally in the hole. The hole was then filled and tamped manually with the soil excavated beforehand to ensure the same density. Following this, the circular footing was positioned on the buried sensor, concentrically with the centre of the tank and checked that it was even. Four LDS sensors were placed on the footing's wings with the help of magnetic bases fixed on the tank's flange by adhesive. Once the LDS were set to a zero reading, the small base of the movable cylinder was placed carefully on the centre of the footing, which had been marked beforehand. The frame assembly was carefully positioned on top of the wider base of the movable cylinder. This accuracy was essential to avoid any shock and vibration to the footing as the loading (80 kPa) included the weight of the movable cylinder and frame assembly.

Readings for temperature and from the LDS sensors were taken simultaneously from the movable cylinder and frame, these readings recorded automatically at one-minute intervals. The soil was left under their weight (i.e. frame and movable cylinder, 12 kg) until the observed deformation remained constant. Thereafter the load increased in three increments, each 6 kg. On the same day, the target load of 80 kPa was reached, this load left for 24 hours to allow all the settlement to take place. After the loading step was completed, the inundation stage was started. ER was measured before the next loading step and wetting stage.

The testing programme comprised three cases of footing test to simulate gypseous soil behaviour under different conditions: (i) a quick test without heating or breeze whereby the footing was loaded, the groundwater level increased at very short intervals; (ii) a slow test without heating or breeze whereby the footing was loaded, the groundwater increased over longer intervals; (iii) a third test similar to test 2, but with heating and a breeze.

Regardless of test condition, the increase in groundwater level was simulated by adding water to the tank's base, this rising through the filter layer and up through the soil deposit. The process was repeated in stages, each with a known amount of water, until failure of the deposit was observed. Failure could occur due to punching, shear or cracking at the upper deposit (see Chapter Five). After failure occurred, the water content and gypsum content were calculated from five depths along the soil column, at three locations for each depth (under the footing, 90 mm to both the right and left of the footing). In Case 3, two infrared lamps and one small fan were used to simulate a hot climate. The lamps were suspended over both sides of the tank in order to ensure homogeneity of the soil surface temperature. A photograph of the setup is shown in Figure 4-17. It is worth mentioning that although the heating source was applied only in Case 3, all cases were insulated with thermal material. This was to compensate for variations of temperature into soil column which in turn, influence measurements of soil resistivity.



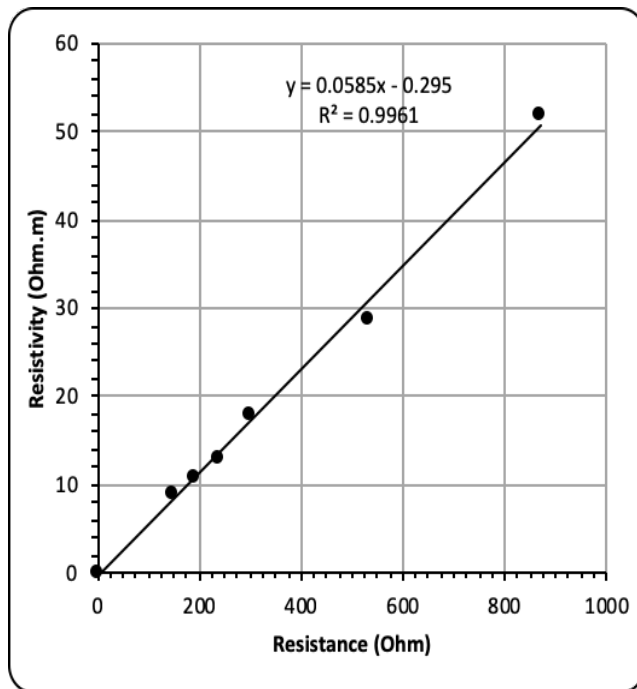
Figure 4-17: Photograph of the test setup; (left) test in laboratory conditions (without heat and breeze), (right) test with heating and breeze sources.

4.6 Electrical Resistivity Calibration

4.6.1 Calibration of the Configuration

Because of the arrangement of electrode pins within the cylindrical cell, there was the possibility of the 2D geometry having an effect on resistivity measurements (ρ). As such, the geometric factor (K) had to be calculated either numerically or experimentally (Sreedeeep et al., 2004; Sheffer et al., 2007; Beck et al., 2011; Hassan, 2014; Al-Obaidy, 2017; Farooqy, 2018). In this study, the geometric factor was experimentally calculated following the procedure by ASTM G57, (2006). Six NaCl solutions of varying concentrations, ranging from 0.1 g/l to 0.6 g/l, were created using distilled water resulting in a range of electrical conductivities. These solutions were poured into the cell to a height of 400 mm in the evaporation cell and 450 mm in the settlement tank. A temperature probe was inserted into the

solution to monitor variations in temperature during the tests. A portable conductivity meter by HANNA instruments (type HI 8733), which itself was calibrated using a standard solution, HI 7030, was used to measure the electrical conductivity (EC) of these solutions, which were in turn converted to resistivity (ρ) (the resistivity is the reciprocal value of conductivity, i.e. $\rho = 1/EC$). The resistance readings (R) for each configuration obtained by the acquisition system, ($R = V/I$), were compared with the EC measured by a standard conductivity meter (HANNA device). The geometric factor was then derived as the gradient of resistivity and resistance line (Figure 4-18), given that $\rho = K \cdot R$. In this process, all the solutions and the instruments were accommodated in a temperature-controlled room at 20°C. According to ASTM G57 (2006), laboratory calibration is recommended to be conducted at 20°C, or a temperature correction factor should be applied.



(a)

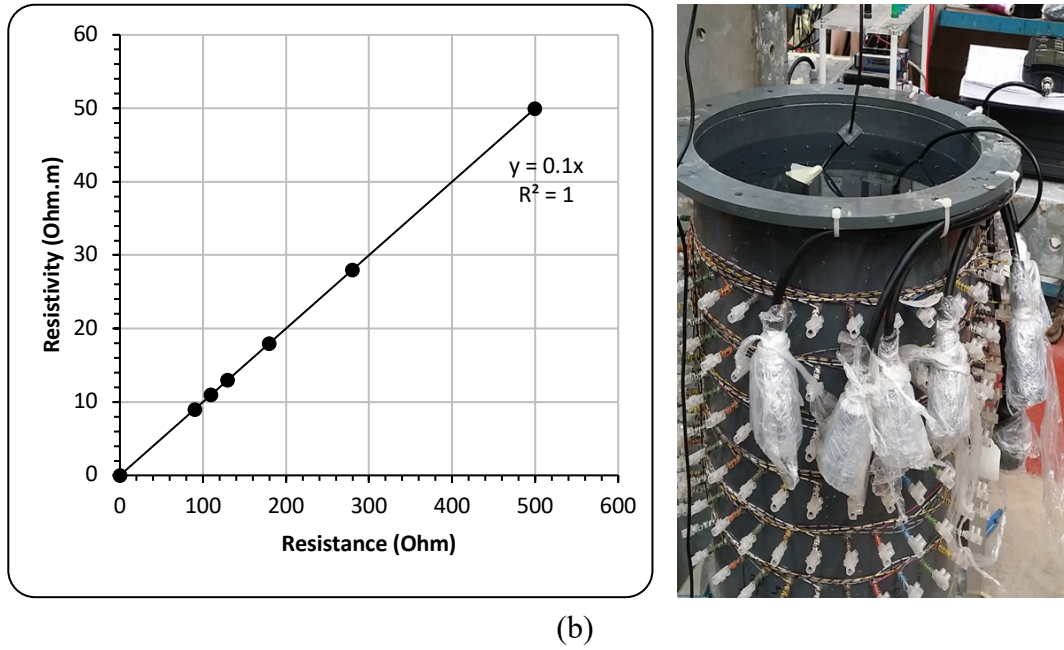


Figure 4-18: Calibration of the electrodes; (a) evaporation cell, (b) settlement cell.

4.6.2 Temperature Correction

Electrical conduction in soils is influenced, among other factors, by the mobility of ions in pore water. Mobility of the ions, however, is controlled by temperature, salt type and its concentration (Rhoades et al., 1976; Sen et al., 1988; Kalinski and Kelly, 1993; Zhou et al., 2013). The mobility of ions increases with increasing temperature as the viscosity of the water is decreased. The resistivity of soil decreases with increased temperature. Campbell et al. (1949) found that the ER of an electrolyte in the temperature range 15-35°C, decreases with an increase in temperature per degree by approximately 2.02%. Therefore, comparisons of resistivity data measured at various temperatures, need to be corrected to a standard reference temperature. To account for temperature variations Equation 4.3 (Keller and Frischknecht, 1966) is commonly applied (e.g. Abu-Hassanein et al., 1996; Kibria, 2014; Hassan, 2014; Farooqy, 2018).

$$\rho_o = \rho_T * [1 + \alpha(T - T_o)] \quad \text{Eq. 4.3}$$

Where; ρ_o is the resistivity measured at a reference temperature T_o ; ρ_T resistivity at soil temperature (T); and α the temperature coefficient for resistivity (correction factor). Keller and Frischknecht (1966) report that the correction factor is 0.025 for most electrolytes at any reference temperature.

4.6.2.1 Investigating the Temperature-Resistivity Relationship for the Gypseous Soils using McMiller Boxes

In order to investigate the influence of temperature on the resistivity of the gypseous soils, a McMiller box (Figure 4-19) was used. This box with internal dimensions of: 108 mm length, 30 mm width and 23 mm height, was made of Perspex with electrodes installed in the side walls. The current and potential electrodes were made of steel plate and brass rods, respectively, (Figure 4-19). The nailed potential electrodes were extended 10 mm into the sample to provide point measurements, the interior spacing between them 6.9 mm. Following the procedure described in Section 4.6.1, the geometric factor of the box was determined to be 0.0102 m.



Figure 4-19: McMiller resistivity box.

This box was utilized to measure the resistivity of the manufactured gypseous soil in its saturated state. Resistivity readings were undertaken using the same data acquisition system used for the evaporation and settlement cells. Four McMiller boxes were available in the

laboratory, therefore two samples for each gypsum content were prepared (10% and 20% gypsum contents). Sand-gypsum mixtures were pluviated into the McMiller box via a funnel, levelled off and weighed, loaded for 2 hours, soaked by placing a filter paper on the soil surface to maintain it without disturbance while dropping distilled water on to the surface using a syringe, and finally dried at 25°C to develop gypsum bonds.

A predetermined volume of water was added to the prepared samples to achieve saturation samples, 83% and 85% degree of saturation corresponding to 10% and 20% gypsum content, respectively, before the box was sealed using cling film to prevent changes in water content. These were left for 24 hours to equalise in a temperature-controlled room at $20 \pm 0.5^\circ\text{C}$. The samples were then tested over a temperature range of 14 to 47°C, replicating the minimum and maximum temperatures likely to be encountered within the samples during the evaporation testing in the larger experimental cell.

To achieve this range of temperatures, the samples were initially cooled down to 14°C in a temperature-controlled incubator. The samples were then allowed to equilibrate to room temperature. Temperature and resistivity were measured at every increase in temperature until the samples reached room temperature ($\sim 20^\circ\text{C}$). The temperature of the samples was then increased to 47°C using an oven. As before, temperature and resistivity were measured at every decrease in temperature until the samples reached room temperature ($\sim 20^\circ\text{C}$). Figure 4-20 shows the resistivity-temperature relationship over the range of temperatures tested. This indicated that resistivity changed between 1.5% and 2.7% per 1°C in soil containing 10% gypsum content, and 1.2%-3.9% in soil with 20% gypsum content. From the resistivity-temperature relationships, it was concluded that the correction factor of temperature varies

marginally based on the temperature range and soil type. However, in this study, the ER on average decreased by 2.4% per 1°C between 14 and 47°C making the correction factor (α) equal to 0.024, which is slightly lower than the value suggested by Keller and Frischknecht (1966) and Hassan (2014).

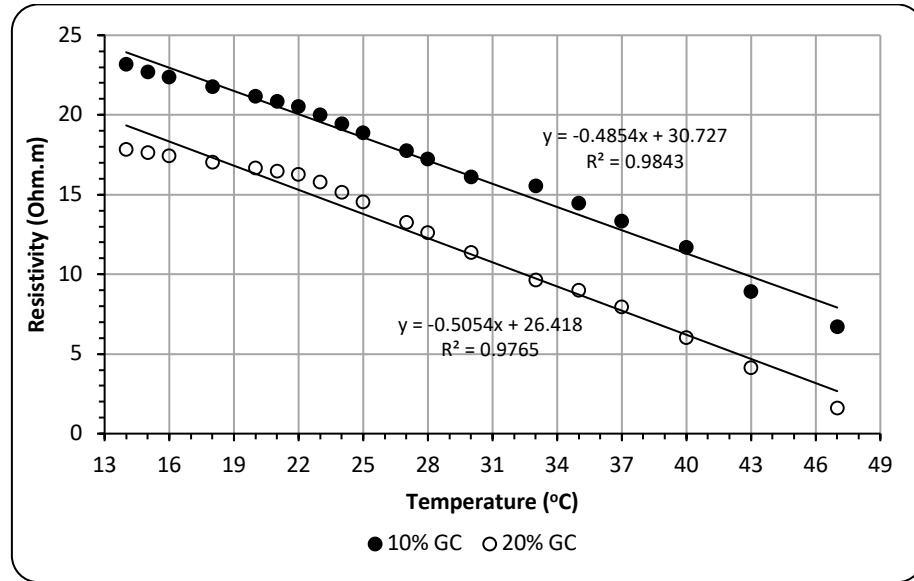


Figure 4-20: Resistivity variation with temperature ranging 14-47°C.

4.6.2.2 Limitations with ER Corrections

Observations from the ER calibration testing suggested that the behaviour of the gypseous samples experiencing a variety of environmental conditions, will be complex and this will impact on the possibility of calibrating the ER data with any degree of accuracy. Testing within the main experimental cell indicated that determining a correction factor for each sample was problematic. For example, gypsum dissolution coupled with changing temperatures and groundwater movements, vaporisation of the water and precipitation of the gypsum near the upper surface, resulted in a transitory system. Therefore, as it was not possible to calculate a temperature correction factor for the aforementioned reasons, it was

decided to implement the commonly used Eq. 4.3.

This may seem an unusual approach, however the aim of this study was not to identify the change in resistivity of the gypseous soil under the range of environmental conditions. Instead, ER was being trialled as a potentially non-destructive method to help indicate if/when changes occur within samples during testing and to potentially complement the destructive methods used post testing. In this case, it was hoped that detecting relative changes, rather than identifying absolute values, in ER over the duration of the experiment might provide insight into the changing conditions within the samples (following the findings of Hassan, 2014; Al-Obaidy, 2017; Farooq, 2018).

4.7 Summary

This chapter provides the development of the bespoke tests, the evaporation and footing tests, and ER method. It also includes the details of the design and description of a bespoke test arrangement and the justification for the decisions made. Furthermore, it includes a description of the experimental apparatus, experimental set up, soil formation, test programme and procedures for running the tests. The design of the resistivity cells which were developed and the test procedure, including calibration tests and data processing, were also detailed. The results of the trial samples exhibited an acceptable deviation in water and gypsum contents along the soil column. The influence of temperature on the resistivity was investigated over the temperature range 14 to 47°C. It was found that soil resistivity was significantly affected by temperature, decreasing with an increase in temperature by approximately 2.4%.

CHAPTER FIVE

EXPERIMENTAL RESULTS AND DISCUSSION

5.1 Introduction

In this chapter, the observations and results from the bespoke experiments are presented. The outcomes are discussed for both the evaporation column and simulated footing tests. Data from both the conventional investigation and the ER survey are incorporated and evaluated appropriately.

5.2 Experimental Results and Analysis of Evaporation Test

Due to the time required to create and test the samples (approximately three months, as described in Section 4.2), two gypsum contents (10% and 20%) were chosen to investigate the influence of evaporation, coupled with groundwater movement and heat transport in the unsaturated zone. Having created the samples, the experiments were undertaken following the procedure as described in Section 4.4.4 (see Figure 5-1 that recalled from Chapter Four: Section 4.4.4).

The data obtained was initially compared between samples to determine the replicability of the process before comparing the behaviour of the datasets (water loss in the water tank, temperature gradient, final gypsum and water contents) with respect to the experimental timeline to determine changes within the samples. It should be noted that there were two sets of data for each percentage of gypsum. The ER was undertaken only for the second sample as there was initially a technical problem with data acquisition (an update in the operating

system compromised the data acquisition software).

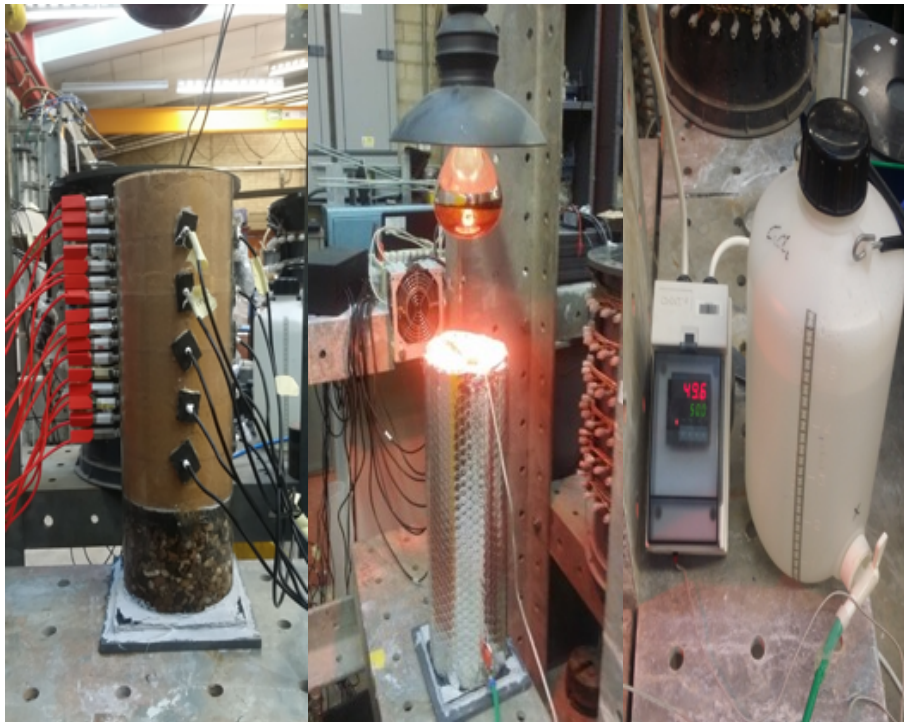


Figure 5-1: Running test. From left to right; soaking the soil by capillary action, starting the test, water tank and temperature controller.

5.2.1 Evaporation, Temperature Gradient, and ER Results with Respect to the Experimental Timeline

The results of the evaporation experiments are first introduced in terms of cumulative evaporation by summing up the daily loss of water from the water tank, versus time for 10% and 20% of gypsum content, with each gypsum content repeated twice (Figure 5-2). It can be seen that the repetition for 10% gypsum content is fairly close, while for 20% gypsum content, there is slightly greater variation although the trends are still similar. Comparing the results between gypsum contents, it can be observed that the cumulative evaporation from samples containing 10% gypsum content were higher than samples with 20% gypsum content.

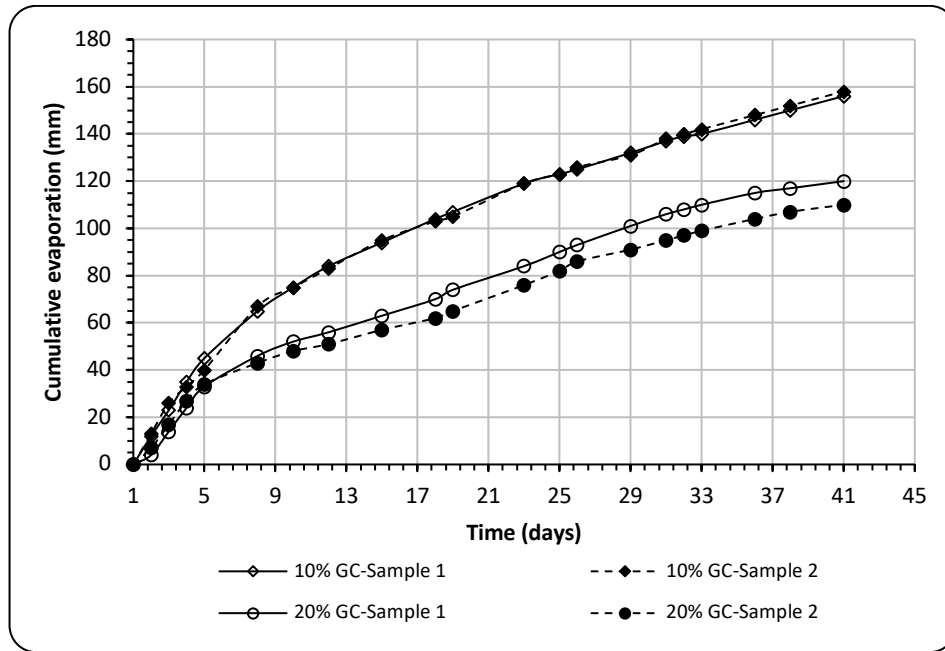


Figure 5-2: Time evolution of cumulative evaporation in manufactured gypseous soil columns with 10% and 20% gypsum contents.

There are two likely causes for this difference. Firstly, this could be attributed to the greater hydraulic conductivity of the sand relative to the moderate hydraulic conductivity of the gypsum (based on findings by Al-Muftly (1997) and Yoon et al. (2015)), thus, increasing gypsum content decreases the permeability of the sample. Secondly, the appearance of a gypsum crust, formed via precipitation caused by evaporation in the upper layers of the samples, creates changes in the properties of the soil. These include, a decrease in porosity, reductions in thermal conductivity and reductions in water vapor diffusivity meaning that evaporation will decrease (Fookes et al., 1985; AlQaissy, 1989; Gran et al., 2011). In this study, it was noticed that a continuous, hard, salt crust varying in thickness from 2 to 3 mm across samples, formed on the surface of the soil in the samples with 20% gypsum content. In contrast, a fragile and very thin crust formed on the surface of the soil which contained 10% gypsum content. This may explain why soil containing 10% gypsum content has the higher evaporation rate as there is a greater void ratio at the surface. It should be noted that

measuring the void ratio without disturbing the soil sample and hence compromising the results, was problematic. As such, this is an assertion which requires corroboration.

It appears that the soil evaporation curves (Figure 5-3) indicate three evaporation stages. The first is characterized by a relatively high evaporation rate, which represents a ‘high energy’ consumption via groundwater. This rapid evaporation rate results in migration of gypsum up through the soil column from the phreatic zone through the vadose zone to be precipitated out near the surface, changing the fabric of the soil and its physical properties as it does. This results in the development of the second stage where the evaporation rate falls as groundwater cannot be transmitted to the soil surface fast enough to meet ‘evaporative demand’ (this is defined as a measure of the extent to which the environment is trying to evaporate water from soil surface) due to lowered permeability with precipitation of the gypsum in the upper layers. Eventually, equilibrium is reached (the third stage). These three stages are consistent with Smits et al. (2011) and Song et al. (2013) who investigated the evaporation of salty water (NaCl) within soil columns.

Variations of soil temperature and electrical resistivity (ER) for 10% and 20% gypsum content over time are shown in Figures 5-4 and 5-5. From these data, it can be seen that the temperature gradient between the soil surface and at a depth of 25 cm, fluctuated over time. The highest temperature was measured at the soil surface, the lowest at 25 cm depth. This is attributed to inconsistent ambient temperatures within the laboratory.

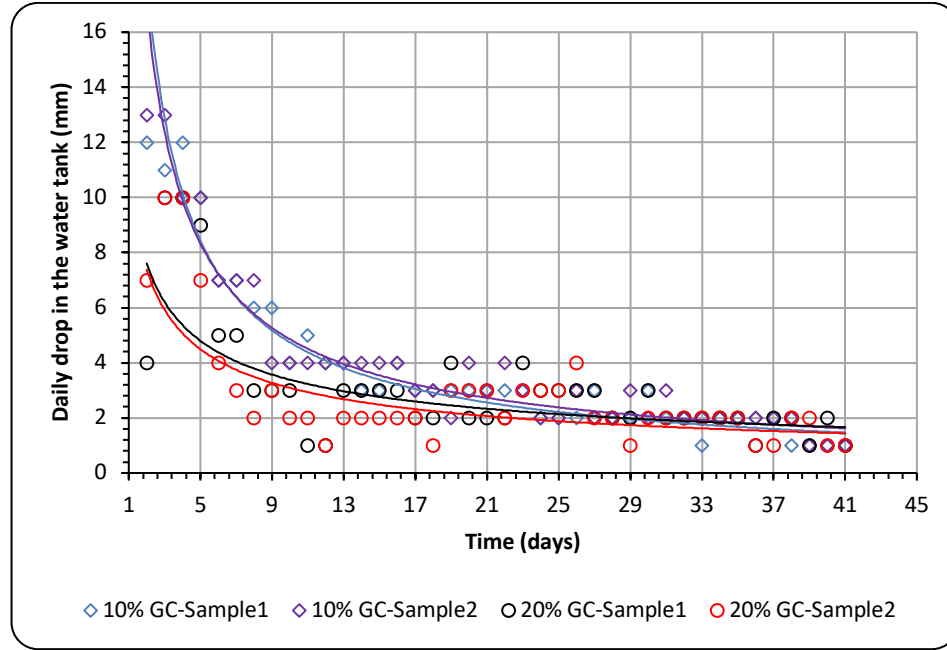
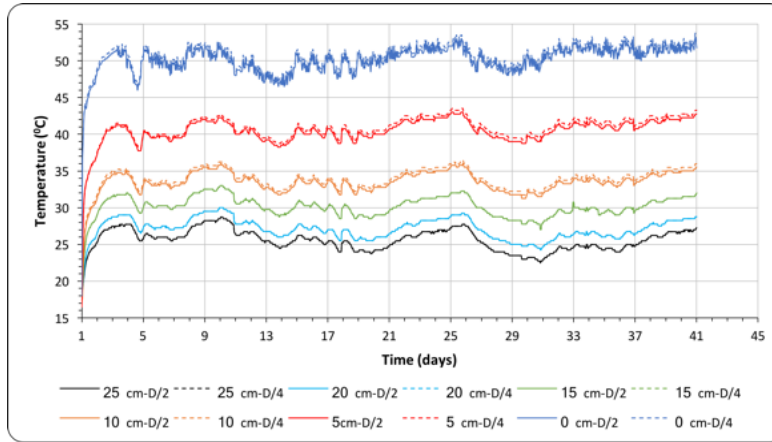
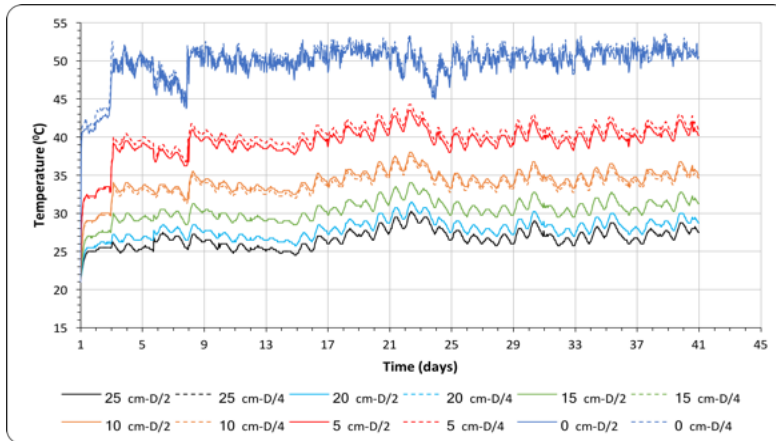
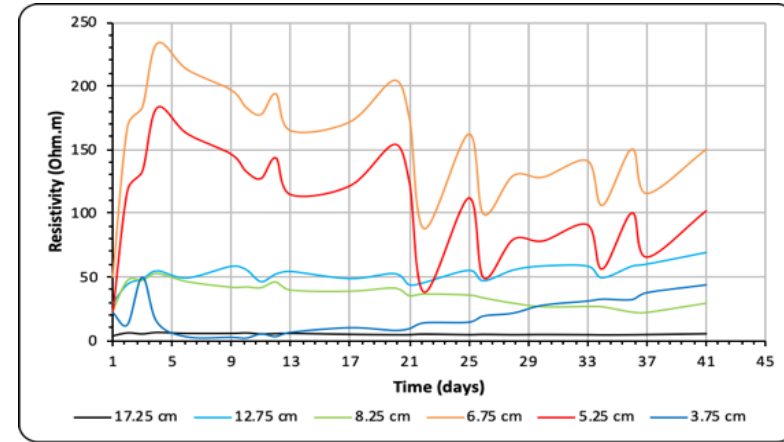


Figure 5-3: The drop daily in water height within the water tank during the whole experiment for 10% and 20% gypsum content.

On occasion, the lab was open to the external environment it being a working civil engineering laboratory, large doors located along the side of the building often opened to allow equipment/materials to be brought into/out of the facility. The laboratory temperature itself varied between 16.5-22°C, thereby influencing the soil temperature. In addition, the energy required to transform liquid water to water vapor (i.e. the evaporation process), resulted in further heat loss (Saito et al., 2006; Smits et al., 2011). However, the variations recorded by the thermistors between pluviated layers were deemed acceptable for the experiment to continue. It can be observed that in the case of 20% gypsum content, the soil temperature increased gradually during the first five days until reaching the desired temperature, while the columns with 10% gypsum content achieved the desired temperature within the first two days.

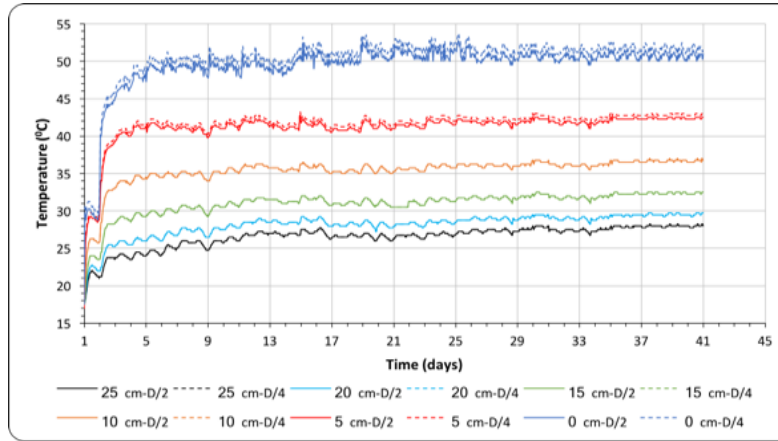


(a)

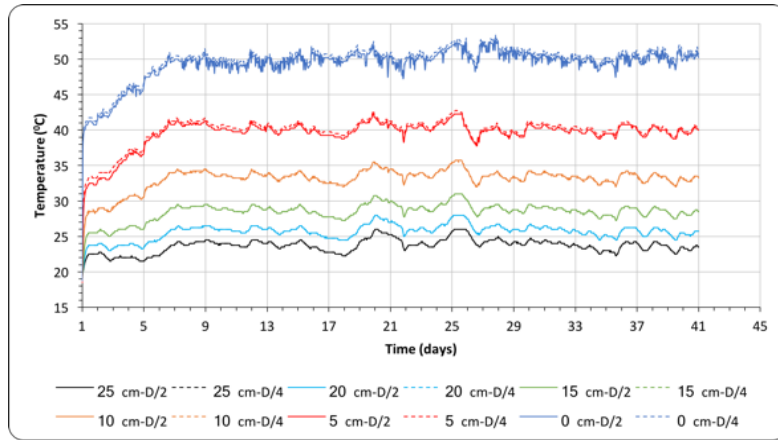
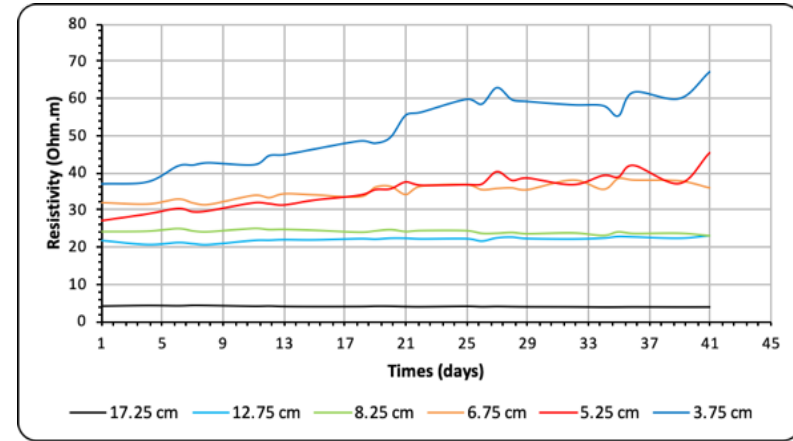


(b)

Figure 5-4: Variation in temperature and ER for; (a) 10% GC-Sample 2, (b) 10% GC-Sample 1. (NB. All these distances start from the surface of the soil; D/2: at centre of sample (7.2 cm); D/4: at distance 3.6 cm from cell wall).



(a)



(b)

Figure 5-5: Variation in temperature and ER for; (a) 20% GC-Sample 2, (b) 20% GC-Sample 1. (NB. All these distances start from the surface of the soil; D/2: at centre of sample (7.2 cm); D/4: at distance 3.6 cm from cell wall).

There does appear to be a slight variation in temperature recorded by the two thermistors in the first three upper layers, in the order of 0.25°C to 0.5°C. Once again, this variation was considered within acceptable limits. In these upper layers, slightly higher temperatures were recorded by the thermistors nearer the cell wall due to the intensity of lamp heating around the cells, although this relationship changed with depth (distance from the heat source) as the lower thermistors recorded the same temperatures at the centre of the samples and close to the cell wall.

Regarding soil resistivity, the values of measured ER corresponding to temperature, were corrected for a reference temperature (25°C) using Eq. 4.3 in Chapter Four. This reference temperature was chosen according to the lowest temperature in the soil columns, 25 cm from the soil surface (the first layer). This standard reference temperature is used by many researchers (e.g. Abu-Hassanein et al., 1996; Sreedeeep et al., 2004). The magnitude of ER in conjunction with temperature over time is presented in Figures 5-4 and 5-5. These figures show that the soil resistivity for the 10% gypsum sample is higher than that for the sample with 20% gypsum content. Increasing the concentration of salt provides more ions for electrical conduction, leading to a reduction in pore water resistivity, thereby diminishing soil resistivity (Rinaldi and Cuestas, 2002; Zha et al., 2010; Long et al., 2012; Hassan, 2014). The lowest ER was measured under the water table, showing as more or less constant with time, this attributed to the distilled water content rather than gypsum content. It was noticed that the variation in ER at a depth of 3.75 cm in soil with 10% gypsum content, decreases over time until 21 days into the experiment. Thereafter, it increases, while the 20% gypsum soil increases with time at the same depth. ER in the column with 10% gypsum content fluctuates significantly over time at all depths in comparison to 20% gypsum content soil. This due to

the fluctuation of the temperature over time which influences the evaporation rate and thus the water content.

5.2.2 Investigating the Water Content, Gypsum Content, Temperature and ER at the End of Test

Post-test sampling was undertaken to determine the gypsum and water contents. This data is augmented with end temperature and ER values (plotted with depth) as it is believed that this further highlights changes induced within the soil column (and as a snap-shot reduces the natural noise within the system, as exhibited by Figures 5-6, 5-7 and Table 5-1).

Looking at the distribution of gypsum post-test, the formation of a phreatic surface (distilled water: 100 mm height within the manufactured soil), results in the dissolution of gypsum below this depth. As a result of capillarity, suction (due to unsaturated soil condition) and the application of a thermal gradient across the sample, gypsum dissolution migrates to the upper zone of the soil column until the water vaporises and the gypsum reprecipitates out of the solution and into the soil. During the experiments, it was observed that the accumulation of gypsum on the soil surface develops with time, progressing in depth with evaporation and an increase in drying volume (within the upper 5 cm of the 30 cm columns). The post-test gypsum distribution (Figure 5-6 and 5-7) illustrates that the gypsum content profiles for the 10% and 20% gypsum content samples, appear to differ at 5 to 25 cm deep. It is suggested that this is the transitional zone between the precipitation zone (at the surface) and the leaching zone below. Dissolution, transportation and precipitation of gypsum in the soil columns is further validated by examination of the gypsum content profiles in both 10% and 20% gypsum content soils.

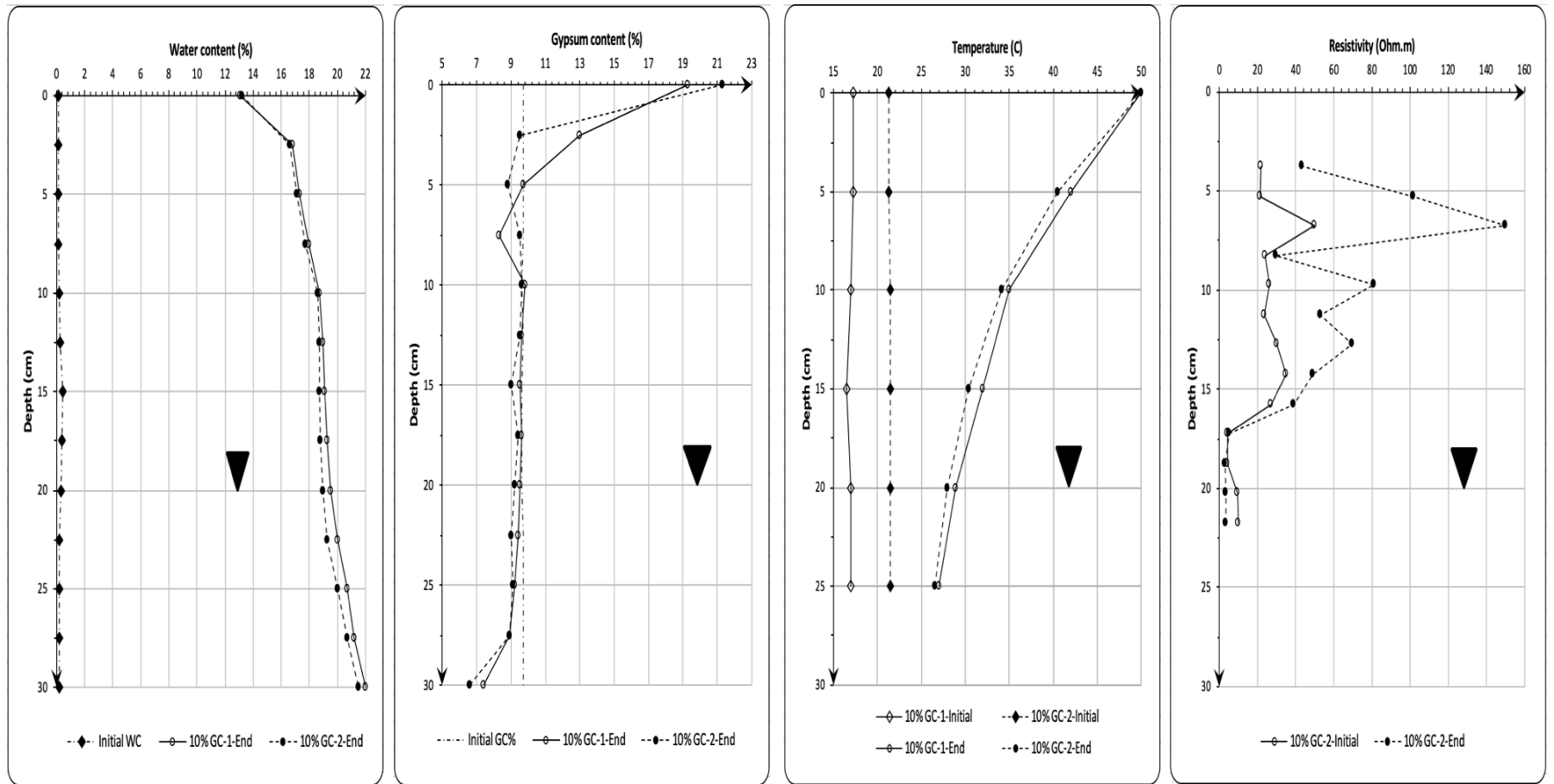


Figure 5-6: Profile of water content, gypsum content, temperature and ER along the soil column at the end of the test with 10% gypsum content, the first sample (10% GC-1) investigated without ER, while the second sample (10% GC-2) tested with ER.

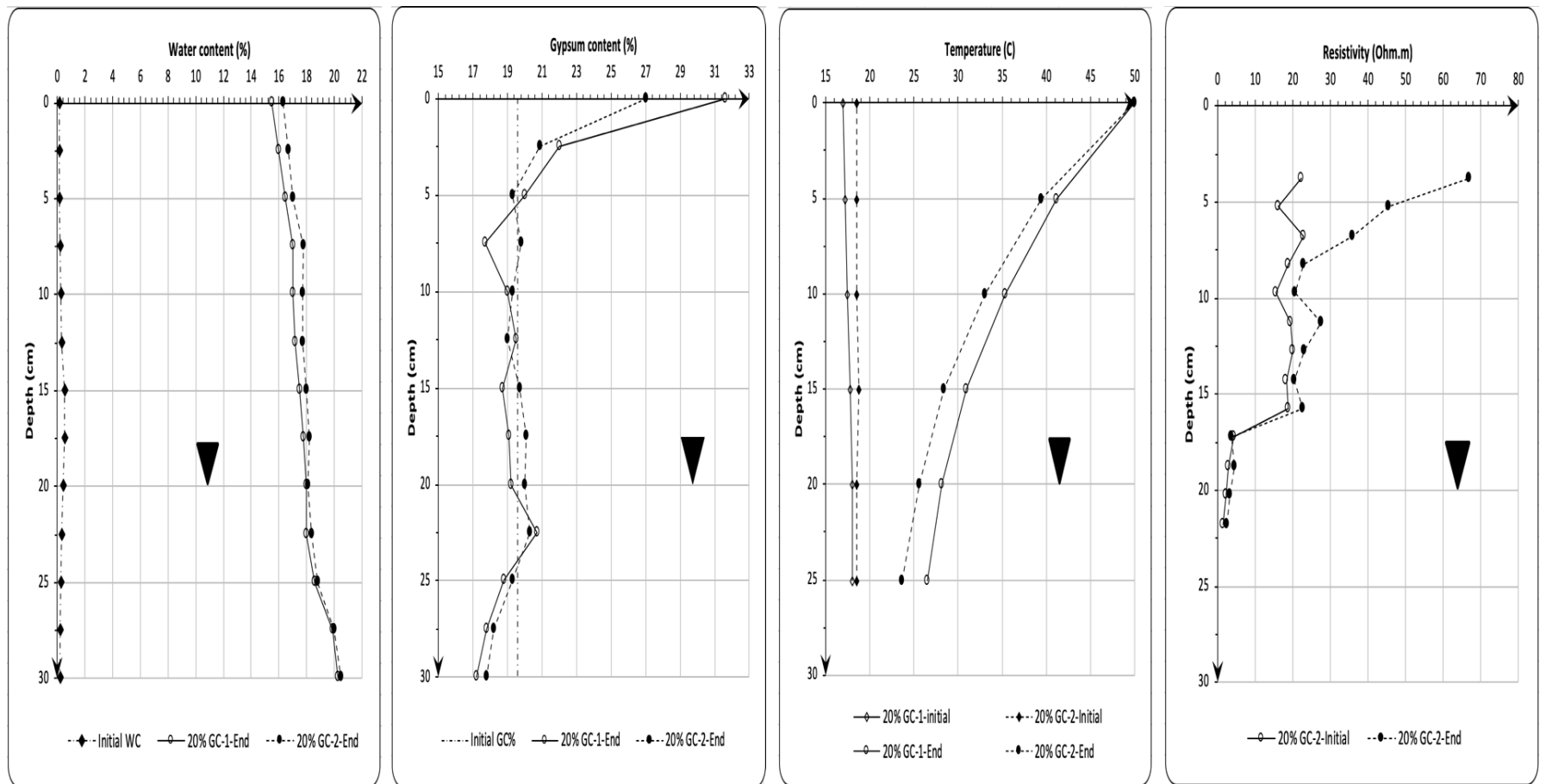


Figure 5-7: Profiles of water content, gypsum content, temperature and ER along the soil column at the end of the test with 20% gypsum content, the first sample (20% GC-1) investigated without ER, while the second sample (20% GC-2) tested with ER.

Table 5-1: Water content and gypsum content measurements with depth (with 0 cm taken at the upper surface) for all soil columns at the end of test.

Sample depth (cm)	Water content (%)				Gypsum content (%)			
	10%-1	10%-2	20%-1	20%-2	10%-1	10%-2	20%-1	20%-2
0.0	13.1	13.2	15.5	16.3	19.3	21.3	31.6	27.0
2.5	16.8	16.6	16.0	16.7	13.0	9.5	22.0	20.9
5.0	17.3	17.1	16.5	17.0	9.7	8.8	20.0	19.3
7.5	18.0	17.7	17.0	17.8	8.3	9.5	17.7	19.8
10.0	18.7	18.6	17.0	17.7	9.8	9.6	19.0	19.3
12.5	19.0	18.7	17.2	17.7	9.6	9.5	19.5	19.0
15.0	19.1	18.7	17.5	18.0	9.5	9.0	18.7	19.7
17.5	19.3	18.8	17.8	18.2	9.6	9.4	19.1	20.1
20.0	19.5	19.0	18.0	18.1	9.5	9.2	19.2	20.0
22.5	20.0	19.3	18.0	18.4	9.4	9.0	20.7	20.3
25.0	20.7	20.0	18.6	18.8	9.2	9.1	18.8	19.3
27.5	21.2	20.7	19.9	20.0	8.9	8.9	17.8	18.2
30.0	22.0	21.5	20.3	20.5	7.4	6.6	17.2	17.8

Both soils reveal high gypsum content values on the soil surface, while the lowest gypsum content was encountered at the base of the soil columns within the ground water especially in the first layer, this due to the distilled water entering the soil column from the water tank, slowly forming an equilibrium with the gypsum in the pores. Below the area of precipitation, the gypsum content falls suddenly below the initial values. For 10% gypsum content columns, the fall is only slightly lower the initial value, this fall coinciding with increasing water contents. These gypsum content values remain lower than the initial value through the soil column, decreasing noticeably towards the bottom (leaching zone). The trend in the first sample with 20% gypsum content (20% GC-1) is similar for 10% gypsum content but the fall below the initial value is significantly higher, while the sample 20% GC-2, indicated more fluctuating gypsum contents between the precipitation and leaching zones, this attributed to experimental error and natural heterogeneity in the samples. These differences between 10%

and 20% gypsum contents could be attributed to the water content and the temperature gradient along the soil column as the samples with 10% gypsum content had higher water contents and temperature gradients below the evaporation front.

It should be noted that measurement of the gypsum content could not be undertaken before the start of the test, as this would disrupt the soil fabric. Initial values were obtained from tests where the samples were created but not permeated with water (for more details, see Section 4.4.3). Although not ideal, this generated an indication of the initial gypsum contents within the samples.

The temperature profiles for 10% and 20% gypsum content samples show two variant temperature gradients corresponding with the different water content zones. The gradient is higher in the dry zone, this reflecting the high heat flux and the low thermal conductivity of the dry soil. Underneath the evaporation zone, the soil is damp making its thermal conductivity higher (Gens et al., 2009). Nevertheless, the temperature gradient in the 10% columns remains higher relative to that in the 20% columns. This difference may be explained as the thermal conductivity of soil columns decreasing with an increase in gypsum content, the accumulation of a gypsum crust reducing thermal conductivity (see Section 5.2.1), this reduction in thermal conductivity leading to a reduction in the temperature of the soil column.

The soil resistivity profiles corresponding to the gypsum and water contents, also reveal significant differences between the two soil types. The initial ER was measured after the sample was saturated in water for one day, at laboratory temperatures. The lowest resistivity was measured under the water table at the beginning and end the test. This was due to the

distilled water content rather than gypsum content. At the end of testing, it was observed that although the gypsum content increased towards the soil surface, the soil resistivity abruptly increased in conjunction with the decrease in water content and presumed increased precipitation of gypsum crystals with vaporisation of the water; this was more pronounced in the 20% gypsum content sample. In comparison to the soil column with 10% gypsum content, the ER revealed a different trend at depths nearer to the soil surface: the ER fluctuated at depths of 5 to 10 cm below the soil surface, decreasing to 43.5 Ohm.m at a depth of 3.75 cm from the surface. This increases in temperature, the measured conductivity of the soil and consequent decrease in ER was true for the 10% column (the ER on average decreases by 2.4% per 1°C between 14 and 47°C: see Section 4.6.2.1). In the 20% column, the ER increases although the temperature is high nearer the soil surface. This difference between both gypsum contents may be contributed to the water content, temperature gradient and the formation of duricrust on the soil surface.

5.3 Results and Analysis of the Simulated Footing Experiment

The simulated footing experiment was carried out in three cylindrical apparatus, which originally was used for a previous doctoral study undertaken within the civil engineering laboratory of Birmingham University (see Al-Obaidy, 2017), having a simulated circular footing of diameter 70 mm. These tests were carried out on a pluviated sand-gypsum mixture containing 20% gypsum content. This content was selected as it is commonly encountered in the Iraqi study area as mentioned in Chapter Four. In order to investigate the performance of a foundation erected on a gypseous soil under different conditions, a series of three footing tests were created:

- Case 1: a quick test without the application of external heating and breeze. Loading the footing was followed by increases in groundwater at very short intervals.
- Case 2: a slow test without the application of external heating and breeze. Loading the footing was followed by an increase in groundwater over long intervals.
- Case 3: a slow test with the application of external heating and a breeze were applied to simulate hot, arid conditions akin to those encountered in the test area (Sissakian et al., 2013; Al-Bahrani et al., 2014; Al-Dabbas et al., 2014; Al-Zubaydi, 2017). The details of the setup and test procedure, were given in Chapter Four. This section describes the results obtained from the settlement tank test.

5.3.1 Mechanism of Wetting the Soil

Water was added to the test tank from the water tank via a clear tube. The water was added slowly by controlling the tap opening, so that no air gaps were left between the gravel particles and that there was no disturbance of the soil particles. At each wetting stage, the water was added to reach the top of the filter layer. The volume of water required to cover the filter layer was measured and found to be 5 litres for the three tanks (for more detail see Section 4.5.2.1). Table 5-2 shows the amount of water that was added at each stage for all cases, this inundation included the water in the filter layer, referred to as W1 (5 litres).

Table 5-2: Volume of water for each wetting stage for all cases.

Wetting stage	Volume of water added in each stage (liters)		
	Case 1	Case 2	Case 3
W1	5	5	5
W2	1	1	1
W3	1	1	1
W4	1	1	1
W5	1	1	-
W6	1.65	1	-
W7	0.4	0.7	-
Total	11.05	10.7	8

5.3.2 Stress-Settlement Characteristics of the Foundation before Wetting Stage

Four LDS sensors with a travel limit of 50 mm, were placed on the footing's wings with the help of magnetic bases (described in Section 4.5.1.1 and 4.5.1.2), to monitor the deflection of the foundation. The load was gradually increased up to 80 kPa, each loading increment maintained until no further deformation was recorded. The temperature of the soil was monitored by thermistors previously inserted along soil column (as described in Section 4.5.2.2). The load-settlement characteristics for the footing founded on the manufactured gypseous soil, are illustrated in Figure 5-8. The load carrying capacity of the foundation, supported on a dry deposit at a vertical movement of 0.65 to 0.82 mm (0.9 to 1.2% of the footing diameter), in its dry state without soaking, was determined from the resultant curve. This was expected as gypseous soils are usually stiff, having very low compressibility when in a dry condition due to the cementing action of the gypsum crystals within the fabric of the soil as encountered via the oedometer testing (Section 3.6.2).

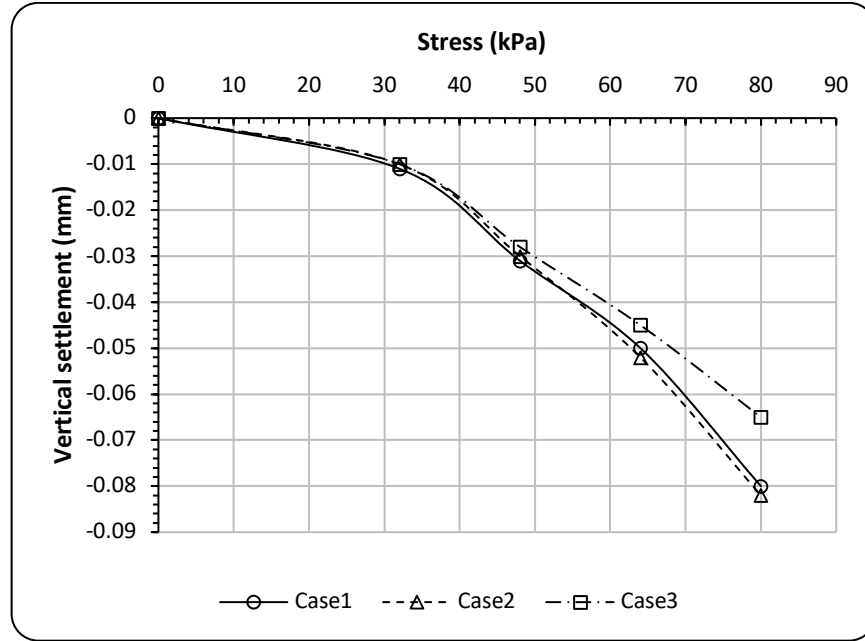


Figure 5-8: Stress-settlement relationships of the foundation settled on dry manufactured gypseous soils (with 20% gypsum content).

5.3.3 Time-Settlement, -ER and -Temperature and Failure Profiles of the Foundation- Manufactured Soil upon Wetting

5.3.3.1 Case 1: Quick Test without Heating Source and Breeze

In this case, the footing, settled on dry manufactured gypseous soil, was loaded and then wetted from below, simulating a rise in groundwater level. As mentioned in Chapter Four: Section 4.5, soil temperature and footing settlement were recorded using the temperature and LDS sensors, respectively. The water was added in seven stages (termed W1, W2, W3, W4, W5, W6, and W7: the volumes added in W1-W7 are presented in Table 5-2) and comprised 11.05 litres in total. This included the initial volume required to fill the filter layer at the base of the apparatus (W1=5 litres). At each wetting stage, sufficient water was added to ensure the water table was level with the upper surface of the filter layer, this achieved by keeping the water level in the water tank at the filter's height in the main experimental apparatus. After

each wetting stage, the water valve was closed to give the opportunity to collect data using ER, the level of the water tank adjusted again by adding water to be level with the top of the filter layer.

Figures 5-9, 5-10, and 5-11 show the vertical displacement of the footing, ER and temperature, respectively, across time during wetting phase, the initial wetting taking place at time zero. With reference to settlement, there was no increase in settlement with W1 and W2 (total= 6 litres), and small settlements between W3 to W5 (total= 9 litres). However, the footing settlement increased considerably at W6 (total= 10.65 litres) causing a total vertical displacement of 6.87 and 7.09 mm, this corresponding to Ch1&Ch4 and Ch2&Ch3, respectively, by the end of 23 hours. An extra 0.4 litre of water was added at W7 (total= 11.05 litres) which was sufficient to cause failure of the footing. The total collapse settlement of the footing was 40.56 and 40.89 mm for Ch1&Ch4 and Ch2&Ch3, respectively. Punching shear failure and cracking are shown in Figure 5-12.

It was evident that the footing punched through the wet upper layer of soil (Figure 5-12) there are clear cracks on the soil surface which developed in a radial pattern. Collapse of the soil structure occurs upon wetting the upper layers because soil suction is reduced leading to a softened, weakened interparticle bond (gypsum crystals) between sand particles, which eventual breaks down. Although the water content on the top layer was 18.7%, which is equal to a degree of saturation of 72% (assuming a void ratio of 0.67, which represents the value before starting the test), this is sufficient to soften the gypsum and cause collapse.

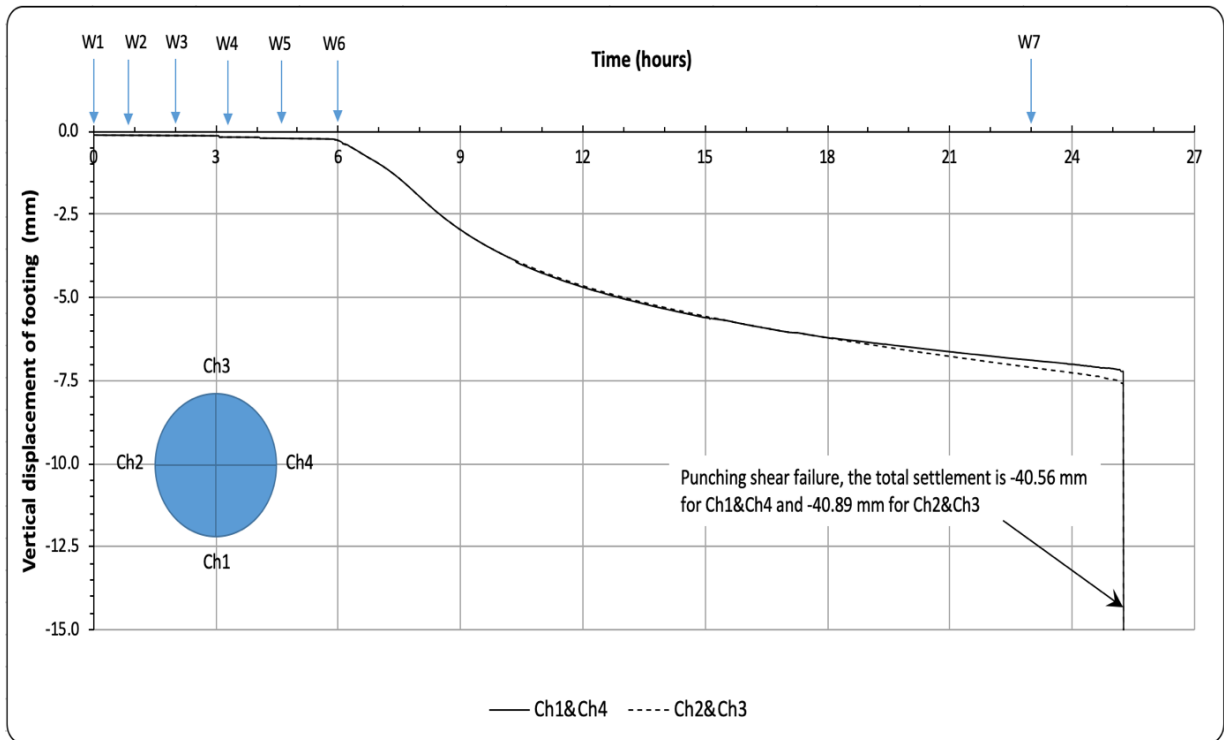


Figure 5-9: Vertical displacement of footing during wetting over time for Case 1. (NB. Ch1, Ch2, Ch3, and Ch4 refer to the channel numbers for the LDS sensors).

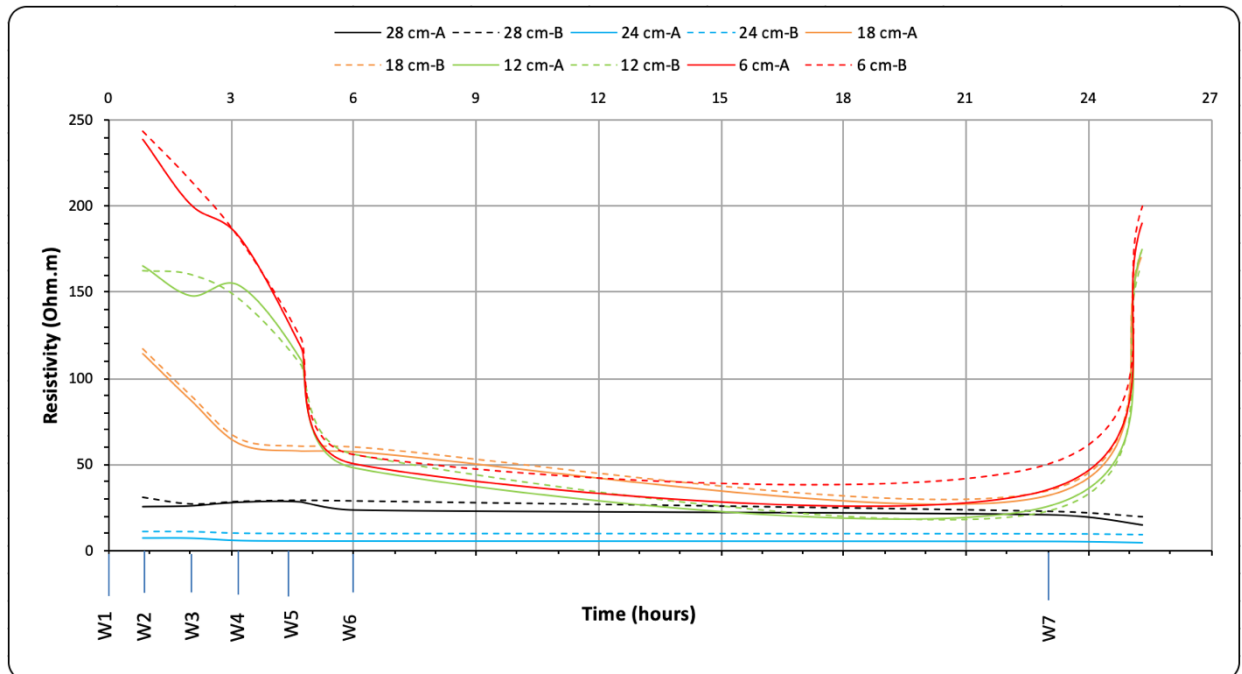


Figure 5-10: ER values along soil deposit during wetting over time for Case 1. (NB. A and B refer to the arrays, number refers to the depth of ER value from the soil surface).

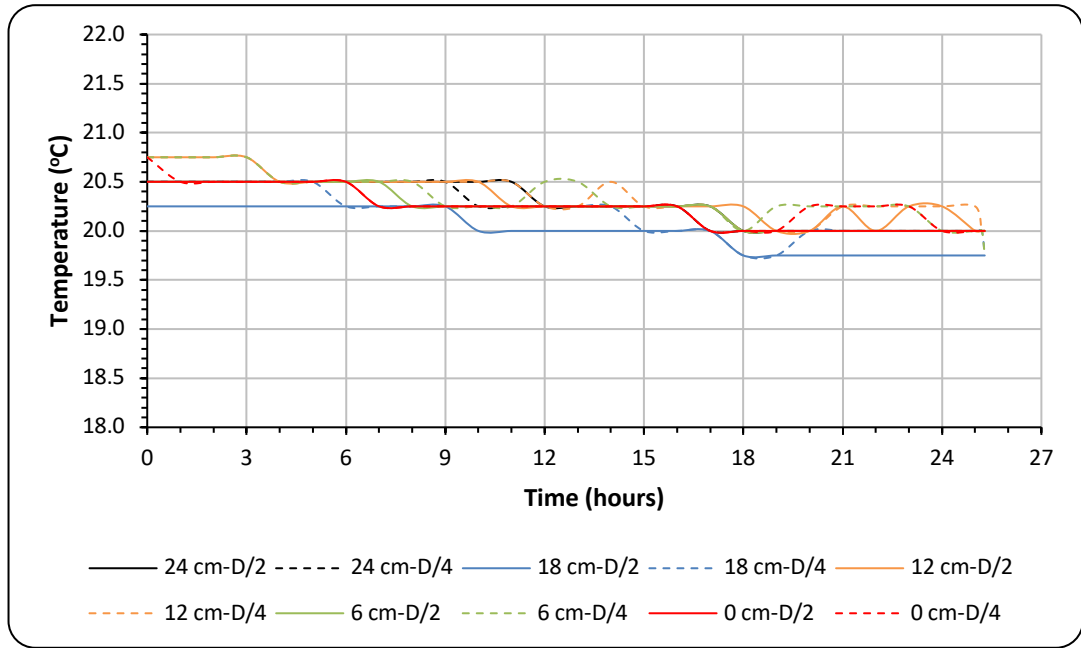


Figure 5-11: Temperature variation along soil deposit during wetting with time for Case 1. (NB. All these distances start at the surface of the soil; D/2: at centre of sample; D/4: at distance 8.73 cm from cell wall).

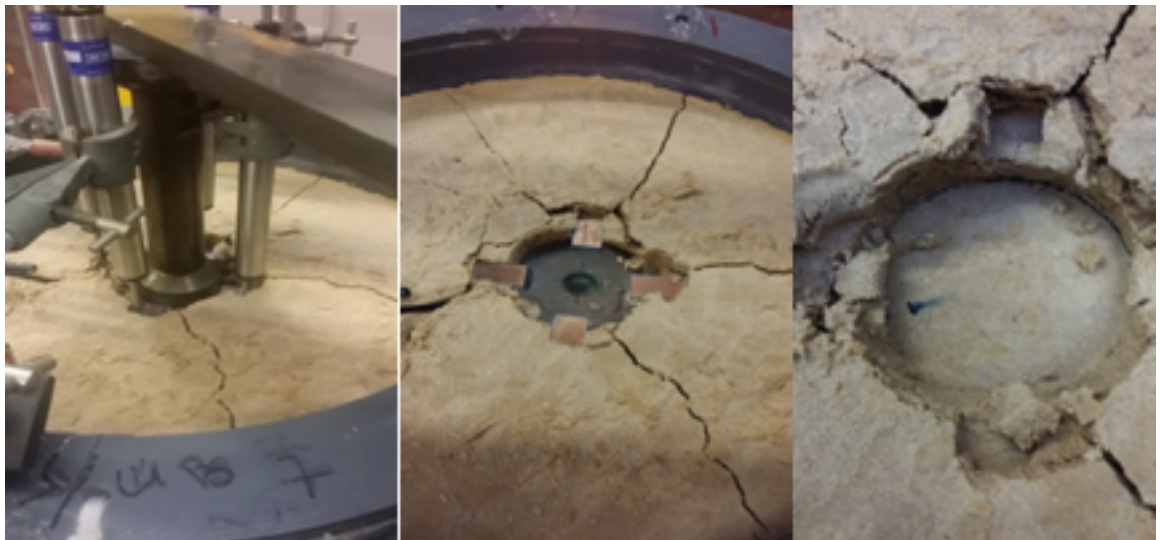


Figure 5-12: Photographs showing the footing failure in Case 1.

It was noticed that when the upper layer became wet, differential settlement occurred. Figure 5-9 shows that there were two periods of differential settlement (dash line deviating from

solid line), the second one greater in magnitude. In the first segment, the settlement in Ch2&Ch3 (dash line) was slightly lower than that for Ch1&Ch4 by 0.05 mm (between 10 and 15 hours). At 18 hours, there was more settlement on Ch2&Ch3 than Ch1&Ch4 (by 0.02 mm) this gradually increasing to 0.33 mm by the end of test. This might be explained by the fact that before the start of the test, some white spots (salty spots) were observed on the soil surface. This phenomenon was observed for all samples although it was vacuumed with water from the soil base and left to air-dry. This could be attributed to the evaporation of water from the upper surface during the drying process. This implies that the soil beneath the foundation was not completely uniform and hence differential settlement was experienced when the water approached this layer. Figure 5-13 shows the soil surface with these salty spots.



Figure 5-13: Salty spot on the soil surface after drying process.

To investigate the relationship between ER and gypseous soil under loading, water and temperature variation, the data from the geophysical investigation were analysed based on the Wenner configuration (see Chapter Four) of the 16 electrodes positioned in two vertical arrays along each test tank. ER values were corrected to 25°C after applying a temperature correction using Eq. 4.3 in Chapter Four. The two vertical arrays positioned on the sides of the tank,

were referred to as A and B, the numbers referring to the depth of ER values from the surface of the soil, as shown in Figure 5-10. It can be noticed from this figure that the highest ER was recorded at 6 cm from the soil surface, the lowest ER was at 24 cm from the soil surface. The readings at 28 cm depth are higher than that taken at 24 cm from the soil surface, although the former was the closest to the filter layer, this true for all cases (Section 5.3.3.2 and 5.3.3.3). This could be attributed to the influence of the gravel and crushed stones layers. There is been a slight difference in the ER readings between the two vertical arrays. This could be attributed to the length of time between the readings taken as the ER measurement for both sides (i.e. arrays A and B) took approximately 30 minutes.

Soil resistivity along soil column, significantly decreased with the increase of additional water from 5 to 10.65 litres, reaching between 55 and 6 Ohm.m. ER then markedly increased after failure at 11.05 litres. This increase in ER was noticed only at depths of 6, 12, and 18 cm from soil surface, these corresponding to 200, 175, and 165 Ohm.m, respectively. ER at depths of 24 and 28 cm, is relatively constant with time. This increase in ER readings could be due to a substantial reduction in the soil pores (high densification) and water drainage at the soil surface. A similar observation was noticed in one compression test (oedometer test), as documented by Comina et al. (2008) and Ghorbani et al. (2013), who debated that this increase in ER due to the decrease in the concentration of salt in the saline as a result of reducing the pores size in the sample.

Figure 5-11 shows the soil temperature along the soil column over time. It can be noticed that the readings in the test period are quite close, their values ranging between 20 and 21°C. The water and gypsum contents and temperature profiles by depth after failure, were calculated along the wet deposit (Figure 5-14). The wettest part of the soil was found to be at the base of the tank (20.6% water content corresponding to 80% saturation degree, assuming a void ratio of 0.67), the water content decreasing towards the surface of the soil, ranging between 18.7% and 18.8% (72% saturation degree) with one exception at mid-height which recorded 19.7% (75% saturation degree). The gypsum content is more or less homogenous along the soil deposit, ranging between 19.5% and 19.6%. This means that there is no gypsum migration, the failure due to weakened interparticle bonding during the wetting stages, resulting in rapid particle reorientation. The temperature gradient profile along soil column is fairly constant and this due to the insulation material around the tank.

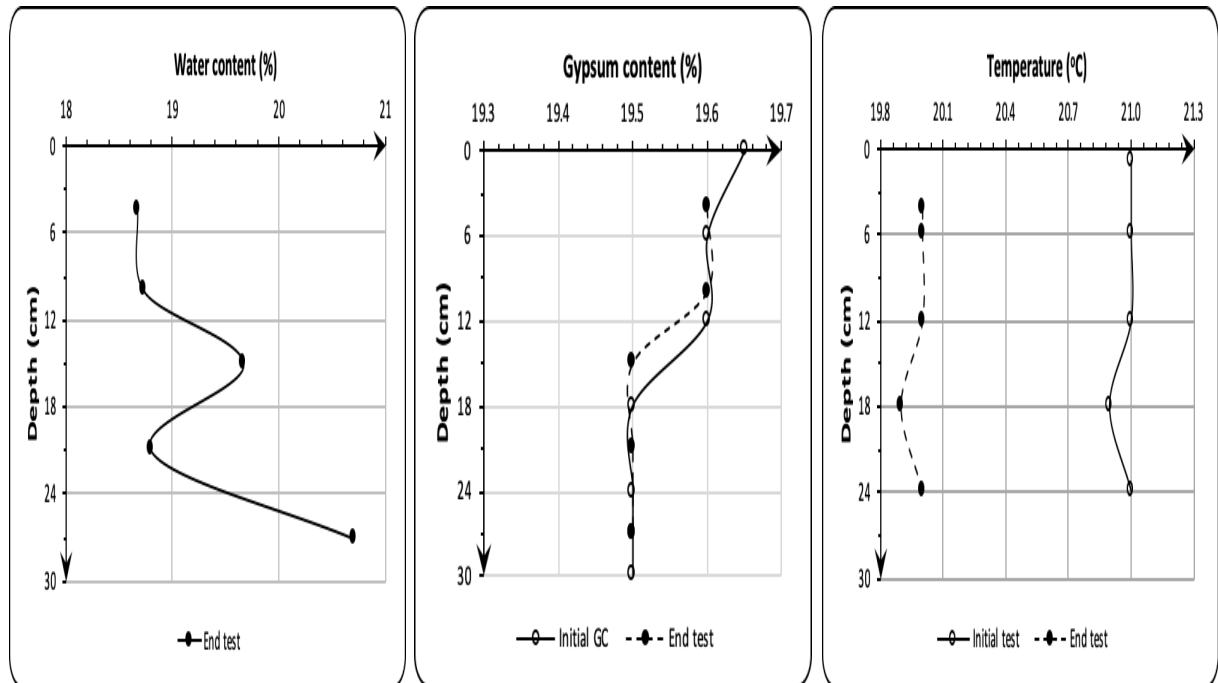


Figure 5-14: Water and gypsum contents and temperature profiles over depth after failure for Case 1.

5.3.3.2 Case 2: Slow Test without Heating Source and Breeze

In this study, the footing was loaded under dry conditions and then wetted. This test was carried out under laboratory conditions, i.e. without heating or breeze as in Case 1. However, the difference between this Case and Case 1 is the timings for the wetting stage which was three days with the exception of W2 which was added 24 hours after the addition of filter water. The footing settlement, ER and temperature over time during the wetting stages, are shown in Figure 5-15, 5-16, and 5-17. The water was added at seven stages, including filter layer water (W1, W2, W3, W4, W5, W6, and W7 as shown in Table 5-2; total=10.7 litres). The settlement increased gradually until wetting stage W7 when the settlement sharply increased. At wetting stage W8, no water entered the soil (this stage is not shown on the graph). Five days after adding W7 (total= 10.7 litres), failure occurred, the footing punching through the wet upper layer, cracks developing on the soil surface in a radial pattern but this time finer than those in Case 1 as shown in Figure 5-18. Collapse of the soil structure occurred upon wetting, because soil suction is reduced, the cementing bonds between particles softened and weakened. This process creates a metastable structure resulting in particle slippage which creates a denser configuration. The total collapse settlement was 38.81 and 38.50 mm (with 0.31 mm differential settlement) corresponding to Ch1&Ch2 and Ch3&Ch4, respectively, by the end of test, these values smaller than that obtained in Case 1 by 5%. This could be because the amount of water and the soil temperature which varied between 16 and 19°C as shown in Figure 5-17, was lower than those in Case 1, leading to a decrease in the rate of dissolution of gypsum crystals in the soil pores.

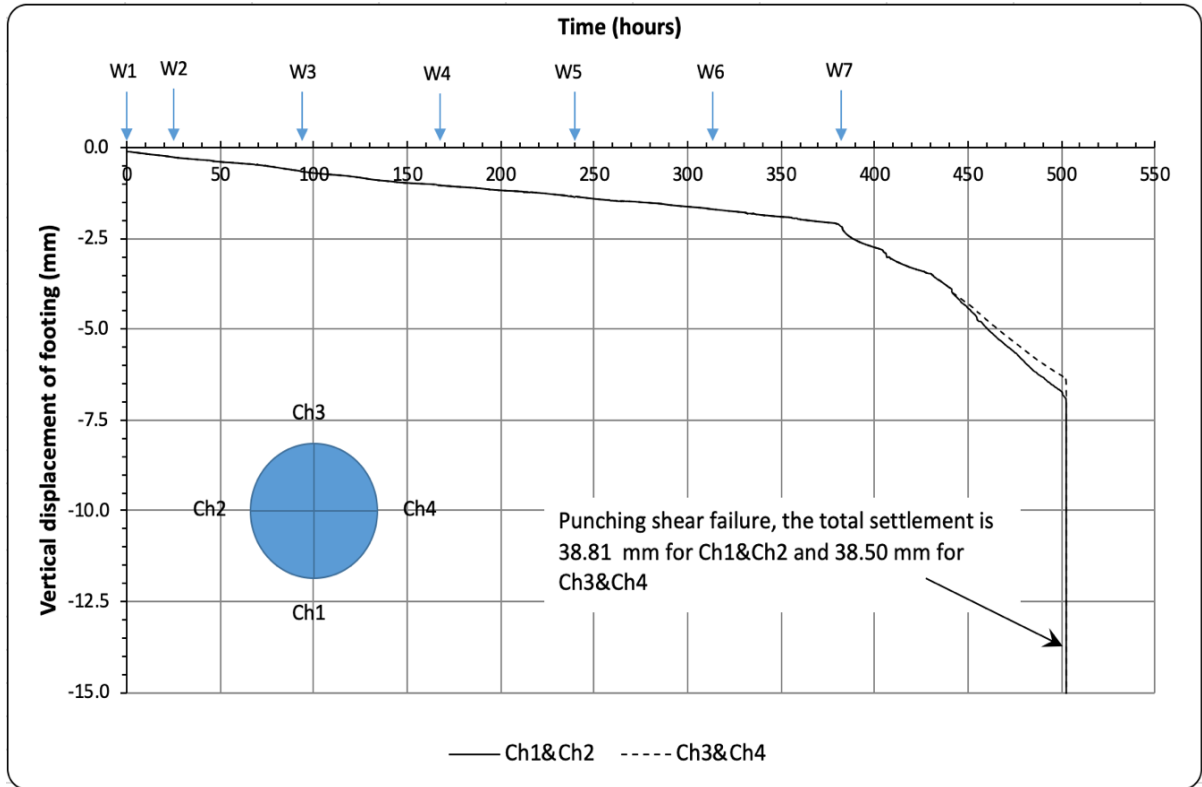


Figure 5-15: Vertical displacement of footing during wetting over time for Case 2. (NB. Ch1, Ch2, Ch3, and Ch4 refer to the channel numbers for the LDS sensors).

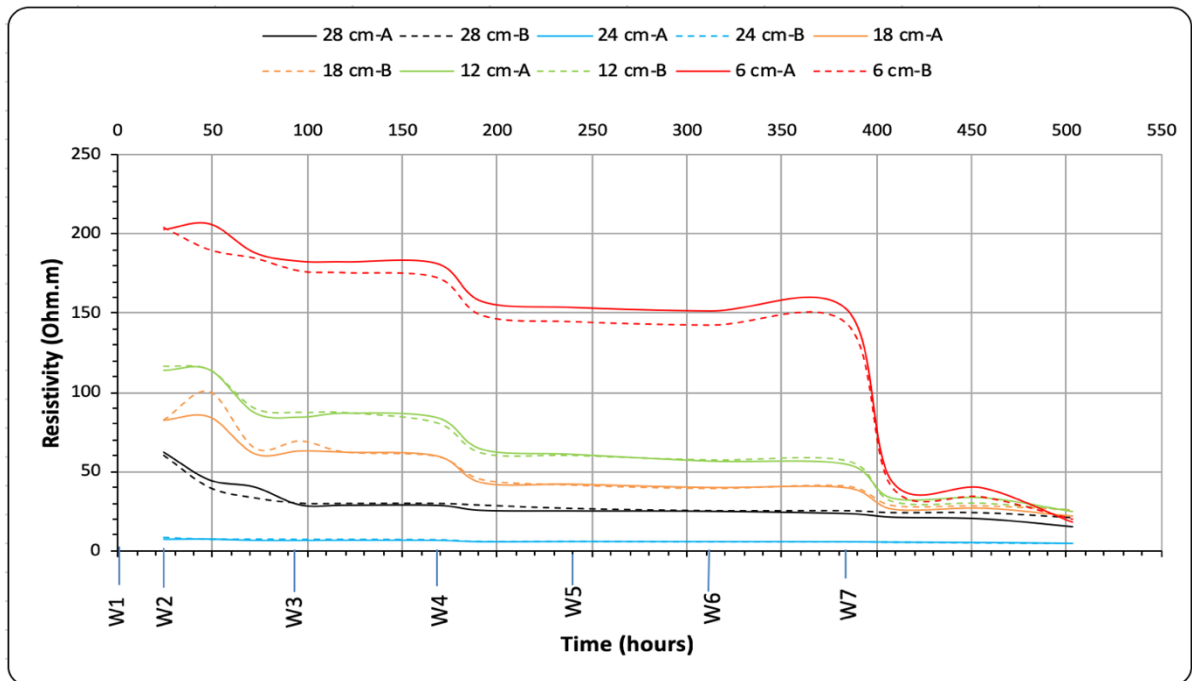


Figure 5-16: ER values along soil deposit during wetting over time for Case 2. (NB. A and B refer to the arrays, number refers to the depth of ER value from the soil surface).

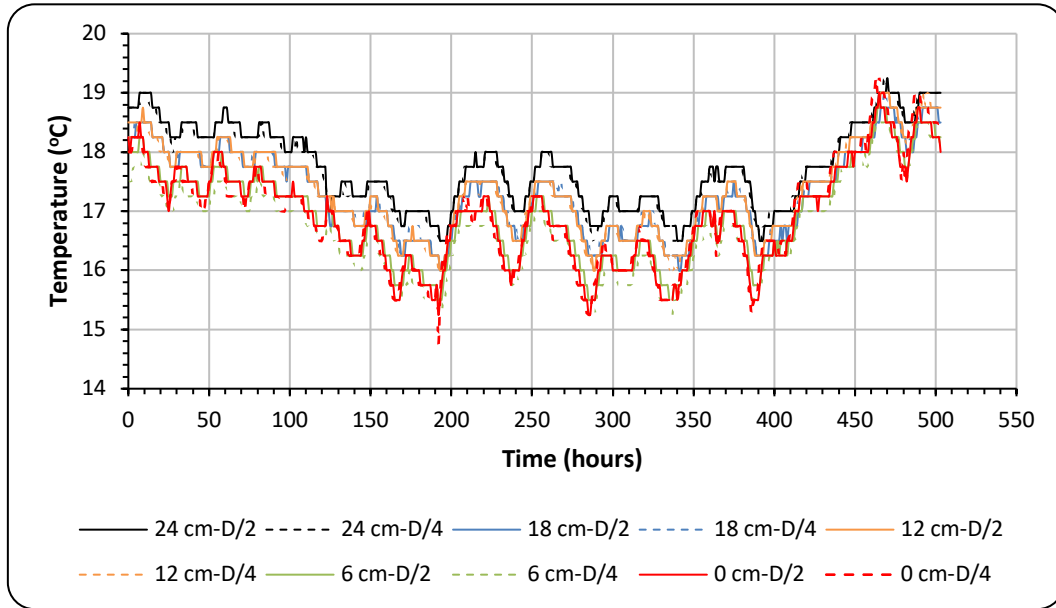


Figure 5-17: Temperature variation along soil deposit during wetting with time for Case 2. (NB. All these distances start at the surface of the soil; D/2: at centre of sample; D/4: at distance 8.73 cm from cell wall).



Figure 5-18: Photographs of the soil surface before and after the failure for Case 2; (a) salt over the soil surface when water approached the upper layer, (b) and (c) punching shear and cracking around the footing model.

Figure 5-16 illustrates the ER observations along soil column over time. It can be seen that the trends are similar to those seen in Case 1 with the exception that after failure, resistivity

continued to decrease. As shown in Figure 5-16, the ER for the three upper layers (6, 12 and 18 cm from soil surface), decreased with an increase in the amount of water and settlement, falling to 20.0, 26.2 and 28.8 Ohm.m, respectively, after failure.

Figure 5-19 shows the water and gypsum contents and temperature profiles. It is noted that the average water content in the soil in Case 2, is lower than that in Case 1. This due to the amount of added water in this case, lower than that used in Case 1 by 0.35 litre and because of possible water loss by evaporation during the longer testing time, approximately 21 days. However, the water contents for Case 2 in the upper and lower layers were 16.8 and 20.5%, respectively. In common with Case 1, the gypsum content and temperature profiles were comparatively homogenous along the soil deposits.

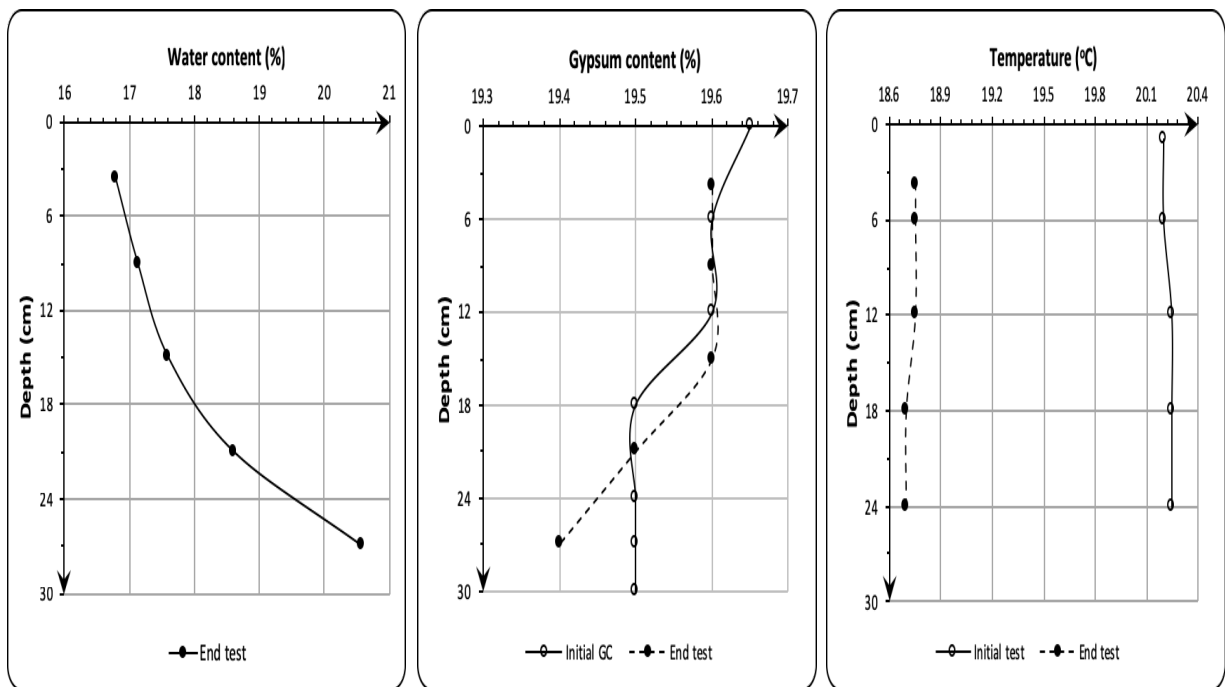


Figure 5-19: Water and gypsum contents and temperature profiles over depth after failure for Case 2.

5.3.3.3 Case 3: Slow Test with Heating Source and Breeze

This study aimed to investigate the performance of a footing resting on dry manufactured gypseous soil with groundwater, temperature and breeze simulating an arid climate. It was conducted following the same procedure as Case 2, but with the addition of heating and a breeze. Because of the presence of a frame in the middle of the set up, it was decided to use two infrared lamps suspended over both sides of the tank to distribute the temperature evenly on the soil surface. The soil surface temperature (50-52°C) was controlled via two sensors positioned on the soil surface (see Chapter Four). Both the lamps and fan were switched on after the footing model was positioned on the soil surface, the rest of the procedure the same as described in Section 4.5.4. The water was added in four stages (W1, W2, W3, and W4; see Table 5-2), to a total= 8 litres. The vertical displacement of footing, ER and temperature over time during soaking, is shown in Figure 5-20, 5-21, and 5-22, respectively. This graph shows that there was been a steep increase in settlement at wetting stage W2 (total= 6 litres) reaching 8.51 mm when 96 hours into the procedure in comparison to Case 2 which reached 0.67 mm with the same amount of water. At W3 (total= 7 litres) the displacement measured 10.83 mm at 168 hours. At W4 (total= 8 litres), the readings from the LDS sensors recorded total settlements of 12.39 and 12.02 mm at Ch1&Ch4 and Ch2&Ch3, respectively, with a differential settlement 0.37 mm observed. It should be noted that 24 hours after W4, a fine crack appeared around one side of the footing and from this point onwards, the LDS sensors recorded a difference in the readings. As shown in Figure 5-23, circular cracks appeared around the footing model. After removing the foundation, the area located directly below the footing had a water content of 7.2% corresponding to 28% degree of saturation, while the area around the foundation (uncover) was approximately dry with a water content of 0.7%, and the duricrust thickness was approximately 11 mm (see Figure 5-23g).

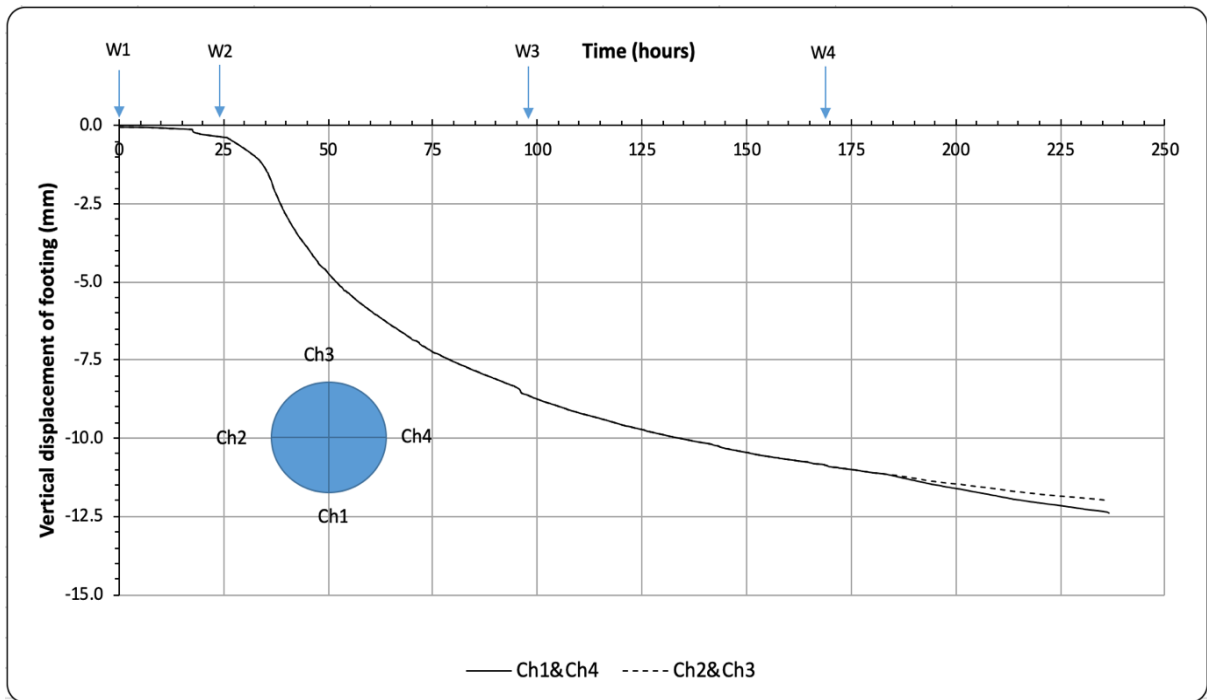


Figure 5-20: Vertical displacement of footing during wetting over time for Case 3. (NB. Ch1, Ch2, Ch3, and Ch4 refer to the channel numbers for the LDS sensors).

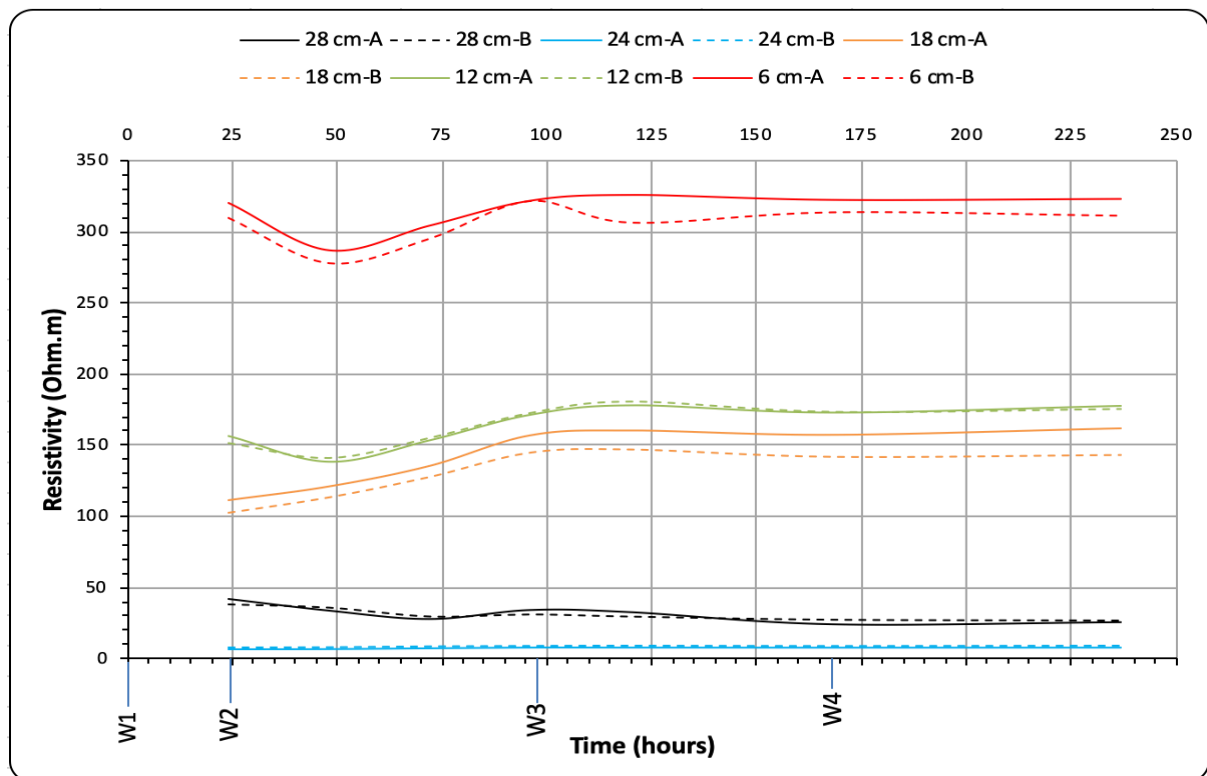


Figure 5-21: ER values along soil deposit during wetting over time for Case 3. (NB. A and B refer to the arrays, number refers to the depth of ER value from the soil surface).

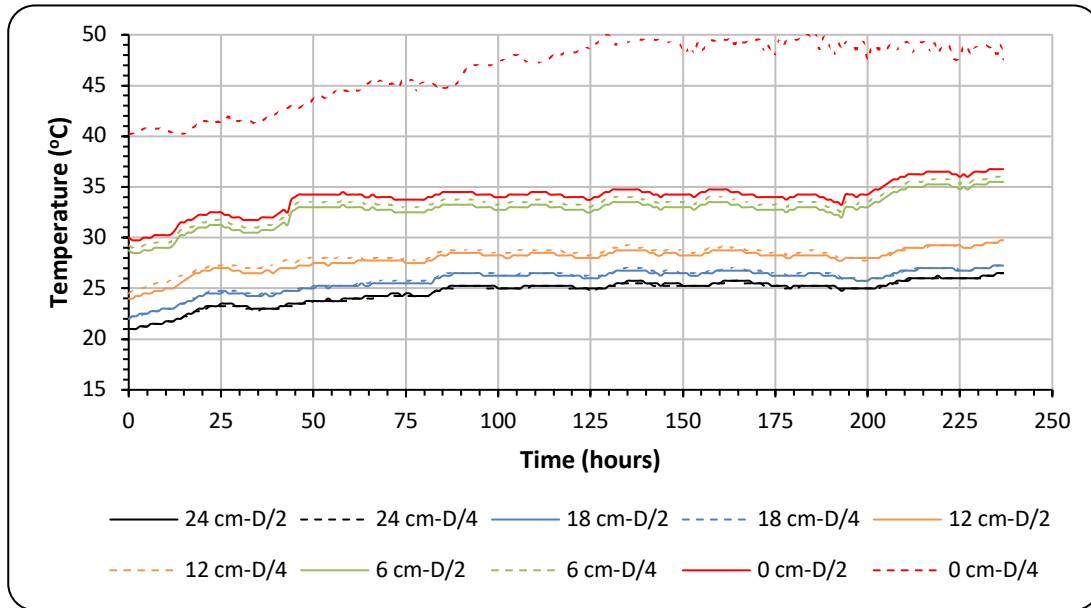


Figure 5-22: Temperature variation along soil deposit during wetting with time for Case 3. (NB. All these distances start at the surface of the soil; D/2: at centre of sample; D/4: at distance 8.73 cm from cell wall).

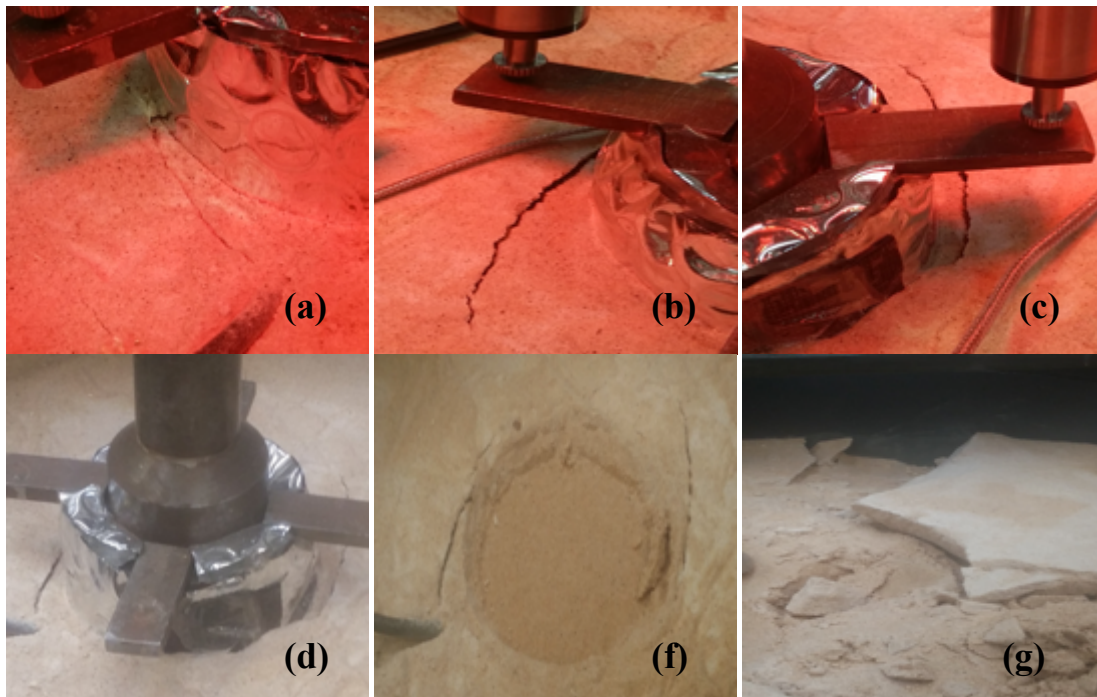


Figure 5-23: The profile of failure of Case 3; (a) first crack after 24 hours after adding 8 litres (W4), (b) and (c) close view for the final failure, (d) failure after switching off the heating system, (f) the area under the footing, (d) the duricrust around the footing area.

This finding is consistent with Tomlinson (1978) who found that in situ during the summer season, the moisture content below paving was higher than under open ground (without paving) at Baghdad Civil Airport, Iraq. The soil surface temperature was measured at 40°C falling to 25°C at a depth of 5 m below the soil surface. It was also noted that the moisture content sharply increased just beneath the pavement, causing a low CBR value. Arutyunyan and Manukyan (1982) found that capillary water is sometimes sufficient to cause the collapse of the soil structure in gypseous sandy soils. This Case has shown that much less water is needed to cause failure under temperature, breeze, water and loading in comparison to Cases 1 and 2. The high thermal gradient of the soil column accelerates to attract groundwater towards the soil surface via capillary forces in addition to high suction seen in dry soil. Gran et al. (2011) proved that vapour pressure in salty unsaturated soil is affected not only by temperature but also by suction and salt concentration. However, the relative movement of the capillary fringe is faster than in the field due to the relative thickness of the laboratory and field samples. This will result faster settlement of the footing model and probably more movement.

The behaviour of ER in this case (3), is completely different from the previous Cases (Case 1 and 2). ER over depth, with exception of 18 cm deep, decreases at the beginning of wetting due to the water added, increases gradually when water content increases. At the end of the test, the ER returns to a value very close to the value measured at the beginning of the wetting phase, as shown in Figure 5-21.

Figure 5-24 illustrates the water and gypsum contents and temperature profiles. The water content was lower than previous tests (Case 1 and 2) as a result of the lower amount of water

added (8 litres) this decreasing in a linear pattern closer to the soil surface. The lowest water content was directly below the foundation (7.2%), while a higher water content was measured at the base of the tank (13.1%). Although water was added in small amounts at a time, the water drawn up through the soil deposit reflects the capillary action of this soil by thermal gradient. As shown from the temperature profiles, there is a bigger difference in temperature gradients in the soil column in comparison to Cases 1 and 2. Once again, the gypsum content is more or less homogenous, varying between 19.4% and 19.6%, indicating that there is no gypsum migration due to the short testing time, this associated with a low volume of water insufficient to leaching gypsum upwards soil surface.

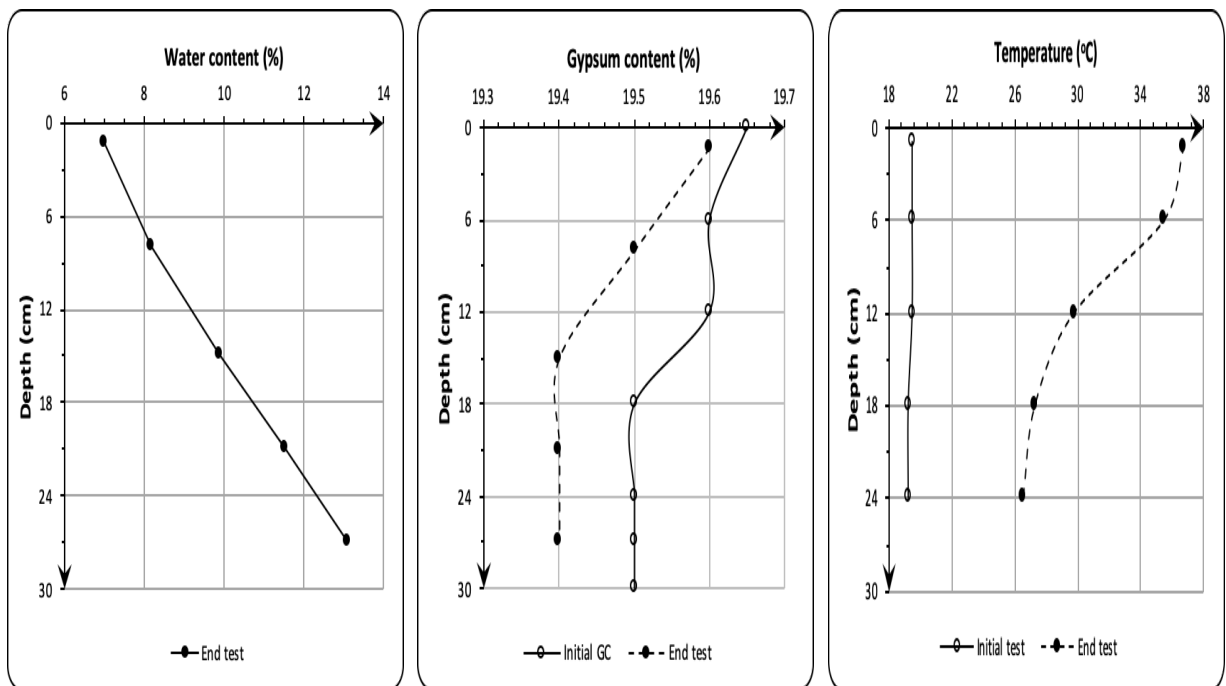


Figure 5-24: Water and gypsum contents and temperature profiles over depth, after failure for Case 3.

5.4 Discussion

5.4.1 Producing a Metastable Response in Samples of Various Sizes

The focus of this study was to develop a method to manufacture gypseous soils that broadly replicate the behaviour of these types of aeolian deposits in hot, arid conditions. Once they were developed, samples were manufactured and tested to investigate the behaviour of these soils when exposed to vertical groundwater flow, with/without the addition of a temperature gradient and surface breeze, as these conditions constitute major issues with shallow foundation movements in Iraq (Seleam, 1988; Al-Ani and Seleam, 1993; Al-Mufti, 1997; Fattah et al, 2008; Al-Farouk et al., 2009; Ahmad et al., 2012; Fattah et al., 2015).

Naturally occurring aeolian gypseous soils in the Middle East are usually found to be loose, open structured fabrics that are stiff when they are dry (or have a low degree of saturation) with very low compressibility (Akili and Torrance, 1981; Fookes et al., 1985; Al-Mufti, 1997; Livneh et al., 1998; Royal, 2012). However, when subjected to changes in water content causing a sudden compression (a metastable response), their response is immediate and substantial. The pluviation method was successful with small-scale samples (see Figure 5-25, also shown in Chapter 3) regarding the reproduction of collapsible soil in the laboratory. It was reassuring to note that metastability was also observed in large-scale samples (i.e. Figures 5-9 and 5-12; 5-15 and 5-18; and 5-20 and 5-23), illustrating the flexibility of the method developed and highlighting a notable contribution to the science emanating from this study.

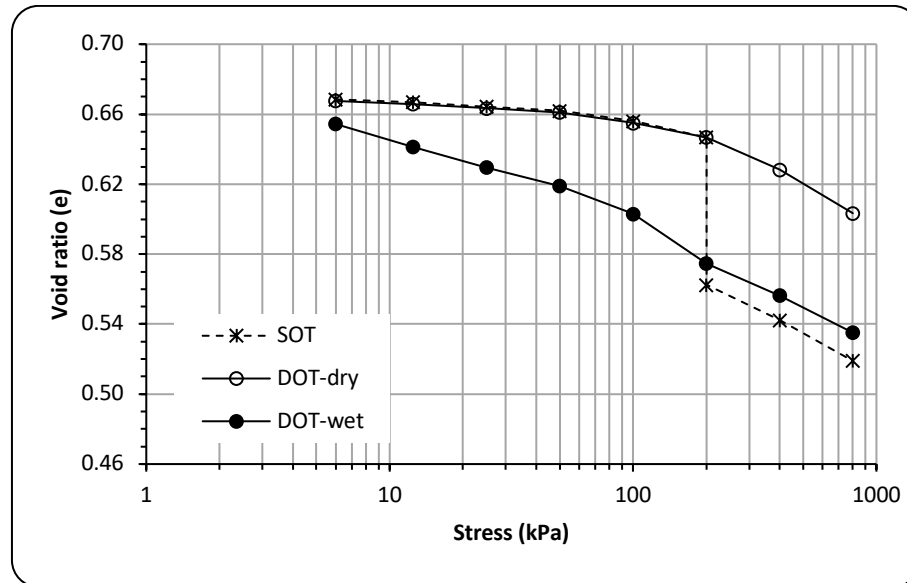


Figure 5-25: Single and double oedometer test for 20% gypsum content.

As such, the aim to produce representative gypseous soil samples in the laboratory has clearly been met, although perhaps more significantly, the method developed allows the creation of much larger samples than those traditionally manufactured in the laboratory. This will allow more complex testing regimes than those that are commonly associated with standard bench scale tests (i.e. the oedometer and UCS).

5.4.2 Observations on the Collapse of the Metastable Soils in the Footing Experiments and Comments on the Possible Mechanisms Controlling this Response

Post-wetting compression of metastable, aeolian gypseous sand found in hot, arid environments has been examined by a number of researchers, and at least four mechanisms have been identified that contribute to the compression response (AlNouri and Saleam, 1994; Al-Mufti, 1997; Nashat, 2011): (1) compression mechanisms associated with the majority of soils; (2) a weakening of intergranular bonds, resulting in particle slippage, forming a denser configuration; (3) compression due to the dissipation of suction and a possible build-up of

positive pore water pressures, followed by consolidation settlements with the dissipation of these pore water pressures due to water moving up the soil column; (4) dissolution of gypsum crystals in the pores of the soil. A combination of these processes will trigger considerable settlement in the soil upon loading and inundation.

It should be noted that much of the literature examining the engineering properties of these types of gypseous soils focuses on weakening and/or changes in soil properties due to dissolution and precipitation of the gypsum within the soil (Seleam, 1988; Al-Ani and Seleam, 1993; AlNouri and Saleam, 1994; Ismail and Mollah, 1998; Al-Farouk et al., 2009; Namiq and Nashat, 2011; Razouki and Salem, 2014). Clearly, the removal of cementitious particles from the soil structure must have a weakening effect and is worthy of investigation.

5.4.2.1 Gypsum Dissolution and Reprecipitation within Soil Columns

Gypsum dissolution and reprecipitation was encountered in this study during the evaporation column tests, where exposure to vertically seeping water from a phreatic surface, up through the unsaturated soil to the surface, where the water then evaporated, appeared to result in relocation of the gypsum (post-testing gypsum contents reproduced in Figure 5-26). Looking at the distribution of post-tested gypsum, the formation of the phreatic surface results in the dissolution of gypsum below this depth. This gypsum is subsequently transported up the soil column via suction, presumably due to unsaturated soil conditions and the application of the thermal gradient across the sample, until the water evaporates and the gypsum reprecipitates out of solution and into the soil. This would appear to take place in the shallow layers of the soil columns (within the upper 5 cm of the 30 cm columns).

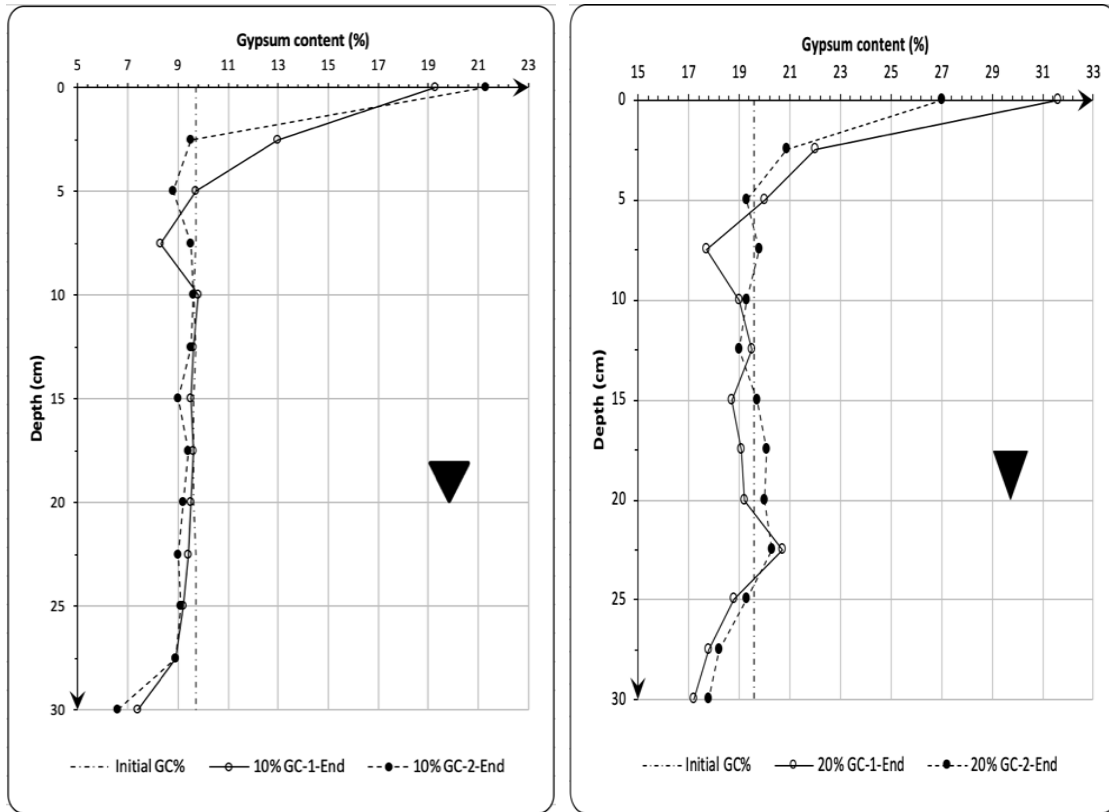


Figure 5-26: Post-testing gypsum content profiles for initial gypsum contents of 10% (left) and 20% (right) (both repeated twice) (previously presented in Figures 5-6 and 5-7), after 40 days of testing.

Upon reflection, the method used to determine the gypsum content was less than ideal, as it involved drying the soil to initially drive off the pore water and then to dehydrate the calcium sulphate crystals, instead of first attempting to separate out the pore water from the soil structure (i.e. via the use of other alternative method). This does not allow easy identification of the amount of gypsum in the pore that is dissolved within the liquid or left as a solid between the particles. Whilst the total gypsum content was measured, it might have been useful to be able to identify the proportions of gypsum content in dissolved and crystalline forms during testing. The development of a more refined method of analysing the gypsum content is recommended as follow-up work from this study.

Limitations regarding the measurement of gypsum content notwithstanding, it is clear that the results of the evaporation testing indicate that gypsum dissolution and precipitation will occur within the manufactured soil samples, which further illustrates that these samples replicate the behaviour of deposits in situ, reinforcing the view that the methodology developed herein is fit for purpose. However, and perhaps more importantly, the post-test gypsum content profiles were developed after 40 days exposure to changes in temperature and unsaturated flow. Such changes in gypsum content were not observed in the footing test with a temperature gradient and a breeze (Case 3 took 11 days to complete), and this suggests that whilst gypsum dissolution and reprecipitation might be an important factor in the long term, in the short term it would appear to be of lesser importance in comparison to other mechanisms. This is considered in more detail in the subsection below.

5.4.2.2 Failure Observations in the Footing Tests

Punching failure was observed in all three cases. This occurred within a short period of time after the addition of the final volume of water into the soil column. This suggested that it is the water permeating into the soil, softening it with the associated dissipation of suction (and possible weakening of the cementing bonds), that is having the most significant effect on the soil structure in the short term rather than water dissolving the gypsum crystals. In all three footing cases, collapse of the soil structure occurred in the uppermost layer when a ‘trigger volume of water’ had permeated into the sample (the curing time for this layer was lower than the others at approximately 30 days, although findings from the UCS testing suggest that the gypseous soil should have fully cured in this time). This was attributed to reductions in soil suction and the bonding material (gypsum) between sand particles, which may be softened, weakened, and broken. Figure 5-27 shows the punching shear within the first upper layer (60

mm thickness) for all cases. The potential importance of this finding is that any rise in groundwater might only have a significant influence on foundations as it approaches the superficial soil deposits where the ground is comparatively heavily loaded due to the location of the foundation. Hence, a far greater risk might be from leaking pipelines and surface water such as rain and irrigation systems, as these are more likely to affect the upper layers of soil, where loading has the greatest effect on the soil. In Iraq, leaking pipelines (water and sewage) and water from garden irrigation have resulted in total, or differential, settlement to structure (see Chapter One) (AlQaissy, 1989; AlNouri and Saleam, 1994; Al-Mufti, 1997; Sissakian and Al-Mousawi, 2007; Ahmed, 2013; Al-Obaidi, 2014).

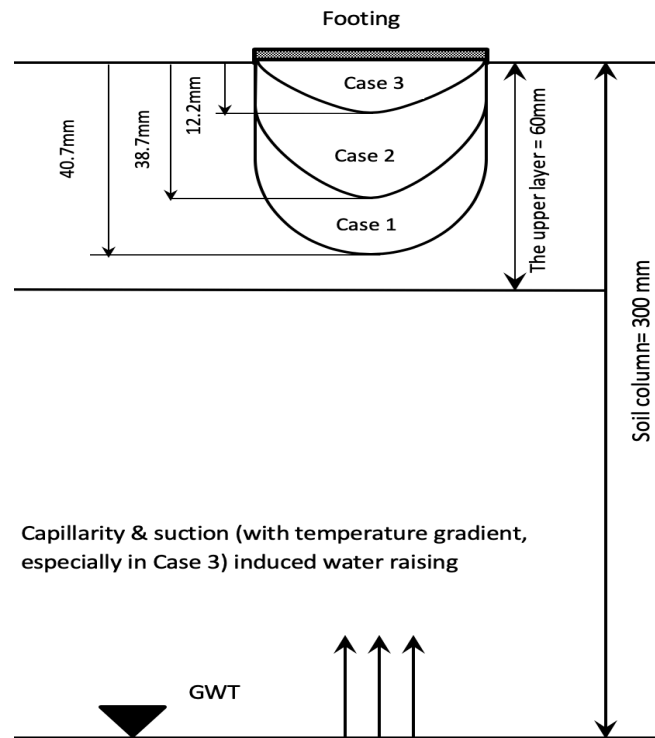


Figure 5-27: Schematic presentation of settlement depth, groundwater level (GWT), and stress bulb for each case (Case 1= 45.13 kPa at settlement 40.7 mm and water content (WC)= 18.7%, Case 2= 47.4 kPa at settlement 38.7 mm and WC= 16.8%, and Case 3= 77.1 kPa at settlement 12.2 mm and WC=7.2%).

This change in response to wetting can be observed also in the oedometer and suction tests, which although not wholly comparable with the foundation testing due to different boundary conditions and different samples, it is hoped that these observations will prove useful. In these cases, inundation resulted in rapid softening and settlement. When considering suction on the wetting curve, it is apparent that there is a significant reduction with wetting (Figure 5-28 and Chapter 3: Section 3.7.4.3). Figure 5-28 illustrates the potential magnitude of dissipation in suction (for footing Case 3) by plotting the approximate suction near the beginning and at the end of the test, based on the water content at failure, and before starting the test based on the trial test, which was on average 1.2% for the soil deposit (Section 4.5.3). It was found that there was a significant reduction in the suction with wetting for all cases, and the mean water content of the soil deposit upon failure for Cases 1, 2, and 3 were 19.3%, 18.1%, and 10%, corresponding to suctions of 4 kPa, 5 kPa, and 15 kPa, respectively.

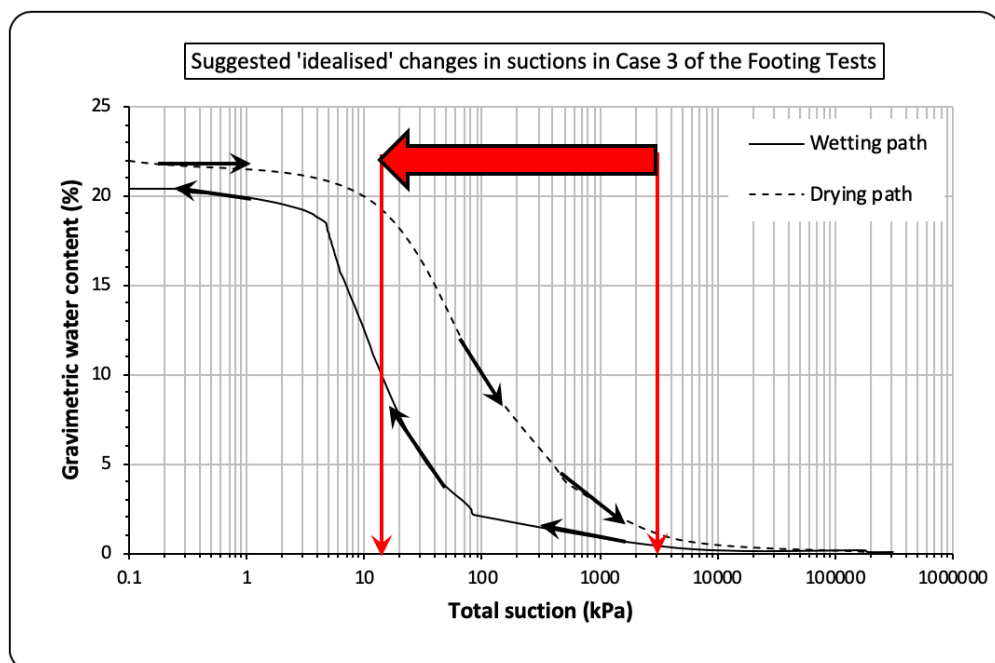


Figure 5-28: Gravimetric water content versus total suction for 20% gypsum content.

Suction testing was undertaken following the ASTM D 6836-07, and as such was conducted at approximately 20°C. Whilst this generated the SWCC for the soils, it did not reflect conditions when the thermal gradient was applied to them. It is presumed that the high temperatures applied to the surface of the soil samples (approximately 50°C) would result in additional suction, although this could not be confirmed with the equipment available in the laboratory and is also worthy of further investigation.

In Case 3 (with heating and a breeze), it was noticed that post testing (with the removal of the foundation), the volume of soil located directly below the footing (covered by the surface area of the foundation) had a water content of 7.2%, corresponding to (approximately) 28% degree of saturation, whilst the soil surrounding the footing (uncovered and hence directly exposed to the infrared lamp) had a water content of 0.7%. In addition, the temperature directly beneath the foundation (a covered area) was lower than the temperature around the foundation (an uncovered area) by approximately 10°C. Hence, the simulated foundation inhibits evaporation, thus the water content of the soil underneath the structure gradually increases as the water rises to the upper layers by capillary action under the effect of the temperature. It has been suggested that non-uniform migration of water through the soil to the ground surface would occur due to the ‘shadowing’ effects of structures that cover part of the ground surface, and that this differential flow of water through the soil would have a negative impact upon the strength of the soil. The difference in the observed water content between the exposed and covered soil here would appear to support this assertion. The higher water content directly under the foundation clearly produces a weakened zone, and this interacts with the soil experiencing the external load, and as a result, the soil's load-bearing capacity is reduced.

Case 3 (although the gypsum content did not vary significantly with depth) resulted in the formation of a duricrust (see the upper layer in Figure 5-23, suggesting that there may have been uncharacterised changes within this thin layer; the lack of characterisation is due to limitations in the facilities available in this study). This would be expected to have strengthened the upper surface (although this could not be verified due to difficulties with post-test handling). However, it is clear that the difference in water content in the superficial layers, due to the ‘shadowing’ by the foundation, resulted in a loss of suction and a punching failure, regardless of the duricrust. Whilst the settlements were not the same order of magnitude as in Case 1 and 2, it occurred for a lower volume of water added to the sample and over a shorter period time. Thus, it is suggested that duricrust formation is not sufficient to prevent collapse of these materials, and hence a hard, dry surface might not be a suitable indicator for potential metastable collapse. In this study, the depth of the duricrust did not approach the depth of the influence of the external load within the soil, and metastable collapse still occurred. Therefore, perhaps the depth of the duricrust formation should be determined, and the depth of the influence of the external load within the soil should be estimated before a decision is taken as to the susceptibility of a soil deposit to metastable collapse with change in groundwater conditions in situ. Certainly, more research into this area should be undertaken.

5.4.3 Observations on the Use of Resistivity to Monitor Changes in Geotechnical Properties of the Gypseous Soil Samples with Movement of Water through the Soil Columns

The application of ER to the evaporation and footing tests appear to show that soil resistivity was very sensitive to moisture and temperature induced variations rather than crystal gypsum

variation. During the evaporation tests, three distinct trends arising from ER could be observed. Lower ER values were observed in the deeper layers of soil (nearer, or below the phreatic surface) when compared to those nearer the surface, and these only marginally changed with time. This was attributed to the relatively constant water content (once water was introduced into the sample and the phreatic surface formed), rather than gypsum content (which decreased with partial dissolution and was transported upwards through the soil column). The intermediate soil deposits (between the relatively constant deep deposits and the changing superficial deposits) experienced a change in ER with fluid flow. This flow increased the volume of saline water within the pores, causing a reduction in the measured resistivity. Initial gypsum content impacts upon the amount of gypsum dissolved (changing the concentration of ions for electrical conduction within the fluid, thus leading to an increase in the pore water conductivity); as a consequence, the ER for a soil column with 20% gypsum content was lower than a soil column with 10% gypsum content in the evaporation tests. Finally, in the superficial deposits, where the water vaporises and evaporates from the soil column, precipitating the transported calcium sulphate into the soil (reforming gypsum crystals) and forming a dryer duricrust layer, ER was observed to significantly increase or decrease in conjunction with a decrease in water content and a high temperature, although the gypsum content increased towards the soil surface. This means the ER tests were inconclusive and it was hard to interpret the results with the formation of duricrust.

During the footing tests, the ER broadly indicated that soil collapsibility upon wetting influenced the resistivity values in the upper layers in all three cases due to the associated variations in soil densification and water content. In Cases 1 and 2, the ER values decreased with time until they approached the failure point, whereupon the behaviour for both varied. In

Case 1 (the quick test), the ER significantly increased upon failure, whereas in Case 2 the ER abruptly decreased, although this case experienced rapid collapse for the same amount of water (11.05 and 10.7 litres for Case 1 and 2, respectively). The increase in ER in Case 1 was attributed to rapid soil densification and water drainage in the upper layer with punching failure (and the associated failure) (recognised as a rapid densifying failure mechanism in loose soils). This was ascribed to the reduction in the salt concentration in the saline water as a result a decrease in the pores' volumes in the sample. The ER behaviour in Case 3 (a slow test under a temperature gradient and breeze) was completely different from Cases 1 and 2. This case showed that in the first wetting stage, ER slightly decreased and then increased gradually when the water content increases, stabilising very close to the value measured at the beginning of wetting phase.

5.5 Summary

It is apparent from the evaporation test that, over time, the manufactured soil experiences partial dissolution and re-precipitation of its gypsum, with precipitation taking place in the upper layers of the soil as the water evaporates from the soil under increasing temperatures. It was found that the evaporation rate is sensitive to the gypsum content as there is more evaporation in soil that has 10% gypsum content in comparison to soil with 20% gypsum content. However, as gypsum crystals are moderately soluble, 2.6 g/l at 25°C under one atmosphere of pressure, this process takes time to develop. In this research, the evaporation tests ran for 40 days. This was not the case in the footing tests, where the gypsum content profiles of the three footing tests did not change significantly. This suggests that dissolution-reprecipitation is not the dominant process in these cases, and partial dissipation of suction and possible softening of cementitious bonds via the gypsum crystals appears to have a more

pronounced impact due to both the time taken for collapse to occur and the volume of water required to trigger an event.

While collapsible soils in hot, arid conditions such as those encountered in Iraq commonly exhibit high stiffness in their dry (or low degree of saturation) state, they are subject to substantial reductions in volume upon wetting. As such, adequate control of surface water (i.e. drainage) and maintenance of buried water pipes are critical in order to prevent wetting of shallow deposits and thus maintain a stable zone for foundations in these soils.

The stress level applied to the samples was 80 kPa, and in all three footing cases, collapse of the soil structure occurred in the upper layer when a trigger volume of water had permeated into the sample. This was attributed to reductions in soil suction and the bonding material (gypsum) between sand particles may be softened, weakened, and broken.

Full collapse was obtained at an approximate (as it was very difficult to subsample and measure the void ratio/dry density of the material, due to its friable nature, thus it has been assumed based on approximated layer properties) degree of saturation of 72% and 65% for to Case 1 and Case 2, respectively. In Case 3, the thermal gradient within the soil column was high, leading to increased water movement towards the surface of the soil. It failed at a 27% degree of saturation. 8 litres of water, including the volume required to fill the filter (5 litres), was sufficient for failure to occur, as opposed to 11.05 and 10.7 litres for Cases 1 and 2, respectively. Consequently, environmental conditions appear to have a critical influence on the behaviour of gypseous soil and could create problematic conditions for construction if not taken into consideration when planning.

The application of ER to the evaporation and footing tests appear to show that soil resistivity was very sensitive to moisture and temperature-induced variations, rather than crystal gypsum variation. However, the variation in the ER of manufactured gypseous soil is due to complicated deformation mechanisms, including the behaviour of gypsum under different conditions, such as variations in temperature, water, and load, which, in turn, significantly influenced the dissolution of the gypsum. ER was also influenced by many other factors, such as salinity, temperature, water, and soil structure; all of these parameters were included in this study.

CHAPTER SIX

CONCLUSION AND RECOMMENDATIONS

6.1 Introduction

The literature review revealed that although previous research has been done into the effects of physical and environmental factors of arid, aeolian, gypseous soils, including the effects of soaking, the wetting-drying cycle, thawing-freezing, and leaching on collapse, compressibility, creep, and shear strength using standard apparatus, there several knowledge gaps (Arutyunyan and Manukyan, 1982; AlNouri and AlQaissy, 1990; Livneh et al., 1998; Razouki and El-Janabi, 1999; Azam, 2000; Razouki and Kuttah, 2006; Razouki and Ibrahim, 2007; Razouki et al., 2007; Sajedi et al., 2008; Estabragh et al., 2013; Aldaood et al., 2015; Fattah et al., 2015). These include:

- 1) The apparent lack of a manufacturing method that can be used to create metastable and collapsible soil samples in the laboratory. The key limitation was the inability to create samples of various sizes (potentially much larger than traditional oedometer samples) that can also produce samples with the desired geotechnical properties (e.g. loose packing conditions with low dry density and relatively high void ratio that are stiff and strong at low degrees of saturation).
- 2) The lack of understanding of how these soils behave in complex loading and environmental conditions. It is acknowledged that in situ behaviour has been reported, where complex conditions clearly occur, although it is often difficult to identify the key mechanism(s) in such uncontrolled conditions. Laboratory testing predominantly has focused upon standard geotechnical testing (i.e. using the oedometer), although

there have been examples where larger samples have been exposed to temperature gradients, water movement and breeze. However, these experiments have not provided a complete picture, and are often not undertaken as parametric studies to confirm the relative influences of the various mechanisms. For example, what effect does the application of vertical groundwater movement, driven by thermal gradients and suction, through these unsaturated soils have on the soil whilst it experiences external loading?

- 3) Laboratory testing of these soils has traditionally used post-sample analysis to attempt to infer changes in the samples during testing. Real-time (or quasi-real-time) monitoring could potentially be undertaken using non-destructive geophysical testing (such as electrical resistivity (ER)), and if successfully applied, could monitor changes during testing. However, this does not appear to have taken place to date.

Therefore, this study aimed to develop a technique to manufacture reproducible gypseous soil samples of different sizes in the laboratory. This study also monitored the change in water and gypsum content within the soil as a response to suction-induced movement of groundwater (via unsaturated conditions and the application of a thermal gradient), and how this influenced the deformation response when loaded by a simulated circular foundation. ER (using a linear array) was trialled as a non-destructive monitoring method to determine if changes in water and gypsum content could be observed over time.

It should be noted that the structure adopted in this thesis aimed, where possible, to ensure that the chapters were self-contained (hence Chapter 3 focused on the development of the methodology and the associated validation testing, while in Chapter 5 the results from the

evaporation and foundation tests were presented and discussed, etc.). These conclusions draw together the key findings from the research and present this study's contributions to knowledge before suggesting further work that should emanate from this research.

6.2 Conclusions

6.2.1 Manufacturing Gypseous Soil and the Associated Validation Testing

The method developed (in Chapter 3) involved a four-stage process:

1. The pluviation of damp sand-gypsum mixtures (potentially in layers, depending on the sample size), to create the desired open, loose soil structure.
2. The subsequent application of a seating load (5 kPa) to develop the desired dry densities/void ratios.
3. and 4. Wetting and drying of the sample (in a low-temperature oven, or in ambient conditions, depending on the sample size) to promote gypsum crystal growth, hence cementing the soil particles and creating the metastable structure.

This method was successfully developed to replicate the desired engineering aspects of naturally occurring (superficial aeolian) soils, located in hot arid environments (i.e. as encountered in Iraq) using materials sourced in the UK. It was clear from the findings that it is possible to produce repeatable samples with the desired properties (within a limited range) that facilitate the option of undertaking systematic study within the laboratory. The sizes of these samples could easily be varied from the standard ones used in geotechnical testing (i.e. for compression testing with the oedometer) to larger samples (349 mm in diameter) for bespoke testing. The production of larger samples is achievable using a multiple-layer approach, providing that the layer thickness is sufficient to prevent the interlayer boundary

(which can be improved by scarifying the sample before pluviating the next layer) from heavily influencing the deformation response of the sample; and that the sample has had sufficient time to ‘cure’ before applying the next layer.

A series of validation testing, including oedometer, unconfined compressive strength, and suction tests, was conducted on this soil. The results showed that:

- i. The manufactured samples were strong and stiff when dry, or at low degrees of saturation (especially those containing higher gypsum content), experienced rapid repacking akin to hydrocollapse when inundated under load, and the stiffness and strength fundamentally decreased with wetting. These responses were more pronounced with increased gypsum content and when external load was applied. Hence the manufactured samples simulated the deformation response encountered within these types of deposits in hot, arid environments. Increasing the applied load presumably results in progressive failure of the interparticle bonds, with associated particle movements in the relatively open soil structure; hence the large corresponding volumetric strains. Secondary compression/creep testing undertook a load step of 90 days, and were found to be important mechanisms when considering settlements with inundation of water, suggesting that longer duration load steps should be used in compression tests than the normal 24-hour period if the metastable nature of these materials are not to be underestimated.
- ii. Outcomes from unconfined compressive strength testing (UCS) indicated that the peak strengths were achieved at very low strains (the range of strains being between 0.32 to 0.68%) due to shearing of the cementing bonds. Hence the deformation response was

brittle, with strain-softening post peak strength. It was noted that, in many cases, the deformation responses observed were not smooth curves, appearing instead to be ‘stepped’ in nature prior to peak strength. This was attributed to the shearing of a proportion of the gypsum bonds and the associated increased frictional forces mobilised as the particles within the loose structure moved closer together; once sufficient bonding was destroyed, then the peak strength was exceeded and the sample was weakened. It was found that the thickness of the layer is critical: too thin and the strength and stiffness of the material was significantly reduced; the interface between layers, especially for samples with higher gypsum content, can dominate the development of the failure plane. It was found that if the layers were of sufficient thickness, then the strength of the overall sample was not overly negatively affected and therefore a multi-layered approach is preferable for the creation of very large samples.

- iii. It was found that as the gypsum content increases, the total suction in drying and wetting paths significantly increases. Residual total suction increased, while the equivalent residual water content decreased as gypsum content increased. Also, it was found that the air-entry value (AEV) happened in a comparatively low range of suction values and slightly increased as gypsum content increased. This is due to the soil structure not being able to hold water within the pore space due to its relatively coarse particle size distribution, even with a low value of suction. This behaviour could be ascribed to the high permeability of the manufactured soil and weak intergranular tension forces of the manufactured soil structure.

Altogether, these tests illustrated the flexibility and repeatability of the method. Therefore, the

method developed herein offers the research community a tool to create samples for study within the laboratory, hence circumventing the problematic procedure of sampling in situ and transporting samples to the laboratory.

6.2.2 Bespoke Testing (Evaporation Column and the Simulated Foundation)

The parametric nature of the study undertaken herein has produced some interesting findings regarding the behaviour of metastable gypseous sand soils when exposed to changing environmental and loading conditions. This includes:

- i. A practical demonstration that environmental conditions appear to have a critical influence on the behaviour of gypseous soil over time and could create problematic conditions for construction if not taken into consideration when planning. This includes:
 - a. It was found that the evaporation rate is sensitive to the gypsum content, presumably due to the hydraulic conductivity of the bonded soil structure, and the reduction of the pore spaces in the near-surface deposits (hence reducing the hydraulic conductivity) with the precipitation of gypsum over time, as soils with 10% gypsum content experienced greater volumes of water evaporating from the samples compared to soil with 20% gypsum content. The precipitation of gypsum within the upper layers of the soil reduces the hydraulic conductivity (and presumably the vapour conductivity) over time, hence the evaporation losses through the soil column would appear to be non-linear with time.
 - b. The formation of a duricrust does not necessarily prevent failure from below due to softening as the water content changes, and hence a hard, dry surface might not be a suitable indicator for potential metastable collapse.

- c. The foundation appeared to provide a ‘shadowing effect’ in Case 3 (the application of a thermal gradient and breeze, as well as the introduction of the water) as the water content of the soil directly below the foundation was much higher than in the soil (at the same depth) where the surface was exposed to the atmosphere (and hence the infrared lamp). This has significant connotations for constructing in these soils, as a temperature gradient and unsaturated conditions drawing water up towards the surface will result in a non-linear distribution of water within the upper layers of the soil and hence will have a non-linear impact upon the shear strength of the soil. This differential softening, and hence differential movements, could have significant implications for the ‘relative’ health of the structure.
- ii. Much of the reported literature on the behaviour of these soils appears to focus upon the dissolution-reprecipitation of the gypsum as a governing mechanism in their engineering behaviour. Whilst this mechanism was encountered in evaporation testing, the solubility of gypsum means that this mechanism takes time to develop. The findings of the simulated foundation test indicated that gypsum content did not change significantly, and it is suggested that it was the loss of suction (due to vertical seepage of water) that resulted in a loss of strength, and thus the punching shear was observed. This short-term response, linked to suction dissipation, clearly has implications for natural soil deposits (potentially even those that have formed a duricrust) if a rapid change in water content is experienced (for example, from failed drainage or leaking utility, as well as changing groundwater regime). Secondary compression/creep testing in the oedometer did illustrate that in the long term, compression could increase (when compared to those observed after a short load step); therefore, gypsum dissolution is not to be discounted, but it should be

acknowledged that the dissolution-reprecipitation process is time-dependent and is not the dominant process in the short term.

- iii. The potential importance of this finding is that any rise in groundwater might only have a significant influence on foundations as it approaches the superficial soil deposits where the ground is comparatively heavily loaded due to the location of the foundation. Hence, a far greater risk is from leaking pipelines and surface water, such as rain and irrigation systems, as these are more likely to affect the upper layers of soil, where loading has the greatest effect on the soil.

6.2.3. Reflections on the Use of Electrical Resistivity

An automated electrical resistivity (ER) system was used to determine if changes in water and gypsum contents can be observed in (quasi) real time with the movement of water vertically upwards through a soil column under a thermal gradient. The potential for using this approach in these conditions (monitoring gypseous soil experiencing external loading and changes in environmental conditions) had not appeared to have been considered to date.

The outcomes from the evaporation and foundation tests showed that soil resistivity was very sensitive to moisture, temperature, and load-induced variations within the soil rather than crystal gypsum variation. Conditions of stress, temperature, and wetting substantially affected the current passing through the soil fabric. This sensitivity to the environmental conditions (where the temperature changed significantly over the 300 mm sample height, and where water changed from fluid to vapour in the upper reaches of the sample) makes detailed analysis of ER all but impossible. For example, ER measurements requires calibrating to a

reference temperature (commonly 25°C or thereabouts is used; see Abu-Hassanein et al., 1996; Sreedeeep et al., 2004), but what reference temperature is suitable when the gradient ranges from approximately 20°C to 50°C? In addition, non-linear vaporisation of water (and precipitation of miscible salts, hence changing geotechnical properties of the soil with time, which will also impact fluid flow) in the upper layers of the soil samples over time also complicates matters. Therefore, whilst generic trends can be seen with ER, a detailed characterisation of the changes within the soil column (i.e. dissolution and reprecipitation fronts within the soil column) could not be achieved. For this to take place, a far more nuanced ER method must be developed that can cope with these challenging, and transitional, conditions. Furthermore, the soil resistivity for the three footing tests was completely different upon failure, and this was due to the test conditions (amount of water, the densification of the upper layer, temperature, and the test time).

6.4 Recommendations for Further Work

This study has provided significant insight into the impact of changing gypsum content and environmental conditions (such as water, temperature, and load) on metastable gypseous soil behaviour (manufactured to emulate superficial aeolian deposits formed in hot, arid conditions such as in the Middle East). It has highlighted the need for further work and future research, including:

- Investigating the influence of groundwater depth on the evaporation rate, and gypsum precipitation, in the gypseous soils.
- Investigating the impacts of cyclic drying-rewetting on the evaporation rate and the gypsum migration within the soil column.

- This research cannot determine the dry density, void ratio, and degree of saturation of soil upon failure as the soil is very loose/friable upon wetting. Therefore, it is necessary to develop a suitable method to obtain undisturbed samples post-testing.
- An investigation into the behaviour of gypseous soils under different wetting conditions, such as infiltration from sources other than a phreatic surface (such as a simulated broken, and leaking, water pipe) close the foundation, is highly recommended for future work. This is believed to be a significant issue, and it would be useful to confirm the impacts of leaking utilities on metastable soil behaviour.
- An investigation into the suctions developed due to high temperature gradients would also be useful, as these undoubtedly contribute to the response of the soil, but were not characterizable in this study. This would require modification to the equipment and processes if the effects of high-temperature suction are to be determined.
- The method used to determine gypsum content did not distinguish between liquid and solid phases within the soil. It would be beneficial to determine the relative effects of these phases, so the development of a modified method to determine gypsum content would be advisable.
- The ER measurements did not function as desired. Whilst some coarse, generalised trends could be inferred, the extreme conditions (i.e. high temperature gradients, changes in water salinity, changes in water content, changes in hydraulic conductivity, vaporization of the water, and changes in gypsum content) within the tests undertaken prevented detailed characterization using this non-destructive technique. A new method is required to allow the calibration/characterization of the ER in these challenging conditions.
- It would be useful to develop a three-dimensional ER visualization to determine what is taking place below the foundation prior to/at failure.

LIST OF REFERENCES

- Abdul-Ameer, E.A. (2012) *A geomorphological study of dune fields and their environmental effects at Al-Muthana Governorate-Iraq*. PhD thesis, University of Baghdad, Iraq.
- Abduljawwad, S.N. (1993) Study on the performance of calcareous expansive clays. *Bulletin of the Association of Engineering Geologists*, 30 (4): 481–498.
- Abduljawwad, S.N. and Al-Amoudi, O.S.B. (1995) Geotechnical behaviour of saline sabkha soils. *Geotechnique*, 45 (3): 425–445.
- Abduljawwad, S.N., Azam, S. and Al-Shayea, N.A. (1999) “Effect of phase transformation of calcium sulfate on the volume change behavior of calcareous expansive soil.” *In Proc., 2nd Int. Conf. on Engrg. for Calcareous Sediments*. 1999. Citeseer. pp. 209–218.
- Abood, M.K. (1994) *Treatment of Gypseous soil with sodium silicate*. M.Sc. thesis, Building and Construction Engineering Department, University of Technology, Iraq.
- Abu-Hassanein, Z.S., Benson, C.H. and Blotz, L.R. (1996) Electrical resistivity of compacted clays. *Journal of Geotechnical Engineering*, 122 (5): 397–406.
- Adamo, N. and Al-Ansari, N. (2016) Mosul Dam the Full Story: Engineering Problems. *Journal of Earth Sciences and Geotechnical Engineering*, 6 (3): 213–244.
- Afaj, H.A.H. and Mohammed, H.A. (2018) Creep behaviour of Iraqi gypsiferous soil. *Journal of Engineering and Sustainable Development*, 21 (2): 93–102.
- Ahmad, F., Said, M.A. and Najah, L. (2012) Effect of leaching and gypsum content on properties of gypseous soil. *IJSRP*, 2 (9): 1–5.
- Ahmed, K.I. (2013) *Effect of gypsum on the hydro-mechanical characteristics of partially saturated sandy soil*. PhD thesis, Cardiff University, UK.
- Akili, W. (2006) “Salt encrusted desert flats (sabkha): problems, challenges and potential solutions.” *In Unsaturated Soils 2006*. pp. 391–402.
- Akili, W. and Torrance, J.K. (1981) The development and geotechnical problems of sabkha, with preliminary experiments on the static penetration resistance of cemented sands. *Quarterly Journal of Engineering Geology and Hydrogeology*, 14 (1): 59–73.

- Al- Khafaji, A. (1997) "Densification of gypseous soil by compaction." *In Symposium on ground improvement geosystems*. London, 1997.
- Al-Aghbari, M.Y. and Mohamedzein, Y.E.A. (2004) Bearing capacity of strip foundations with structural skirts. *Geotechnical & Geological Engineering*, 22 (1): 43.
- Al-Amoudi, O.S.B. (1994) Chemical stabilization of sabkha soils at high moisture contents. *Engineering geology*, 36 (3–4): 279–291.
- Al-Anbari, M., Thameer, M., Al-Ansari, N., et al. (2016) Estimation of Domestic Solid Waste Amount and Its Required Landfill Volume in Najaf Governorate-Iraq for the Period 2015-2035. *Engineering*, 8 (6): 339–346.
- Al-Ani, M.M. and Seleam, S.N. (1993) Effect of initial water content and soaking pressure on the geotechnical Properties of gypseous soil. *journal of Al-Muhandis*, 116.
- Al-Ansari, N., Barazanji, A., Al-Jabbari, M., et al. (1984) *Geological Investigation of Mosul Dam Site. Co- fidential Report, Ministry of Irrigation*.
- Al-Bahrani, H.S., Al-Mousawi, A.S., Al-Dujaili, A.M., et al. (2014) Statistical Test for Water Quality Parameters of Euphrates River at Najaf Province during Winter and Summer Seasons. *European Journal of Advances in Engineering and Technology*, 1 (2): 35–38.
- Al-Barrak, K. and Rowell, D.L. (2006) The solubility of gypsum in calcareous soils. *Geoderma*, 136 (3–4): 830–837.
- Al-Bayati, A.Z. (2000) *Behaviour of Gypseous Soil under Cyclic Loading*. M.Sc. thesis, Civil Engineering Department, University of Baghdad, Iraq.
- Al-Dabbas, M.A., Schanz, T. and Yassen, M.J. (2012) Proposed engineering of gypsiferous soil classification. *Arabian Journal of Geosciences*, 5 (1): 111–119.
- Al-Dilaimy, F.K. (1989) *Effect of gypsum content on strength and deformation of a remolded clayey soil*. M.Sc. thesis, University of Salladin, Erbil.
- Al-Dulaimi, N.S.. (2004) *Characteristics of Gypseous Soils Treatment with Calcium Chloride Solution*. M.Sc. thesis, Civil Engineering Department, University of Baghdad, Iraq.
- Al-Farouk, O., Al-Damluji, S., Al-Obaidi, A.L.M., et al. (2009) "Experimental and numerical investigations of dissolution of gypsum in gypsiferous Iraqi soils." *In Proceedings of the 17th International Conference on Soil Mechanics and Geotechnical Engineering:*

- The academia and practice of geotechnical engineering, Alexandria, Egypt. 2009. pp. 5–9.*
- Al-Gabri, M.K.A. (2003) *Collapsibility of gypseous soils using three different methods*. M.Sc. thesis, Building and Construction Engineering Department, University of Technology, Iraq.
- Al-Heeti, A.A.H. (1990) *The engineering properties of compacted gypsified soil*. M.Sc. thesis, Civil Engineering Department, University of Baghdad, Iraq.
- Al-Khuzai, H.M.A. (1985) *The effect of leaching on the engineering properties of Al-Jazirah soil*. M.Sc. thesis, Mosul University, Iraq.
- Al-Layla, M.T. and Al-Obaydi, M.A. (1993) “Lime Stabilization of Gypseous Soil.” *In Proceedings of the 5th Arab Conference of Structural Engineering, Vol. 2, Civil Engineering Department*. Al-Fateh University, Tripoli, 1993. pp. 1001–1013.
- Al-Mohmmadi, N.M., Nashat, I.H. and Bako, G.Y. (1987) “Compressibility and collapse of gypseous soils.” *In Proc. 6th Asian Conf. on Soil Mechanics, Tokyo*. 1987.
- Al-Mufti, A.A. (1997) *Effect of gypsum dissolution on the mechanical behavior of gypseous soils*. PhD thesis, Civil Engineering Department, University of Baghdad, Iraq.
- Al-Mufti, A.A. and Nashat, I.H. (2000) “Gypsum content determination in gypseous soils and rocks.” *In Proceedings of the 3th Jordanian international mining conference, Amman*. 2000. pp. 485–492.
- Al-Obaidi, Q.A.J. (2014) *Hydro-mechanical behaviour of collapsible soils*. PhD thesis, University of Bochum, Germany.
- Al-Obaidy, N. (2017) *Treatment of collapsible soil using encased stone columns*. PhD thesis, University of Birmingham, UK.
- Al-Taiee, M. and Rasheed, A.M. (2009) “Simulation Tigris River Flood Wave in Mosul City Due to a Hypothetical Mosul Dam Break.” *In Proceeding of Thirteenth International Water Technology Conference*. IWTC 13: Hurgada, Egypt, 2009.
- Al-Zubaydi, J.H.A. (2017) Study of the Engineering Properties of Dunes Field at Al-Najaf Governorate- Middle of Iraq. *Journal of Babylon University/Pure and Applied Sciences*, 25 (3).

- Alaithawi, A.H. (1990) *Time dependent deformation of a gypseous silty soil*. M.Sc. thesis, Civil engineering department, University of Baghdad, Iraq.
- Aldood, A., Bouasker, M. and Al-Mukhtar, M. (2015) Effect of long-term soaking and leaching on the behaviour of lime-stabilised gypseous soil. *International Journal of Pavement Engineering*, 16 (1): 11–26.
- Ali, T.S. and Fakhraldin, M.K. (2016) Soil parameters analysis of Al-Najaf City in Iraq: case study. *J Geotech Eng*, 3 (1): 1987–2394.
- AlNouri, I. and AlQaissy, F. (1990) “Effect on compressibility and shear strength.” *In Conference, Vol. (6)*. Singapore, 1990. pp. 8–14.
- AlNouri, I. and Saleam, S. (1994) Compressibility characteristics of gypseous sandy soils. *Geotechnical testing journal*, 17 (4): 465–474.
- Alonso, E.E. and Ramon, A. (2013) Heave of a railway bridge induced by gypsum crystal growth: field observations. *Géotechnique*, 63 (9): 707.
- AlQaissy, F.F. (1989) *Effect of gypsum content and its migration on compressibility and shear strength of the soil*. M.Sc. thesis, Department of Building and Construction, University of Technology, Iraq.
- Alzayani, N.J., Royal, A.C.D., Ghataora, G.S., et al. (2017) Cement-bentonite in comparison with other cemented materials. *Environmental Geotechnics*, 4 (5): 353–372.
- Arulanandan, K. and Smith, S.S. (1973) Electrical dispersion in relation to soil structure. *Journal of Soil Mechanics & Foundations Div*, 99 (sm2).
- Arutyunyan, R.N. and Manukyan, A. V. (1982) Prevention of piping deformations in gypseous soils in Erevan. *Soil Mechanics and Foundation Engineering*, 19 (4): 151–154. doi:10.1007/BF02314830.
- Asghari, S., Ghafoori, M. and Tabatabai, S.S. (2014) The evaluation of changes in permeability and chemical composition of gypseous soils through leaching in southern Mashhad, Iran. *Malaysian Journal of Civil Engineering*, 26 (3): 337–348.
- ASTM-G57 (2006) *Standard test method for field measurement of soil resistivity using the Wenner four-electrode method*, American Society for Testing and Materials. Pennsylvania, USA.

- Awn, S.H.A. (2010) A modified collapse test for gypseous soils. *DIYALA JOURNAL OF ENGINEERING SCIENCES*, pp. 299–309.
- Azam, S. (2000) Collapse and compressibility behaviour of arid calcareous soil formations. *Bulletin of Engineering Geology and the Environment*, 59 (3): 211–217.
- Azam, S. and Abduljawwad, S.N. (2000) Influence of gypsification on engineering behavior of expansive clay. *Journal of Geotechnical and Geoenvironmental Engineering*, 126 (6): 538–542.
- Azam, S., Abduljawwad, S.N., Al-Shayea, N.A., et al. (1998) Expansive characteristics of gypsiferous/anhydritic soil formations. *Engineering geology*, 51 (2): 89–107.
- Aziz, L.J. (2008) *Lateral Resistance of a Single Pile Embedded in Sand with Cavities*. PhD thesis, University of Technology, Iraq.
- Barzanji, A. (1973) *Gypsiferous soils of Iraq*. PhD thesis, University of Ghent, UK.
- Beck, Y.L., Lopes, S.P., Ferber, V., et al. (2011) Microstructural Interpretation of water content and dry density influence on the DC-electrical resistivity of a fine-grained Soil. *Geotechnical Testing Journal*, 34 (6): 1–14.
- Bell, F.G. (1981) Geotechnical properties of some evaporitic rocks. *Bulletin of the International Association of Engineering Geology-Bulletin de l'Association Internationale de Géologie de l'Ingénieur*, 24 (1): 137–144.
- Bell, F.G. (1994) A survey of the engineering properties of some anhydrite and gypsum from the north and midlands of England. *Engineering Geology*, 38 (1–2): 1–23. doi:10.1016/0013-7952(94)90021-3.
- Bera, T.K. and Nagaraju, J. (2011) Switching of the surface electrode array in a 16-electrode EIT system using 8-Bit parallel digital data. *World Congress on Information and Communication Technologies (WICT)*, pp. 1288–1293.
- Berner, R. (1971) *Principles of chemical sedimentary*. New York: McGraw-HillBook Co.
- Blatt, H., Middleton, G. and Murray, R. (1980) *Origin of sedimentary rocks*. 2nd edn. New York: Prentice–Hall.
- Bolton, M.D. and Lau, C.K. (1989) “Scale effects in the bearing capacity of granular soils.” *In Proceedings of the 12th International Conference on Soil Mechanics and Foundation*

- Engineering*. 1989. AA Balkema. pp. 895–898.
- Boyadgiev, T.G. and Verheye, W.H. (1996) Contribution to a utilitarian classification of gypsiferous soil. *Geoderma*, 74 (3–4): 321–338. doi:10.1016/S0016-7061(96)00074-2.
- Brandon, T.L., Clough, G.W. and Rahardjo, P.P. (1991) Fabrication of silty sand specimens for large-and small-scale tests. *Geotechnical Testing Journal*, 14 (1): 46–55.
- Brune, G. (1965) Anhydrite and gypsum problems in engineering geology. *Engineering Geology*, 2 (1): 26–38.
- BSI (1990) *Methods of test for soils for civil engineering purposes. British Standard 1377*, British Standard Institution, London, UK.
- Buringh, P.D. (1960) *Soils and Soil Conditions In Iraq*. Ministry of agriculture.
- Campbell, R.B., Bower, C.A. and Richards, L.A. (1949) Change of Electrical Conductivity With Temperature and the Relation of Osmotic Pressure to Electrical Conductivity and Ion Concentration for Soil Extracts 1. *Soil Science Society of America Journal*, 13 (C): 66–69.
- Chen, X.Y. (1997) Pedogenic gypcrete formation in arid central Australia. *Geoderma*, 77 (1): 39–61.
- Cheshomi, A., Eshaghi, A. and Hassanpour, J. (2017) Effect of lime and fly ash on swelling percentage and Atterberg limits of sulfate-bearing clay. *Applied Clay Science*, 135: 190–198. doi:10.1016/j.clay.2016.09.019.
- Choi, S.-K., Lee, M.-J., Choo, H., et al. (2009) Preparation of a large size granular specimen using a rainer system with a porous plate. *Geotechnical Testing Journal*, 33 (1): 45–54.
- Comina, C., Foti, S., Musso, G., et al. (2008) EIT oedometer: An advanced cell to monitor spatial and time variability in soil with electrical and seismic measurements. *Geotechnical Testing Journal*, 31 (5): 404–412. doi:10.1520/GTJ101367.
- Cooper, A. (2007) “Gypsum dissolution geohazards at Ripon, North Yorkshire, UK.” *In In: Engineering geology for tomorrow’s cities [conference proceedings]/[by IAEG. Nottingham: IAEG. 2007. International Association for Engineering Geology.*
- Cooper, A.H. (1988) Subsidence resulting from the dissolution of Permian gypsum in the

- Ripon area; its relevance to mining and water abstraction. *Geological Society, London, Engineering Geology Special Publications*, 5 (1): 387–390.
- Cooper, A.H. (1989) Airborne multispectral scanning of subsidence caused by Permian gypsum dissolution at Ripon, North Yorkshire. *Quarterly Journal of Engineering Geology and Hydrogeology*, 22 (3): 219–229.
- Cooper, A.H. and Saunders, J.M. (2002) Road and bridge construction across gypsum karst in England. *Engineering Geology*, 65 (2–3): 217–223.
- Cooper, A.H. and Waltham, A.C. (1999) Subsidence caused by gypsum dissolution at Ripon, North Yorkshire. *Quarterly Journal of Engineering Geology and Hydrogeology*, 32 (4): 305–310.
- Czerewko, M.A., Cripps, J.C., Culshaw, M., et al. (2006) Sulfate and sulfide minerals in the UK and their implications for the built environment. *IAEG*, pp. 1–12.
- Dahlin, T. and Loke, M.H. (1998) Resolution of 2D Wenner resistivity imaging as assessed by numerical modelling. *Journal of Applied Geophysics*, 38 (4): 237–249.
- Damasceno, V.M., Fratta, D. and Bosscher, P.J. (2009) Development and validation of a low-cost electrical resistivity tomographer for soil process monitoring. *Canadian Geotechnical Journal*, 46 (7): 842–854.
- Dave, T.N. and Dasaka, S.M. (2012) Assessment of portable traveling pluviator to prepare reconstituted sand specimens. *Geomechanics and Engineering*, 4 (2): 79–90.
- Devadasi, R.K., Naickb, P., Reddy, T. V., et al. (2014) Automatic switching multi-electrode electrical resistivity profiling system. *International Journal of Electronics, Communication & Instrumentation Engineering Research and Development (IJECIERD)*, 4 (1): 47–52.
- El Sawwaf, M.A. and Nazir, A.K. (2012) Cyclic settlement behavior of strip footings resting on reinforced layered sand slope. *Journal of Advanced research*, 3 (4): 315–324.
- Estabragh, A.R., Kargar, S. and Javadi, A.A. (2013) Investigation on the mechanical properties of gypsum soil. *Proceedings of the Institution of Civil Engineers-Construction Materials*, 167 (5): 251–257.
- Eswaran, H. and Gong, Z.-T. (1991) Properties, genesis, classification, and distribution of

soils with gypsum. *Occurrence, characteristics, and genesis of carbonate, gypsum, and silica accumulations in soils*, (occurrencechara): 89–119.

Fang, H.Y. (1997) *Introduction to environmental geotechnology*. New York: CRC press.

FAO (1990) *Management of gypsiferous soils*, Food and Agricultural Organization of the United Nations, Rome.

FAO (1998) *World Reference Base for Soil Resources. World Soil Resources Report Vol. 84* FAO, Rome,.

Faroqy, A. (2018) *Investigation the changes in the geophysical and geotechnical properties of fine-grained soils when exposed to changes in vertically applied loads*. PhD thesis, University of Birmingham, UK.

Fattah, M.Y., Al-Ani, M.M. and Al-Lamy, M.T.A. (2015) Wetting and drying collapse behaviour of collapsible gypseous soils treated by grouting. *Arabian Journal of Geosciences*, 8 (4): 2035–2049.

Fattah, M.Y., al-Musawi, H.H.M. and Salman, F.A. (2012) Treatment of Collapsibility of Gypseous Soils by Dynamic Compaction. *Geotechnical and Geological Engineering*, 30 (6): 1369–1387. doi:10.1007/s10706-012-9552-z.

Fattah, M.Y., Al-Shakarchi, Y.J. and Al-Numani (2008) Long-Term Deformation Of Some Gypseous Soils. *Engineering and Technology Journal*, 26 (12): 1461–1483.

Feng-e, Z., Ji-xiang, Q., Yao-ru, L., et al. (2013) Mechanism of Karst Formation in Sulfate Rocks. *Procedia Earth and Planetary Science*, 7: 944–947.

Fookes, P.G. (1976) Road geotechnics in hot deserts. *Highway Engineer*, 23 (10): 11–23.

Fookes, P.G., French, W.J. and Rice, S.M.M. (1985) The influence of ground and groundwater geochemistry on construction in the Middle East. *Quarterly Journal of Engineering Geology and Hydrogeology*, 18 (2): 101–127.

Fredlund, D.G., Sheng, D. and Zhao, J. (2011) Estimation of soil suction from the soil-water characteristic curve. *Canadian Geotechnical Journal*, 48 (2): 186–198. doi:10.1139/t10-060.

Fredlund, D.G. and Xing, A. (1994) Equations for the soil-water characteristic curve. *Canadian Geotechnical Journal*, 31 (4): 521–532.

- French, W.J., Poole, A.B., Ravenscroft, P., et al. (1982) Results of preliminary experiments on the influence of fabrics on the migration of groundwater and water-soluble minerals in the capillary fringe. *Quarterly Journal of Engineering Geology and Hydrogeology*, 15 (3): 187–199.
- Fretti, C., Presti, D.C.F. Lo and Pedroni, S. (1995) A pluvial deposition method to reconstitute well-graded sand specimens. *Geotechnical testing journal*, 18 (2): 292–298.
- Frydman, S. (1979) “Use of pressuremeter in clean and variably cemented sands.” In *Proc. 7th European Conf. Soil Mechanics and Foundation Engineering, Brighton, England. 1979.* p. 217.
- Fukue, M., Minato, T., Horibe, H., et al. (1999) The micro-structures of clay given by resistivity measurements. *Engineering geology*, 54 (1–2): 43–53.
- Furley, P.A. and Zouzou, R. (1989) The origin and nature of gypsiferous soils in the Syrian mid-Euphrates. *Scottish geographical magazine*, 105 (1): 30–37.
- Gens, A., Sánchez, M., Guimaraes, L.D.N., et al. (2009) A full-scale in situ heating test for high-level nuclear waste disposal: observations, analysis and interpretation. *Géotechnique*, 59 (4): 377.
- Ghorbani, A., Cosenza, P., Badrzadeh, Y., et al. (2013) Changes in the electrical resistivity of arid soils during oedometer testing. *European Journal of Environmental and Civil Engineering*, 17 (2): 84–98. doi:10.1080/19648189.2012.747782.
- Gran, M., Carrera, J., Massana, J., et al. (2011) Dynamics of water vapor flux and water separation processes during evaporation from a salty dry soil. *Journal of hydrology*, 396 (3–4): 215–220.
- Guinea, A., Playà, E., Rivero, L., et al. (2012) The electrical properties of calcium sulfate rocks from decametric to micrometric scale. *Journal of Applied Geophysics*, 85: 80–91.
- Gumusoglu, M.C. and Ulker, R. (1982) The investigation of the effect of gypsum on foundation design. *Bulletin of the International Association of Engineering Geology-Bulletin de l'Association Internationale de Géologie de l'Ingénieur*, 25 (1): 99–105.

- Haeri, S.M., Hamidi, A. and Tabatabaee, N. (2005) The effect of gypsum cementation on the mechanical behavior of gravely sands. *Geotechnical Testing Journal*, 28 (4): 380–390.
- Hassan, A. (2014) *Electrical resistivity method for water content characterisation of unsaturated clay soil*. PhD thesis, UK.
- Hawkins, A.B. and Pinches, C.M. (1987) “Expansion due to gypsum growth.” *In Proceedings of the 6th international conference on expansive soils, New Delhi*. 1987. pp. 183–187.
- Herrero, J. (2004) Revisiting the definitions of gypsic and petrogypsic horizons in Soil Taxonomy and World Reference Base for Soil Resources. *Geoderma*, 120 (1–2): 1–5.
- Herrero, J., Artieda, O. and Hudnall, W. (2009) Gypsum, a tricky material. *Soil Science Society of America Journal*, 73 (6): 1757–1763.
- Herrero, J. and Porta, J. (1987) “Gypsiferous soils in the North-East of Spain.” *In Réunion internationale de micromorphologie des sols*. 7. 1987. pp. 187–192.
- Herrero, J. and Porta, J. (2000) The terminology and the concepts of gypsum-rich soils. *Geoderma*, 96 (1–2): 47–61.
- Hesse, P.R. (1976) Particle size distribution in gypsic soils. *Plant and Soil*, 44 (1): 241–247.
- Hijab, S.R. and Al-Jabbar, M.A. (2006) *Geophysical Investigation on Mosul Dam Area, Stage One, Emergency Microgravity Survey*. Iraq Geological Survey Library. internal report.
- Holiday, D. (1978) The origin of gypsum and anhydrite, some effects of its solution. *Quarterly Journal of Engineering Geology*, 11: 325–33.
- Holtz, R.D. and Kovacs, W.. (1981) *An introduction to geotechnical engineering*. Printice-Hall, Inc., Englewood Cliffs, New Jersey.
- Horta, J.D.O.S. (1980) Calcrete, gypcrete and soil classification in Algeria. *Engineering Geology*, 15 (1–2): 15–52.
- Huang, A.-B., Chang, W.-J., Hsu, H.-H., et al. (2015) A mist pluviation method for reconstituting silty sand specimens. *Engineering geology*, 188: 1–9.
- Huang, J.T. and Airey, D.W. (1998) Properties of artificially cemented carbonate sand. *Journal of Geotechnical and Geoenvironmental Engineering*, 124 (6): 492–499.
- Ismael, N.F. (1993) Laboratory and field leaching tests on coastal salt-bearing soils. *Journal*

- of geotechnical engineering*, 119 (3): 453–470.
- Ismael, N.F. and Mollah, M.A. (1998) Leaching effects on properties of cemented sands in Kuwait. *Journal of geotechnical and geoenvironmental engineering*, 124 (10): 997–1004.
- Ismail, M.A., Joer, H.A. and Randolph, M.F. (2000) Sample preparation technique for artificially cemented soils. *Geotechnical Testing Journal*, 23 (2): 171–177.
- Jafarzadeh, A.A. and Burnham, C.P. (1992) Gypsum crystals in soils. *Journal of soil science*, 43 (3): 409–420.
- James, A.N. and Edworthy, K.J. (1985) The effects of water interactions on engineering structures. *Hydrological sciences journal*, 30 (3): 395–406.
- James, A.N. and Kirkpatrick, I.M. (1980) Design of foundations of dams containing soluble rocks and soils. *Quarterly Journal of Engineering Geology and Hydrogeology*, 13 (3): 189–198.
- James, A.N. and Lupton, A.R.R. (1978) Gypsum and anhydrite in foundations of hydraulic structures. *Geotechnique*, 28 (3): 249–272.
- Jassim, S.Z. and Goff, J.C. (2006) *Geology of Iraq*. Dolin.
- Jennings, J.E. and Knight, K. (1975) “A guide to construction on or with materials exhibiting additional settlement due to collapse of grain structure.” In *In Proceeding of the 6th African Conference on Soil Mechanics and Foundation Engineering*. South Africa, 1975. pp. 99–105.
- Jha, A.K. and Sivapullaiah, P. V (2016) Volume change behavior of lime treated gypseous soil—influence of mineralogy and microstructure. *Applied Clay Science*, 119: 202–212.
- Jinguuji, M. (2011) *Development of multi-transmission high speed survey system and the application of geyser monitoring. International Workshop within the frame of the FWF project TEMPEL (TRP 175-N21) and the 7th FP European project SafeL and November 30 th - December 2 nd,*.
- Johnson, K.S. (2008) Gypsum-karst problems in constructing dams in the USA. *Environmental geology*, 53 (5): 945–950.

- Kadhim, A.J. (2014) Stabilization of gypseous soil by cutback asphalt for roads construction. *Journal of Engineering and Sustainable Development*, 18 (1): 46–67.
- Kalinski, R.J. and Kelly, W.E. (1993) Estimating water content of soils from electrical resistivity. *Geotechnical Testing Journal*, 16 (3): 323–329.
- Kattab, S.A. (1986) *Effect of gypsum on the strength of granular soil treated and untreated with cement*. M.Sc. thesis, University of Mosul, Iraq.
- Keller, G.V. and Frischknecht, F.C. (1966) *Electrical methods in geophysical prospecting*. Pergamon Press, New York, N.Y.
- Kelley, J.R., Wakeley, L.D., Broadfoot, S.W., et al. (2007) *Geologic setting of Mosul Dam and its engineering implications*. ENGINEER RESEARCH AND DEVELOPMENT CENTER VICKSBURG MS.
- Kemna, A., Binley, A. and Slater, L. (2004) Crosshole IP imaging for engineering and environmental applications. *Geophysics*, 69 (1): 97–107.
- Keren, R., Kreit, J.F. and Shainberg, I. (1980) Influence of size of gypsum particles on the hydraulic conductivity of soils. *Soil Science*, 130 (3): 113–117.
- Kezdi, A. (1974) *Handbook of soil mechanics*. Amsterdam: Vol. 1, Soil Physics, Elsevier Scientific Publishing Company.
- Khan, N.A. (1994) Influence of dilution and particle size on gypsum solubility of gypsiferous soils. *Sarhad Journal of Agriculture*.
- Khan, S.U. and Webster, G.R. (1968) Determination of gypsum in solonchic soils by an x-ray technique. *Analyst*, 93 (1107): 400–402.
- Khari, M., Kassim, K.A. and Adnan, A. (2014) Sand samples' preparation using mobile pluviator. *Arabian Journal for Science and Engineering*, 39 (10): 6825–6834.
- Kibria, G. (2014) *Evaluation of Physico-Mechanical Properties of Clayey Soils Using Electrical Resistivity Imaging Technique*. University of Texas at Arlington.
- Kim, J.H., Yoon, H.-K. and Lee, J.-S. (2010) Void ratio estimation of soft soils using electrical resistivity cone probe. *Journal of geotechnical and geoenvironmental engineering*, 137 (1): 86–93.
- Klein, C. and Hurlbut, Csj. (1985) *Manual of Mineralogy, after J.D. Dana*. 20th Editi. New

- York: John Wiley and Sons.
- Klimchouk, A. (1996) The dissolution and conversion of gypsum and anhydrite. *International Journal of Speleology*, 25 (3): 2.
- Knight, K. (1963) The origin and occurrence of collapsing soils. *Proc. 3rd Reg. African CSMFE*, 1: 127–130.
- Krauskopf, K.B. (1979) *Introduction to geochemistry. International series in the earth and planetary science*. Tokyo: Mc Grow-Hill.
- Kusakabe, O. (1995) “Chapter 6: Foundations.” *In Geotechnical centrifuge technology*. London: R. N. Taylor, ed., Blackie Academic & Professional. pp. 118–167.
- Ladd, R.S. (1978) Preparing test specimens using undercompaction. *Geotechnical Testing Journal*, 1 (1): 16–23.
- Lebron, I., Herrero, J. and Robinson, D.A. (2009) Determination of gypsum content in dryland soils exploiting the gypsum–bassanite phase change. *Soil Science Society of America Journal*, 73 (2): 403–411.
- Lee, G.W., Clemence, S.P., Bhatia, S.K., et al. (1984) *Subsidence Affects Due to Gypsum Solution in Syracuse, New York*.
- Lee, M.-J., Hong, S.-J., Choi, Y.-M., et al. (2010) Evaluation of deformation modulus of cemented sand using CPT and DMT. *Engineering Geology*, 115 (1–2): 28–35.
- Lees, G.M. and Falcon, N.L. (1952) The geographical history of the Mesopotamian plains. *The Geographical Journal*, 118 (1): 24–39.
- Lins, Y. (2009) *Hydro-mechanical properties of partially saturated sand*, PhD thesis, University Bochum.
- Livneh, M., Livneh, N.A. and Hayati, G. (1998) Site investigation of sub-soil with gypsum lenses for runway construction in an arid zone in Southern Israel. *Engineering geology*, 51 (2): 131–145.
- Loke, D.M. (1999) *Electrical imaging surveys for environmental and engineering studies. A practical guide to 2-D and 3-D surveys*.
- Loke, M.H., Chambers, J.E. and Kuras, O. (2011) Instrumentation, electrical resistivity, Solid Earth Geophysics Encyclopedia (2nd edition.). *Electrical & Electromagnetic*, H. Gupta

- (Ed.), Springer, Berlin, pp. 599–604.
- Loke, M.H., Chambers, J.E., Rucker, D.F., et al. (2013) Recent developments in the direct-current geoelectrical imaging method. *Journal of applied geophysics*, 95: 135–156.
- Long, M., Donohue, S., L’Heureux, J.-S., et al. (2012) Relationship between electrical resistivity and basic geotechnical parameters for marine clays. *Canadian Geotechnical Journal*, 49 (10): 1158–1168.
- Mandal, J.N. and Manjunath, V.R. (1995) Bearing capacity of strip footing resting on reinforced sand subgrades. *Construction and Building Materials*, 9 (1): 35–38.
- Mashali, A. (1986) “Physical and chemical properties of gypsiferous soil related reclamation and management practice.” *In Symposium on gypsiferous soils their effect on construction and agriculture production*. 1986.
- Merriam–Webster (1994) *Merriam–Webster’s Collegiate Dictionary*. 10th edn.
- MESF (2007) *The Mosul Dam Issue File’, The Middle East Seismological Forum Special Reporting*.
- Miura, S. and Toki, S. (1982) A sample preparation method and its effect on static and cyclic deformation-strength properties of sand. *Soils and foundations*, 22 (1): 61–77.
- Moret-Fernández, D. and Herrero, J. (2015) Effect of gypsum content on soil water retention. *Journal of Hydrology*, 528: 122–126.
- Mori, K., Seed, H.B. and Chan, C.K. (1977) *Influence of sample disturbance on sand response to cyclic loading*. CALIFORNIA UNIV BERKELEY COLL OF ENGINEERING.
- Nafie, F.A.A. (1989) *The properties of highly gypsiferous soils and their significance for land management*. PhD thesis, University of London, UK.
- Namiq, L. and Nashat, I. (2011) Influence of leaching on volume change of a gypsiferous soil. *Geo-Frontiers: Advances in Geotechnical Engineering ASCE*, pp. 2611–2620.
- Nashat, I.H. (1990) *Engineering characteristics of some gypseous soils in Iraq*. PhD thesis, University of Baghdad, Iraq.
- NCCLR (National Centre for Construction Labs and Research) (2005) *Soil Investigation for Electrical Transformation Station at AL-Najaf City, Report No.1/1/20, Baghdad, Iraq*.

- Nelson, R.E., Klameth, L.C. and Nettleton, W.D. (1978) Determining Soil Gypsum Content and Expressing Properties of Gypsiferous Soils 1. *Soil Science Society of America Journal*, 42 (4): 659–661.
- Oda, M., Koishikawa, I. and Higuchi, T. (1978) Experimental study of anisotropic shear strength of sand by plane strain test. *Soils and foundations*, 18 (1): 25–38.
- Okpoli, C.C. (2013) Sensitivity and resolution capacity of electrode configurations. *International Journal of Geophysics*, 2013.
- Olayinka, A.I. and Yaramanci, U. (2000) Assessment of the reliability of 2D inversion of apparent resistivity data. *Geophysical Prospecting*, 48 (2): 293–316.
- Ovesen, N.K. (1975) Centrifugal testing applied to bearing capacity problems of footings on sand. *Geotechnique*, 25 (2): 394–401.
- Pandey, L.M.S., Shukla, S.K. and Habibi, D. (2015) Electrical resistivity of sandy soil. *Géotechnique Letters*, 5 (3): 178–185.
- Pando, L., Pulgar, J.A. and Gutiérrez-Claverol, M. (2013) A case of man-induced ground subsidence and building settlement related to karstified gypsum (Oviedo, NW Spain). *Environmental earth sciences*, 68 (2): 507–519.
- Pearson, M.J., Monteith, S.E., Ferguson, R.R., et al. (2015) A method to determine particle size distribution in soils with gypsum. *Geoderma*, 237: 318–324.
- Petrukhin, V.P. and Arakelyan, E.A. (1984) Strength of gypsum-clay soils and its variation during the leaching of salts. *Soil Mechanics and Foundation Engineering*, 21 (6): 264–268.
- Poch, R.M., Artieda, O., Herrero, J., et al. (2010) *Gypsic Features*. Elsevier B.V. doi:10.1016/B978-0-444-53156-8.00010-6.
- Polydorides, N. (2002) *Image Reconstruction algorithms for soft-field tomography*. University of Manchester, Manchester, United Kingdom.
- Porta, J. (1998) Methodologies for the analysis and characterization of gypsum in soils: A review. *Geoderma*, 87 (1–2): 31–46.
- Porta, J. and Herrero, J. (1990) “Micromorphology and genesis of soils enriched with gypsum.” In *Developments in Soil Science*. Elsevier. pp. 321–339.

- Presti, D.C.F. Lo, Berardi, R., Pedroni, S., et al. (1993) A new traveling sand pluviator to reconstitute specimens of well-graded silty sands. *Geotechnical Testing Journal*, 16 (1): 18–26.
- Presti, D.C.F. Lo, Pedroni, S. and Crippa, V. (1992) Maximum dry density of cohesionless soils by pluviation and by ASTM D 4253-83: A comparative study. *Geotechnical Testing Journal*, 15 (2): 180–189.
- Puppala, A.J., Acar, Y.B. and Tumay, M.T. (1995) Cone penetration in very weakly cemented sand. *Journal of Geotechnical Engineering*, 121 (8): 589–600.
- Rad, N.S. and Tumay, M.T. (1986) Effect of cementation on the cone penetration resistance of sand: A model study. *Geotechnical Testing Journal*, 9 (3): 117–125.
- Rad, N.S. and Tumay, M.T. (1987) Factors affecting sand specimen preparation by raining. *Geotechnical Testing Journal*, 10 (1): 31–37.
- Random House Value (1996) *Webster's encyclopedic unabridged dictionary of the English language*. Random House, New York.
- Ransome, F.L. (1928) Geology of the Saint Francis dam site. *Economic Geology*, 23 (5): 553–563.
- Razouki, S.S. and Al-Azawi, M. (2003) Long-Term Soaking Effect On Strength And Deformation Characteristics Of A Gypsiferous Subgrade Soil. *Engineering Journal of the University of Qatar*, 16: 49–60.
- Razouki, S.S. and El-Janabi, O.A. (1999) Decrease in the CBR of a gypsiferous soil due to long-term soaking. *Quarterly Journal of Engineering Geology and Hydrogeology*, 32 (1): 87–89.
- Razouki, S.S. and Ibrahim, A.N. (2007) “Improving a gypsum sand roadbed soil by increased compaction.” *In Proceedings of the Institution of Civil Engineers-Transport*. 2007. Thomas Telford Ltd. pp. 27–31.
- Razouki, S.S. and Kuttah, D.K. (2006) “Predicting long-term soaked CBR of gypsiferous subgrade soils.” *In Proceedings of the Institution of Civil Engineers-Transport*. 2006. Thomas Telford Ltd. pp. 135–140.
- Razouki, S.S., Kuttah, D.K. and Abood, M.H. (2010) Compaction and design of gypsiferous

- fill for hot desert road pavements. *Proceedings of the Institution of Civil Engineers-Construction Materials*, 164 (1): 3–11.
- Razouki, S.S., Kuttah, D.K., Al-Damluji, O.A., et al. (2007) Strength erosion of a fine-grained gypsiferous soil during soaking. *Arabian Journal for Science and Engineering*, 32 (1B): 147.
- Razouki, S.S., Kuttah, D.K., Al-Damluji, O.A., et al. (2008) Using gypsiferous soil for embankments in hot desert areas. *Proceedings of the Institution of Civil Engineers-Construction Materials*, 161 (2): 63–71.
- Razouki, S.S. and Salem, B.M. (2014) Soaking–drying frequency effect on gypsum-rich roadbed sand. *International Journal of Pavement Engineering*, 15 (10): 933–939.
- Redfield, R.C. (1963) Report on attendance at the 1st International Conference on Public Works in Gypsiferous Terrain, Madrid, 20–29 Sept 1962. *US Bureau of Reclamation, Amarillo*.
- Reynolds, J.M. (1997) An introduction to applied and environmental geophysics. *Chichester: John Wiley & Sons*.
- Rhoades, J.D., Raats, P.A.C. and Prather, R.J. (1976) Effects of liquid-phase electrical conductivity, water content, and surface conductivity on bulk soil electrical conductivity 1. *Soil Science Society of America Journal*, 40 (5): 651–655.
- Rinaldi, V.A. and Cuestas, G.A. (2002) Ohmic Conductivity of a Compacted Silty Clay. *Journal of Geotechnical and Geoenvironmental Engineering*, 128 (10): 824–835. doi:10.1061/(asce)1090-0241(2002)128:10(824).
- Rogers, C.D.F., Dijkstra, T.A. and Smalley, I.J. (1994) Hydroconsolidation and subsidence of loess: studies from China, Russia, North America and Europe: in memory of Jan Sajgalik. *Engineering Geology*, 37 (2): 83–113.
- Royal, A. (2012) *Arid Soils*. In *ICE Manual of Geotechnical Engineering*. London: Volume 1, Geotechnical Engineering Principles, Problematic Soils and Site Investigation.
- Royal, A.C.D., Makhover, Y., Moshirian, S., et al. (2013) Investigation of cement–bentonite slurry samples containing PFA in the UCS and triaxial apparatus. *Geotechnical and Geological Engineering*, 31 (2): 767–781.

- Royal, A.C.D., Opukumo, A.W., Qadr, C.S., et al. (2018) Deformation and Compression Behaviour of a Cement–Bentonite Slurry for Groundwater Control Applications. *Geotechnical and Geological Engineering*, 36 (2): 835–853.
- Saaed, S.A., Alomary, R. and Nazhat, N. (1989) “Shear behaviour of gypsiferous soils.” *In Proc. Of the 2nd int. Symposium on Environmental Geotechnology, Shanghai*. 1989.
- Saito, H., Šimůnek, J. and Mohanty, B.P. (2006) Numerical analysis of coupled water, vapor, and heat transport in the vadose zone. *Vadose Zone Journal*, 5 (2): 784–800.
- Sajedi, K., Huat, B.B.K. and Bazaz, J.B. (2008) "Effects of cyclic test in decreasing damages to structures and roads on gypsum soils". *6th international conference on case histories in geotechnical engineering, Arlington, VA, August, pp. 11-16*
- Salas, J.A.J., Justo, J.L., Romana, M., et al. (1973) “The collapse of gypseous silts and clays of low plasticity in arid and semiarid climates.” *In Proceedings of the 8th International Conference on Soil Mechanics and Foundation Engineering, Moscow. Dunod Press, Paris*. 1973. pp. 193–199.
- Salih, N.B. (2013) *Stability of dams constructed on problematic substrates*. PhD thesis, School of Engineering and Design, Brunel University, UK.
- Samouëlian, A., Cousin, I., Richard, G., et al. (2003) Electrical resistivity imaging for detecting soil cracking at the centimetric scale. *Soil Science Society of America Journal*, 67 (5): 1319–1326.
- Samouëlian, A., Cousin, I., Tabbagh, A., et al. (2005) Electrical resistivity survey in soil science: a review. *Soil and Tillage research*, 83 (2): 173–193.
- Seleam, S.N.M. (1988) *Geotechnical characteristics of a gypseous sandy soil including the effect of contamination with some oil products*. M.Sc. thesis, University of Technology. Baghdad, Iraq.
- Sen, P.N., Goode, P.A. and Sibbit, A. (1988) Electrical conduction in clay bearing sandstones at low and high salinities. *Journal of Applied Physics*, 63 (10): 4832–4840.
- Sheffer, M.R., Reppert, P.M. and Howie, J.A. (2007) A laboratory apparatus for streaming potential and resistivity measurements on soil samples. *Review of Scientific Instruments*, 78 (9): 94502.

- Sheikha, A.A.H. (1994) *The Collapsibility of Gypseous Soil and Effect of Leaching on its Behavior*. University of Technology, Baghdad, Iraq.
- Sievert, T., Wolter, A. and Singh, N.B. (2005) Hydration of anhydrite of gypsum (CaSO_4 . II) in a ball mill. *Cement and concrete research*, 35 (4): 623–630.
- SIGIR (2007) *Relief and Reconstruction Funded Work at Mosul Dam, Mosul-Iraq', Special Inspector General for Iraq Reconstruction, 29 October 2007*.
- Singh, R.B. and Al-Layla, M.T. (1980) "Engineering behaviour and microstructures of a collapsible Mosul clay under physico-chemical reversal of leaching." *In Proceedings of the 6th Southeast Asian Conference on Soil Engineering, Taipei*. 1980. pp. 127–137.
- Sirwan, K., Majeed, A.H. and Wadood, B.A. (1991) Consolidation characteristics of gypsiferous soils. *Geological Society, London, Engineering Geology Special Publications*, 7 (1): 503–508.
- Sissakian, V., Al-Ansari, N. and Knutsson, S. (2013) Sand and dust storm events in Iraq. *Journal of Natural Science*, 5 (10): 1084–1094.
- Sissakian, V., Al-Ansari, N. and Knutsson, S. (2014) Karstification effect on the stability of Mosul Dam and its assessment, North Iraq. *Engineering*, 6 (2): 84–92.
- Sissakian, V.K. and Al-Mousawi, H.A. (2007) Karstification and related problems, examples from Iraq. *Iraqi Bulletin of Geology and Mining*, 3 (2): 1–12.
- Skarie, R.L., Arndt, J.L. and Richardson, J.L. (1987) Sulfate and Gypsum Determination in Saline Soils 1. *Soil Science Society of America Journal*, 51 (4): 901–905.
- Slater, L.D. and Lesmes, D. (2002) IP interpretation in environmental investigations. *Geophysics*, 67 (1): 77–88.
- Smits, K.M., Cihan, A., Sakaki, T., et al. (2011) Evaporation from soils under thermal boundary conditions: Experimental and modeling investigation to compare equilibrium-and nonequilibrium-based approaches. *Water Resources Research*, 47 (5).
- Solis, R. and Zhang, J. (2008) "Gypsiferous soils: An engineering problem." *In Sinkholes and the engineering and environmental impacts of karst*. pp. 742–749.
- Song, W.-K., Cui, Y.-J., Tang, A.M., et al. (2013) Development of a large-scale

- environmental chamber for investigating soil water evaporation. *Geotechnical Testing Journal*, 36 (6): 847–857.
- Spaargaren (1994) *World reference base for soil resources. Draft. ISSS-ISRIC-FAO, Wageningen/Rome.*
- Sreedeeep, S., Reshma, A.C. and Singh, D.N. (2004) Measuring soil electrical resistivity using a resistivity box and a resistivity probe. *Geotechnical testing journal*, 27 (4): 411–415.
- Soil Survey Staff (1998) *Keys to soil taxonomy*. 8th edn. ashington, DC,: USDA Natural Resources Conservation Service, Washington, DC, pp. 326.
- Stummer, P., Maurer, H. and Green, A.G. (2004) Experimental design: Electrical resistivity data sets that provide optimum subsurface information. *Geophysics*, 69 (1): 120–139.
- Subhi, H.M. (1987) *The properties of salt contaminated soils and their influence on the performance of roads in Iraq*. PhD thesis, Queen Mary, University of London, UK.
- Sweeney, B.P. and Clough, G.W. (1990) Design of a large calibration chamber. *Geotechnical testing journal*, 13 (1): 36–44.
- Taha, S.A.W. (1979) *The effect of leaching on the engineering properties of Qayiara soil*. M.Sc. thesis, Department of Civil Engineering, University of Mosul, Iraq.
- Taimeh, A.Y. (1992) Formation of gypsic horizons in some arid regions soils of Jordan. *Soil Science*, 153 (6): 486–498.
- Tatsuoka, F., Teachavorasinskun, S., Dong, J., et al. (1994) “Importance of measuring local strains in cyclic triaxial tests on granular materials.” *In Dynamic geotechnical testing II*. ASTM International.
- Taylor, R.K. and Cripps, J.C. (1984) *Mineralogical controls on volume change*. Surrey Univ. Press/Blackie Group, Glasgow.
- Tomlinson, M.J. (1978) Middle East—Highway and airfield pavements. *Quarterly Journal of Engineering Geology and Hydrogeology*, 11 (1): 65–73.
- Tumay, M.T., Antonini, M. and Arman, A. (1979) Metal versus nonwoven fiber fabric earth reinforcement in dry sands: a comparative statistical analysis of model tests. *Geotechnical Testing Journal*, 2 (1): 44–56.
- Ueng, T.-S., Wang, M.-H., Chen, M.-H., et al. (2005) A large biaxial shear box for shaking

- table test on saturated sand. *Geotechnical Testing Journal*, 29 (1): 1–8.
- Vaid, Y.P. and Negussey, D. (1984) Relative density of pluviated sand samples. *Soils and Foundations*, 24 (2): 101–105.
- Van Alphen, J.G. and de los Ríos Romero, F. (1971) *Gypsiferous soils: Notes on their characteristics and management*. ILRI.
- Vanapalli, S.K., Fredlund, D.G. and Pufahl, D.E. (1999) The influence of soil structure and stress history on the soil-water characteristics of a compacted till. *Geotechnique*, 49 (2): 143 – 159.
- Verheye, W.H. and Boyadgiev, T.G. (1997) Evaluating the land use potential of gypsiferous soils from field pedogenic characteristics. *Soil Use and Management*, 13 (2): 97–103.
- Watson, A. (1979) Gypsum crusts in deserts. *Journal of Arid Environments*, 2 (1): 3–20.
- Watson, A. (1983) *Gypsum crusts*. In Goudie, A.S. & Pye, K. (eds.), *Chemical Sediments and Geomorphology: Precipitates and Residua in the Near-surface Environment*. Academic Press, London, pp. 133–161.
- Yamamuro, J.A. and Wood, F.M. (2004) Effects of depositional method on the undrained behaviour and microstructure of sand with silt. *Soil Dyn. Earthq. Eng*, 24 (9–10): 751–760.
- Yamnova, I.A. and Pankova, E.I. (2013) Gypsic pedofeatures and elementary pedogenetic processes of their formation. *Eurasian soil science*, 46 (12): 1117–1129.
- Yan, M., Miao, L. and Cui, Y. (2012) Electrical resistivity features of compacted expansive soils. *Marine Georesources & Geotechnology*, 30 (2): 167–179.
- Yilmaz, I. (2001) Gypsum/anhydrite: Some engineering problems. *Bulletin of Engineering Geology and the Environment*, 60 (3): 227–230. doi:10.1007/s100640000071.
- Yilmaz, I. and Civelekoglu, B. (2009) Gypsum: an additive for stabilization of swelling clay soils. *Applied Clay Science*, 44 (1–2): 166–172.
- Yoon, H.-K., Truong, Q.H., Byun, Y.-H., et al. (2015) Capillary effect in salt-cemented media of particle sizes. *Journal of Applied Geophysics*, 112: 20–28.
- Zanbak, C. and Arthur, R.C. (1986) Geochemical and engineering aspects of anhydrite/gypsum phase transitions. *Bulletin of the Association of Engineering*

Geologists, 23 (4): 419–433.

- Zha, F., Liu, S., Du, Y., et al. (2010) Characterization of compacted loess by electrical resistivity method. *Soil Behavior and Geo-Micromechanics, GeoShanghai 2010*, pp. 68–73.
- Zhou, M., Wang, J. and Liu, F. (2013) “Proposal of new temperature correction models for soil electrical resistivity.” *In 11th IEEE International Conference on Solid Dielectrics - June 30th - July 4th*. Bologna, Italy, 2013.